

Alma Mater Studiorum – Università di Bologna

DOTTORATO DI RICERCA IN

CHIMICA

Ciclo XXIX

Settore Concorsuale di afferenza: 03/C1

Settore Scientifico disciplinare: CHIM/06

**ELECTROPHILIC AND NUCLEOPHILIC ACTIVATION OF
ALLENAMIDES AND ALLENOATES: USEFUL BUILDING
BLOCKS IN ORGANIC SYNTHESIS**

Presentata da: Elisabetta Manoni

Coordinatore Dottorato

Prof. Aldo Roda

Relatore

Prof. Pier Giorgio Cozzi

Co-relatore

Prof. Marco Bandini

Esame finale anno 2017

INDEX

1. INTRODUCTION: ALLENAMIDES	1
2. REACTIVITY	4
2.1 <u>Cycloaddition</u>	4
2.1.1 <i>Inverse Electron-Demand Hetero [4+2] Cycloaddition</i>	4
2.1.2 <i>Formal [4+2] and [2+2] Cycloaddition</i>	6
2.1.3 <i>[4+3] Cycloaddition</i>	14
2.2 <u>Isomerization Reaction</u>	22
2.3 <u>Palladium-Catalysed Cascade Reaction</u>	28
2.4 <u>Electrophilic Activation</u>	34
3. ELECTROPHILIC ACTIVATION OF ALLENAMIDES BY CHIRAL PHOSPHORIC ACIDS	43
3.1 <u>Metal-Free Enantioselective Dearomatization of Indoles</u>	43
3.1.1 <i>Experimental Section</i>	56
3.2 <u>Organocatalytic Enantioselective Synthesis of 1-Vinyl Tetrahydroisoquinoline</u>	77
3.2.1 <i>Experimental Section</i>	84

4. INTRODUCTION: ALLENOATES	104
4.1 <u>Electrophilic Activation</u>	105
4.2 <u>Nucleophilic Activation</u>	109
5. GOLD-CATALYSED [3,3]-SIGMATROPIC REARRANGEMENT OF PROPARGYLIC CARBOXYLATE	113
5.1 <u>Catalytic α-Allylation of Enones with Alcohols</u>	113
5.1.1 <i>Experimental Section</i>	124
6. INTRODUCTION: C–H ACTIVATION	139
6.1 <u>Stoichiometric Reaction</u>	139
6.2 <u>Catalytic Reaction</u>	142
7. MANGANESE-CATALYSED C–H ACTIVATION	155
7.1 <u>Mn-Catalysed C–H alkynylation</u>	155
7.1.1 <i>Experimental Section</i>	168
8. CONCLUSIONS	178

The studies undertaken in these three years of my PhD resulted in the sequent publications:

1. Metal-Free Enantioselective Electrophilic Activation of Allenamides: Stereoselective De-Aromatization of Indoles”, C. Romano, M. Jia, M. Monari, **E. Manoni** and M. Bandini, *Angew. Chem. Int. Ed.*, **2014**, 53, 13854-13857 (*described in paragraph 3.1*);
2. Stereoselective Organocatalytic Addition of Nucleophiles to Isoquinolinium and 3,4-dihydroisoquinolinium Ions: A simple Approach for the Synthesis of Isoquinoline Alkaloids”, A. Gualandi, L. Mengozzi, **E. Manoni** and P. G. Cozzi, *Catal. Lett.*, **2015**, 145, 398-419;
3. Organocatalytic Enantioselective Synthesis of 1-Vinyl Tetrahydroisoquinolines through Activation with Chiral Brønsted Acids” **E. Manoni**, A. Gualandi, L. Mengozzi, M. Bandini and P. G. Cozzi, *RSC Adv.*, **2015**, 5, 10546-10550 (*described in paragraph 3.2*);
4. New Opportunities in the Stereoselective Dearomatization of Indoles”, **E. Manoni**, A. De Nisi and M. Bandini, *Pure & Appl. Chem.*, **2016**, 88, 207-214;
5. Catalytic α -allylation of enones with alcohols via [gold (I)]-mediated [3,3]-sigmatropic rearrangement of propargylic carboxylates”, **E. Manoni**, M. Daka, M. M. Mastandrea, A. De Nisi, M. Monari and M. Bandini, *Adv. Synth. Catal.*, **2016**, 358, 1404-1409 *Selected as a VIP article by the Editorial Board* (*described in paragraph 5.1*);
6. *N*-allenyl amides and *O*-allenyl ethers in asymmetric catalysis”, **E. Manoni** and M. Bandini, *Eur. J. Org. Chem.*, **2016**, 3135-3142;
7. From QCA (Quantum Cellular Automata) to Organocatalytic Reactions with Stabilized Carbenium Ions”, A. Gualandi, L. Mengozzi, **E. Manoni** and P. G. Cozzi, *Chem. Rec.*, **2016**, 16, 1228-1243;
8. Manganese-Catalyzed C–H Alkynylation: Expedient Peptide Synthesis and Modification”, Z. Ruan, N. Sauermann, **E. Manoni** and L. Ackermann, *Angew. Chem. Int. Ed.*, *accepted* (*described in paragraph 7.1*).

1. INTRODUCTION: ALLENAMIDES

In recent years, the interest in allenes drastically increased due to their importance as building blocks in a large variety of synthetic transformations.^[1,2] The allenes were largely employed in cycloaddition reactions,^[3] but their challenging synthesis and their poor predisposition toward electrophilic activation encouraged the development of allene-equivalent compounds. Heteroatom-substituted allenes, in particular allenamines, have received low attention from the scientific community, so far. In this class of compounds, the π -donating ability of the nitrogen atom makes allenamines more electron-rich than allenes allowing their easy electrophilic activation. Despite their synthetic potential, few developments have been achieved in their manipulation due to the high sensibility toward hydrolysis and the tendency toward polymerization and isomerization even at low temperature. In order to overcome these issues, it was identified an allenamine-equivalent where the heteroatom is bonded to an electron-withdrawing group. This functionalization reduces the reactivity of the allenic framework but, at the same time, makes the allenic system more stable (Figure 1).^[4-6]

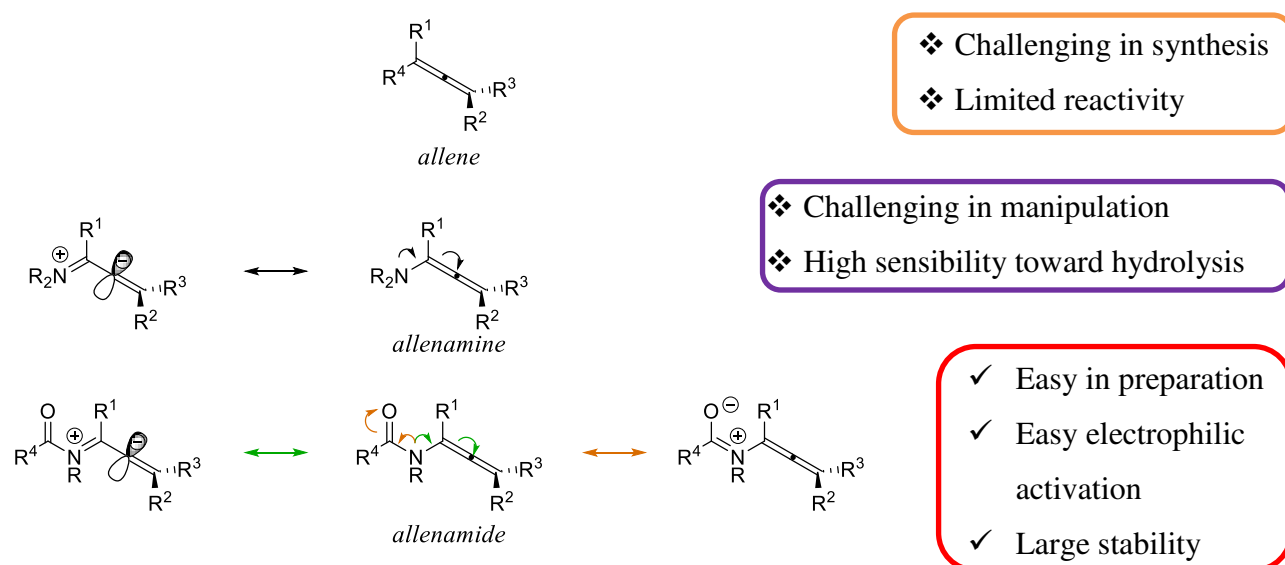
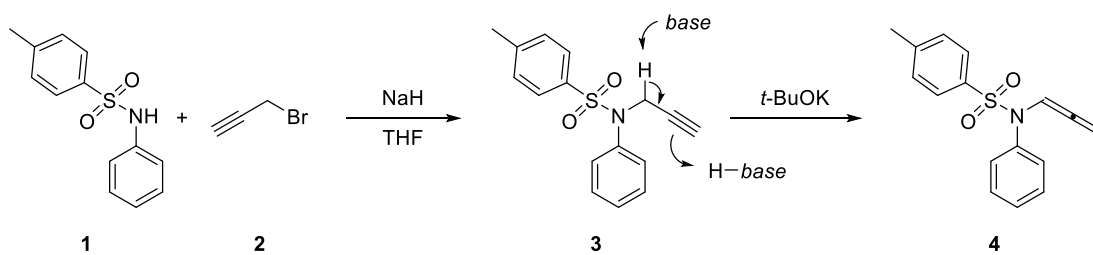


Figure 1: Disadvantages and advantages in the use of allene, allenamines and allenamides.

Allenamides were prepared the first time by Dickinson^[7] in 1967 by treating 2-pyrrolidinone with NaH and propargyl bromide. In contrast, when less reactive amides (for example *N*-tosylaniline or 2-oxazolidinone) were used in place of the 2-pyrrolidone moiety was not possible to obtain the desired allenamides using the synthetic procedure reported by Dickinson. Indeed, the reaction was not complete and it was possible to isolate only the propoargylamide intermediate **3** (Scheme 1). A treatment of the latter with catalytic amount (30 mol%) of *t*-BuOK is required to drive the reaction toward the formation of desired product **4** (Scheme 1).



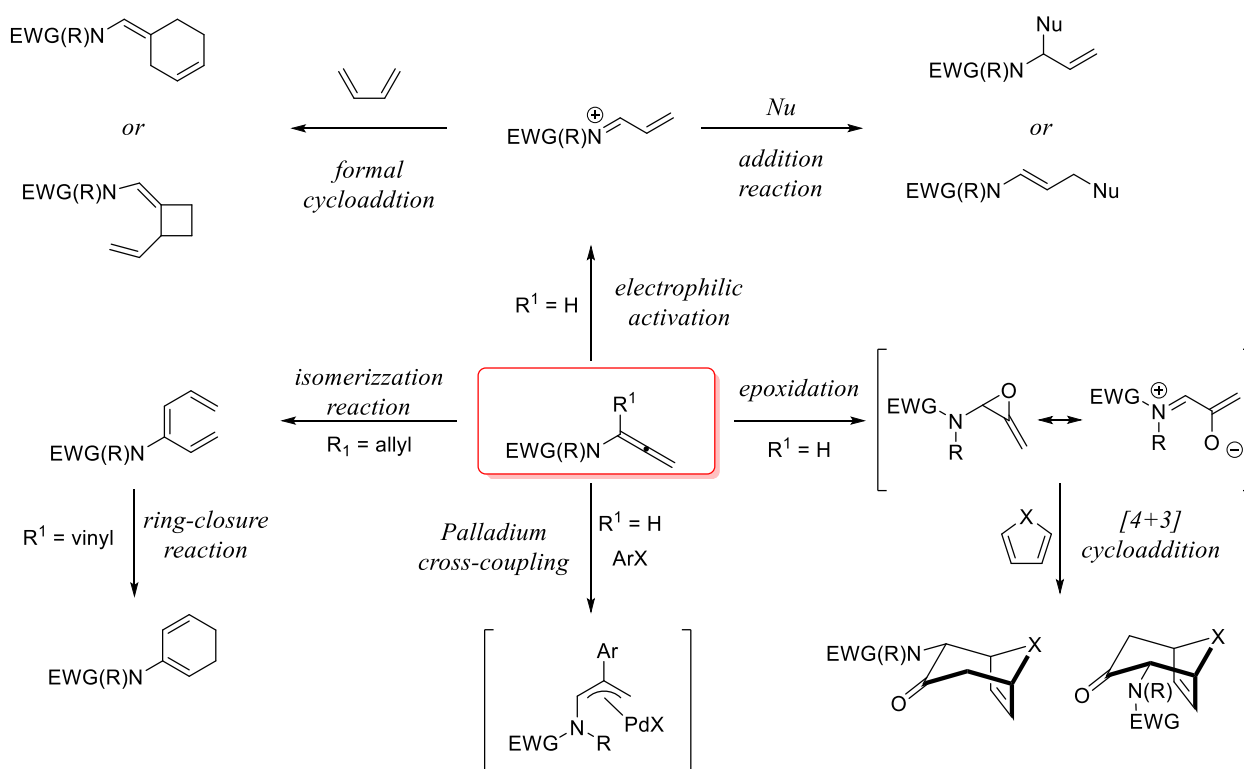
Scheme 1: Preparation of allenamide 4.

Bibliography

- [1] K. M. Brummond, J. L. Kent, *Tetrahedron* **2000**, *56*, 3263–3283.
- [2] S. Ma, *Chem. Rev.* **2005**, *105*, 2829–2872.
- [3] F. López, J. L. Mascareñas, *Chem. Soc. Rev.* **2014**, *43*, 2904–2915.
- [4] L.-L. Wei, H. Xiong, R. P. Hsung, *Acc. Chem. Res.* **2003**, *36*, 773–782.
- [5] T. Lu, Z. Lu, Z.-X. Ma, Y. Zhang, R. P. Hsung, *Chem. Rev.* **2013**, *113*, 4862–4904.
- [6] E. Manoni, M. Bandini, *Eur. J. Org. Chem.* **2016**, 3135–3142.
- [7] W. B. Dickinson, P. C. Lang, *Tetrahedron Lett.* **1967**, *8*, 3035–3040.

2. REACTIVITY

The allenamides have been employed in numerous methodologies. Their electrophilic activation promoted by soft-metals (such as gold-based catalysts) or Brønsted acid leads to the formation of an iminium ion intermediate which in turn could be employed in addition reactions as well as in formal cycloaddition reactions. Additionally, the α -substituted allenamides can undergo an isomerization reaction with consequent formation of dienes (or trienes) which can be used in further cycloaddition reactions. Moreover, the large flexibility of allenamides allowed their employment in other reactions such as palladium-catalysed cross coupling reactions as well as in epoxidation reaction and followed by [4+3] cycloadditions (Scheme 1).



Scheme 1: Allenamides as powerful building blocks in organic synthesis.

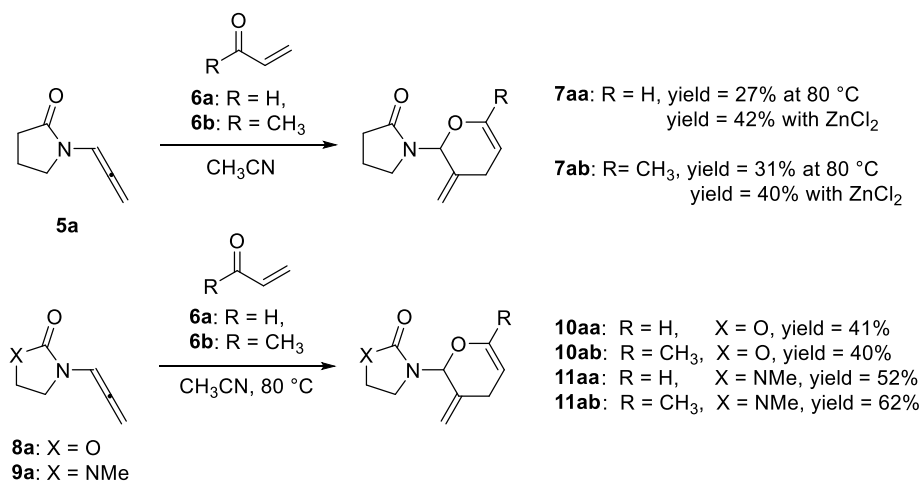
In the following chapter some examples about the use of allenamides in organic synthesis are reported in order to highlight their large versatility as building blocks.

2.1 Cycloaddition

2.1.1 Inverse Electron-Demand Hetero[4+2] Cycloaddition

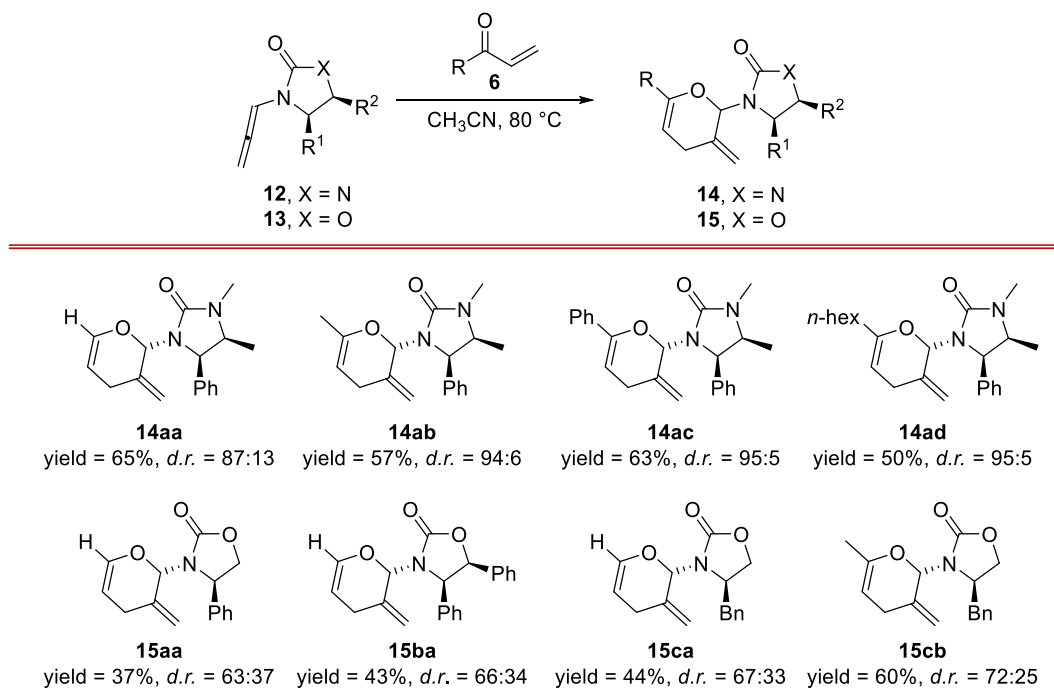
In 1999 Hsung and co-workers^[8] documented the inverse electron-demand hetero[4+2] cycloaddition reaction of allenamide **5** with α,β -unsaturated carbonyl compounds **6** under both

thermal and acidic conditions obtaining the corresponding products in moderate yields. The authors reported that allenamides featuring an oxazolidinone or imidazolidinone scaffold resulted more reactive (Scheme 2).



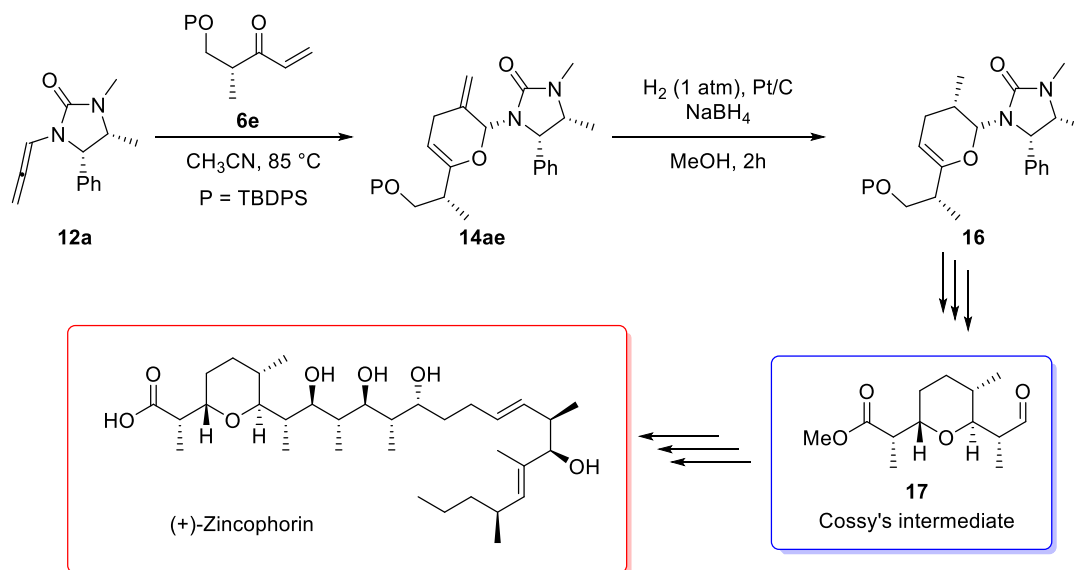
Scheme 2: Pioneering studies in inverse demand hetero[4+2] cyclization reactions with allenamides.

Subsequently, Hsung reported the first stereoselective variant^[9] of title cycloaddition reaction using a chiral allenamide as substrate. A range of chiral allenamides as well as heterodienes were submitted under optimized reaction conditions resulting in the corresponding products in good yields and excellent stereoselectivity (Scheme 3).



Scheme 3: First stereoselective inverse demand hetero[4+2] cycloaddition reactions with allenamides.

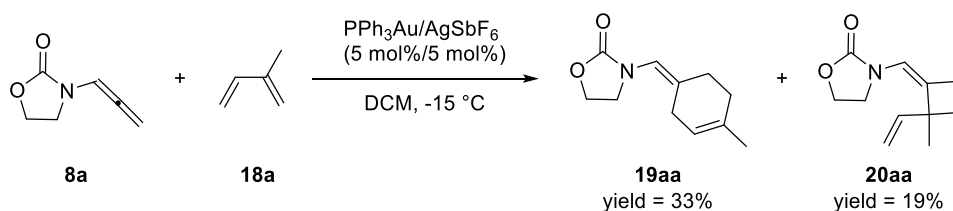
The value of these 2-substituted pyranil heterocycles was demonstrated with their employment in the synthesis of the C1—C9 subunit (Cossy's intermediate) of (+)-Zincophorin (Scheme 4).^[10]



Scheme 4: Synthesis of (+)-Zincophorin.

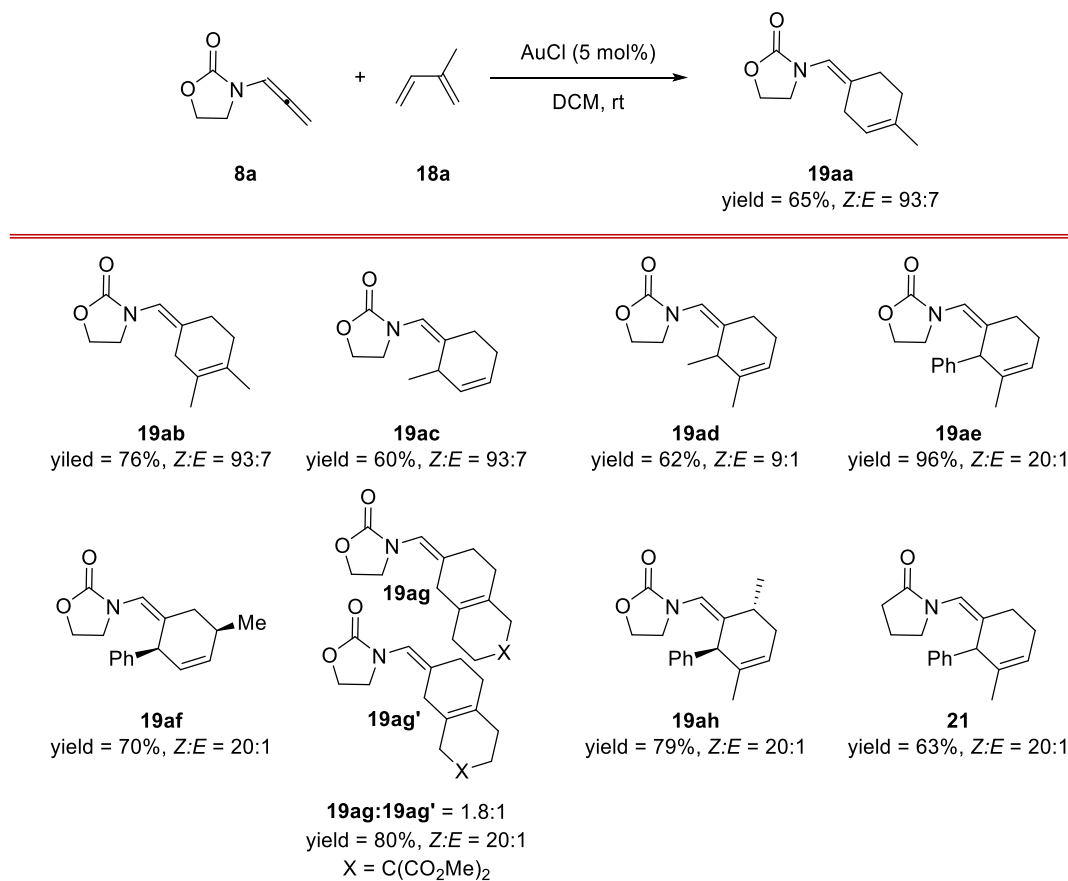
2.1.2 Formal [4+2] and [2+2] Cycloaddition

The [4+2] Diels-Alder reaction is among the most powerful synthetic methods for the synthesis of unsaturated six-membered rings due to its ample scope and simplicity of operation. López and Mascareñas^[11], as well as Toste^[12–14] and Fürstner^[15], reported gold-catalysed intramolecular [4+2] cycloaddition of allene-tethered-dienes in order to develop a very efficient protocol for *trans*-fused bicyclic system. Subsequently, López and Mascareñas, with the aim of extending the use of this intramolecular cycloaddition toward more challenging intermolecular variant, developed the first transition metal-catalysed [4+2] cycloaddition between non-activated 1,3-dienes and allenamides.^[16] They started their investigation trying to use electronically neutral allenes instead of allenamides in the process but no satisfactory results were achieved. On the contrary, the use of electron-rich allenamides in the condensation with isoprene in the presence of $\text{PPh}_3\text{AuCl/AgSbF}_6$ resulted in the generation of the desired [4+2] cycloadduct product although with the concomitant and unexpected formation of the [2+2] cycloadduct side-product (Scheme 5).



Scheme 5: First transition metal-catalysed [4+2] cycloaddition of allenamides.

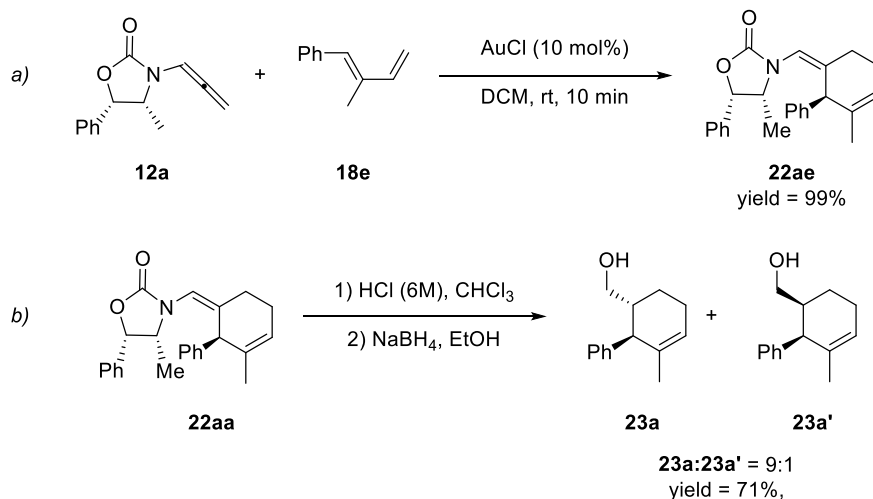
In order to avoid the formation of product **20**, they carried out the condensation between **8a** and isoprene in the presence of different cationic Au-catalysts, but also the cyclobutane derivatives have been isolated in all of the cases. Finally, the neutral AuCl catalyst promoted the reaction with complete regio- and very high stereoselectivity toward the selective formation of the [4+2] cycloadduct **19aa** in 65% yield. In order to prove the scope of the methodology, several differently substituted dienes and allenamides were submitted under optimized reaction conditions resulting in the corresponding products in good to excellent yields and in some cases with complete stereoselectivity (Scheme 6).



Scheme 6: Optimized reaction conditions and scope of the regio- and stereoselective [4+2] cycloaddition.

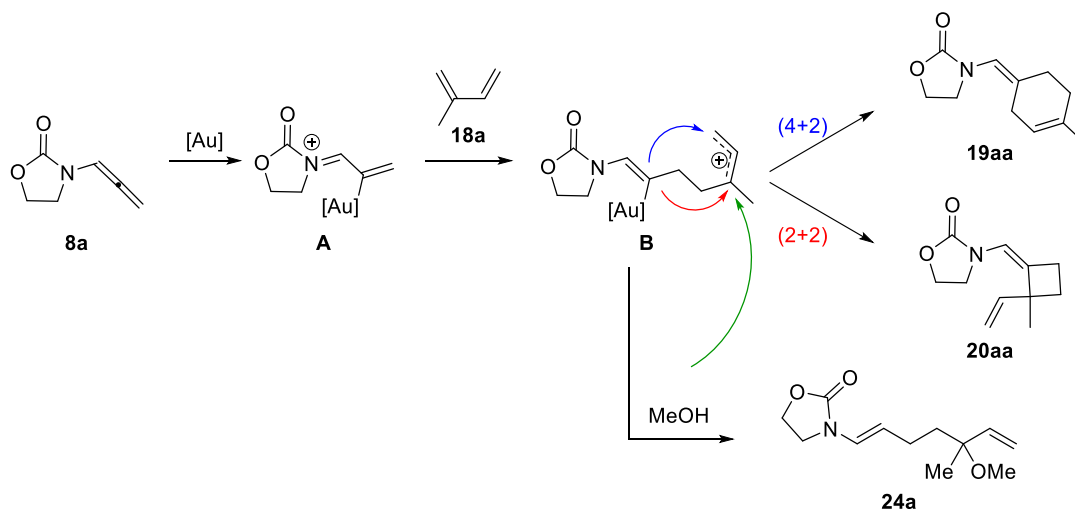
With the use of chiral allenamide **12a** it was also possible to develop an enantioselective variant of this methodology. Furthermore, product **19** presents an enamide group which is a powerful building

block for further functionalizations. Indeed, under acidic conditions followed by reduction with NaBH_4 , it was possible to isolate the desired alcohol **23** in good yield and 9:1 diastereoisomeric ratio (Scheme 7).



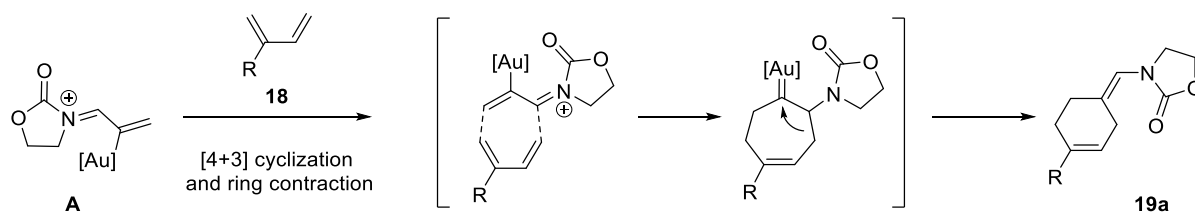
Scheme 7: Enantioselective variant of the [4+2] cycloaddition (a) and highly diastereoselective reduction (b).

Mechanistically, the formation of undesired [2+2] cycloadduct and the presence of small amounts of allylether **24a**, observed when the reaction has been carried out in the presence of MeOH , suggested the formation of an iminium ion as the intermediate. Indeed the first nucleophilic trapping of the iminium ion **A** intermediate results in the formation of allyl cation intermediate **B** which can undergo the second nucleophilic attack in the terminal carbon, resulting in a cyclohexene adduct **19aa** or in the more substituted carbon, resulting in the cyclobutane adduct **20aa** (Scheme 8).



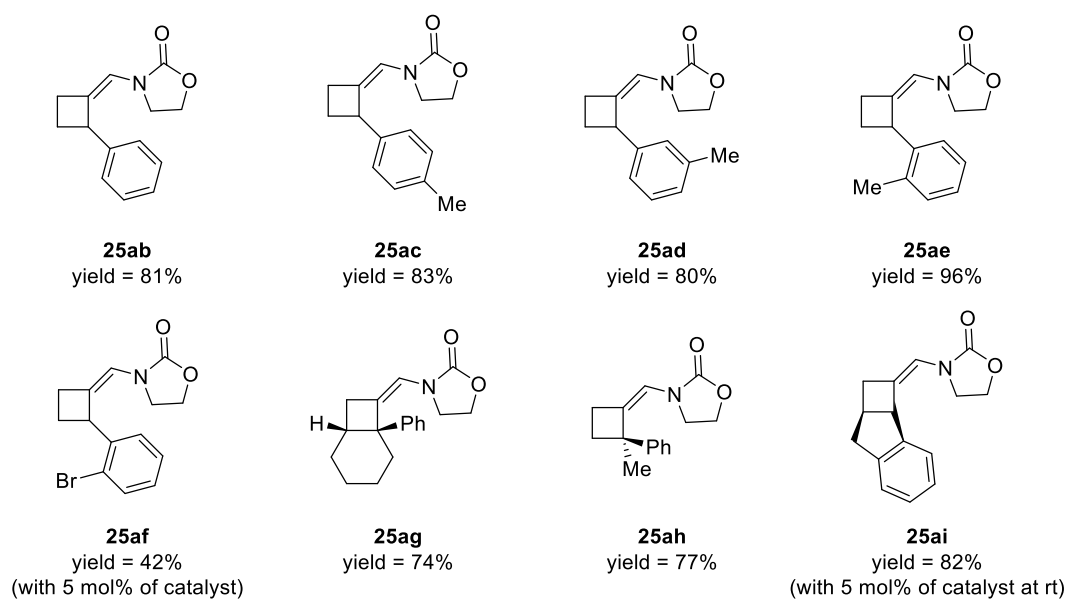
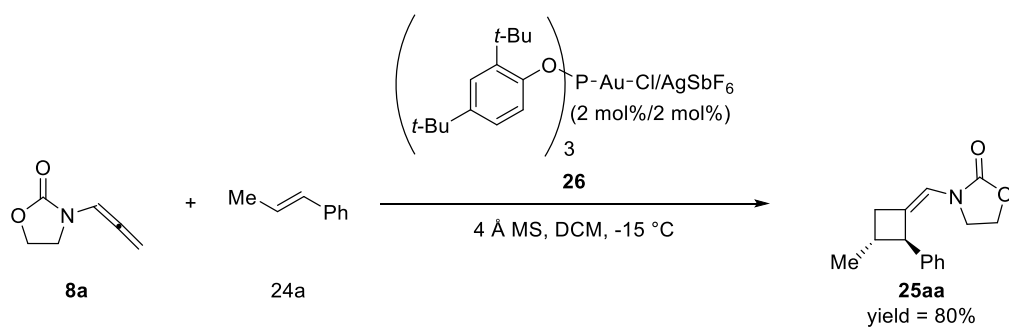
Scheme 8: Proposed mechanism for the formation of **24aa**, **20aa** and **23a**.

Subsequently, in particular in 2013, the same authors, in collaboration with Ujaque, performed combined experimental and computational studies in order to shed light on the reaction mechanism of the process.^[17] Based on the obtained results, they demonstrated the formation of metal allyl cation from the electrophilic activation of allenamide by gold-catalyst, but the formation of desired [4+2] product took place through concerted [4+3] cycloaddition followed by ring contraction event (Scheme 9).



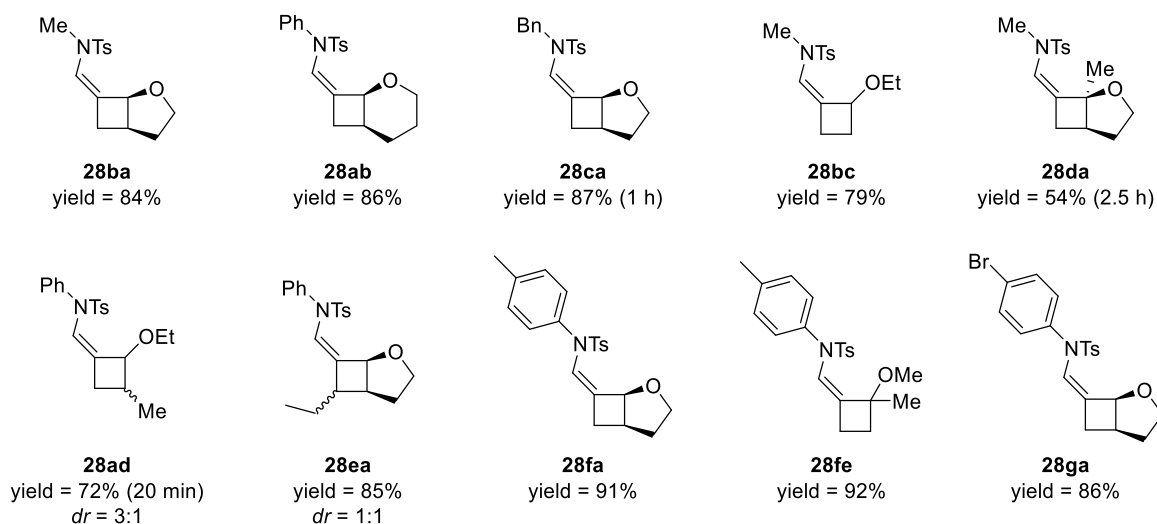
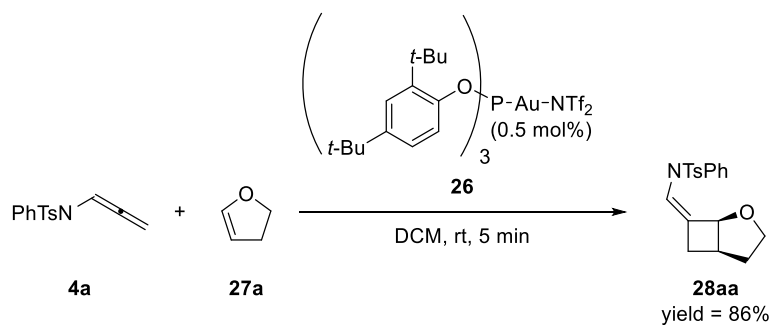
Scheme 9: Mechanism for the formation of **19a**.

Considering the synthetic and medicinal relevance of the cyclobutane framework, the authors developed a gold-catalysed intermolecular [2+2] cycloaddition between allenamides and *trans*-methyl styrene.^[18] They found that the best catalyst to obtain the cyclobutane derivatives in selective manner was the π -acidic cationic phosphite gold(I) catalyst. They were able to isolate the desired cyclobutane **25aa** in 51% yield, but by performing the reaction in the presence of 4 Å molecular sieves in the mixture and by adding the allenamide **8a** over one hour, the yield of **25aa** increased up to 80%. Subsequently they demonstrated the scope of the method by submitting differently substituted styrenes in the reaction with allenamide **8a** and by isolating the desired cyclobutane derivatives in good to excellent yields (Scheme 10).



Scheme 10: Optimized reaction conditions for the Au(I)-catalysed [2+2] cycloaddition of the allenamides and its ample scope.

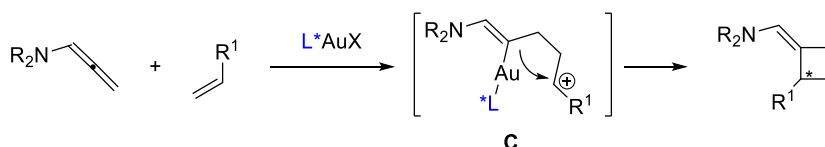
In the same time González and co-workers in 2012, reported an intermolecular [2+2] cycloaddition of allenamides using electron-rich enol ethers as alkenes.^[19] The phosphite-based gold-catalyst **26** used by López and Mascareñas resulted to be the best promoting agent also for this transformation. It delivered the product from the condensation of allenamide **4** and 2,3-dihydrofuran **27a** in 86% yield with complete *cis*-selectivity for the configuration of bicycle linking and *Z* configuration for the double bond. The scope of the reaction has been investigated by submitting differently substituted allenamides as well as enol ethers under optimized reaction conditions (Scheme 11).



Scheme 11: Optimized reaction conditions and scope for the intermolecular [2+2] cycloaddition with electron-rich enol ethers.

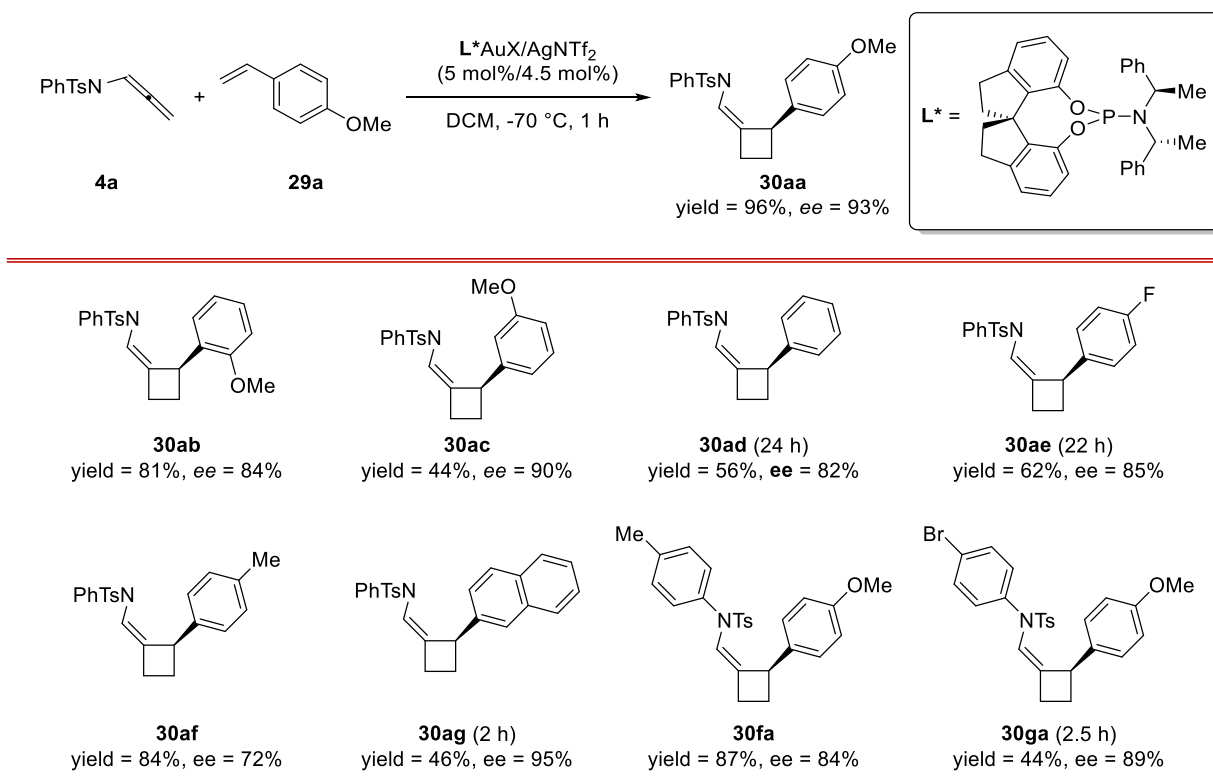
The reaction was tolerant toward different functional groups delivering the corresponding products in good to excellent yields and complete stereoselectivity when cyclic enol ethers were used. Also acyclic enol ethers were employed in the transformation resulting in the desired products in good yields.

In this line, González and co-workers in 2012 reported the first enantioselective gold(I)-catalysed intermolecular [2+2] cycloaddition in order to develop a synthetic procedure for enantioenriched cyclobutane derivatives.^[20] The enantioselective step of the process is the nucleophilic attack from the enamide in the intermediate **C** to the allyl cation and they suggested that the enantioselectivity could be controlled by a chiral ligand on the gold catalyst (Scheme 12).



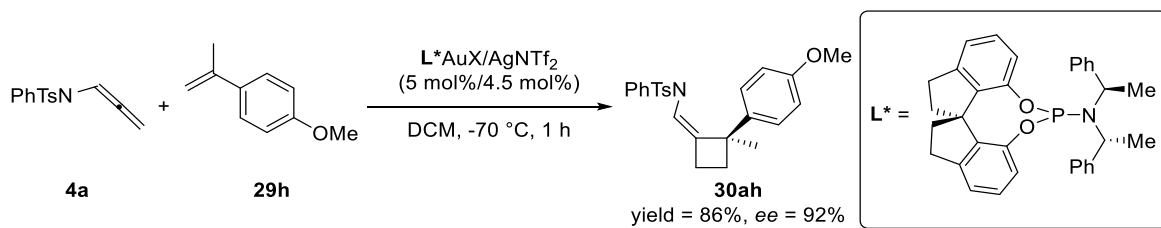
Scheme 12: First enantioselective Au(I)-catalysed intermolecular [2+2] cycloaddition.

In this line, they started their investigation by testing different chiral phosphine ligands for gold(I) catalysts in the condensation of allenamide **4a** and 4-methoxystyrene **29a** in dichloromethane and very low temperature due to the high reactivity of allenamide. Subsequently, the investigation continued by testing the effect of the nature of the sulfonyl group bonded to the nitrogen confirming the sulfonyl group as the best one. The scope of the reaction was proved by submitting several differently substituted styrene derivatives and allenamides under optimized catalytic conditions. The methodology resulted to be tolerant toward different functional groups and the enantiomeric excesses of the products were not influenced by the nature of the substituent (Scheme 13).



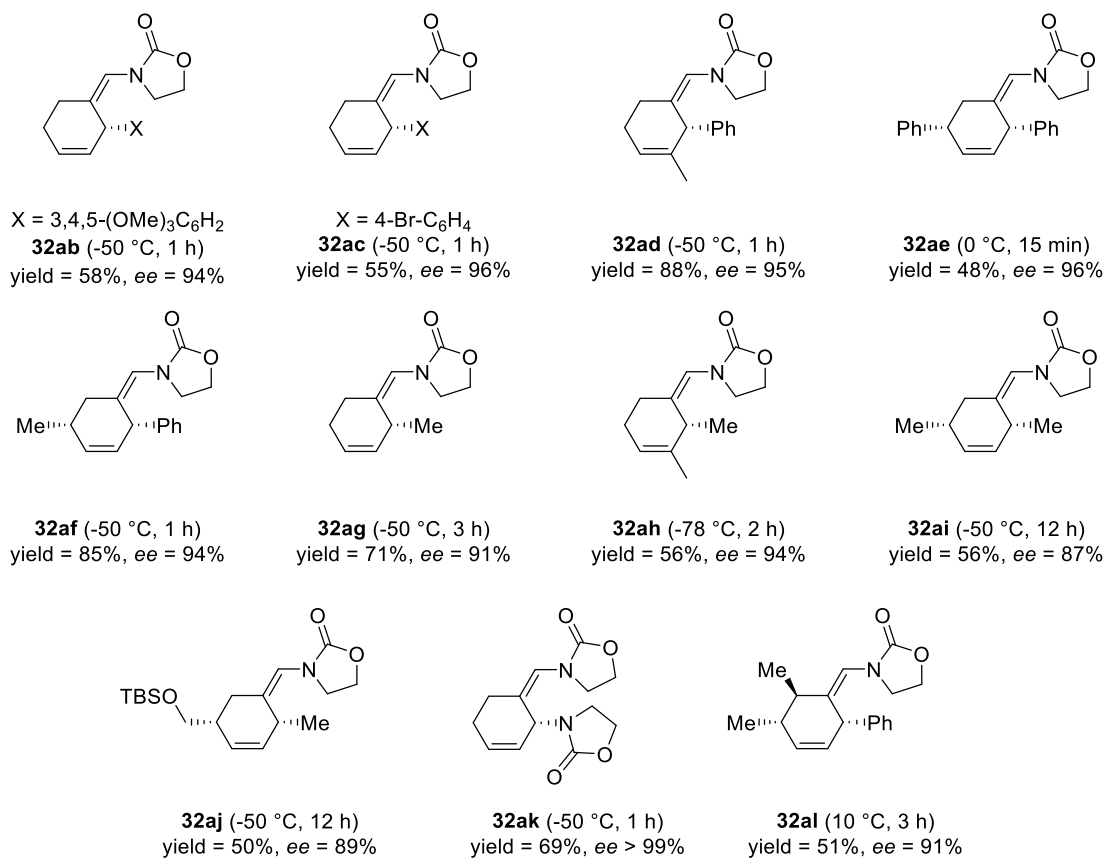
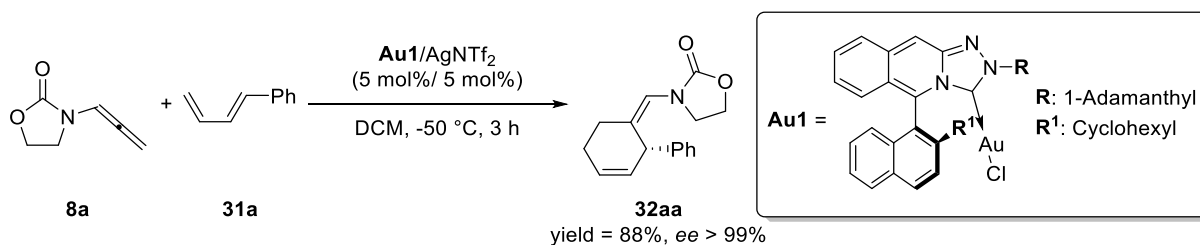
Scheme 13: Optimized reaction conditions for enantioselective [2+2] cycloaddition and scope of the reaction.

Furthermore, the enantioselective methodology was also used to prepare cyclobutanes containing challenging quaternary carbon centers.^[21] Using α -methylstyrene as alkene in the reaction the desired product has been obtained without significant variations in term of yield and enantiomeric excess respect the model reaction (Scheme 14).



Scheme 14: Synthesis of cyclobutane containing quaternary center.

In order to develop the first asymmetric variant of intermolecular [4+2] cycloaddition of allenamides and dienes, López and Mascareñas designed a new chiral NHC-gold(I) complex^[22] since chiral acyclic diaminocarbene gold-complexes were recently employed in enantioselective applications.^[12,23]



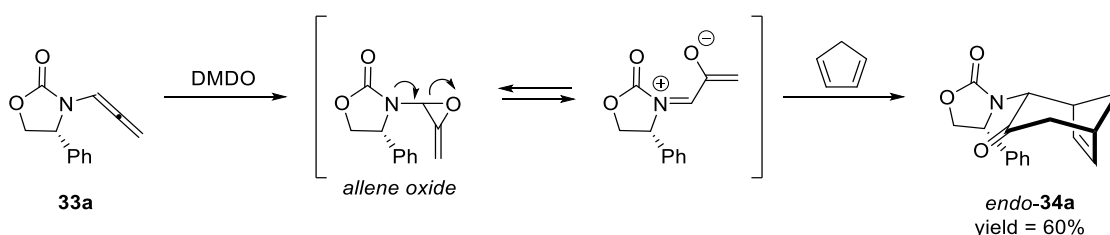
Scheme 15: First asymmetric variant of intermolecular [4+2] cycloaddition of allenamides and scope of the reaction.

They synthesized a rigid bicyclic structure to fix the orientation of the C(carbene)-Au bond and the closer groups R and R¹ in order to promote the asymmetric induction and subsequently, the efficiency of the title catalyst was proved in the [4+2] cycloaddition of allenamide **8a** and differently substituted dienes (Scheme 15).

The methodology resulted to be tolerant toward different functional groups and all the products were isolated with good to excellent yields. Moreover, the enantioselectivity was not influenced by the nature of the substituent on the dienes and in most of the cases the enantiomeric excesses was more than 90%.

2.1.3 [4+3] Cycloaddition

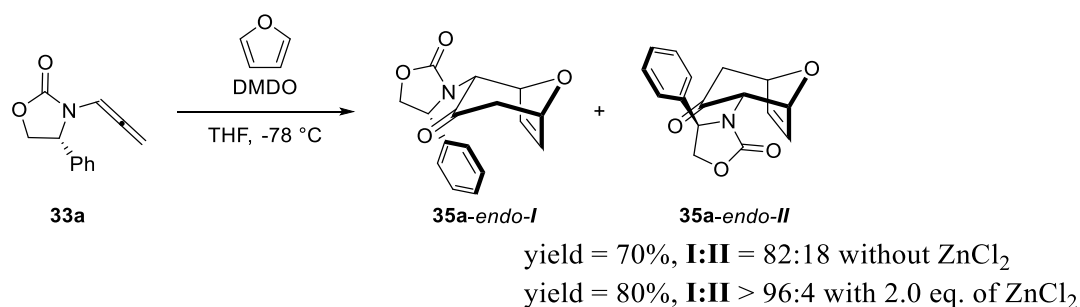
[4+3] cycloaddition is a useful route to seven-membered carbocycles. Allyl or oxyallyl cations are commonly used as 3 atom π -system and the presence of heteroatoms in particular oxygen, nitrogen or sulfur, stabilizes the oxyallyl cation. The epoxidation of allenamides is an easy and facile way to obtain nitrogen-substituted oxyallyl cations. The first epoxidation of allenamide was reported by Hsung and co-workers^[24] in 2001 using the chiral allenamide **33a** and dimethyldioxirane (DMDO) as oxidizing agent. At the time, they also demonstrated that the oxyallyl cation obtained from allenamide could be used in a [4+3] cycloaddition with cyclic diene. They started their investigation using cyclopentadiene as partner in the reaction and they were able to isolate the desired product in 60% yield as single *endo*-diastereoisomer (Scheme 16).



Scheme 16: First epoxidation of allenamide and reaction with cyclopentadiene.

Subsequently, they investigated the [4+3] cycloaddition using furan as diene. Also in this case only the *endo*-isomer was obtained but with moderate diastereoselectivity. They continued the investigation, by screening different solvents and temperatures and they also tried to use additives in order to improve the yield and the diastereoselectivity. Adding two equivalents of ZnCl₂ in the

mixture and decreasing the temperature up to $-78\text{ }^{\circ}\text{C}$ it was possible to isolate the bicycle product **35a** in 80% yield and diastereoisomeric ratio more than 96:4.



Scheme 17: [4+3] cycloaddition between allenamide and furan.

The presence of the Zn(II) cation should increase the conformational rigidity of the oxyallyl cation and consequently promote the diastereomeric induction (Figure 1).

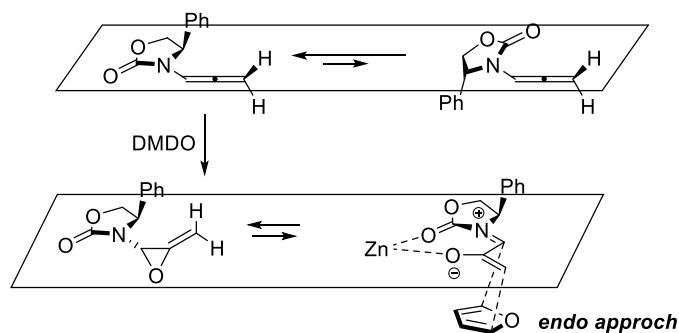


Figure 1: Role of the Zn(II) in diastereomeric induction.

Differently substituted allenamides were submitted under optimized reaction conditions with furan. The yields were satisfactory and allenamides with bulky groups in α position to the nitrogen in oxazolidinone ring resulted in the corresponding *endo*-products in high diastereoselectivity also without ZnCl_2 as additive. Indeed the addition of diene would proceed from the less hindered face of the oxyallyl cation.

Inspired by these satisfactory results, the authors envisioned the possibility to develop an enantioselective [4+3] cycloaddition of achiral allenamides and dienes using chiral Lewis acid-catalyst.^[25] They considered the activation promoted by Zn(II) in the transformation and the differentiation of the two faces in the oxyallyl cation intermediate effected by the substituent in the oxazolidinone ring. They rationalized that the replacement of achiral ZnCl_2 with a chiral Lewis acid which can fix the conformation of oxyallyl cation and promote the diastereoselectivity (Figure 2).

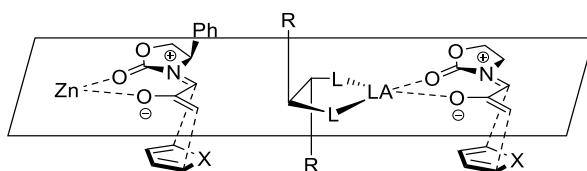
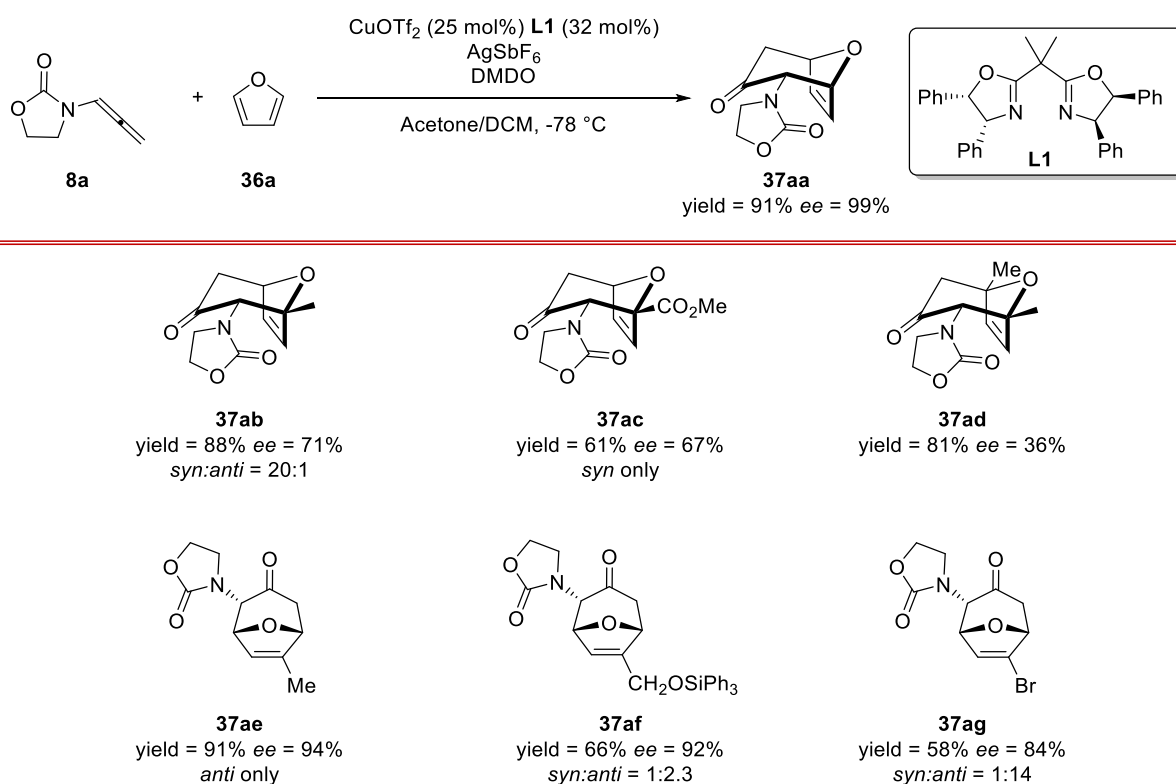


Figure 2: Use of chiral Lewis acid in enantioselective [4+3] cycloaddition.

In this line, they started to screen different Lewis acids and chiral ligands in order to find the best promoting agent in term of yield and enantioselectivity. Using $\text{Cu}(\text{OTf})_2$ and ligand **L1** they were able to obtain the desired cycloadduct in 46% yield and 90% enantiomeric excess. Subsequently they demonstrated that the yield and the enantiomeric excess can be further increase using AgSbF_6 as additive at the mixture. Allenamide **8a** was submitted with differently substituted furans under optimized reaction conditions in order to prove the scope of the methodology (Scheme 18).



Scheme 18: Optimized reaction conditions for the [4+3] cycloaddition with furan and scope of the reaction.

The predominant formation of the *S*-enantiomer can be justified by considering the *endo*-1 and *endo*-2 approaches shown in Figure 3. In the *endo*-2 approach it is presents an interaction between the hydrogen on C3 carbon of the furan and the phenyl group of the ligand and this causes the preference toward the *endo*-1 approach and consequent formation of *S* enantiomer. The 3-substituted furans resulted in the corresponding *anti*-isomer in high enantiomeric excesses. The preference in the formation of *anti*-isomers is due to interaction between $\text{R}^{3\text{syn}}$ on C3 of the furan

and the phenyl group of the ligand forcing the furan to an orientation where the substituent in C3 position is in *anti* respect the oxazolidinone. On the contrary, the 2-substituted furans present a lower enantiomeric excess and a prevalence of *syn*-isomers. This evidence can be rationalized by considering the interaction between the substituent in C2 position of furan and the oxyallyl framework: this interaction can be reduced with a movement of the furan but in this way also the interaction with hydrogen in C3 and the phenyl group of the ligand decreases making it easier the *endo-2* approach (Figure 3).

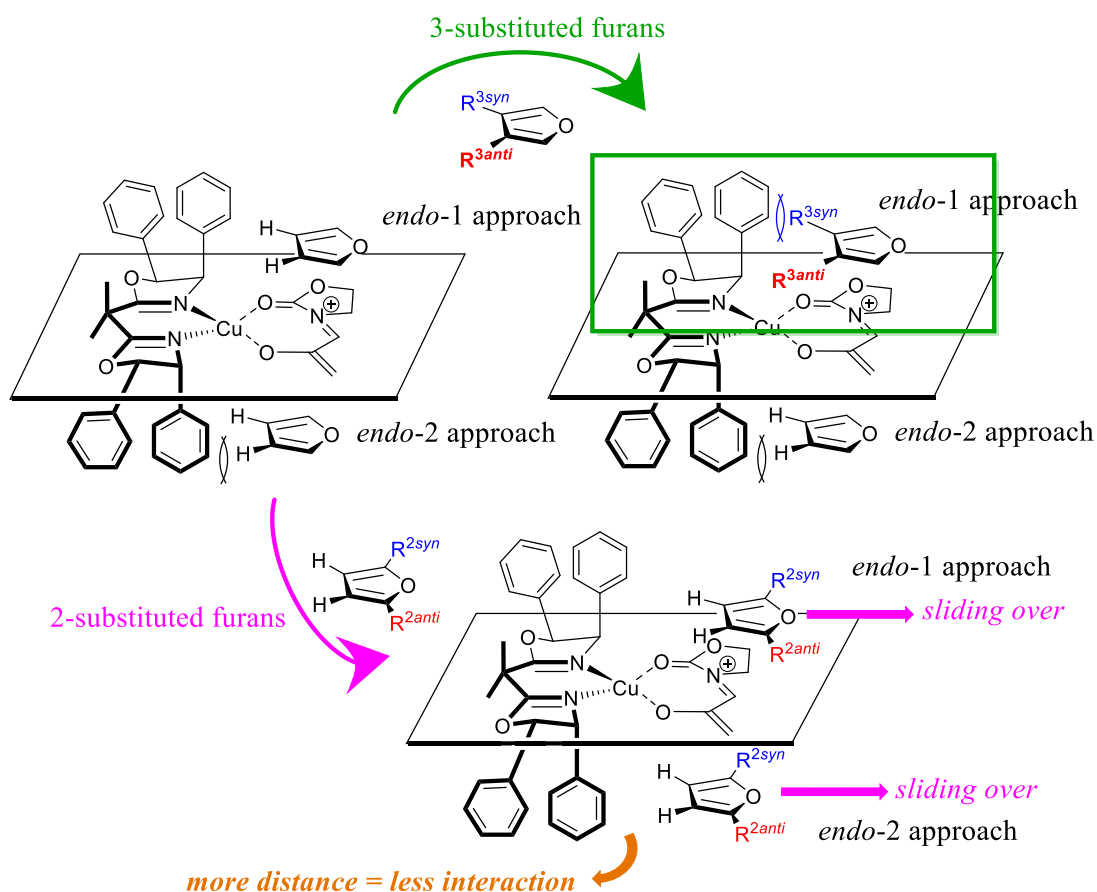
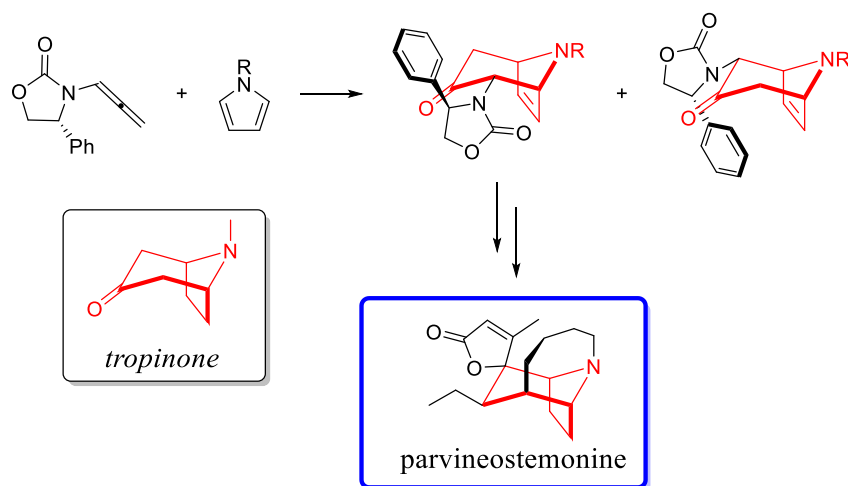


Figure 3: *endo-1* and *endo-2* approaches

In this line Hsung and co-workers in 2007^[26] reported an intermolecular [4+3] cyclization of chiral allenamides and pyrroles which can be a useful way to obtain tropinone derivatives in high stereoselectivity. Furthermore the tropinone obtained can be used for the synthesis of alkaloids such as parvineostemonine (Scheme 19).



Scheme 19: Synthetic procedure for the tropinone and parvineostemonine.

They started their investigation in order to optimize the reaction conditions and immediately they realized that the nitrogen of the pyrrole needs to be substituted with an electron-withdrawing group such as Boc or Bz to avoid its oxidation by DMDO. Despite further optimizations, it was not possible to obtain high diastereoselectivity for the reaction with pyrroles as that achieved in the process with the furans. Therefore, in order to improve the diastereomeric induction, different chiral allenamides were submitted under cyclization reaction with pyrrole. The products **38** and **39** were obtained in good yields and excellent diastereoselectivity, but on the contrary of the process with furans, the diastereoisomeric ratio is inexplicably in favour of the *endo-II* products also in the presence of $ZnCl_2$ (Figure 4).

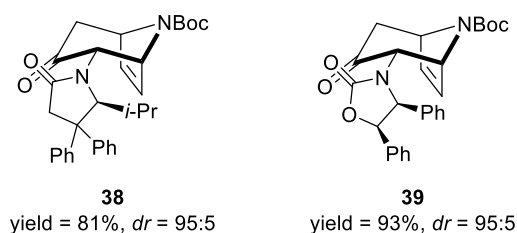


Figure 4: *endo-II* product favoured in the reaction with pyrrole.

Mechanistically, this result cannot be justified by the model described above, which should provide the diastereoisomer *endo-I* as main one.

Another unexpected result was observed in the intermolecular [4+3] cycloaddition reaction between chiral allenamide **33a** and 2-methylfurfanoate.^[27] Also in this case the major product was the *endo-II* diastereoisomer and furthermore a decrease of diastereoselectivity was observed when $ZnCl_2$ was employed as additive. To rationalize this result, the possible conformations of the oxyallyl framework were considered. In particular, the *endo-I* approach is favourite by the double

coordination of the oxygens to the Zn(II) cation, but in this configuration there are two aligned dipoles (red arrows in Figure 5). On the contrary, in the *endo-II* approach the dipole interaction is lower and this conformer is more favourite when 2-methyl furanoate was used (Figure 5).

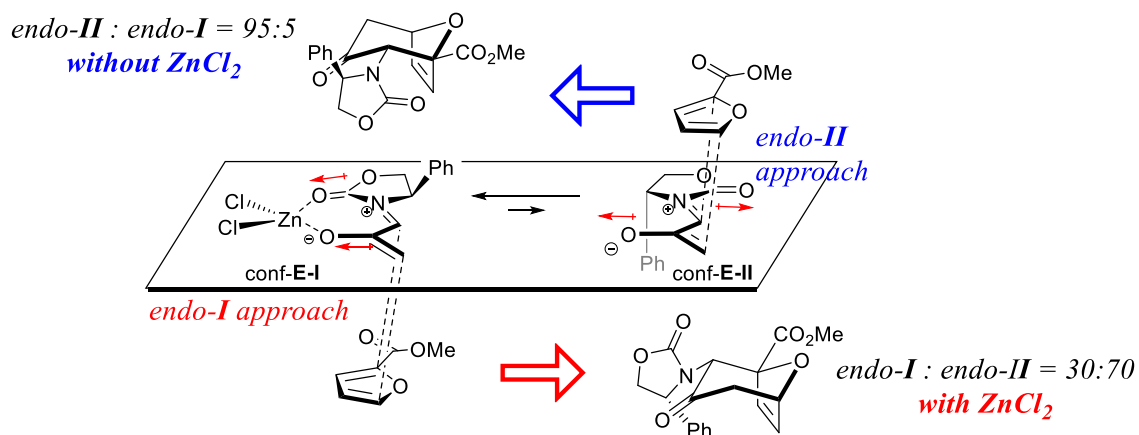


Figure 5: New proposed model for *endo-I* and *endo-II* approaches.

This new model can also justify the lower diastereoselectivity observed when ZnCl₂ was used as additive. Indeed, in the absence of the additive the conformer *conf-E-II* reacts very fast to form the *endo-II* product, but in the presence of a cation able to coordinate the oxyallyl cation, the equilibrium of the two possible conformers is heavily in favour of *conf-E-I* causing a decrease of diastereoselectivity. To prove this new model, the authors made further experiments. In particular, they performed the reaction using a large excess of ZnCl₂ (7 eq) to move the equilibrium toward the complete formation of *conf-E-I*. Under these conditions the reaction failed and only products of decomposition were obtained. This means that the conformer *conf-E-I* reacts more slowly through the *endo-I* approach than the decomposition reaction. Furthermore, when 2-cyanofuran was employed in the reaction, only the corresponding *endo-II* product was isolated (with and without the use of ZnCl₂). This can be rationalized by considering the strong dipole of cyano group which causes the preference of the transition state with less dipole interaction. Finally, in order to exclude the possible steric factor, 2-methyl furan was used in the reaction resulting only in the corresponding *endo-I* product.

These unexpected results inspired Hsung, Houk and their co-workers to shed light on the real mechanism of the [4+3] cycloaddition of allenamides with dienes through computational studies.^[28] Initially, the four possible transition-state geometries in the reaction between allenamide **33a** and furan were considered. Originally, it was supposed that the *Z* configuration was the favourite because of the increment of the diastereoselectivity for the double chelation with the ZnCl₂, but detailed studies revealed that only the *E* isomer was located as an energy minimum in the reaction.

The less stability (14 kcal mol^{-1}) shown by *Z* conformation is due to the electrostatic repulsion between the oxyallyl framework and carbonyl oxygen. For the *E* geometry, there are two concerted transition states which provide the *endo-I* and *endo-II* products (Figure 6).

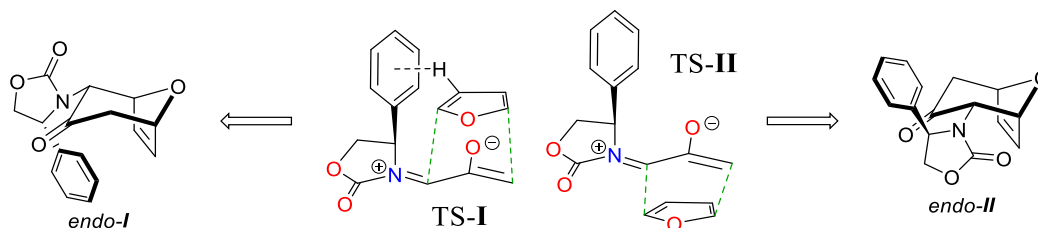


Figure 6: Transition states for *E*-geometry.

In TS-II the furan is located on the less crowded face and initially this approach was considered the favourite, but instead, for furan is easier to add to more crowded face as shown in TS-I. Indeed, there is an attractive interaction between furan and phenyl group in α position on the oxazolidinone ring respect to the nitrogen. In particular, this interaction between the hydrogen bonded to the C3 carbon and the negative cloud of the phenyl ring, makes the TS-I more favourite than the TS-II of $0.2 \text{ kcal mol}^{-1}$, which is a possible value for a diastereomeric ratio of 82:18. Also in the presence of ZnCl_2 as additive, the *E* geometry results to be more stable than the *Z* configuration of $6.2 \text{ kcal mol}^{-1}$ and it was demonstrated that the role of the ZnCl_2 in the transformation is to decrease the activation energy. With the coordination to Zn(II) cation the difference between two possible approaches is $1.1 \text{ kcal mol}^{-1}$, a reasonable value for a diastereomeric ratio of 96:4. When the 2-methyl furanoate was used as diene it was obtained the opposite stereochemistry and it can be explained by this new model. Indeed, the repulsion interaction between the phenyl ring and the methyl carbonate is higher than the attractive interaction between the hydrogen bonded to C3 and the phenyl group. For this reason the TS-II is more favourite than the TS-I and the DFT calculations revealed also that the *syn*-adduct is more stable than the *anti*-adduct of $5.9 \text{ kcal mol}^{-1}$.

However, those studies demonstrated that the regioselectivity was influenced by the presence of a phenyl group on the oxazolidinone moiety. Until then, no examples of how the regioselectivity is influenced by the substituents on the dienes were reported. In this line, Houk, Hsung and their co-workers developed an experimental and theoretical studies of the regioselectivity of the achiral allenamide **8a** toward unsymmetrical furans.^[29] The monosubstituted furans were taken in exam and methyl group was chosen as electron-donating group (EDG) and carboxylic esters as electron-withdrawing groups (EWG). Several experiments were performed under thermal conditions and in the presence of Lewis acids and it was possible to demonstrate that the regioselectivity was not influenced by the use of Lewis acid. Moreover the regioselectivity was not dependent by electronic

character of the substituents; indeed all the furans with substituent in C2 resulted in *syn*-adducts while the C3-substituted furans gave the corresponding *anti*-adducts (Figure 7).

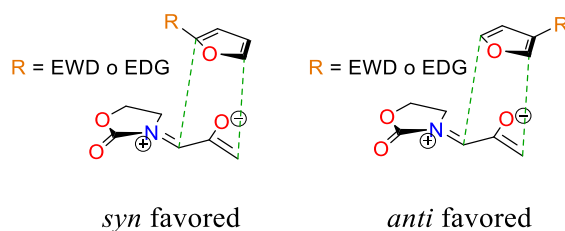


Figure 7: *syn* and *anti* approaches.

In order to develop a model to anticipate the stereochemistry of the products, it was studied the cycloaddition between chiral allenamide **33a** and differently substituted furans.^[30] Using chiral allenamides it was possible to obtain four *endo* products: *endo-I* and *endo-II* where the oxazolidinone framework and the substituent of the furans are *syn*, and *endo-I* and *endo-II* where the oxazolidinone framework and the substituent of the furans are *anti*.

The investigation started by studying the cycloaddition between the 2-substituted furans and the allenamide **33a**. Considering that the C α of the oxyallyl framework is more electrophilic and the C γ is more nucleophilic, the *syn*-adduct is expected as product when the furan has a EWG in position 2. Moreover, only the *endo-I* adduct was observed due to the CH- π interaction between the hydrogen atom on C3 of furan and the phenyl ring. On the contrary, also the regioselectivity for 2-EDG-furans is unexpectedly *syn*. Here the electronic effects cannot be considered and the regioselectivity derived only from a preference for the transition state that allows the more advanced bonding interaction. In this case, the *endo-II* adduct was isolated as only isomer when the 2-CO₂Me furan was employed as diene. As previously reported, the repulsion interaction between the ester group and the phenyl group allows the addition of diene only on the less-hindered face of oxyallyl, but when cyano group was used instead of CO₂Me, the prevailing formation of *endo-I* adduct was observed. This result can be explained because the 2-CN group is further away from the phenyl ring than the 2-CO₂Me group and therefore the repulsion interaction is absent. All the 3-substituted furans employed for the reaction with allenamide **33a**, resulted in the corresponding *anti-I* adducts (Figure 8).

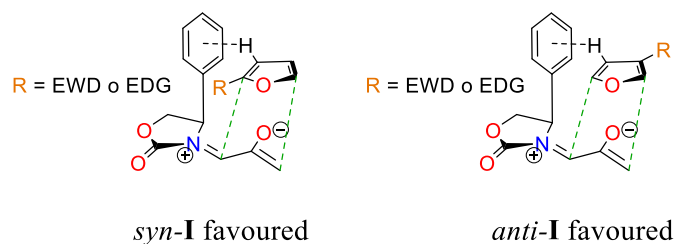
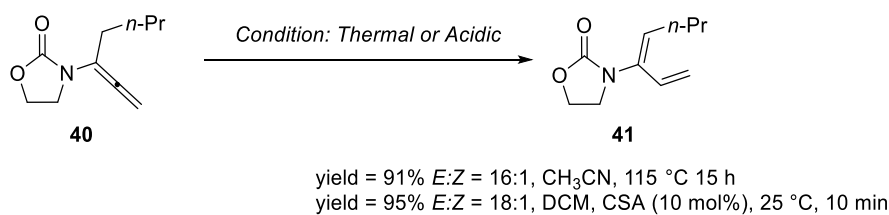


Figure 8: Favoured approaches for 2- and 3-substituted furans.

In conclusion, the 3-substituted furans resulted in the corresponding *anti-I* adducts regardless the electronic character of the substituent, while when the 2-substituted furans were employed, it was possible to isolate only the *syn-I* adduct except for the 2-CO₂Me furan which led to the formation of *syn-II* adduct due to its repulsion interaction with the phenyl ring. Subsequently, unsymmetrical disubstituted furans were employed for the reaction in order to explore the generality of the stereo- and regiochemical control.^[31] Several 2-EWG-3-EDG furans as well as 2-EDG-3-EWG furans were used in the screening and finally it is possible to conclude that the 2-substituted furans promote the formation of *syn-I* adducts except: 1) the C2 substituent is the COOR group, or 2) there is another substituent in 3-position because in these cases the predominant product is the *syn-II* adduct. The regio- or the stereochemical control of the process was not influenced by the electronic character of the substituents.

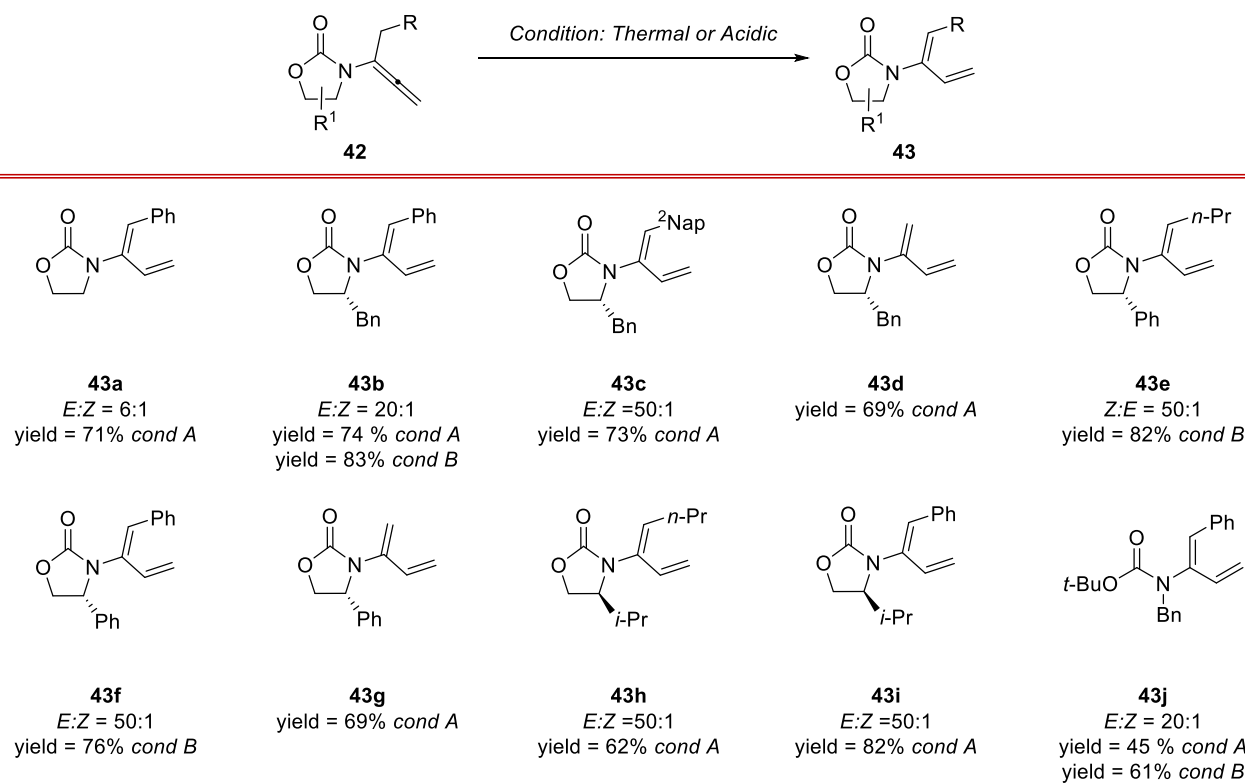
2.2 Isomerization Reaction

Another type of cyclization where the allenamides have been involved is the 6π -ring closure. In particular, to develop this new type of reactivity, a previous isomerization reaction of the allene framework to form a diene was necessary. In this line, Hsung and co-workers in 2009 developed a regio- and stereoselective isomerization of allenamides.^[32] In particular, they submitted the allenamide **40** under several thermal conditions and good to excellent yields were achieved in the formation of desired diene **41**. The success of the reaction didn't request strictly high temperature; indeed in the presence of camphorsulfonic acid (CSA) it was possible to obtain the desired product in 95% yield in DCM under very mild reaction conditions (Scheme 20).



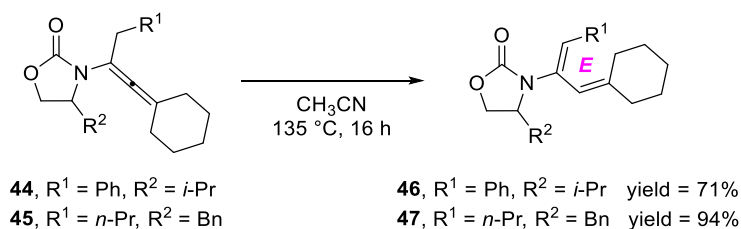
Scheme 20: Regio- and stereoselective isomerization of allenamide **40**.

The predominant formation of the *E* isomer was unambiguously determined through single-crystal X-ray analysis. The isomers *E* were also obtained when several α -derivated allenamides have been submitted under thermal (*cond A*) and acidic (*cond B*) reaction conditions and all the corresponding products were isolated in good to excellent yields (Scheme 21).



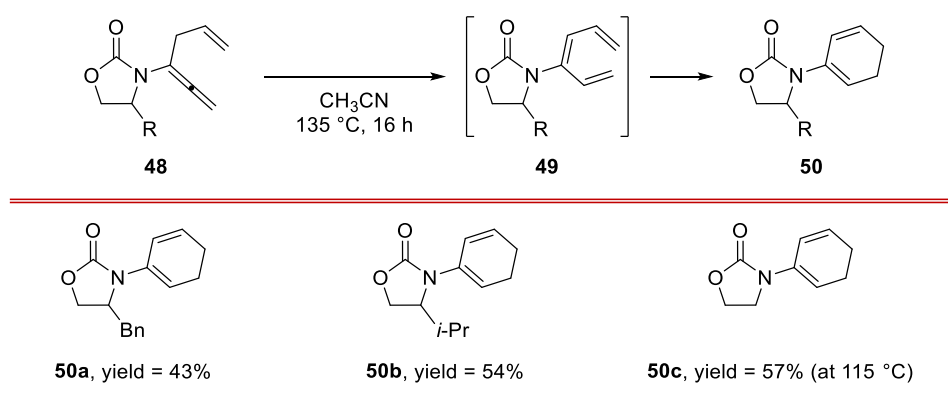
Scheme 21: Scope of the isomerization of allenamides.

The isomerization reaction demonstrated to be not limited in the use of α -derivated allenamides but also γ -derivated allenamides proved to be suitable substrates for the formation of 1-amido-dienes exclusively as *E*-isomers. High yields were achieved when several γ -allenamides were submitted under acidic conditions but to obtain satisfactory yields under thermal condition, higher temperatures and/or longer reaction times were necessary. This finding suggested to the authors to develop a regioselective thermal isomerization of α - γ -disubstituted allenamides at 135 °C in acetonitrile. Gratefully, only the desired 2-amino-dienes were obtained in good yields (Scheme 22).



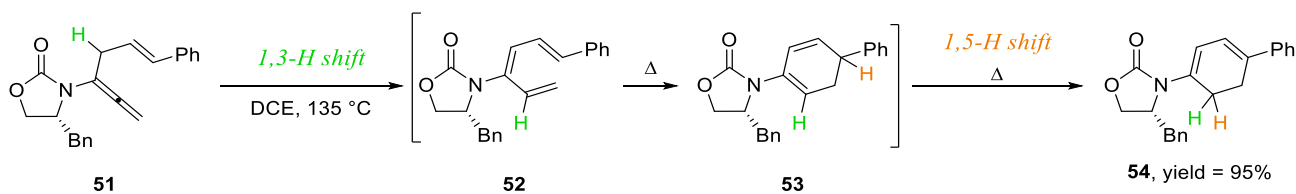
Scheme 22: Regioselective thermal isomerization of allenamides.

The title transformation resulted to be an efficient way to synthesize dienes which are largely employed in pericyclic reactions. In particular, the authors reported a 6 π -ring-closure tandem reaction of allenamides obtaining the cyclic-2-amido-dienes in good yields (Scheme 23).



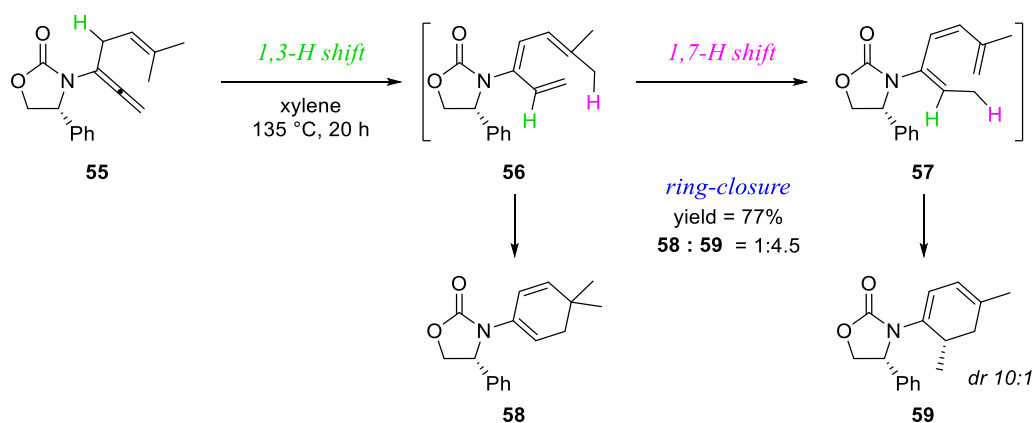
Scheme 23: 6 π -ring-closure tandem reaction of allenamides.

Subsequently, the authors observed that, heating the chiral allenamide **51** in DCE at 135 °C, the triene **54** has been formed as product instead of the expected cyclodiene **53** (Scheme 24).^[33]



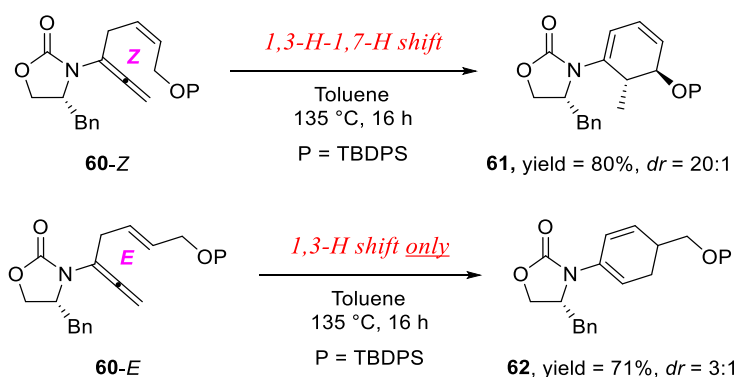
Scheme 24: Unexpected 1,5-H shift.

The 1,5-H shift necessary to form the final product **54** was also observed using the triene **52** (obtained by acidic treatment of allenamide **51**) resulting in the corresponding cyclodiene in comparative yield. In order to prevent the 1,5-H shift, the phenyl group was replaced with two methyl groups, but also in this case a second unexpected result was observed. Indeed, a mixture of two products were obtained: the desired 2-amido-diene and the unexpected product delivered from 1,7-H shift reaction of the triene intermediate and consequent ring closure reaction (Scheme 25).



Scheme 25: Unexpected 1,7-H shift.

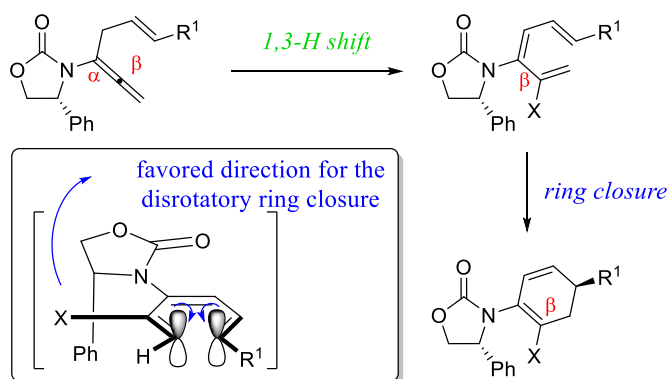
Comparative results in term of yield and ratio of two products were achieved when the triene was isolated and used as starting material. The stereochemistry of the product **59**, unambiguously determined by single-crystal X-ray analysis, proved that the ring closure reaction proceeds through a favourite disrotatory route due to a 1,6-induction. Several amido trienes were submitted under thermal conditions and in all of the cases the products delivered by tandem 1,3-H-1,7-H shift resulted to be the major products. Through further investigations, it was demonstrated that the 1,7-H shift was discouraged using allenamide bearing two methyl groups in γ position of the allene framework. Moreover, it was also demonstrated that the 1,7-H shift depended to the olefinic geometry. In particular, while the 1,3-H-1,7-H shift occurred using **60-Z**, the 1,7-H shift was completely dropped using the corresponding *E* isomer (Scheme 26).



Scheme 26: Dependence of the 1,7-H shift to the olefin geometry.

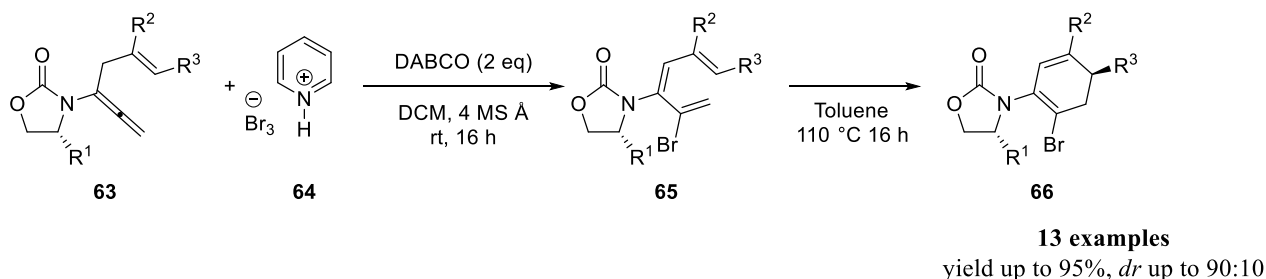
The low 1,6-induction achieved in the formation of the previous product (*dr* 3:1), suggested to the authors to develop a more efficient procedure to increase the stereoselection in the 6π -electron ring closure step.^[34] They considered the possible transition state of the 1,3,5-hexatriene for the ring closure step: the presence of a large substituent in C2 position of the amidotriene could improve the

stereoselection of the title step due to the bigger steric hindrance than the hydrogen atom (Scheme 27).



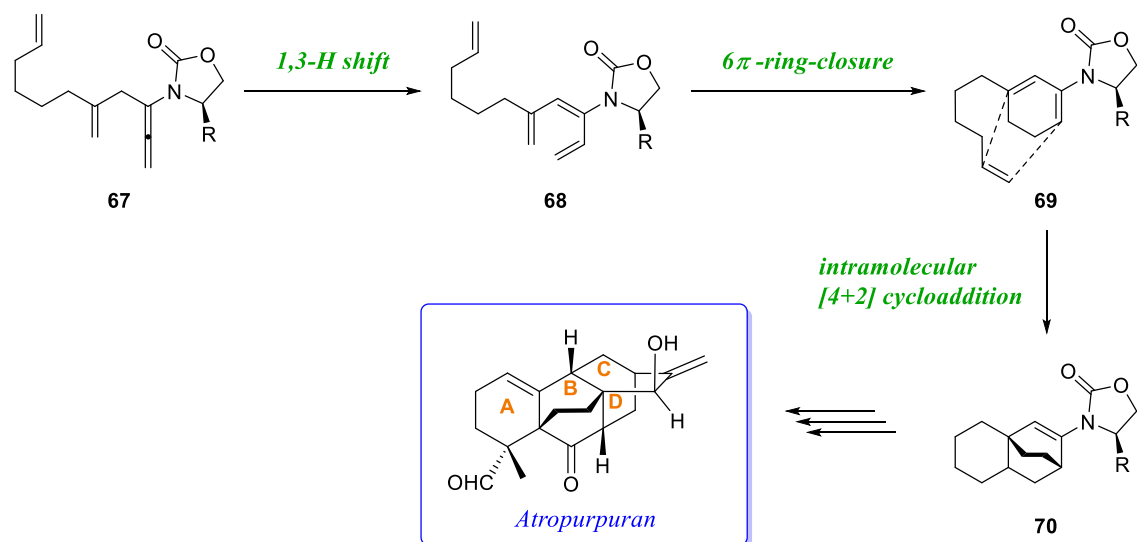
Scheme 27: Possible transition state of the triene for the ring closure step.

As functionalization of the C2 of the aminotriene (which corresponds of the β carbon of the allene framework), was chosen a bromine atom added through electrophilic halogenation with pyridinium tribromide salt. Several chiral allenamides were submitted under optimized bromination conditions resulting in the corresponding products in good to excellent yields. Subsequently, the bromo-amidotrienes were tested in the stereoselective electrocyclicization furnishing the desired cyclodienes in good yields and good diastereoisomeric ratio (Scheme 28).



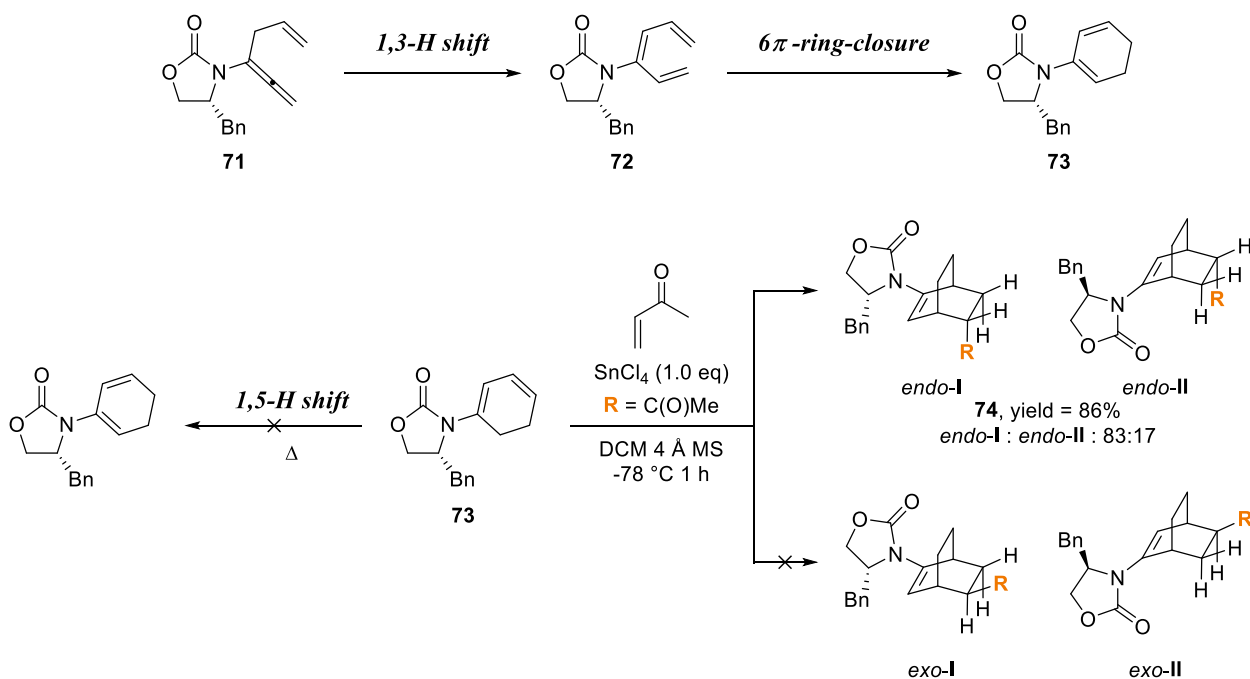
Scheme 28: Stereoselective electrocyclicization of the bromo-amidotrienes.

A useful application for the methodology have been demonstrated by Hsung and co-workers^[35] when, in 2012, they developed a tandem 1,3-H-shift-6 π -electrocyclization followed by an intramolecular Diels-Alder cycloaddition reaction in order to synthesize the BCD-ring of Atropurpuran^[36–38] which is an important compound due to its medicinal properties (Scheme 29).^[39]



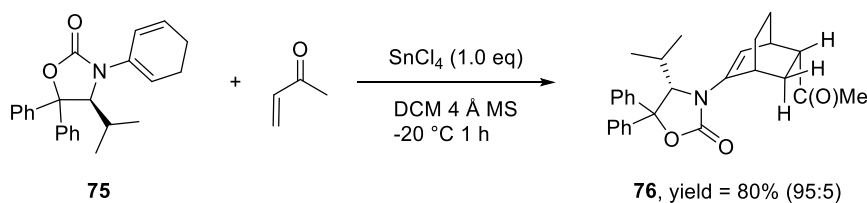
Scheme 29: Application of the tandem 1,3-H-shift-6 π -electrocyclization-Diels-Alder reaction in the synthesis of the BCD-ring of the Atropurpuran.

In the same line, Hsung developed a highly stereoselective variant of the Diels-Alder cycloaddition between the 2-amidodienes derived from allenamides and enones.^[40] The first challenge for the authors was to avoid the competitive 1,5-H shift of the 2-amidocyclodiene. They chose the condensation between the cyclic diene derived from chiral allenamide **71** with methyl vinyl ketone as model reaction. After several experiments, the SnCl₄ has been evaluated as best promoting agent providing only the *endo*-cycloadduct in good yield and good diastereoisomeric ratio (Scheme 30).



Scheme 30: Stereoselective Diels-Alder reaction using SnCl₄ as additive to suppress the 1,5-H shift.

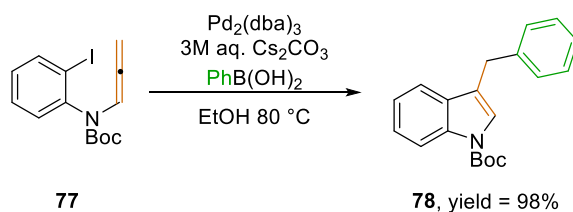
The stereoselectivity of the process was improved when the chiral 2-oxazolidinone was replaced with other chiral amides as auxiliaries. In particular, diastereoisomeric ratio up to 95:5 was achieved using the allenamide **75**, as shown in Scheme 31.



Scheme 31: Highly stereoselective Diels-Alder reaction of allenamide **76**.

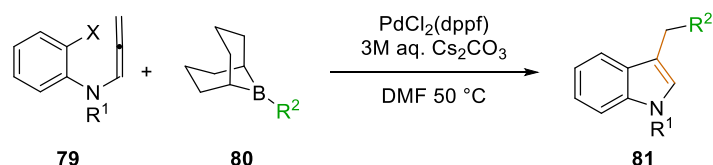
2.3 Palladium-Catalysed Cascade Reaction

Another field where recently the allenamides found interesting applications is the palladium-catalysed cascade reaction. For example, in 2007 Fuwa and Sasaki^[41] reported a facile and useful strategy to synthesize 2,3-disubstituted indoles starting from *N*-(*o*-halophenyl) allenamides. In particular, using allenamide **77** in the presence of the phenylboronic acid they were able to find the optimal catalytic conditions to obtain the indole **78** in excellent yield (Scheme 32).



Scheme 32: Palladium-catalysed cascade reaction for the synthesis of 2-substituted indoles.

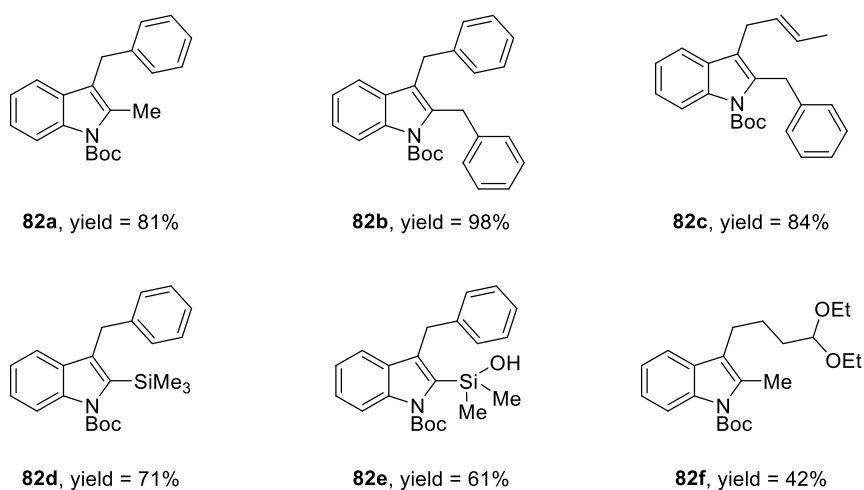
Mechanistically, the palladium(0) underwent the initial oxidative addition of the aryl iodide followed by the formation of π -allylpalladium intermediate *via* carbopalladation. The latter compound has been trapped by the phenyl boronic acid providing the desired 3-benzylic indole. Several aryl boronic acids were employed in the reaction with allenamide **77** promoted by $\text{Pd}_2(\text{dba})_3$ and the corresponding products were isolated in good yields. Unfortunately, not satisfactory results were achieved when alkylboranes were employed in the reaction instead of the aryl boronic acids. Therefore the authors found new reaction conditions for the use of alkylboranes (Scheme 33).



Scheme 33: Optimized reaction conditions in the use of alkylboranes.

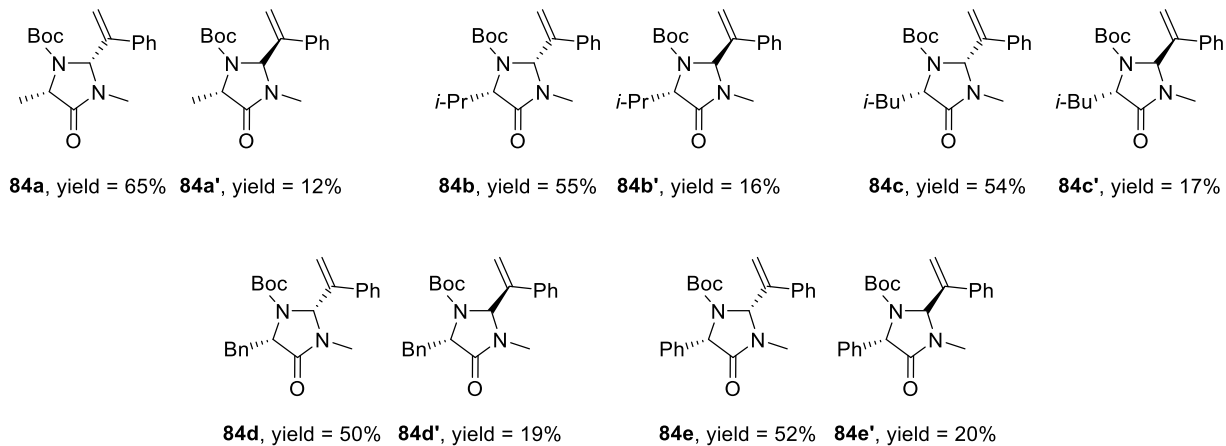
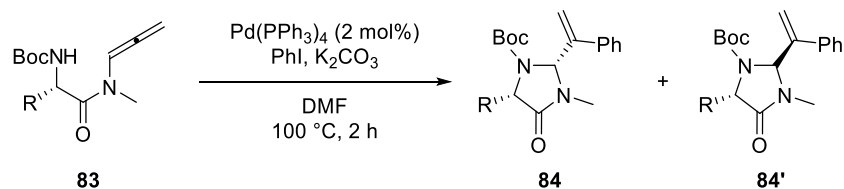
Finally, with the optimized catalytic conditions in their hands, also different alkylboranes were submitted in the reaction with allenamide **79** resulting in the desired products in good yields.

In order to extend the methodology and to synthesize 2,3-disubstituted indoles, the reaction was performed using α -substituted allenamides (Scheme 34).



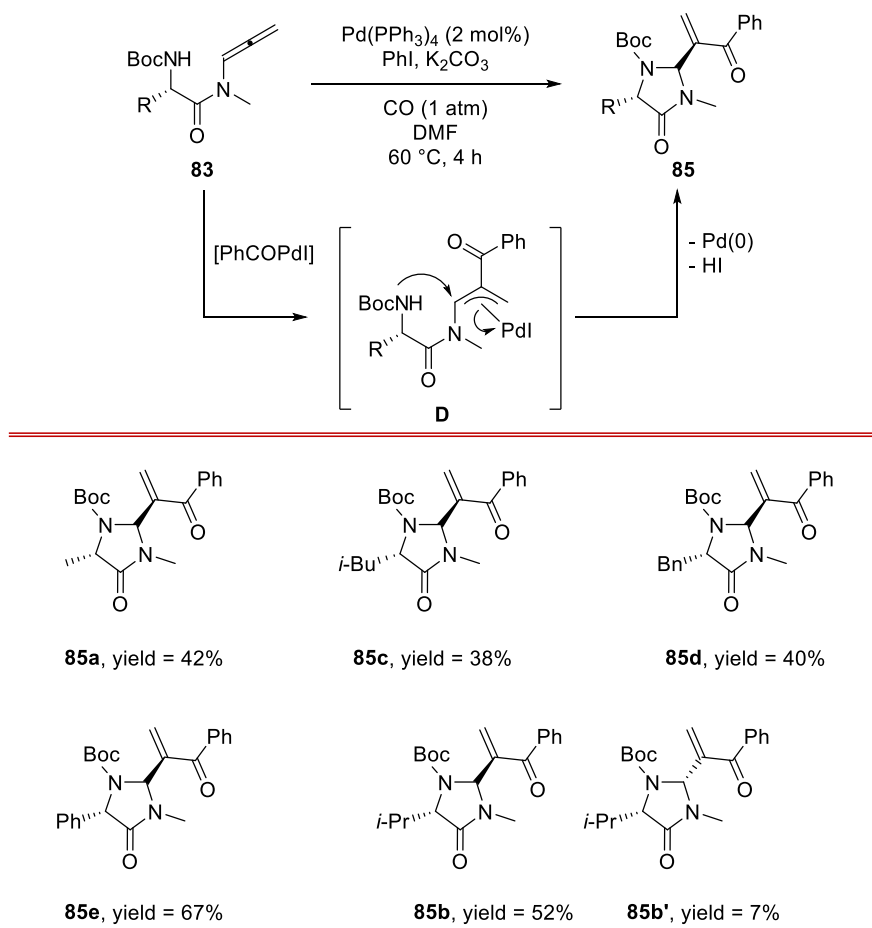
Scheme 34: Synthesis of 2,3-disubstituted indoles *via* Pd-catalysed-cascade reaction.

In the same line, Broggini and co-workers reported an efficient procedure for the synthesis of enantiopure imidazolidinones from α -amino allenamides.^[42] Several chiral allenamides were prepared from the corresponding *L*- α -aminoacids in excellent yields and subsequently, they were submitted under optimized heterocyclization reaction conditions. The desired compounds have been isolated in good yields and the absolute configuration was determined by X-ray single crystal analysis (Scheme 35).



Scheme 35: Synthesis of enantiopure imidazolidinones from α -amino allenamides.

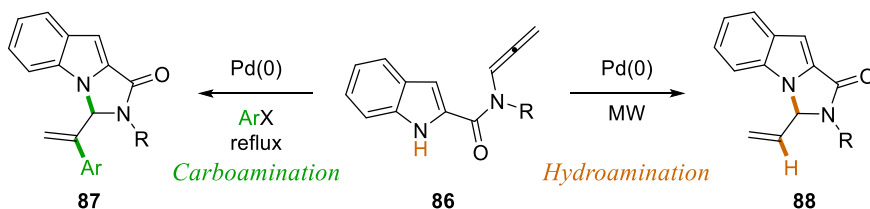
In order to extend the methodology, 2-enoyl imidazolidinones were obtained through a palladium-catalysed carbonylative cyclization of corresponding allenamides making the reaction under CO atmosphere. Mechanistically, the carbometallation reaction, that the allenamide undergoes to form the π -allyl complex **D**, has been preceded by insertion of carbon monoxide on the initially generated PhPdI complex. The corresponding imidazolidinones have been isolated in moderate yields and only in *trans*-configuration (except for the product **85b** which has been isolated in 6:1 diastereoisomer ratio) (Scheme 36).



Scheme 36: Optimized reaction conditions for the Pd-catalysed carbonylative cyclization.

It is noteworthy that the products present the vinyl group as substituent which is a powerful building block for further functionalizations.

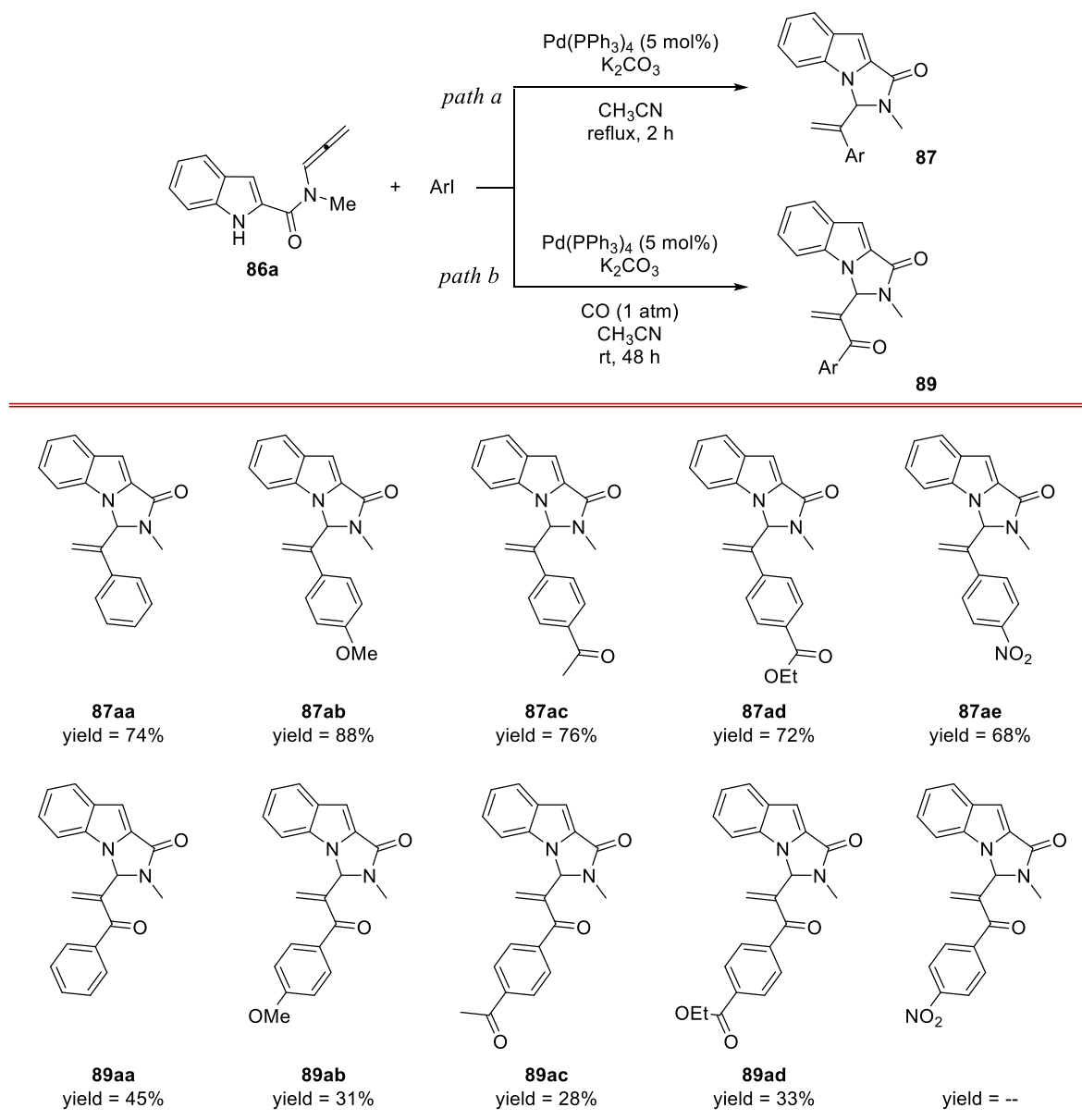
In line with their interest in intramolecular palladium-catalysed procedure, Brogini and co-workers developed a Pd-catalysed carboamination and a Pd-catalysed hydroamination from indole bearing the allenamide moiety (Scheme 37).^[43]



Scheme 37: Pd-catalysed carboamination and hydroamination from indoles bearing allenamide moiety.

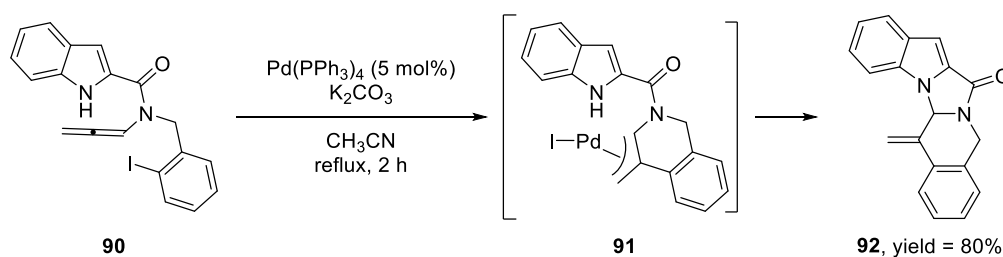
They started to prepare the allenamide **86a** from the indole-2-carboxylic acid and then they submitted the title allenamide in a reaction with different aryl iodides in the presence of $\text{Pd}(\text{PPh}_3)_4$. The corresponding products were isolated in good yields after 2 hours. In order to develop also the

carbonylative amination they repeated the reactions under the same conditions but using a CO atmosphere. Not satisfactory results were obtained in the formation of the corresponding products, but the yields have been improved by performing the reactions at room temperature and for a prolonged time (Scheme 38).



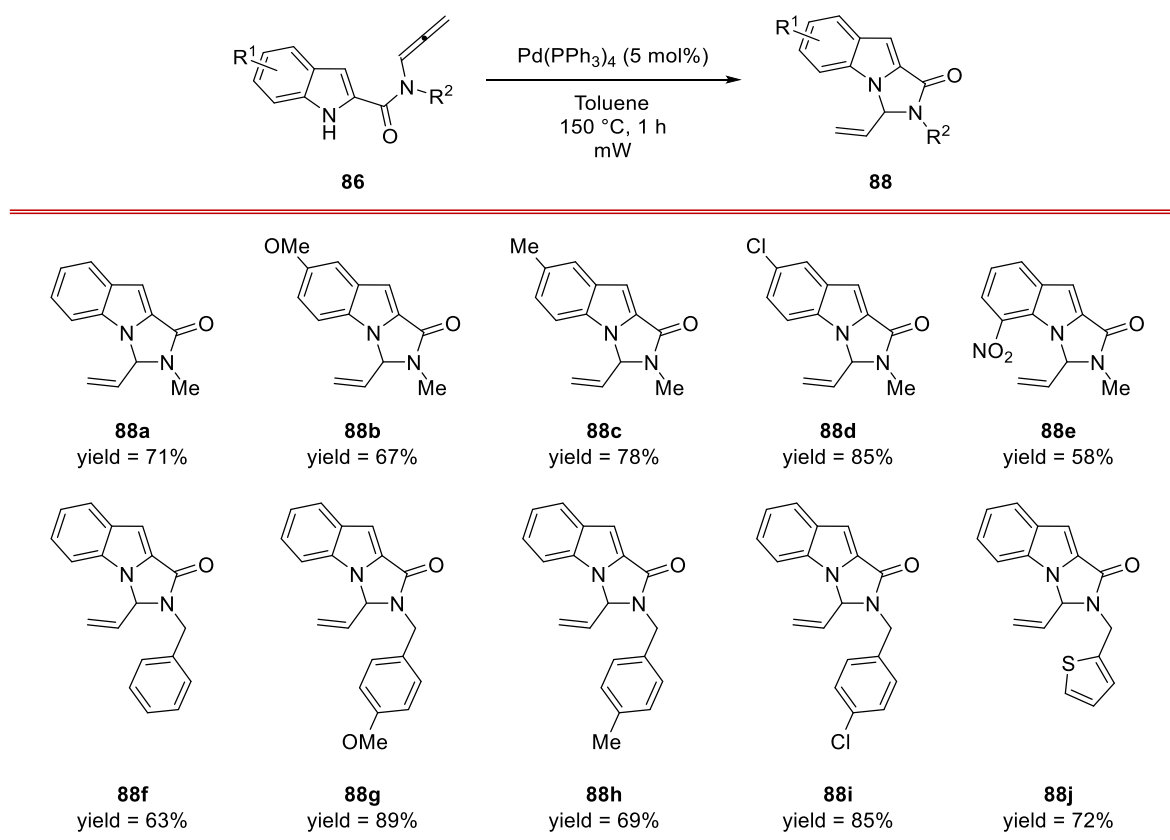
Scheme 38: Optimized reaction conditions for carboamination and carbonylative amination of allenamides.

Finally, it was also developed a totally intramolecular variant of the carboamination reaction and the authors were able to isolate the desired pentacyclic imidazolinone in high yield (Scheme 39).



Scheme 39: Intramolecular carboamination of allenamide **90**.

The hydroamination reaction is a facile way to prepare nitrogen-containing heterocycles with an unsubstituted vinyl pendant which is a powerful building block for further transformations. The authors were able to find that the allenamide **86a** under microwave activation provided the corresponding product in good yield in the presence of the $\text{Pd(PPh}_3)_4$ as catalyst. Subsequently, differently substituted indoles bearing allenamide moiety were submitted under optimized reaction conditions furnishing all the products in good yields (Scheme 40).



Scheme 40: Optimized reaction conditions for hydroamination protocol.

Through deuterium-labelled experiments it was proposed a reaction mechanism: initially, the Pd(0) -catalyst reacts with the indole to generate the Pd(II) -hydride complex **E**, which in turn undergoes the insertion of the allenene framework into the Pd-H bond. The π -allyl- Pd(II) complex **F** provides the

final product through the intramolecular formation of the new C-N bond and subsequent reductive elimination of a Pd(0) specie (Figure 9).

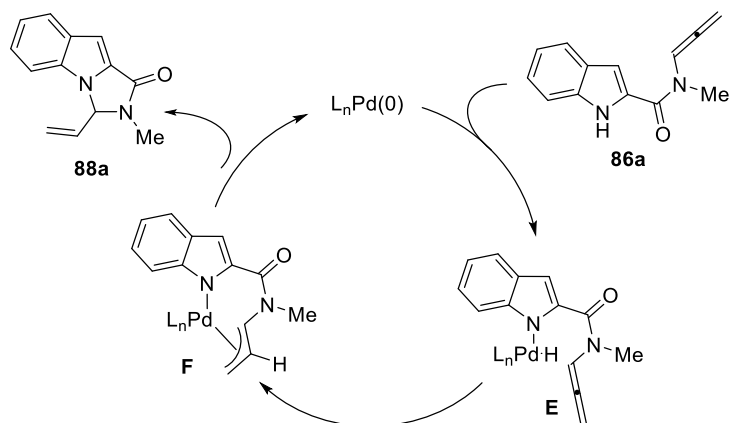


Figure 9: Proposed reaction mechanism.

2.4 Electrophilic Activation

The allenamides can undergo an electrophilic activation promoted by soft-metals (for example gold-based catalysts) or Brønsted acids resulting in a positively charged intermediate (**G** and **H**, Figure 10). After the electrophilic activation, the *in situ* formed intermediates show two electrophilic positions, the α -position which will result in a linear product and the γ -position which will result in the branched one.

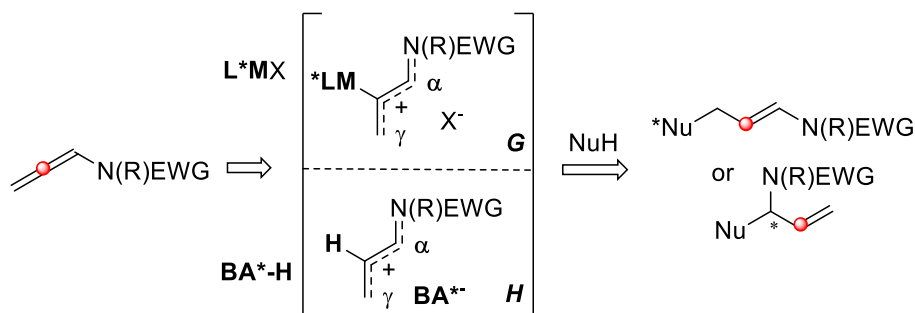
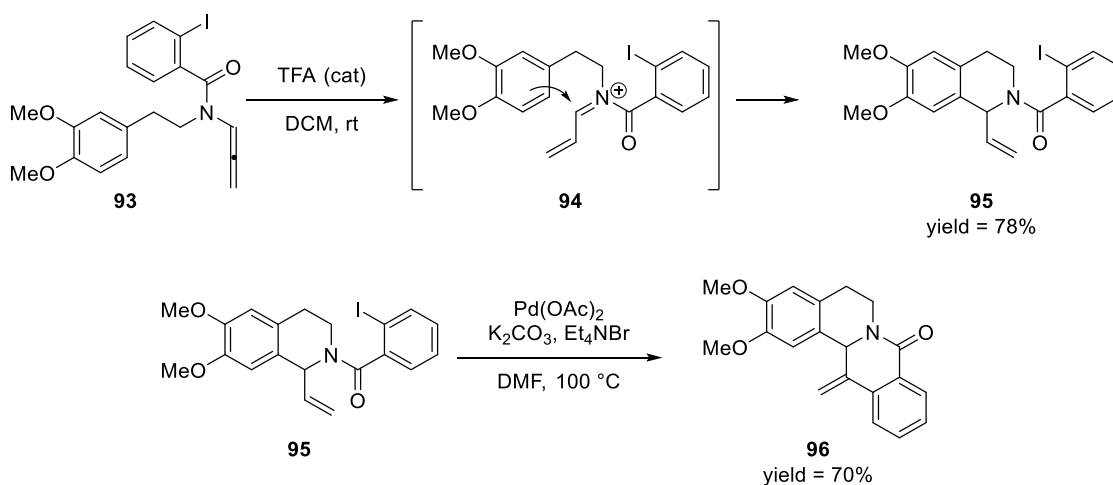


Figure 10: Electrophilic activation of allenamides.

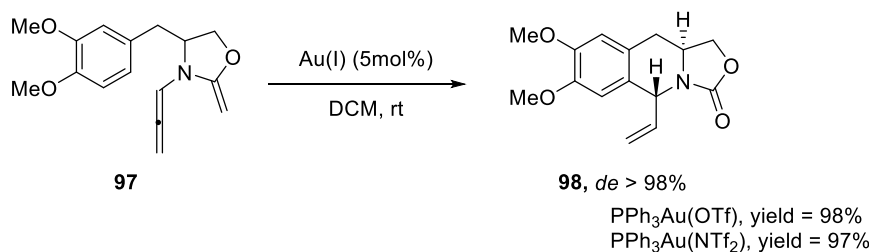
Already in 2007 it was hypothesized the formation of an acyliminium ion by treatment of an allenamide with a Brønsted acid. As matter of facts, Navarro-Vázquez and co-workers^[44] reported a new synthesis of functionalized protoberberines through cyclization of intermediate acyliminium ion promoted by TFA. In particular, the primary formation of intermediate acyliminium resulted

from electrophilic activation of allenamide by TFA, was followed by intramolecular electrophilic aromatic substitution on the electron-rich arene (Scheme 41).



Scheme 41: Synthesis of functionalized protoberberines.

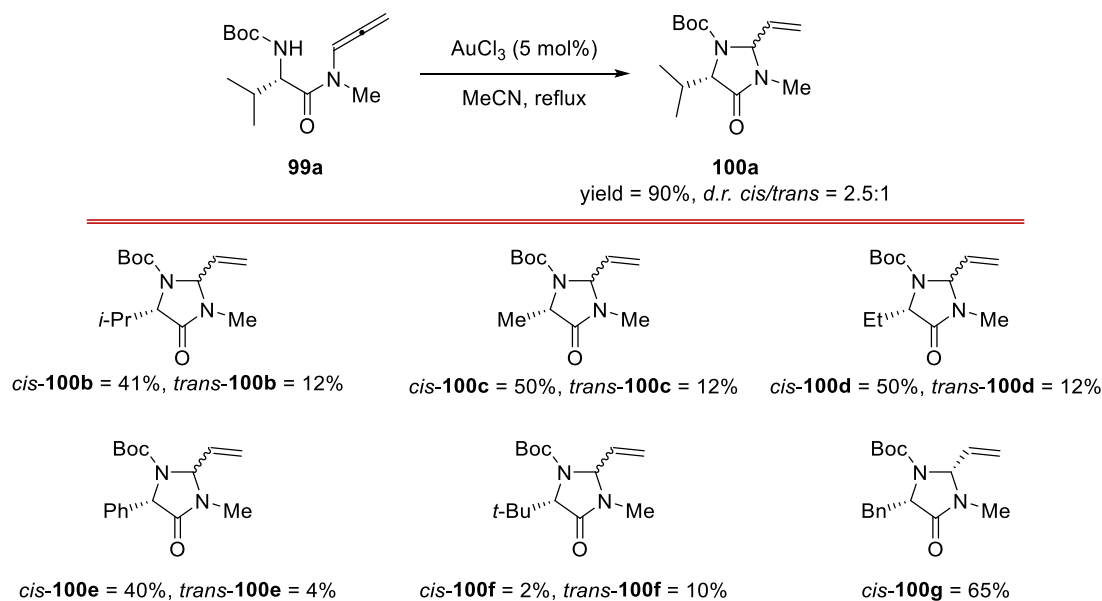
A evidence that the allenamides can also undergo electrophilic activation by transition metal is reported by Kimber and co-worker in 2012^[45] when they reported a procedure to prepare α -vinyl tetrahydroisoquinolines using allenamides as substrate and gold(I) catalyst as promoting agent (Scheme 42).



Scheme 42: Preparation of tetrahydroisoquinolines promoted by Au(I) catalysts.

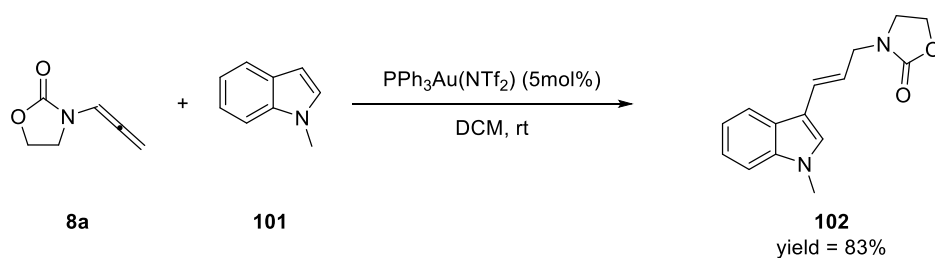
Excellent yields were achieved when gold(I) catalysts $\text{PPh}_3\text{Au(OTf)}$ and $\text{PPh}_3\text{Au(NTf}_2)$ were employed in the process. Further analysis demonstrated high selectivity in the transformation giving the diastereoisomeric excess up to 98%.

Inspired by previously heterocyclization of α -amino allenamides under base-promoted^[46] and palladium^[42] catalysed conditions, Manzo and Brogini^[47] envisioned the possibility to use gold salts to promote a gold-catalysed intramolecular hydroamination of allenamides (Scheme 43). They were able to obtain the desired differently substituted 4-imidazolidinones in good yields. Moreover, the vinyl group in position 2 plays an important role for further functionalizations.



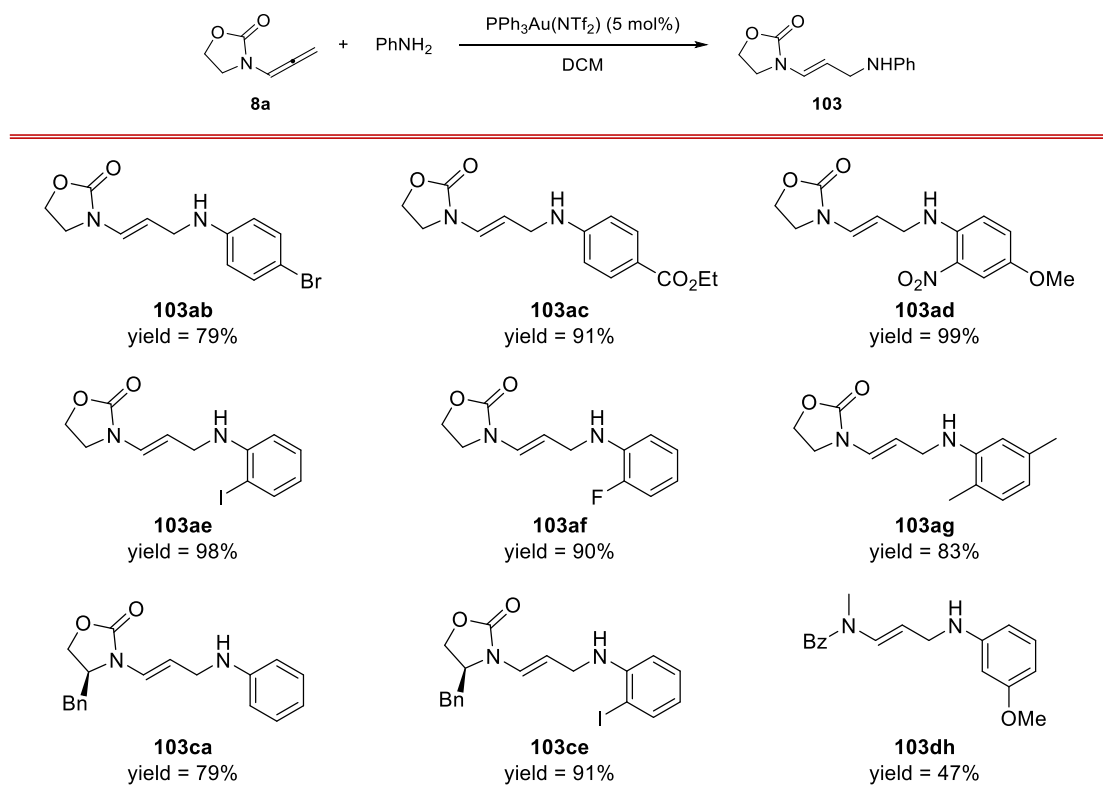
Scheme 43: Au-catalysed intramolecular hydroaminations.

The electrophilic activation of allenamides by gold salts until 2010 was principally used in intramolecular reactions with consequent formation of a cycle. Kimber and co-workers developed the first intermolecular gold-catalysed addition to allenamides promoted by gold(I)-catalysts. In this way it was developed a facile and mild synthesis of enamides.^[48] Using the electron-rich aromatics as nucleophiles through a Friedel-Crafts-type reaction, he was able to prepare numerous enamides differently substituted with high regioselectivity toward the terminal carbon of the allenamides (Scheme 44).



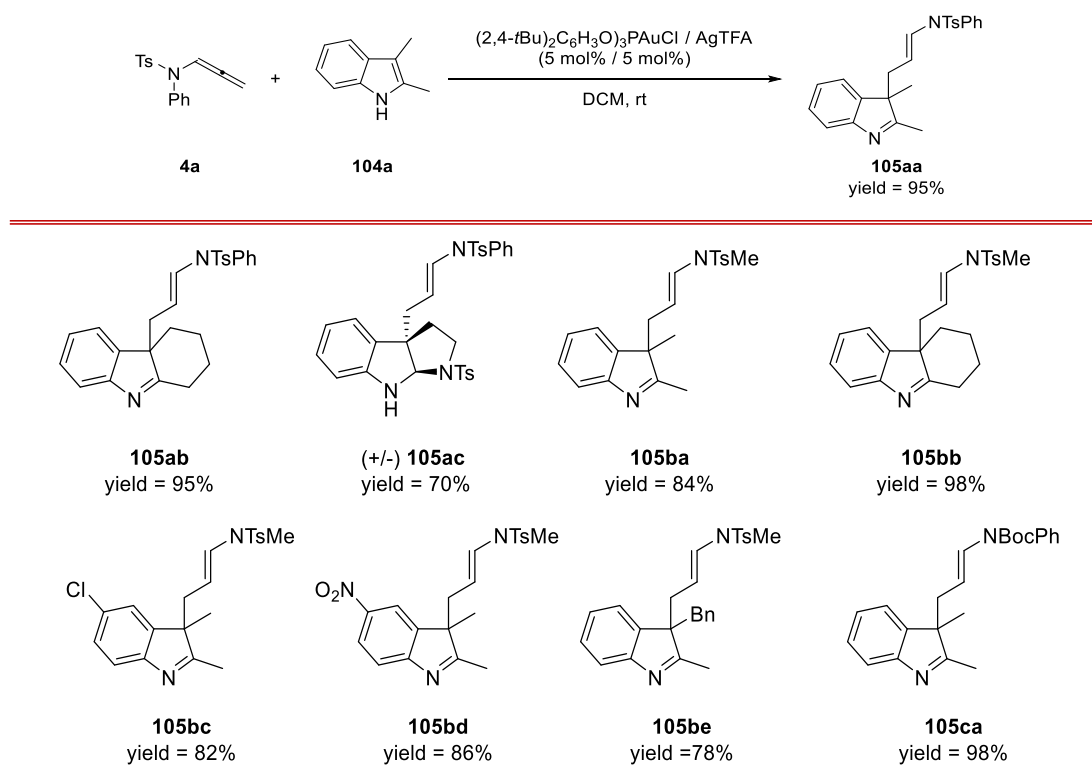
Scheme 44: First intermolecular gold-catalysed addition to allenamide.

Inspired by these satisfactory results in the intermolecular hydroarylation of allenamides, subsequently he developed an intermolecular hydroaminations of allenamides with arylamines.^[49] The products of this reaction were allylamino enamides which result to be important building blocks in organic synthesis and often present in biological systems (Scheme 45). All the allylamines in this protocol were obtained in good to excellent yields and in all of the cases the configuration of the C–C double bond was *E*.



Scheme 45: Au-catalysed hydroamination of allenamides with arylamines.

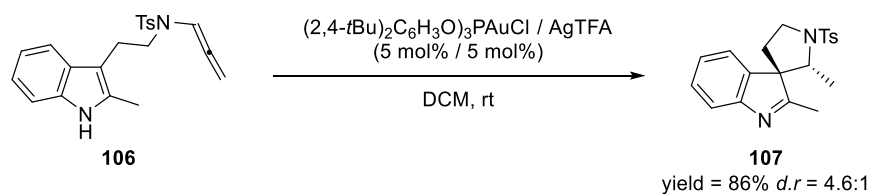
In this line, the interest of Bandini and co-workers in gold(I)-catalysed manipulation of π -system^[50-53], resulted in 2014 into the development of the gold(I)-dearomatization of 2,3-disubstituted indoles with allenamides in order to synthesize indolenine cores that are common motifs in countless naturally occurring compounds.^[54] Several *N*-tosylallenamides as well as *N*-Boc- (Boc = *tert*-butoxycarbonyl) and *N*-oxazolylallenamides with aromatic and aliphatic substituent bonded to the *N* of the allenamides were submitted under optimized reaction conditions resulting in the corresponding products in good to excellent yields (Scheme 46).



Scheme 46: Au-catalysed de-aromatization of indoles with allenamides.

The role of the counterion^[55,56] of the gold(I) catalyst was investigated; in particular, weakly coordinating anion gave high conversion but modest regioselectivity while more coordinating species depressed the reaction rates but increased the regioselectivity toward the C3 site. The optimal compromise has been achieved using trifluoroacetic anion as the counterion.

Finally, it was also synthesized the 5-membered spiroindolenine **107** in 86% yield through an intramolecular de-aromatization of indole core with allenamide with complete *5-exo-trig* regiochemistry on the α -position of allenamide (Scheme 47).



Scheme 47: Synthesis of the spiroindolenine **107**.

In conclusion, the examples reported above demonstrated the large flexibility of the allenamides in organic synthesis.

The first part of this thesis has the aim the development of new enantioselective methodologies involving allenamides and their electrophilic activation.

Bibliography

- [1] K. M. Brummond, J. L. Kent, *Tetrahedron* **2000**, *56*, 3263–3283.
- [2] S. Ma, *Chem. Rev.* **2005**, *105*, 2829–2872.
- [3] F. López, J. L. Mascareñas, *Chem. Soc. Rev.* **2014**, *43*, 2904–2915.
- [4] L.-L. Wei, H. Xiong, R. P. Hsung, *Acc. Chem. Res.* **2003**, *36*, 773–782.
- [5] T. Lu, Z. Lu, Z.-X. Ma, Y. Zhang, R. P. Hsung, *Chem. Rev.* **2013**, *113*, 4862–4904.
- [6] E. Manoni, M. Bandini, *Eur. J. Org. Chem.* **2016**, 3135–3142.
- [7] W. B. Dickinson, P. C. Lang, *Tetrahedron Lett.* **1967**, *8*, 3035–3040.
- [8] L. L. Wei, H. Xiong, C. J. Douglas, R. P. Hsung, *Tetrahedron Lett.* **1999**, *40*, 6903–6907.
- [9] L.-L. Wei, R. P. Hsung, H. Xiong, J. a. Mulder, N. T. Nkansah, *Org. Lett.* **1999**, *1*, 2145–2148.
- [10] Z. Song, R. P. Hsung, T. Lu, A. G. Lohse, *J. Org. Chem.* **2007**, *72*, 9722–9731.
- [11] I. Alonso, B. Trillo, F. López, S. Montserrat, G. Ujaque, L. Castedo, A. Lledós, J. L. Mascareñas, *J. Am. Chem. Soc.* **2009**, *131*, 13020–13030.
- [12] P. Mauleón, R. M. Zeldin, A. Z. González, F. D. Toste, *J. Am. Chem. Soc.* **2009**, *131*, 6348–6349.
- [13] D. Benitez, E. Tkatchouk, A. Z. Gonzalez, W. a Goddard, F. D. Toste, *Org. Lett.* **2009**, *11*, 4798–4801.
- [14] A. Z. Gonza, F. D. Toste, *Org. Lett.* **2010**, *12*, 200–203.
- [15] M. Alcarazo, T. Stork, A. Anoop, W. Thiel, A. Fürstner, *Angew. Chem. Int. Ed.* **2010**, *49*, 2542–2546.
- [16] H. Faustino, F. López, L. Castedo, J. L. Mascareñas, *Chem. Sci.* **2011**, *2*, 633.
- [17] S. Montserrat, H. Faustino, A. Lledós, J. L. Mascareñas, F. López, G. Ujaque, *Chem. Eur. J.* **2013**, *19*, 15248–15260.

- [18] H. Faustino, P. Bernal, L. Castedo, F. López, J. L. Mascareñas, *Adv. Synth. Catal.* **2012**, *354*, 1658–1664.
- [19] S. Suárez-Pantiga, C. Hernández-Díaz, M. Piedrafita, E. Rubio, J. M. González, *Adv. Synth. Catal.* **2012**, *354*, 1651–1657.
- [20] S. Suárez-Pantiga, C. Hernández-Díaz, E. Rubio, J. M. González, *Angew. Chem. Int. Ed.* **2012**, *51*, 11552–11555.
- [21] K. W. Quasdorf, L. E. Overman, *Nature* **2014**, *516*, 181–191.
- [22] J. Francos, F. Grande-Carmona, H. Faustino, J. Iglesias-Sigüenza, E. Díez, I. Alonso, R. Fernández, J. M. Lassaletta, F. López, J. L. Mascareñas, *J. Am. Chem. Soc.* **2012**, *134*, 14322–14325.
- [23] S. Handa, L. M. Slaughter, *Angew. Chem. Int. Ed.* **2012**, *51*, 2912–2915.
- [24] H. S. Cycloadditions, H. Xiong, R. P. Hsung, C. R. Berry, C. Rameshkumar, *J. Am. Chem. Soc.* **2001**, *123*, 7174–7175.
- [25] J. Huang, R. P. Hsung, *J. Am. Chem. Soc.* **2005**, *127*, 50–51.
- [26] J. E. Antoline, R. P. Hsung, J. Huang, Z. Song, G. Li, *Org. Lett.* **2007**, *9*, 1275–1278.
- [27] J. E. Antoline, R. P. Hsung, *Synlett* **2008**, *5*, 739–744.
- [28] E. H. Krenske, K. N. Houk, A. G. Lohse, E. Antoline, R. P. Hsung, *Chem. Sci.* **2010**, *1*, 387–392.
- [29] A. G. Lohse, E. H. Krenske, J. E. Antoline, K. N. Houk, R. P. Hsung, *Org. Lett.* **2010**, *12*, 5506–5509.
- [30] J. E. Antoline, E. H. Krenske, A. G. Lohse, K. N. Houk, R. P. Hsung, *J. Am. Chem. Soc.* **2011**, *133*, 14443–14451.
- [31] Y. Du, E. H. Krenske, J. E. Antoline, A. G. Lohse, K. N. Houk, R. P. Hsung, *J. Org. Chem.* **2013**, *78*, 1753–1759.
- [32] R. Hayashi, R. P. Hsung, J. B. Feltenberger, A. G. Lohse, *Org. Lett.* **2009**, *11*, 2125–2128.

- [33] R. Hayashi, J. B. Feltenberger, R. P. Hsung, *Org. Lett.* **2010**, *12*, 1152–1155.
- [34] R. Hayashi, M. C. Walton, R. P. Hsung, J. H. Schwab, X. Yu, *Org. Lett.* **2010**, *12*, 5768–5771.
- [35] R. Hayashi, Z.-X. Ma, R. P. Hsung, *Org. Lett.* **2012**, *14*, 252–255.
- [36] S. W. Pelletier, A.-M. M. Ateya, J. Finer-Moore, N. V. Mody, L. C. Schramm, *J. Nat. Prod.* **1982**, *45*, 779–781.
- [37] C.-H. Yang, X.-C. Wang, Q.-F. Tang, W.-Y. Liu, J.-H. Liu, *Helv. Chim. Acta* **2008**, *91*, 759–765.
- [38] P. Tang, Q.-H. Chen, F.-P. Wang, *Tetrahedron Lett.* **2009**, *50*, 460–462.
- [39] T. Suzuki, A. Sasaki, N. Egashira, K. S., *Angew. Chem. Int. Ed.* **2011**, *50*, 9177–9179.
- [40] L.-C. Fang, R. P. Hsung, Z.-X. Ma, W. R. Presser, *Org. Lett.* **2013**, *15*, 4842–4845.
- [41] H. Fuwa, M. Sasaki, *Org. Biomol. Chem.* **2007**, *5*, 2214–2218.
- [42] E. M. Beccalli, G. Broggin, F. Clerici, S. Galli, C. Kammerer, M. Rigamonti, S. Sottocornola, *Org. Lett.* **2009**, *11*, 1563–1566.
- [43] E. M. Beccalli, A. Bernasconi, E. Borsini, G. Broggin, M. Rigamonti, G. Zecchi, *J. Nat. Prod.* **2010**, *75*, 6923–6932.
- [44] A. Navarro-Vázquez, D. Rodríguez, M. F. Martínez-Esperón, A. García, C. Saá, D. Domínguez, *Tetrahedron Lett.* **2007**, *48*, 2741–2743.
- [45] S. Singh, M. R. J. Elsegood, M. C. Kimber, *Synlett* **2012**, *6*, 565–568.
- [46] G. Broggin, S. Galli, M. Rigamonti, S. Sottocornola, G. Zecchi, *Tetrahedron Lett.* **2009**, *50*, 1447–1449.
- [47] A. M. Manzo, A. D. Perboni, G. Broggin, M. Rigamonti, *Tetrahedron Lett.* **2009**, *50*, 4696–4699.
- [48] M. C. Kimber, *Org. Lett.* **2010**, *12*, 1128–1131.
- [49] A. W. Hill, M. R. J. Elsegood, M. C. Kimber, *J. Org. Chem.* **2010**, *75*, 5406–5409.

- [50] M. Bandini, A. Eichholzer, *Angew. Chem. Int. Ed.* **2009**, *48*, 9533–9537.
- [51] G. Cera, P. Crispino, M. Monari, M. Bandini, *Chem. Commun.* **2011**, *47*, 7803–7805.
- [52] G. Cera, S. Piscitelli, M. Chiarucci, G. Fabrizi, A. Goggiamani, R. S. Ramón, S. P. Nolan, M. Bandini, *Angew. Chem. Int. Ed.* **2012**, *51*, 9891–9895.
- [53] M. Chiarucci, R. Mocci, L.-D. Syntrivanis, G. Cera, A. Mazzanti, M. Bandini, *Angew. Chem. Int. Ed.* **2013**, *52*, 10850–10853.
- [54] M. Jia, G. Cera, D. Perrotta, M. Monari, M. Bandini, *Chem. Eur. J.* **2014**, *20*, 9875–9878.
- [55] M. Bandini, A. Bottoni, M. Chiarucci, G. Cera, G. Pietro Miscione, *J. Am. Chem. Soc.* **2012**, *134*, 20690–20700.
- [56] D. Wang, R. Cai, S. Sharma, J. Jirak, S. K. Thummanapelli, N. G. Akhmedov, H. Zhang, X. Liu, J. L. Petersen, X. Shi, *J. Am. Chem. Soc.* **2012**, *134*, 9012–9019.

3. ELECTROPHILIC ACTIVATION OF ALLENAMIDES BY CHIRAL PHOSPHORIC ACIDS

3.1 Metal-Free Enantioselective Dearomatization of Indoles

Dearomatization of indoles^[1-3] is a useful route to obtain indolenines^[4-6] and indolines^[5,6] derivatives. Alkaloids compounds with indolenine or indoline scaffolds have been developed as promising biological agents due to their relevant therapeutic activity against cancer, inflammation^[3] and hypertension. Many transformations consist of a further functionalization of indoles with C2 or C3 positions being already substituted. The reactivity of the indoles can be compared with the classical reactivity of enamine where the nucleophilic site is the carbon in 3-position (Figure 1).

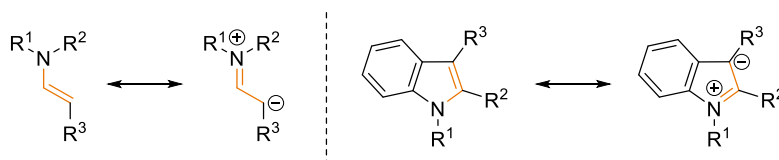
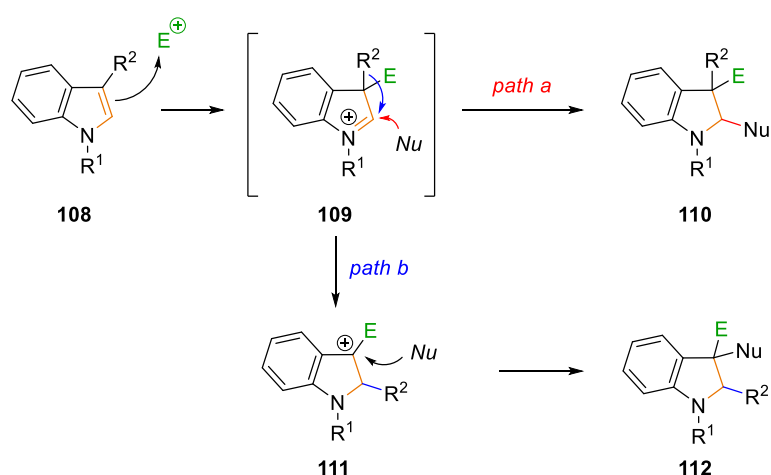


Figure 1: Classical reactivity of the enamine compared with the reactivity of the indole.

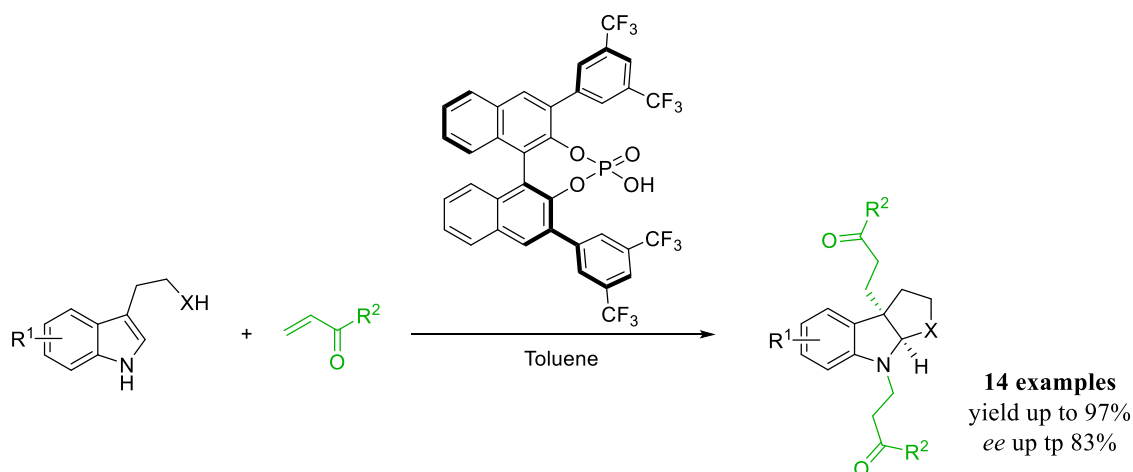
When dearomatization is on C3 position, the resulting intermediate **109** has two possible pathways:

- ✓ the C2 can undergo a nucleophilic attack resulting in the indolenine **110** (path a, Scheme 1);
- ✓ [1,2]-shift of the substituent from C3 to C2 followed by a nucleophilic addition to C3 (path b, Scheme 1).



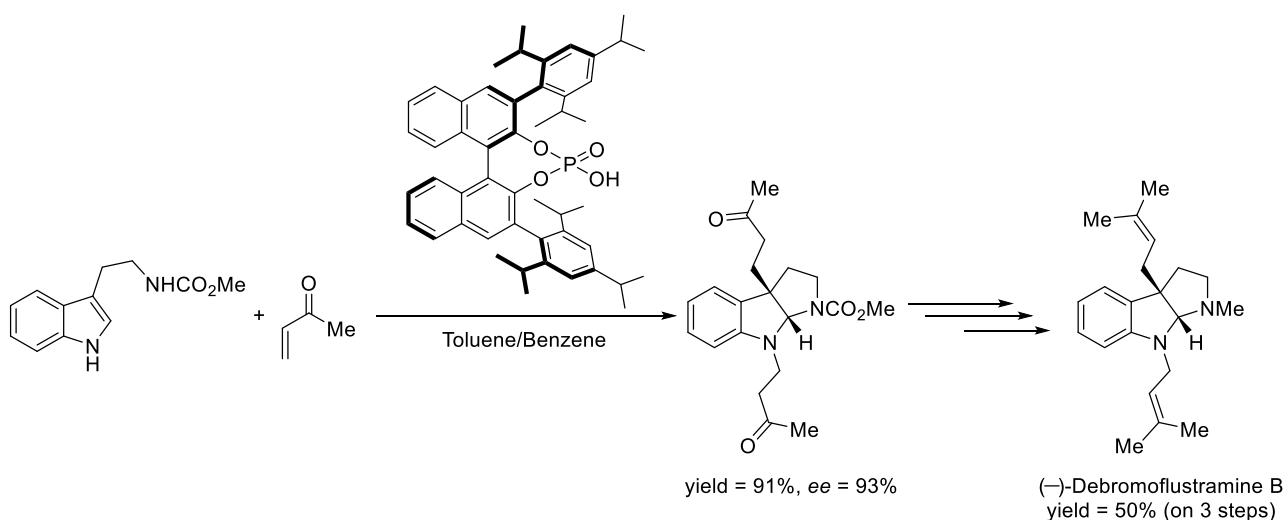
Scheme 1: Dearomatization of 3-substituted indole.

In 2012 You and co-workers reported an enantioselective dearomatization of indoles promoted by chiral phosphoric acids in order to obtain pyrroloindolines.^[7] The authors were able to isolate the desired products in good to excellent yields and with enantiomeric excess up to 83% (Scheme 2).



Scheme 2: Enantioselective dearomatization of indoles promoted by chiral phosphoric acids.

The pyrroloindolines obtained in this transformation is part of an important class of alkaloids which have shown promising application in muscle relaxants, potassium channel-blockers and anti-cancer agents. This type of dearomatization was used by Antilla and Zhang^[8] to develop the total synthesis of one of these alkaloids, in particular the (–)-Debromoflustramine B (Scheme 3).



Scheme 3: Total synthesis of the (–)-Debromoflustramine B.

The possibility to use chiral phosphoric acids to promote an efficient enantioselective dearomatization of indoles and the possibility to activate the allenamides with Brønsted acids as reported by Navarro-Vázquez (Scheme 41, chapter 2),^[9] suggested us to use this class of chiral Brønsted acids^[10–13] in order to develop the first metal-free electrophilic activation of allenamides in

enantioselective transformation. In particular, BINOL-based phosphoric acids introduced as promoting agent for the activation of allenamides, resulted in a tight contact ion pairs between the chiral anion and the α,β -unsaturated iminium intermediate (**B**, Figure 2). It is important to note that using *N*(H)-free disubstituted indoles, not only the C3 position can promote the nucleophilic attack but also the nitrogen and moreover, the iminium intermediate has two possible electrophilic sites which can undergo the attack (Figure 2).

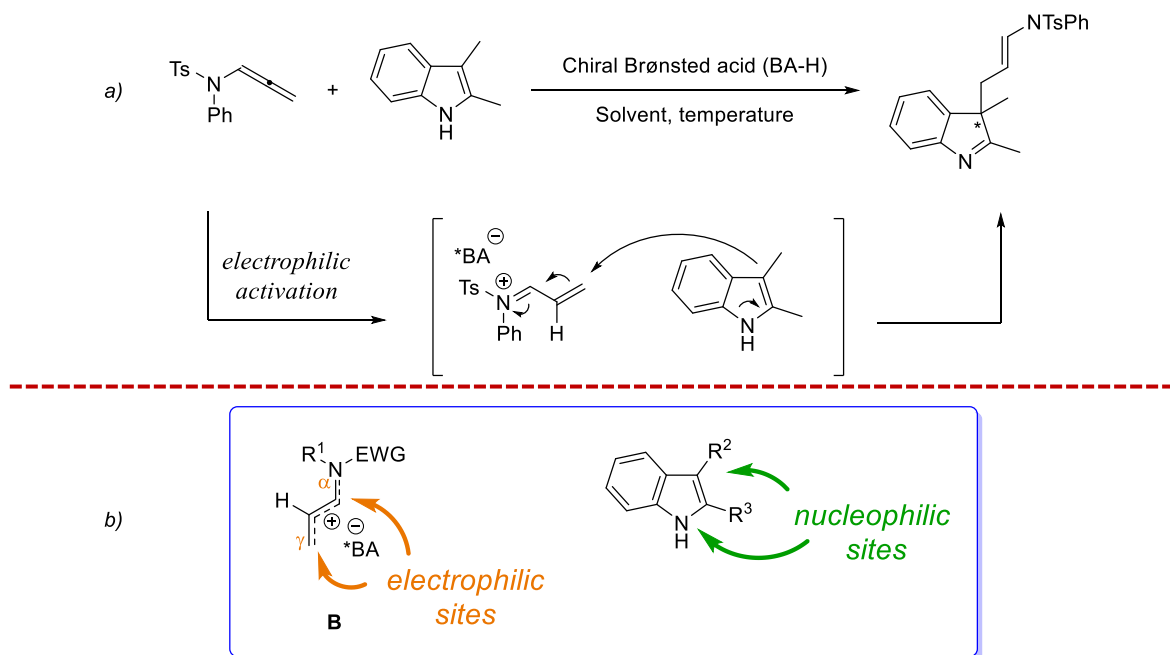


Figure 2: Our hypothesis to develop the enantioselective variant of the title dearomatization using chiral Brønsted acids (a) and electrophilic sites of iminium ion intermediate and nucleophilic sites of 2,3-disubstituted indole (b).

Differently substituted BINOL-based phosphoric acids have been prepared in order to find the best catalyst for the reaction between allenamides and 2,3-dimethyl indole. In particular, **IV**, **V** and **VI** were prepared using the already known synthetic procedures developed by Alexakis^[14] and MacMillan^[15].

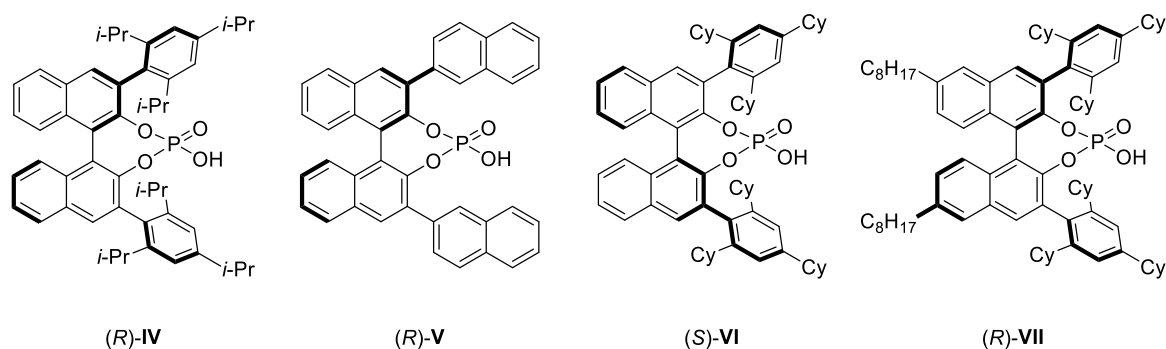
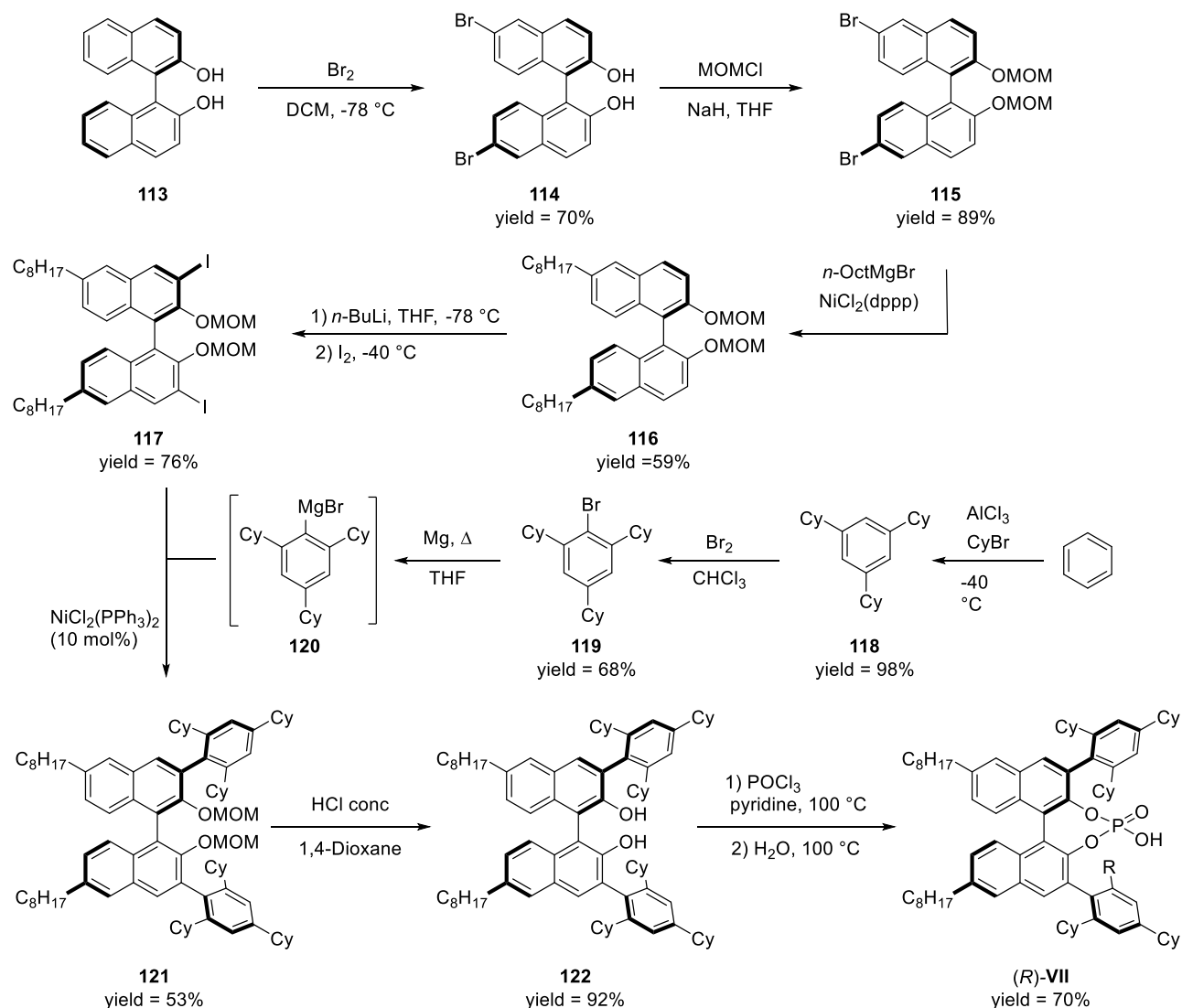


Figure 3: BINOL-base phosphoric acids prepared following the synthetic procedure reported in literature.

The catalyst **VII** was prepared using a modified procedure with respect to the synthesis of **VI** (Scheme 4).



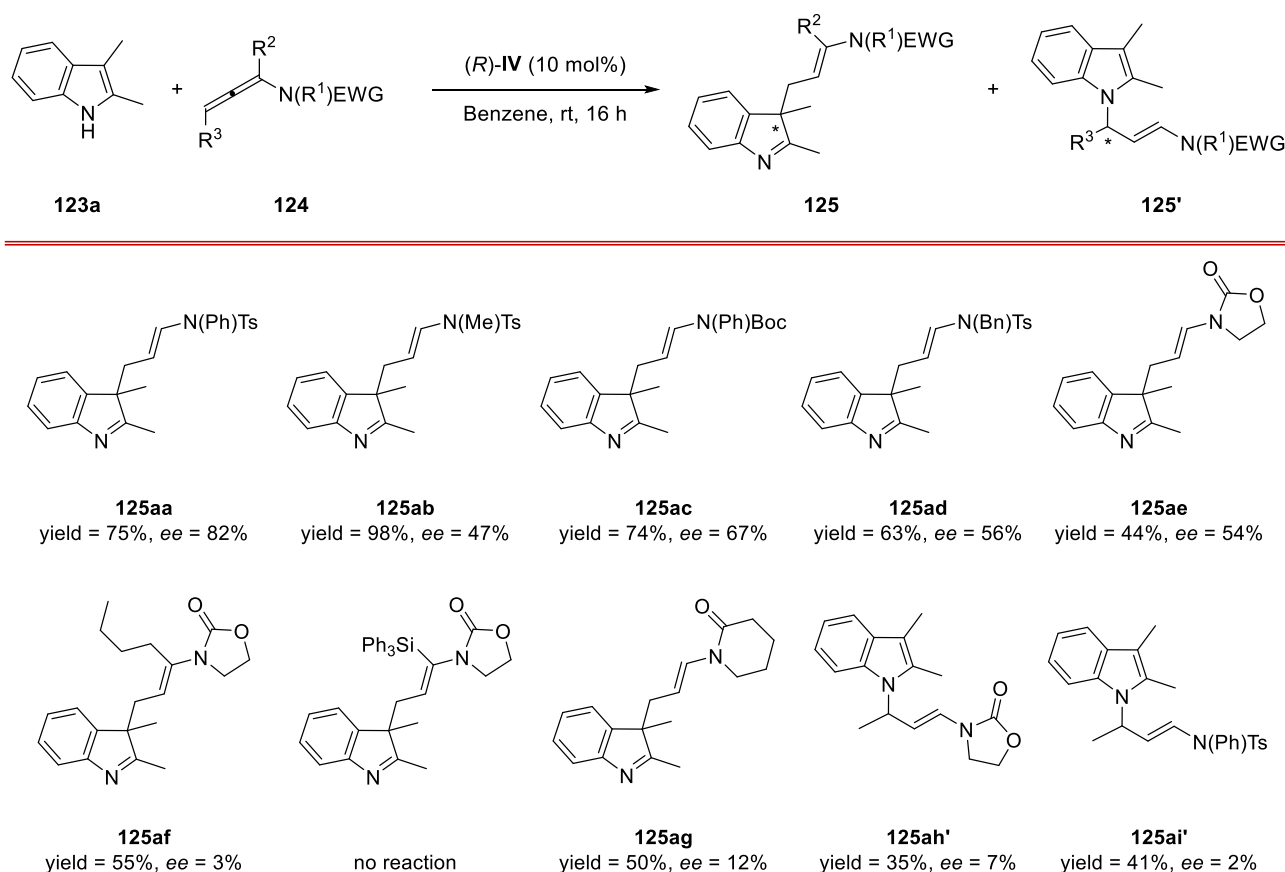
Scheme 4: Synthesis of the (R)-VII.

Although the synthetic procedure to obtain the BINOL-based phosphoric acids was already reported, the synthesis of the desired phosphoric acids didn't proceed smoothly. In particular, the preparation of the Grignard reagent **120** was very challenging due to the large steric hindrance of the cyclohexyl groups that make difficult the insertion of the magnesium in the C–Br bond. The formation of the desired Grignard reagent was monitored by GC-MS analysis and satisfactory results were achieved when the reaction was performed at high temperature and for long time. Also the Kumada cross-coupling was a challenging step. The Grignard reagent was transferred into the solution of the compound **117** and $\text{NiCl}_2(\text{PPh}_3)_2$ via cannula and satisfactory yields of compound **121** were achieved only when the THF used as solvent was previously degassed through freezing-

pump-thaw cycles. Furthermore, it is important to highlight that the formation of the desired phosphoric acid **VII** was monitored via ^{31}P -NMR analysis in order to check the complete hydrolysis of the P-Cl bond intermediate.

With the catalysts in our hands, we submitted differently substituted allenamides in the reaction with 2,3-dimethylindole in the presence of 10 mol% of catalyst **IV**.

As reported in Scheme 5, the allenamides featuring substituent in γ position of the allene framework resulted in the corresponding products in low yields and very low enantiomeric excesses while α -substituted allenamides gave the *N*-adduct instead of the desired C3-adduct. Only modest yields and not satisfactory enantioselectivities were achieved when cyclic allenamides were employed, but the yields increased using acyclic allenamides bearing aliphatic groups. Good yields and high enantiomeric excesses were obtained when allenamide **124a** was used. In order to improve the yield and the *ee* the tosyl group was replaced with Boc group but unfortunately without good results both in term of yield and *ee* (Scheme 5).

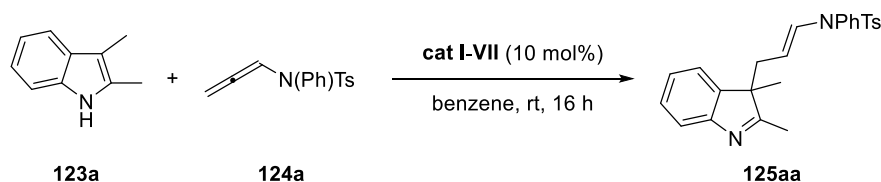


Scheme 5: Screening of the allenamides. All reactions were performed in dry benzene under nitrogen conditions (**123a:124a-i:cat=2:1:0.1**)

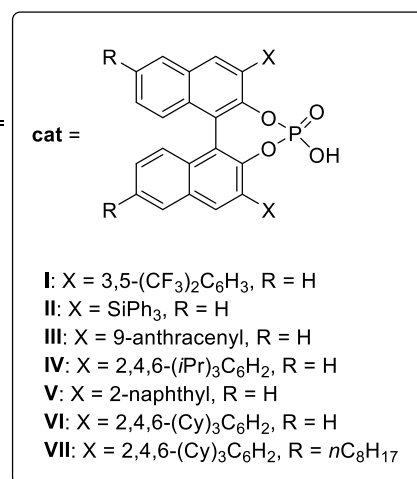
The condensation between *N*-phenyl-*N*-sulfonylallenamide **124a** and 2,3-dimethylindole **123a** was chosen as model reaction and several chiral phosphoric acids were tested as catalysts in anhydrous benzene at room temperature (Table 1).

As reported in Table 1, all the catalysts screened for this transformation gave the desired product in good to excellent yields. C3-adduct was isolated with complete regiochemistry on the γ position of the allenamide. Only catalysts **I**, **II** and **V** gave the product with not satisfactory enantiomeric excesses, since the other catalysts promoted the reaction with good enantioselectivity (more than 72%). In particular, the catalyst (*R*)-**VII** (C8-TCyP) promoted the model reaction giving the indolenine in quantitative yield and excellent enantiomeric excess (entry 7). In order to increase the enantioselection the temperature of the reaction was decreased up to 10 °C (entry 8) resulting in higher *ee* (94%) for the product but lower yield (72%). Finally, the reaction promoted by (*R*)-**VII** was performed in the presence of activated molecular sieves (entry 10), but no significant contribution in terms of yield and enantioselection was recorded. The key role of the catalyst in the enantioselective activation of allenamide was investigated using (*R*)-**VII** at a loading of 1 mol % (entry 10); indeed under these conditions the indolenine was obtained in only 57% yield after 72 hours and 87% *ee*.

Table 1: Optimization of the catalytic system.^[a]

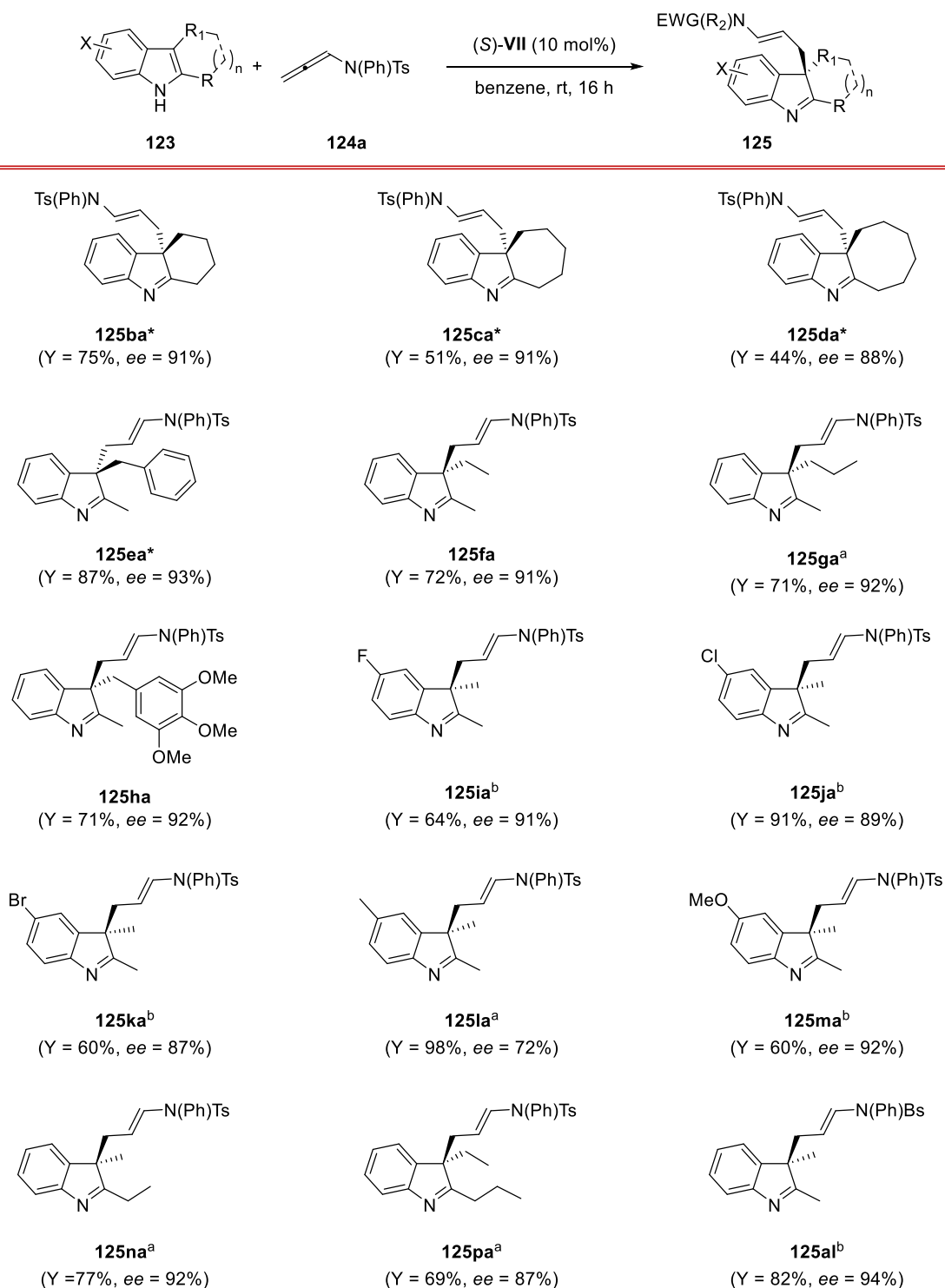


Entry	cat	T(°C) / t (h)	Yield	
			125aa (%) ^[b]	<i>ee</i> 125aa(%) ^[c]
1	(<i>R</i>)- I	25 / 16	53	28 (<i>S</i>)
2	(<i>R</i>)- II	25 / 16	61	8 (<i>S</i>)
3	(<i>R</i>)- III	25 / 16	92	72 (<i>S</i>)
4	(<i>R</i>)- IV	25 / 16	75	82 (<i>S</i>)
5	(<i>R</i>)- V	25 / 16	53	25 (<i>S</i>)
6	(<i>S</i>)- VI	25 / 16	88	84 (<i>R</i>)
7	(<i>R</i>)- VII	25 / 16	98	92 (<i>S</i>)
8 ^[d]	(<i>R</i>)- VII	10 / 16	72	94 (<i>S</i>)
9	(<i>R</i>)- VII	25 / 72	57	87 (<i>S</i>)
10 ^[e]	(<i>R</i>)- VII	25 / 16	95	85 (<i>S</i>)



[a] All reactions were performed in dry benzene under nitrogen conditions (**123a**:**124a**:**cat**=**2**:**1**:**0.1**, unless otherwise specified). [b] Determined after flash chromatography. [c] Determined with chiral HPLC. Absolute configuration in brackets. [d] 1 mol% of catalyst was used. [e] With activated 5 Å molecular sieves.

With the optimized reaction conditions in our hands, the scope of the reaction was investigated by submitting several differently substituted indoles under the dearomatization with allenamide **124** in the presence of (*S*)-**VII** as catalyst (Scheme 6). This methodology was tolerant toward different functional groups providing all the desired indolenines in good to excellent yields and excellent enantiomeric excesses. In particular, indoles featuring aliphatic and benzylic substituents on C3 or C2 positions resulted in the corresponding products in good yields and excellent enantiomeric excesses (up to 93%). Indoles with C(2,3)-fused cycles as substituents proved to be suitable substrates for the reaction. The corresponding products were isolated in good yields and enantiomeric excesses even more than 90%. Also different functional groups on the six-member aromatic ring of the indoles were tolerated. Indoles with electron-withdrawing groups as well as electronic-donating groups resulted in the indolenines in good yields and with high level of enantioselectivity. Finally, also the allenamide featuring benzenesulfonyl group instead of tosyl group was submitted under optimized reaction conditions with the 2,3-dimethylindole resulting in the desired product in 82% yield and 94% *ee*.



Scheme 6: Scope of the enantioselective dearomatization of 2,3-disubstituted indoles with allenamides. * (R)-I was used. [a] Catalyst loading 5 mol%, time 72 h. [b] Catalyst loading 1 mol%, time 72 h. Ts = *p*-toluenesulfonyl, Bs = benzenesulfonyl.

The absolute configuration of the final product **125ka** was determined to be *R* by single-crystal X-ray analysis and on the basis of this finding we postulated the hypothetical model trajectory showed in Figure 4.

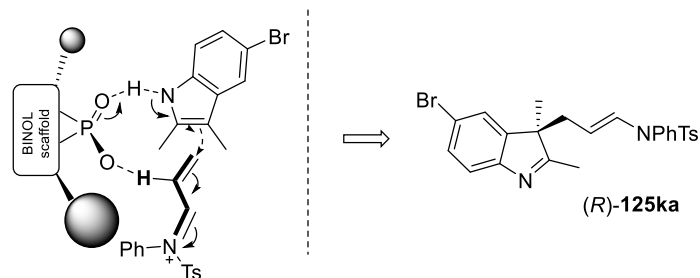


Figure 4: Hypothetical model trajectory.

The initial electrophilic activation of allenamide by the catalyst resulted in the formation of the iminium specie which undergoes a Michael-type nucleophilic addition from the C3 of the indole. It is important to note that the *N*-H free of the indole takes part at the formation of the chiral ion-pair through hydrogen bond interaction.

This protocol proved to be an efficient route to the synthesis of highly functionalized indolenines. Not only indolenines but also indolines^[5,6] are important scaffold in organic chemistry for their biological activity. For this reason we envisioned the possibility to develop a new enantioselective dearomatization/hydrogen transfer cascade reaction in order to obtain enantioenriched, highly functionalized indolines. In this direction, we envisioned a chiral Brønsted acid-catalysed one-pot dearomatization/hydrogenation transfer sequence through a three-component reaction with the indole, the allenamide, and a Hantzsch ester (HE)^[16–20] (Figure 5).

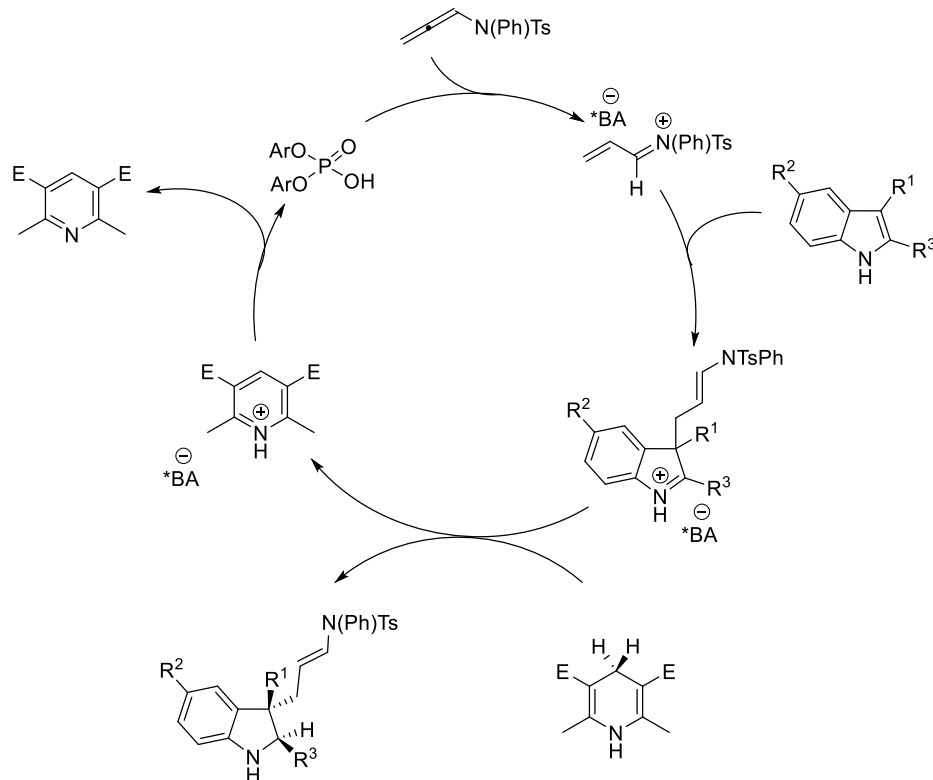
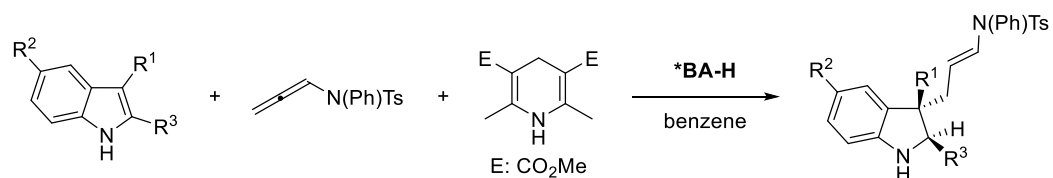
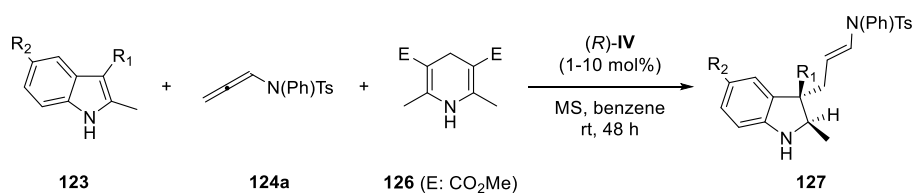


Figure 5: Proposed reaction mechanism for the Brønsted acid catalyzed one-pot dearomatization/hydrogenation transfer sequence through a three-component reaction with the indole, the allenamide, and a Hantzsch ester (HE).

The commercially available (*R*)-**IV** (TRIP) demonstrated to be an optimal catalyst for the enantioselective synthesis of *trans*-C2/C3 indolines resulting from the condensation of 2,3-dimethylindole with *N*-phenyl-*N*-tosylallenamide (Table 2).

Table 2: Enantioselective dearomatization/hydrogen transfer sequence reaction.^[a]



Entry	R ¹ / R ²	Yield 127 (%) ^[b] <i>trans + cis</i>	<i>dr</i> 127 ^[c] <i>trans + cis</i>	<i>ee</i> (%) ^[d] <i>trans + cis</i>
1	Me / H	51	19:1	98:82
2	Et / H	49	15:1	99/33
3	Me / Cl	72	11:1	95/70
4	Me / Br	60	10:1	95/82
5	Me / Me	44	12:1	94/n.d.

[a] All reactions were performed under inert conditions using nitrogen gas (**123:124a:127:cat=2:1:2:0.1**, unless otherwise specified). [b] Determined after flash chromatography. [c] Determined on the reaction crude. [d] Determined with chiral HPLC. n.d. not determined.

High levels of enantioselectivities were also obtained using indoles featuring substituents on the benzenoid ring. Electron-withdrawing groups as well as electron-donating groups were tolerated in the synthetic protocol and the corresponding indolines were isolated in moderate yields and high diastereoisomeric ratio.

In conclusion, the first metal-free enantioselective electrophilic activation of allenamides promoted by chiral BINOL-based phosphoric acids was developed. This methodology demonstrated to be tolerant toward several functional groups regardless their electronic character. It was possible to develop an efficient and highly enantioselective synthesis of indolenines and indolines differently functionalized through dearomatization of 2,3-disubstituted indoles.

Bibliography

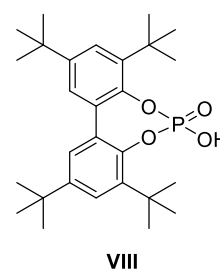
- [1] F. L. Ortiz, M. J. Iglesias, I. Fernández, C. M. A. Sánchez, G. R. Gómez, F. Lo, I. Ferná, C. M. Andu, *Reactions* **2007**, *107*, 1580–1691.
- [2] S. P. Roche, J. A. Porco, *Angew. Chem. Int. Ed.* **2011**, *50*, 4068–4093.
- [3] S. P. Roche, J.-J. Youte Tendoung, B. Tréguier, *Tetrahedron* **2015**, *71*, 3549–3591.
- [4] Y. Zhu, V. H. Rawal, *J. Am. Chem. Soc.* **2012**, *134*, 111–114.
- [5] Q.-L. Xu, L. X. Dai, S.-L. You, *Chem. Sci.* **2013**, 97–102.
- [6] L. M. Repka, S. E. Reisman, *J. Org. Chem.* **2013**, *78*, 12314–12320.
- [7] Q. Cai, C. Liu, X.-W. Liang, S.-L. You, *Org. Lett.* **2012**, *14*, 4588–4590.
- [8] Z. Zhang, J. C. Antilla, *Angew. Chem. Int. Ed.* **2012**, *51*, 11778–11782.
- [9] A. Navarro-Vázquez, D. Rodríguez, M. F. Martínez-Espéron, A. García, C. Saá, D. Domínguez, *Tetrahedron Lett.* **2007**, *48*, 2741–2743.
- [10] T. Akiyama, Y. Honma, J. Itoh, K. Fuchibe, *Adv. Synth. Catal.* **2008**, *350*, 399–402.
- [11] V. Rauniyar, A. D. Lackner, G. L. Hamilton, F. D. Toste, *Science (80-.)*. **2011**, *334*, 1681–1684.
- [12] S. Harada, S. Kuwano, Y. Yamaoka, K.-I. Yamada, K. Takasu, *Angew. Chem. Int. Ed.* **2013**, *52*, 10227–10230.
- [13] W. Zi, Y. M. Wang, F. D. Toste, *J. Am. Chem. Soc.* **2014**, *136*, 12864–12867.
- [14] F. Romanov-Michailidis, L. Guénée, A. Alexakis, *Angew. Chem. Int. Ed.* **2013**, *52*, 9266–9270.
- [15] R. I. Storer, D. E. Carrera, Y. Ni, D. W. C. MacMillan, *J. Am. Chem. Soc.* **2006**, *128*, 84–86.
- [16] J. W. Yang, M. T. Hechavarria Fonseca, N. Vignola, B. List, *Angew. Chem. Int. Ed.* **2005**, *44*, 108–110.
- [17] S. Hoffmann, A. M. Seayad, B. List, *Angew. Chem. Int. Ed.* **2005**, *44*, 7424–7427.

- [18] G. Li, Y. Liang, J. C. Antilla, *J. Am. Chem. Soc.* **2007**, *129*, 5830–5831.
- [19] Q. Kang, Z. A. Zhao, S. L. You, *Adv. Synth. Catal.* **2007**, *349*, 1657–1660.
- [20] S. G. Ouellet, J. B. Tuttle, D. W. C. MacMillan, *J. Am. Chem. Soc.* **2005**, *127*, 32–33.

3.1.1 Experimental Section

¹H-NMR spectra were recorded on Varian 200 (200 MHz) or Varian 400 (400 MHz) spectrometers. Chemical shifts are reported in ppm from TMS with the solvent resonance as the internal standard (deuteriochloroform: 7.27 ppm). Data are reported as follows: chemical shift, multiplicity (s = singlet, d = doublet, t = triplet, q = quartet, sext = sextet, sept = septet, p = pseudo, b = broad, m = multiplet), coupling constants (Hz). ¹³C-NMR spectra were recorded on a Varian 200 (50 MHz), Varian 400 (100 MHz) spectrometers with complete proton decoupling. Chemical shifts are reported in ppm from TMS with the solvent as the internal standard (deuteriochloroform: 77.0 ppm). GC-MS spectra were taken by EI ionization at 70 eV on a Hewlett-Packard 5971 with GC injection. They are reported as: *m/z* (rel. intense). LC-electrospray ionization mass spectra were obtained with Agilent Technologies MSD1100 single-quadrupole mass spectrometer. Chromatographic purification was done with 240-400 mesh silica gel. Anhydrous THF and DCM were distilled respectively from sodium-benzophenone and P₂O₅ prior to use. Other anhydrous solvents were supplied by Fluka or Sigma Aldrich in Sureseal® bottles and used without any further purification. Commercially available chemicals were purchased from Sigma Aldrich, Stream and TCI and used without any further purification. Analytical high performance liquid chromatography (HPLC) was performed on a liquid chromatograph equipped with a variable wave-length UV detector (deuterium lamp 190-600 nm), using a Daicel Chiracel™ AD, IA and ID (0.46 cm I.D. x 25 cm Daicel Inc). HPLC grade isopropanol and *n*-hexane were used as the eluting solvents. Melting points were determined with Bibby Stuart Scientific Melting Point Apparatus SMP 3 and are not corrected. All allenamides **124** were obtained following known procedures^[1] and (**124g**, **124j**),^[2] **124i**.^[3] BAs **I-IV** were purchased by Sigma-Aldrich and directly used in the catalysis. BA **V**^[4] and **VI**^[5] were obtained via known procedures.

Racemic mixtures of products **125** were obtained by using BA **VIII** (10 mol%) in DCM. Racemic mixtures of diastereomerically enriched compounds **127/127'** were obtained by reducing the corresponding indolenines **125** to indolines **127/127'** with NaBH₄ in MeOH at rt. Anhydrous solvents were purchased from Sigma-Aldrich. Agilent Technologies LC/MSD Trap 1100 series (nebulizer: 15.0 PSI, dry Gas: 5.0 L/min,



^[1] S. Suárez-Pantiga, C. Hernández-Díaz, M. Piedrafita, E. Rubio, J. M. González, *Adv. Synth. Catal.* **2012**, *354*, 1651-1657.

^[2] H. Xiong, R. P. Hsung, L.-L. Wei, C. R. Berry, J. A. Mulder, B. Stockwell, *Org. Lett.* **2010**, *2*, 2869-2871.

^[3] R. Hayashi, R. P. Hsung, J. B. Feltenberger, A. G. Lohse, *Org. Lett.* **2009**, *11*, 2125-2128.

^[4] C. Guo, J. Song, L.-Z. Gong, *Org. Lett.* **2013**, *15*, 2676-2679.

^[5] V. Rauniyar, Z. J. Wang, H. E. Burks, F. D. Toste, *J. Am. Chem. Soc.* **2011**, *133*, 8486-8489.

dry Temperature: 325 °C, capillary voltage positive scan: 4000 mA, capillary voltage negative scan: 3500 mA). Some of the indolenine products were already fully characterized in racemic form in one of our recent report (*i.e.* **125aa**, **125ba**, **125ca**, **125da**, **125ea**, **125la**, **125pa**).^[6] In these cases, only $[\alpha]_D$, and ¹H-NMR spectra were reported in order to verify the purity of the compounds.

The X-ray intensity data for **125ka** were measured on a Bruker Apex II CCD diffractometer. Cell dimensions and the orientation matrix were initially determined from a least-squares refinement on reflections measured in three sets of 20 exposures, collected in three different ω regions, and eventually refined against all data. A full sphere of reciprocal space was scanned by 0.3° ω steps. The software SMART^[7] was used for collecting frames of data, indexing reflections and determination of lattice parameters. The collected frames were then processed for integration by the SAINT program,^[5] and an empirical absorption correction was applied using SADABS.^[8] The structures were solved by direct methods (SIR 97)^[9] and subsequent Fourier syntheses and refined by full-matrix least-squares on F² (SHELXTL),^[10] using anisotropic thermal parameters for all non-hydrogen atoms. All the hydrogen atoms were located in difference Fourier maps. Those bonded to aromatic carbons were treated as riding atoms in geometrically idealized positions. The absolute configuration has been established by anomalous dispersion effects in diffraction measurements on the crystal (Flack parameter= 0.015(8)). The molecular graphics were generated by using ORTEP.^[11] Color codes for the molecular graphics: blue (N), red (O), grey (C), white (H), olive green (Br), yellow (S). Crystal data and other experimental details for **125ka** are reported in Table S3 whereas bond lengths [Å] and angles (deg) are shown in Table S4.

^[6] M. Jia, G. Cera, D. Perrotta, M. Bandini, *Chem. Eur. J.* **2014**, *20*, 9875-9878.

^[7] SMART & SAINT Software Reference Manuals, Version 5.051 (*Windows NT Version*), Bruker Analytical X-ray Instruments Inc. Madison, WI, 1998.

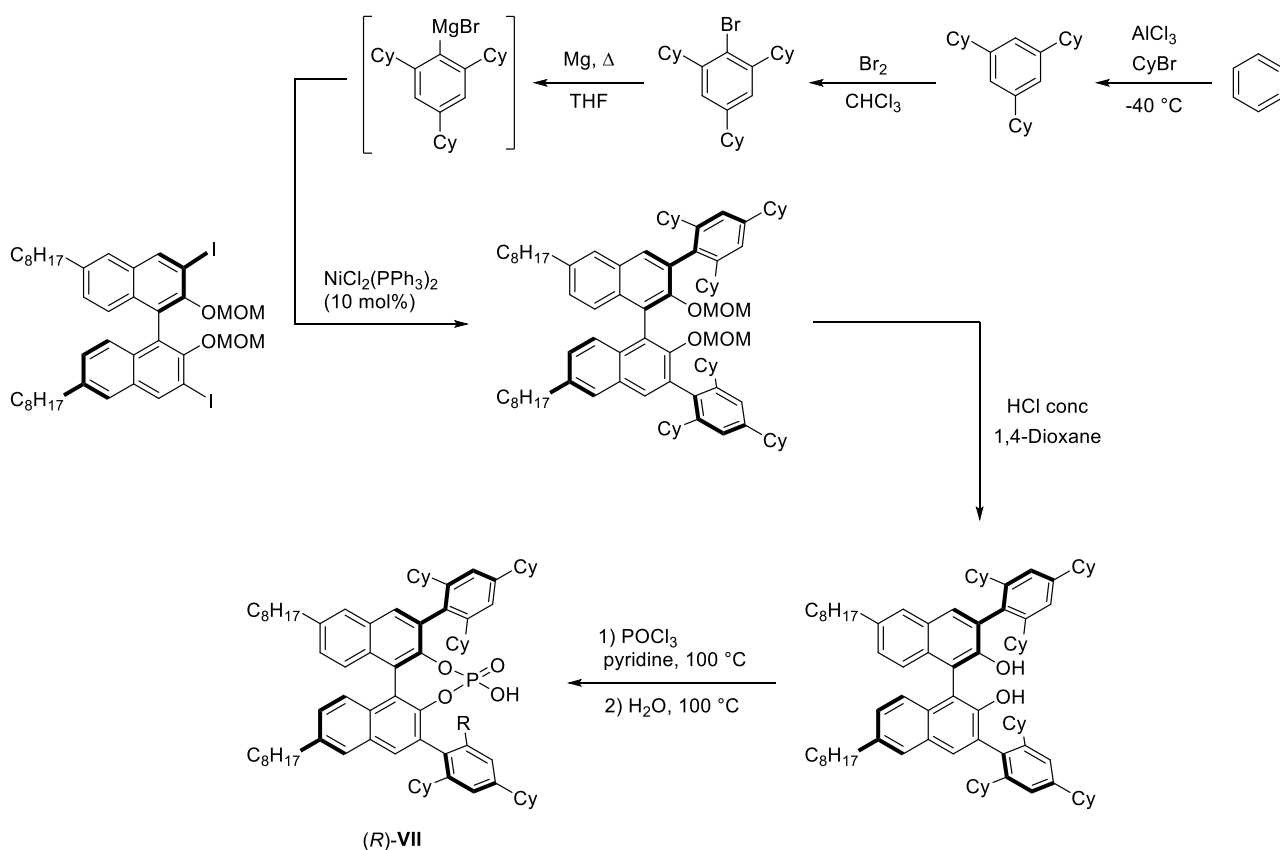
^[8] Sheldrick, G. M. SADABS, program for empirical absorption correction, University of Göttingen, Germany, 1996.

^[9] Altomare, A., Burla, M.C., Camalli, M., Cascarano, G. L., Giacovazzo, C., Guagliardi, A., Moliterni, A. G. G., Polidori, G. & Spagna, R. *J. Appl. Crystallogr.* **32**, 115-119 (1999).

^[10] Sheldrick, G. M. SHELXTLplus Version 5.1 (*Windows NT version*) *Structure Determination Package*; Bruker Analytical XrayInstruments Inc.: Madison, WI, 1998.

^[11] Farrugia, L. J. ORTEP-3, *J. Appl. Cryst.* **45**, 849-854 (2012).

Synthesis of (S)-C₈TCyP (VII).



A modified procedure with respect to the literature^[3] was utilized for the last four steps herein described.

An oven-dried two-necked flask, equipped with a condenser and connected to the inert gas line, was charged with 5 mL of anhydrous THF. The solvent was degassed through freezing-pump-thaw cycles then, Mg (86 mg, 3.6 mmol) and 1-Br-2,4,6-Cy₃C₆H₂^[3] (1.21 g, 3.0 mmol) were added in sequence. To the solution was added 1 bean of I₂ and 10 mL of 1,2-Br₂-ethane. The solution was vigorously kept at reflux with a heat gun as far as the color of the solution tuned to green-gray (≈ 30 min), then to complete the formation of the Grignard reagent, the mixture was kept under reflux (oil bath) for about 1 h. Formation of the Grignard reagent was verified via GC-MS analysis from an aliquot of solution. In a second oven-dried two-necked flask was prepared a solution of $(\text{PPh}_3)_2\text{NiCl}_2$ (33 mg, 60 μmol) and compound A (430 mg, 0.52 mmol) in degassed THF (3 ml). The pale yellow solution was cooled at $0\text{ }^\circ\text{C}$, then the pre-cooled (rt) solution of Grignard reagent was transferred via cannula. The resulting dark-brown mixture was stirred overnight at $55\text{ }^\circ\text{C}$. The mixture was quenched with a saturated solution of NH_4Cl and the THF removed under reduced pressure. The aqueous residue was extracted three times with AcOEt and the organic phases dried

over Na₂SO₄. After removal of the volatiles, the reaction crude was purified via flash chromatography (*n*Hex 100 → *n*Hex:Et₂O 95:5).

(*S*)-**121**: viscous pale yellow oil (350 mg, 53% (not optimized)). ¹*H-NMR* (400 MHz, CDCl₃, diagnostic signals) δ 0.85 (t, *J* = 6.8 Hz, 6H), 2.22-2.39 (m, 6H), 2.47-2.56 (m, 2H), 2.70 (t, *J* = 8.0 Hz, 6H), 4.21 (d, *J* = 5.6 Hz, 2H), 4.30 (d, *J* = 5.6 Hz, 2H), 6.85 (s, 2H), 7.01 (s, 4H), 7.10 (d, *J* = 8.0 Hz, 2H), 7.19 (d, *J* = 8.0 Hz, 2H), 7.54 (s, 2H), 7.63 (s, 2H).

210 mg of (*S*)-**121** were suspended in 3.5 mL of reagent grade dioxane and treated with 1.0 ml of HCl conc. The white slurry was vigorously stirred under reflux for 3.5 h. The reaction mixture was cooled to 0 °C and the solution neutralized with saturated solution of NaHCO₃. The aqueous phase was extracted with DCM, dried over Na₂SO₄ and the volatiles removed under reduced pressure. The crude was purified by flash chromatography (*n*Hex 100 → *n*Hex:CH₂Cl₂ 80:20).

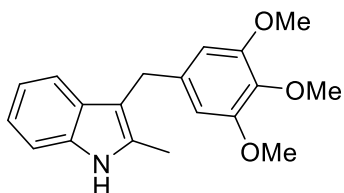
(*S*)-**122**: White foam (300 mg, 92%). *MP* = 153-156 °C. [α]_D = +64.0° (*c* = 0.20, CHCl₃). ¹*H-NMR* (400 MHz, CDCl₃, diagnostic signals) δ 0.92 (t, *J* = 6.8 Hz, 6H), 2.27 (t, *J* = 12.0 Hz, 2H), 2.49-2.61 (m, 4H), 2.77 (t, *J* = 7.6 Hz, 4H), 4.80 (s, 2H), 7.09 (s, 2H), 7.14 (s, 2H), 7.18 (d, *J* = 8.8 Hz, 2H), 7.24 (d, *J* = 8.8 Hz, 2H), 7.64 (s, 2H), 7.67 (s, 2H).

Diol **122** (340 mg, 0.28 mmol) was suspended in 1.0 mL of pyridine and treated with 94 μL of freshly distilled POCl₃ (0.86 mmol). The viscous solution was stirred at reflux for 72 h (TLC monitoring revealed complete consumption of **C**). The reaction was acidified with HCl (1N) than extracted with DCM for three times. After dryness with Na₂SO₄ and removal of the organic solvents under reduced pressure, the crude was suspended in 0.5 mL of water. Then, 0.5 mL of pyridine was then added and the resulting mixture was refluxed for 48 h (complete hydrolysis of the P-Cl intermediate was controlled via ³¹P-NMR, δ = 7.54 ppm, CDCl₃). The reaction was acidified with HCl (1N) than extracted with DCM for three times. The organic solvents were removed under reduced pressure without drying over Na₂SO₄, and the corresponding C8-TCyP was purified via flash-chromatography (*c*Hex:EtOAc 8:2). The resulting white solid was dissolved in Et₂O and the organic phase was washed three times with HCl (6 N) to restore the phosphoric acid (**VII**). After dryness the Brønsted acid was obtained as a white crystalline solid.

(*S*)-**VII**: white solid. Yield = 70%. *MP* = 158-160 °C. [α]_D = +19.2° (*c* = 0.26, CHCl₃). ³¹P-NMR (162 MHz, CDCl₃) δ 1.26 ppm. ¹*H-NMR* (400 MHz, CDCl₃, diagnostic signals) δ 2.42-2.46 (m, 2H), 2.76 (t, *J* = 7.2 Hz, 4H), 6.91 (d, *J* = 8.4 Hz, 4H), 7.12 (d, *J* = 8.4 Hz, 2H), 7.18 (d, *J* = 8.4 Hz, 2H), 7.60 (d, *J* = 16.4 Hz, 4H). ¹³C-NMR (100 MHz, CDCl₃, diagnostic signals) δ 14.0, 22.6, 25.8,

26.2, 26.7, 26.8, 26.9, 27.0, 27.2, 29.2, 29.3, 29.5, 31.1, 31.8, 32.6, 33.2, 33.9, 34.7, 34.9, 36.0, 37.0, 41.6, 41.9, 44.6, 121.2, 121.6, 122.4, 126.2, 126.5, 126.7, 127.6, 130.5, 130.9, 131.1, 131.7, 132.1, 139.8, 140.7, 145.3, 145.6, 145.7, 146.1, 146.7, 146.8.

Synthesis of indole 125h.

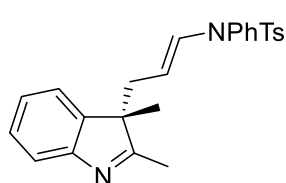


A solution of 2-methylindole (544 mg, 4.15 mmol) in 12 ml of dry DCM is cooled to 0 °C and 5 ml (1.2 eq) of a solution of Et₂AlCl (1M in hexane) was slowly added. The reaction crude was stirred for 10 min then 3,4,5-trimethoxybenzoyl chloride (1.2 equiv), dissolved in 6 ml of dry DCM, was added drop-wise. The reaction was maintained at this temperature for 10-15 minutes and then at room temperature for 16 h. After conventional work-up (H₂O, CH₂Cl₂, Na₂SO₄). Purification by flash chromatography (cHex:AcOEt 65:35). **MP** = 139-141 °C. ¹H-NMR (200 MHz, CDCl₃) δ 2.62 (s, 3H), 3.84 (s, 6H), 3.96 (s, 3H), 7.01 (s, 2H), 7.15-7.27 (m, 2H), 7.35 (d, *J* = 7.6 Hz, 1H), 7.50 (d, *J* = 7.4 Hz, 1H), 8.49 (s broad, 1H). **LC-MS** (m/z): 326 [M+H]⁺, 673 [2M+Na]⁺.

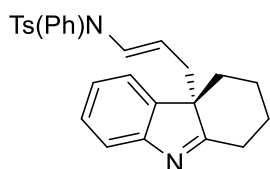
A flamed three-necked flask was charged with 4 ml of dry THF and 4.3 ml of a LiAlH₄ (1 M, 4.3 mmol) are added at 0 °C. Subsequently, the crude ketone dissolved in THF (4 mL), was added dropwise. The reaction mixture was then stirred at 50 °C for 4 h and judged complete by TLC (cHex:AcOEt 1:1). The reaction was quenched with a NaOH (10%) at 0 °C, the aqueous phase extracted with AcOEt (3 x 5 mL) and the collected organic phases dried over Na₂SO₄. Purification by flash chromatography (cHex:AcOEt 7:3) afforded **125h** as a light pink solid in 30% yield (two steps, not optimized). **MP** = 138-139 °C. ¹H-NMR (400 MHz, CDCl₃) δ 2.39 (s, 3H), 2.95 (s, 3H), 3.78 (s, 6H), 4.04 (s, 2H), 7.07 (t, *J* = 8.0 Hz, 1H), 7.13 (t, *J* = 8.0 Hz, 1H), 7.26 (d, *J* = 8.0 Hz, 1H), 7.45 (d, *J* = 8.0 Hz, 1H), 7.93 (s broad, 1H). ¹³C-NMR (100 MHz, CDCl₃) δ 11.7, 30.4, 55.9(2C), 60.7, 105.1(2C), 110.1, 110.2, 118.2, 119.1, 120.9, 128.7, 131.7, 135.2, 135.8, 137.5, 153.0(2C). **LC-MS** (m/z): 312.2 [M+H]⁺.

General procedure for the dearomatization reaction.

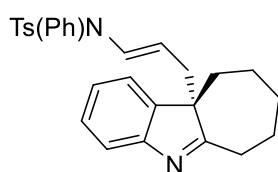
A dried two-necked flask was charged with 1 mL of anhydrous benzene, 0.1 mmol of allenamide **124a** and 0.2 mmol of the desired indole (2 eq. with respect to **124a**). The mixture was cooled to the desired temperature, then (*S*)-**VII** (5-10 mol%) was added. The reaction was allowed to reach the room temperature over the corresponding reaction time (16-48 h). After removal of the solvent under reduced pressure and the crude was purified by column chromatography to give the desired product **125**.



(*S*)-**125aa**.^[4,10] (Entry 10, Table 1). Orange oil. Yield = 98% (*c*Hex-AcOEt: 70:30). *Ee* = 92%. **HPLC**: Chiralcel-AD: eluent: *n*Hex:IPA = 80:20, flow = 0.7 mL/min, T = 40 °C, *Rt_R* (10.2 min), *Rt_S* (10.9 min). [α]_D = -102 ° (*c* = 0.85, CHCl₃). **¹H-NMR** (400 MHz, CDCl₃) δ 1.25 (s, 3H), 2.16 (s, 3H), 2.35 (dd, *J* = 7.6, 14.0 Hz, 1H), 2.45 (s, 3H), 2.49 (dd, *J* = 14.0 Hz, 1H), 3.69-3.76 (m, 1H), 6.64 (d, *J* = 8.0 Hz, 2H), 6.79 (d, *J* = 2.0, 8.4 Hz, 1H), 7.09-7.11 (m, 2H), 7.19-7.26 (m, 5H), 7.33 (d, *J* = 8.0 Hz, 2H), 7.41 (d, *J* = 7.6 Hz, 1H).



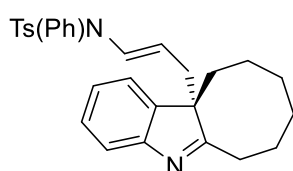
(*S*)-**125ba**.^[4,12] Pale yellow solid. Yield = 75% (*c*Hex-AcOEt: 70:30). *Ee* = 92%. **MP** = 60-62 °C. **HPLC**: Chiralcel-AD: eluent: *n*Hex:IPA = 80:20, flow = 0.7 mL/min, T = 40 °C, *Rt_R* (9.7 min), *Rt_S* (10.6 min). [α]_D = -32.4° (*c* = 0.85, CHCl₃, *ee* = 85%). **¹H-NMR** (400 MHz, CDCl₃) δ 1.14 (td, *J* = 13.6, 4.0 Hz, 1H), 1.28 (d, *J* = 12.8 Hz, 7H), 1.48-1.32 (m, 2H), 1.60-1.85 (m, 2H), 2.27 (d, *J* = 13.2 Hz, 9H), 2.45 (s, 3H), 2.42-2.58 (m, 2H), 2.80 (d, *J* = 13.6 Hz, 1H), 3.68-3.76 (m, 1H), 6.63 (d, *J* = 7.6 Hz, 13H), 6.76 (d, *J* = 14.0 Hz, 1H), 7.00-7.18 (m, 2H), 7.20-7.29 (m, 6H), 7.35 (d, *J* = 8.4 Hz, 2H).



(*S*)-**125ca**.^[4,10] Sticky pale yellow wax. Yield = 51% (*c*Hex-AcOEt: 90:10 \rightarrow 70:30). *Ee* = 91%. **HPLC**: Chiralcel-AD: eluent: *n*Hex:IPA = 95:5, flow = 0.6 mL/min, T = 40 °C, *Rt_R* (36.8 min), *Rt_S* (39.8 min). [α]_D = -14.7° (*c* = 0.25, CHCl₃). **¹H-NMR** (400 MHz, CDCl₃) δ 0.52-0.71 (m, 1H), 0.75-

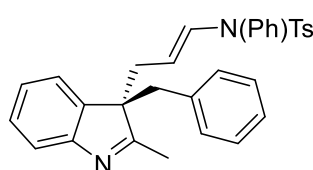
^[12] The reaction was carried out in the presence of (*R*)-**VII**.

0.91 (m, 1H), 1.55-1.62 (m, 2H), 1.65-1.80 (m, 2H), 2.00-2.11 (m, 2H), 2.45 (s, 3H), 2.35-2.57 (m, 2H), 2.78-2.92 (m, 2H), 3.68 (dt, $J = 14.0, 7.2$ Hz, 1H), 6.65 (d, $J = 7.6$ Hz, 2H), 6.75 (d, $J = 13.6$ Hz, 1H), 7.03-7.09 (m, 2H), 7.20-7.24 (m, 6H), 7.31-7.44 (m, 3H).



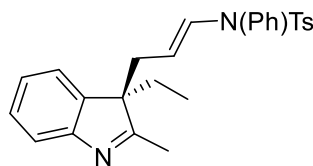
(S)-125da.^[4,10] Pale yellow solid. Yield = 44% (*c*Hex-AcOEt: 80:20). **MP** = 123-125 °C. *Ee* = 88%. **HPLC**: Chiralcel-AD: eluent: *n*Hex:IPA = 80:20, flow = 0.6 mL/min, T = 40 °C, R_{tR} (9.2 min), R_{tS} (9.9 min). $[\alpha]_D = -8.3^\circ$ ($c = 0.30$, CHCl₃, *ee* = 76%). **¹H-NMR** (400 MHz, CDCl₃) δ 0.81-0.92

(m, 3H), 1.24-1.38 (m, 3H), 1.75-1.90 (m, 2H), 2.00-2.15 (m, 2H), 2.19-2.35 (m, 2H), 2.36-2.43 (m, 1H), 2.46 (s, 3H), 2.48-2.55 (m, 1H), 2.55-2.71 (m, 1H), 3.64 (dt, $J = 14.0, 7.6$ Hz, 1H), 6.65 (d, $J = 7.6$ Hz, 2H), 6.71 (d, $J = 14.0$ Hz, 1H), 7.04 (d, $J = 7.2$ Hz, 1H), 7.09 (dt, $J = 1.2, 7.2$ Hz, 1H), 7.27-7.00 (m, 6H), 7.36 (d, $J = 8.0$ Hz, 2H), 7.41 (d, $J = 7.2$ Hz, 1H).



(S)-125ea.^[4,10] Pale yellow wax. Yield = 87% (*c*Hex-AcOEt: 80:20). *Ee* = 93%. **HPLC**: Chiralcel-AD: eluent: *n*Hex:IPA = 80:20, flow = 0.7 mL/min, T = 40 °C, R_{tS} (10.8 min), R_{tR} (11.9 min). $[\alpha]_D = -29.0^\circ$ ($c = 0.5$, CHCl₃).

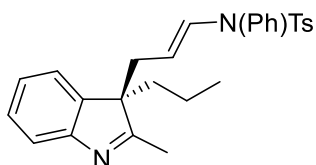
¹H-NMR (400 MHz, CDCl₃) δ 2.18 (s, 3H), 2.41 (s, 3H), 2.49 (dd, $J = 8.4, 13.6$ Hz, 1H), 2.61 (dd, $J = 7.6, 13.6$ Hz, 1H), 2.81 (d, $J = 13.2$ Hz, 1H), 3.13 (d, $J = 13.2$ Hz, 1H), 3.59-3.66 (m, 1H), 6.54 (d, $J = 7.6$ Hz, 2H), 6.71 (d, $J = 6.8$ Hz, 2H), 6.74 (d, $J = 14.4$ Hz, 1H), 6.91 (d, $J = 7.2$ Hz, 1H), 7.02-7.09 (m, 3H), 7.12-7.20 (m, 6H), 7.24-7.28 (m, 4H).



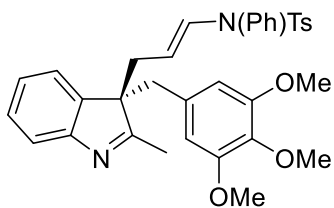
(R)-125fa. Pale yellow solid. Yield = 72% (*c*Hex-AcOEt: 85:15 → 70:30). **MP** = 50-52 °C. *Ee* = 91%. **HPLC**: Chiralcel-AD: eluent: *n*Hex:IPA = 80:20, flow = 0.7 mL/min, T = 40 °C, R_{tR} (9.1 min), R_{tS} (9.9 min). $[\alpha]_D = +56^\circ$ ($c = 0.4$, CHCl₃, *ee* = 87%). **¹H-NMR** (400 MHz,

CDCl₃) δ 0.35 (t, $J = 7.4$ Hz, 3H), 1.75-1.80 (m, 1H), 1.84-1.91 (m, 1H), 2.12 (s, 3H), 2.34 (dd, $J = 7.6, 13.6$ Hz, 1H), 2.45 (s, 3H), 2.51 (dd, $J = 7.6, 13.6$ Hz, 1H), 3.66-3.73 (m, 1H), 6.61 (d, $J = 8.0$

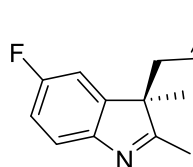
Hz, 2H), 6.77 (d, $J = 7.6$ Hz, 1H), 7.05-7.12 (m, 2H), 7.17-7.26 (m, 6H), 7.31 (d, $J = 8.4$ Hz, 2H), 7.40 (d, $J = 7.2$ Hz, 1H). $^{13}\text{C-NMR}$ (100 MHz, CDCl_3) δ 8.2, 16.1, 21.6, 28.6, 30.9, 37.0, 105.1, 119.4, 121.9, 127.3(2C), 127.4, 128.7, 129.2(2C), 129.5(2C), 129.9(2C), 131.1, 135.4, 136.1, 141.2, 143.7, 155.2, 185.1. **LC-MS** (m/z): 445 $[\text{M}+\text{H}]^+$. **Anal. calcd** for ($\text{C}_{27}\text{H}_{28}\text{N}_2\text{O}_2\text{S}$: 444.19): C, 72.94; H, 6.35, N, 7.20; Found: C, 72.88, H, 6.28, N, 7.19.



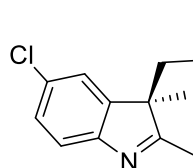
(R)-125ga. Pale yellow oil. Yield = 98% (*c*Hex-AcOEt: 85:15 \rightarrow 70:30). $E_e = 92\%$. **HPLC**: Chiralcel-AD: eluent: *n*Hex:IPA = 90:10, flow = 0.7 mL/min, T = 40 °C, R_{tR} (17.3 min), R_{tS} (19.1 min). $[\alpha]_D = +61.1$ ($c = 0.7$, CHCl_3). $^1\text{H-NMR}$ (400 MHz, CDCl_3) δ 0.69 (t, $J = 4.0$ Hz, 3H), 1.62-1.69 (m, 3H), 1.75-1.81 (m, 1H), 2.09 (s, 3H), 2.32 (dd, $J = 7.6, 14.0$ Hz, 1H), 2.42 (s, 3H), 2.48 (dd, $J = 7.6, 13.2$ Hz, 1H), 3.62-3.70 (m, 1H), 6.59 (d, $J = 6.8$ Hz, 2H), 6.74 (d, $J = 14.0$ Hz, 1H), 7.03-7.09 (m, 3H), 7.16-7.24 (m, 6H), 7.29 (d, $J = 8.0$ Hz, 2H), 7.37 (d, $J = 7.6$ Hz, 1H). $^{13}\text{C-NMR}$ (100 MHz, CDCl_3) δ 14.2, 16.2, 17.2, 21.6, 30.9, 37.2, 38.1, 105.0, 119.5, 121.6, 124.8, 127.3(2C), 127.4, 128.7, 129.2(2C), 129.4(2C), 129.9(2C), 131.1, 135.5, 136.1, 141.6, 143.7, 185.3. **LC-MS** (m/z): 459 $[\text{M}+\text{H}]^+$. **Anal. calcd** for ($\text{C}_{28}\text{H}_{30}\text{N}_2\text{O}_2\text{S}$: 458.20): C, 73.33; H, 6.59, N, 6.11; Found: C, 73.48, H, 6.41, N, 6.10.



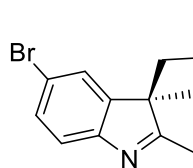
(R)-125ha. White solid. Yield = 42% (*c*Hex-AcOEt: 80:20 \rightarrow 70:30). $M_p = 63-65$ °C. $E_e = 91\%$. **HPLC**: Chiralcel-IA: eluent: *n*Hex:IPA = 75:25, flow = 0.7 mL/min, T = 40 °C, R_{tR} (13.9 min), R_{tS} (22.0 min). $[\alpha]_D = +1.1$ ($c = 0.35$, CHCl_3). $^1\text{H-NMR}$ (400 MHz, CDCl_3) δ 2.16 (s, 3H), 2.44 (s, 3H), 2.50 (dd, $J = 7.6, 14.0$ Hz, 1H), 2.66 (dd, $J = 7.6, 14.0$ Hz, 1H), 2.80 (d, $J = 14.0$ Hz, 1H), 3.17 (d, $J = 14.0$ Hz, 1H), 3.56 (s, 6H), 3.64-3.72 (m, 1H), 3.73 (s, 3H), 5.86 (s, 2H), 6.58 (d, $J = 7.6$ Hz, 2H), 6.80 (d, $J = 14.0$ Hz, 1H), 7.01-7.26 (m 8H), 7.30-7.32 (m, 3H). $^{13}\text{C-NMR}$ (100 MHz, CDCl_3) δ 16.7, 21.6, 36.7, 41.9, 55.8(2C), 60.8, 63.5, 104.5, 106.0, 119.8, 122.7, 124.6, 127.3(2C), 127.6, 128.7(2C), 129.2(2C), 129.5(2C), 129.8(2C), 131.3, 131.5, 135.3, 136.0, 136.6, 141.1, 143.8, 152.3(2C), 155.1, 184.2. **LC-MS** (m/z): 597 $[\text{M}+\text{H}]^+$. **Anal. calcd** for ($\text{C}_{35}\text{H}_{36}\text{N}_2\text{O}_5\text{S}$: 596.23): C, 70.45; H, 6.08, N, 4.69; Found: C, 70.33, H, 6.15, N, 4.61.



(R)-125ia. Pale yellow solid. Yield = 64% (cHex-AcOEt: 80:20). *Ee* = 92%. *Mp* = 53-55 °C. **HPLC:** Chiralcel-AD: eluent: *n*Hex:IPA = 80:20, flow = 0.7 mL/min, T = 40 °C, *Rt_R* (9.4 min), *Rt_S* (10.5 min). $[\alpha]_D = +57.7$ (*c* = 0.35, CHCl₃). **¹H-NMR** (400 MHz, CDCl₃) δ 1.21 (s, 3H), 2.10 (s, 3H), 2.31 (dd, *J* = 7.6, 13.6 Hz, 1H), 2.42 (s, 3H), 2.43 (dd, *J* = 7.6, 13.6 Hz, 1H), 3.64-3.69 (m, 1H), 6.61 (d, *J* = 8.0 Hz, 2H), 6.74-6.78 (m, 2H), 6.86 (dt, *J* = 2.0, 8.4 Hz, 1H), 7.17-7.24 (m, 5H), 7.27-7.33 (m, 1H), 7.33 (d, *J* = 8.0 Hz, 1H). **¹³C-NMR** (100 MHz, CDCl₃) δ 15.8, 21.0, 21.6, 37.5, 58.6 (d, *J* = 1.5 Hz, 1C), 104.7, 109.3 (d, *J* = 18.2 Hz, 1C), 113.9 (d, *J* = 17.6 Hz, 1C), 120.1 (d, *J* = 6.8 Hz, 1C), 127.2(2), 128.8, 129.2(2C), 129.5(2C), 129.8(2C), 131.5, 135.3, 136.1, 143.9, 145.2 (d, *J* = 6.8 Hz, 1C), 150.1, 161.1 (d, *J* = 181.1 Hz, 1C), 185.8 (d, *J* = 2.3 Hz, 1C). **LC-MS** (*m/z*): 471 [M+Na]⁺, 919 [2M+Na]⁺. **Anal. calcd** for (C₂₆H₂₅FN₂O₂S: 448.16): C, 69.62; H, 5.62, N, 7.13; Found: C, 69.55, H, 5.58, N, 7.00.

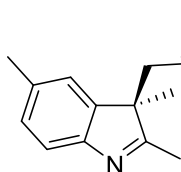


(R)-125ja. White solid. Yield = 91% (cHex-AcOEt: 85:15). *Mp* = 88-90 °C. *Ee* = 89%. **HPLC:** Chiralcel-AD: eluent: *n*Hex:IPA = 80:20, flow = 0.7 mL/min, T = 40 °C, *Rt_R* (10.6 min), *Rt_S* (11.4 min). $[\alpha]_D = +79.0$ (*c* = 1.1, CHCl₃, *ee* = 78%). **¹H-NMR** (400 MHz, CDCl₃) δ 1.24 (s, 3H), 2.15 (s, 3H), 2.32 (dd, *J* = 8.0, 14.4 Hz, 1H), 2.45 (s, 3H), 2.47 (dd, *J* = 8.0, 14.4 Hz, 1H), 3.38-3.74 (m, 1H), 6.69 (d, *J* = 7.6 Hz, 2H), 6.84 (d, *J* = 14.0 Hz, 1H), 7.05 (s, 1H), 7.18-7.34 (m, 7H), 7.37 (d, *J* = 8.0 Hz, 2H). **¹³C-NMR** (100 MHz, CDCl₃) δ 15.8, 21.0, 21.6, 37.4, 58.6, 104.6, 120.4, 122.3, 127.2(2C), 127.7, 128.9, 129.3(2C), 129.6(2C), 129.9(2C), 130.7, 131.6, 135.4, 136.1, 143.9, 145.1, 152.7, 186.7. **LC-MS** (*m/z*): 487 [M+Na]⁺, 503 [M+K]⁺, 951 [2M+Na]⁺. **Anal. calcd** for (C₂₆H₂₅ClN₂O₂S: 464.13): C, 67.16; H, 5.42, N, 7.62; Found: C, 67.01, H, 5.36, N, 7.59.



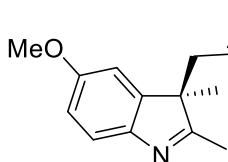
(R)-125ka. Pale yellow solid. Yield = 60% (cHex-AcOEt: 80:20). *Mp* = 124-125 °C. *Ee* = 86%. **HPLC:** Chiralcel-AD: eluent: *n*Hex:IPA = 90:10, flow = 0.9 mL/min, T = 40 °C, *Rt_R* (16.8 min), *Rt_S* (17.7 min). $[\alpha]_D = +118.6$ (*c* = 0.58, CHCl₃). **¹H-NMR** (400 MHz, CDCl₃) δ 1.21

(s, 3H), 2.11 (s, 3H), 2.28 (dd, $J = 7.6, 13.6$ Hz, 1H), 2.41 (s, 3H), 2.43 (dd, $J = 7.2, 13.6$ Hz, 1H), 3.65-3.72 (m, 1H), 6.65 (d, $J = 7.6$ Hz, 2H), 6.82 (d, $J = 13.6$ Hz, 1H), 7.16 (s, 1H), 7.18-7.25 (m, 6H), 7.30-7.36 (m, 3H). $^{13}\text{C-NMR}$ (100 MHz, CDCl_3) δ 15.8, 21.0, 21.6, 37.4, 58.6, 104.6, 118.6, 120.9, 125.2, 127.7(2C), 128.9, 129.3(2C), 129.6(2C), 129.9(2C), 130.6, 135.4, 136.1, 143.9, 145.8, 153.1, 186.8. **LC-MS** (m/z): 286 $[\text{M-indole}]^+$. **Anal. calcd** for ($\text{C}_{26}\text{H}_{25}\text{BrN}_2\text{O}_2\text{S}$: 508.08): C, 61.30; H, 4.95, N, 5.50; Found: C, 61.19, H, 4.87, N, 5.61.



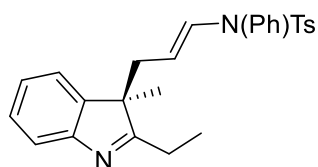
(R)-125la.^[4] Pale yellow solid. Yield = 98% (*c*Hex-AcOEt: 90:10 \rightarrow 70:30). *Ee* = 72%. **Mp** = 129-130 °C. **HPLC**: Chiralcel-AD: eluent: *n*Hex:IPA = 80:20, flow = 0.7 mL/min, T = 40 °C, R_{t_S} (10.4 min), R_{t_R} (11.1 min). $[\alpha]_D = +83.1$ ($c = 0.65$, CHCl_3). $^1\text{H-NMR}$ (400

MHz, CDCl_3) δ 1.24 (s, 3H), 2.14 (s, 3H), 2.20-2.30 (m, 1H), 2.33 (s, 3H), 2.45 (s, 3H), 2.46-2.50 (m, 1H), 3.76-3.82 (m, 1H), 6.70 (d, $J = 7.2$ Hz, 2H), 6.83 (d, $J = 14.0$ Hz, 1H), 6.87 (s, 1H), 7.04 (d, $J = 8.0$ Hz, 1H), 7.23-7.31 (m, 6H), 7.36 (d, $J = 8.0$ Hz, 2H).

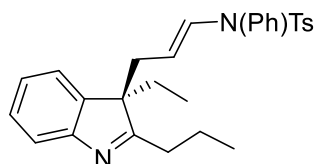


(R)-125ma. Pale brown solid. Yield = 60% (*c*Hex-AcOEt: 85:15). *Ee* = 92%. **Mp** = 108-110 °C. **HPLC**: Chiralcel-IA: eluent: *n*Hex:IPA = 80:20, flow = 0.7 mL/min, T = 40 °C, R_{t_S} (11.7 min), R_{t_R} (13.8 min). $[\alpha]_D = +29.8^\circ$ ($c = 0.32$, CHCl_3). $^1\text{H-NMR}$ (400

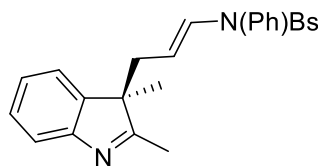
MHz, CDCl_3) δ 1.23 (s, 3H), 2.08 (s, 3H), 2.29 (dd, $J = 8.0, 14.4$ Hz, 1H), 2.40 (s, 3H), 2.43 (dd, $J = 8.0, 14.4$ Hz, 1H), 3.67-3.76 (m, 1H), 3.74 (s, 3H), 6.60 (d, $J = 2.4$ Hz, 1H), 6.64 (d, $J = 7.2$ Hz, 1H), 6.71 (dd, $J = 2.4, 8.0$ Hz, 1H), 6.80 (d, $J = 14.0$ Hz, 1H), 7.15-7.21 (m, 4H), 7.26 (d, $J = 8.4$ Hz, 1H), 7.32 (d, $J = 8.4$ Hz, 1H). $^{13}\text{C-NMR}$ (100 MHz, CDCl_3) δ 15.8, 21.4, 21.6, 37.6, 55.6, 58.2, 105.2, 108.0, 112.5, 119.8, 127.2(2C), 128.7, 129.2(2C), 129.5(2C), 130.0(2C), 131.2, 135.4, 136.2, 143.8, 144.9, 157.7, 183.4. **Anal. calcd** for ($\text{C}_{27}\text{H}_{28}\text{N}_2\text{O}_3\text{S}$: 460.18): C, 70.41; H, 6.13, N, 6.08; Found: C, 70.31, H, 6.09, N, 6.00.



(R)-125na. Pale yellow oil. Yield = 77% (*c*Hex-AcOEt: 90:10→80:20). *Ee* = 92%. **HPLC:** Chiralcel-AD: eluent: *n*Hex:IPA = 85:15, flow = 0.7 mL/min, T = 40 °C, *Rt_S* (9.3 min), *Rt_R* (9.8 min). $[\alpha]_{\text{D}} = +53.2^{\circ}$ (*c* = 0.25, CHCl₃). **¹H-NMR** (400 MHz, CDCl₃) δ 1.23 (s, 3H), 1.24 (t, *J* = 9.2 Hz, 3H), 2.32-2.40 (m, 2H), 2.44 (s, 3H), 2.46-2.52 (m, 2H), 3.65-3.72 (m, 1H), 6.64 (d, *J* = 7.6 Hz, 2H), 6.73 (d, *J* = 13.6 Hz, 1H), 7.10-7.11 (m, 2H), 7.20-7.31 (m, 7H) 7.48 (d, *J* = 8.0 Hz, 1H). **¹³C-NMR** (100 MHz, CDCl₃) δ 10.2, 21.5, 21.6, 23.3, 26.9, 37.8, 105.1, 119.7, 121.5, 124.9, 127.3(2C), 127.4, 128.9, 129.2(2C), 129.5(2C), 129.9(2C), 131.1, 135.4, 136.1, 143.7, 144.3, 190.0. **LC-MS** (*m/z*): 287 [M-indole]⁺, 467 [2M+Na]⁺. **Anal. calcd** for (C₂₇H₂₈N₂O₂S: 444.19): C, 72.94; H, 6.35, N, 6.30; Found: C, 72.77, H, 6.21, N, 6.19.



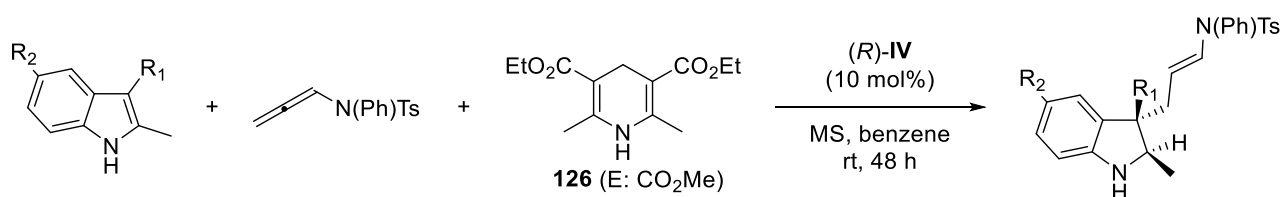
(R)-125pa. White solid. Yield = 69% (*c*Hex-AcOEt: 90:10). *Ee* = 87%. **Mp** = 105-108 °C. **HPLC:** Chiralcel-AD: eluent: *n*Hex:IPA = 85:15, flow = 0.7 mL/min, T = 40 °C, *Rt_S* (7.6 min), *Rt_R* (8.7 min). $[\alpha]_{\text{D}} = +39.6^{\circ}$ (*c* = 0.7, CHCl₃). **¹H-NMR** (400 MHz, CDCl₃) δ 0.34 (t, *J* = 7.6 Hz, 3H), 0.99 (t, *J* = 7.2 Hz, 3H), 1.73-2.05 (m, 4H), 2.32-2.37 (m, 3H), 2.44 (s, 3H), 2.45-2.49 (m, 1H), 3.64-3.72 (m, 1H), 6.62 (d, *J* = 7.2 Hz, 2H), 6.73 (d, *J* = 13.6 Hz, 1H), 7.06-7.11 (m, 2H), 7.21-7.30 (m, 8H) 7.46 (d, *J* = 7.2 Hz, 1H).



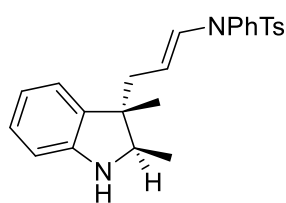
(R)-3al. White wax. Yield = 82% (*c*Hex-AcOEt: 70:30→60:40). *Ee* = 94%. **HPLC:** Chiralcel-AD: eluent: *n*Hex:IPA = 85:15, flow = 0.7 mL/min, T = 40 °C, *Rt_S* (11.6 min), *Rt_R* (12.4 min). $[\alpha]_{\text{D}} = 75.5$ (*c* = 0.4, CHCl₃). **¹H-NMR** (400 MHz, CDCl₃) δ 1.24 (s, 3H), 2.15 (s, 3H), 2.34 (dd, *J* = 8.4, 13.6 Hz, 1H), 2.49 (dd, *J* = 8.0, 113.6 Hz, 1H), 3.69-3.76 (m, 1H), 6.61 (d, *J* = 8.0 Hz, 2H), 6.78 (d, *J* = 13.6 Hz, 2H), 7.09-7.10 (m, 2H), 7.18-7.26 (m, 4H), 7.40-7.45 (m, 5H), 7.56-7.59 (m, 1H). **¹³C-NMR** (100 MHz, CDCl₃) δ 15.8, 21.3, 37.4, 58.2, 105.5, 119.6, 121.7, 124.9, 127.2, 127.5(2C), 128.8, 128.9(2C), 129.2(2C), 129.8(2C), 131.1, 132.9, 136.0, 138.3, 143.2, 154.2, 186.0.

LC-MS (m/z): 272 [M-indole]⁺. **Anal. calcd** for (C₂₅H₂₄N₂O₂S: 416.16): C, 72.09; H, 5.81, N, 6.73; Found: C, 72.22, H, 5.71, N, 6.65.

General procedure for the enantioselective Brønsted acid cascade (dearomatization/hydrogenation) sequence.



A dried two-necked flask was charged with 1 mL of anhydrous benzene and 25 mg of dried 5 Å MS. Then, 50 μmol (14 mg) of allenamide **124a**, 0.1 mmol of Hantzsch ester and 0.1 mmol of the desired indole (2 eq. with respect to **124a**) were added in sequence. After adjusting the temperature, the BINOL-based phosphoric acid (*R*)-**IV** (5-10 mol%) was added. The reaction was stirred at the same temperature for 48 h, the solvent evaporated and the crude directly purified via flash-chromatography.^[13]

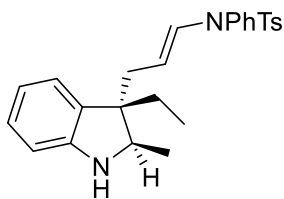


(*2R,3S*)-**127aa**. White wax. Yield = 51% (*c*Hex-AcOEt = 80:20). *Dr* = 96:4. *Ee* = 99% (major), 33% (minor). [α]_D = -65.5° (*c* = 0.65, CHCl₃).

HPLC: Chiralcel-IA: eluent: *n*Hex:IPA = 90:10, flow = 0.8 mL/min, *T* = 40 °C, *Rt*_(*2R,3S*) (12.3 min), *Rt*_(minor II diast.) (15.6 min), *Rt*_(major II diast.) (17.1

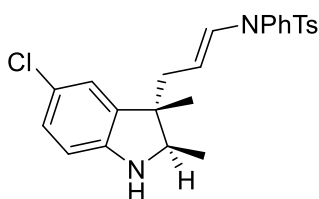
min), *Rt*_(*2S,3R*) (18.1 min). **¹H-NMR** (400 MHz, CDCl₃) δ (major diast.) 1.08 (s, 3H), 1.15 (d, *J* = 6.4 Hz, 3H), 1.86 (dd, *J* = 9.2, 14.0 Hz, 1H), 2.11 (dd, *J* = 9.2, 14.0 Hz, 1H), 2.40 (s, 3H), 3.48 (q, *J* = 6.4 Hz, 1H), 4.21-4.26 (m, 1H), 6.46-6.55 (m, 3H), 6.72 (d, *J* = 14.4 Hz, 1H), 6.87-6.92 (m, 3H), 7.21-7.23 (m, 3H), 7.28-7.31 (m, 2H), 7.45 (d, *J* = 8.4 Hz, 2H). **¹³C-NMR** (100 MHz, CDCl₃) δ (major diast.) 13.9, 21.6, 22.5, 34.5, 46.5, 66.0, 109.0, 123.7, 127.2, 127.4(2C), 128.8, 129.3(2C), 129.5(2C), 130.1(2C), 130.6, 136.0, 136.9, 143.6. **LC-MS** (m/z): 447 [M+H]⁺, 469 [M+Na]⁺.

^[13] In some cases, the product was isolated with small amounts of the reduced form of the HE.



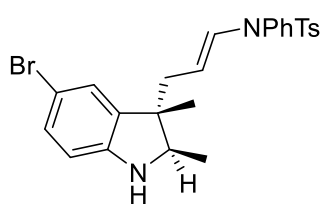
(*2R,3S*)-**127fa**. White yellow solid. Yield = 49% (cHex-AcOEt = 90:10). *Dr* = 96:4. *Ee* = 99% (major), 33% (minor). **HPLC**: Chiralcel-AD: eluent: *n*Hex:IPA = 95:5, flow = 0.7 mL/min, T = 40 °C, *Rt*_(*2R,3S*) (29.9 min), *Rt*_(minor II diast.) (39.8 min), *Rt*_(major II diast.) (44.4 min), *Rt*_(*2S,3R*) (50.5 min). **¹H-NMR**

(400 MHz, CDCl₃) δ (major diast.) 0.85 (t, *J* = 7.4 Hz, 3H), 1.14 (d, *J* = 6.4 Hz, 3H), 1.45-1.50 (m, 1H), 1.51-1.63 (m, 1H), 1.98 (dd, *J* = 7.6, 13.6 Hz, 1H), 2.20 (dd, *J* = 6.8, 13.6 Hz, 1H), 2.43 (s, 3H), 3.66 (q, *J* = 7.2 Hz, 1H), 4.21-4.32 (m, 1H), 6.48-6.57 (m, 2H), 6.79 (d, *J* = 14.4 Hz, 1H), 6.82-6.98 (m, 3H), 7.20-7.22 (m, 2H), 7.28-7.32 (m, 3H), 7.49 (d, *J* = 8.4 Hz, 2H). **¹³C-NMR** (100 MHz, CDCl₃) δ (major diast.) 8.8, 15.4, 21.6, 26.9, 33.0, 50.0, 61.6, 109.1, 117.9, 124.2, 127.0, 127.4, 128.7, 129.2(2C), 129.5(2C), 129.9, 130.1(2C), 134.3, 136.0, 143.6, 149.9. **LC-MS** (*m/z*): 447 [M+H]⁺, 469 [M+Na]⁺.



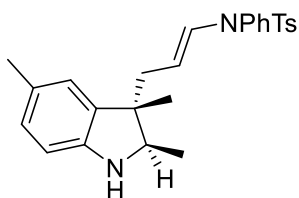
(*2R,3S*)-**127ja**. White solid. Yield = 72% (cHex-AcOEt = 85:15). *Dr* = 93:7. *Mp* = 58-60 °C. *Ee* = 94% (major), 80% (minor). [α]_D = -55.1° (*c* = 0.80, CHCl₃). **HPLC**: Chiralcel-AD: eluent: *n*Hex:IPA = 80:20, flow = 0.7 mL/min, T = 40 °C, *Rt*_(*2R,3S*) (8.8 min), *Rt*_(minor II diast.) (10.9 min),

*Rt*_(*2S,3R*) (11.1 min), *Rt*_(major II diast.) (11.7 min). **¹H-NMR** (400 MHz, CDCl₃) δ (major diast.) 1.10 (s, 3H), 1.17 (d, *J* = 6.4 Hz, 3H), 1.87 (dd, *J* = 8.4, 13.2 Hz, 1H), 2.17 (dd, *J* = 7.2, 13.2 Hz, 1H), 2.46 (s, 3H), 3.55 (q, *J* = 6.4 Hz, 1H), 4.35-4.44 (m, 1H), 6.44 (d, *J* = 8.4 Hz, 1H), 6.48 (d, *J* = 2.0 Hz, 1H), 6.80 (d, *J* = 14.0 Hz, 1H), 6.86 (dd, *J* = 3.2, 12.0 Hz, 1H), 6.92-6.95 (m, 2H), 7.26-7.28 (m, 2H), 7.37-7.39 (m, 2H), 7.50 (d, *J* = 8.0 Hz, 2H). **¹³C-NMR** (100 MHz, CDCl₃) δ (major diast.) 13.8, 21.6, 22.3, 34.1, 46.8, 66.3, 108.1, 109.9, 122.6, 124.0, 126.8, 127.3(2C), 128.9, 129.4(2C), 129.6(2C), 130.1(2C), 130.8, 135.8, 136.7, 138.1, 143.7, 148.2. **LC-MS** (*m/z*): 467 [M+H]⁺, 489 [M+Na]⁺.



(*2R,3S*)-**127ka**. White solid. Yield = 60% (*c*Hex-AcOEt = 80:20). *Dr* = 12:1. *Ee* = 96% (major), 77% (minor). **HPLC**: Chiralcel-IA: eluent: *n*Hex:IPA = 85:15, flow = 0.7 mL/min, T = 40 °C, *Rt*_(*2R,3S*) (11.0 min), *Rt*_(minor II diast.) (14.0 min), *Rt*_(*2S,3R*) (14.8 min), *Rt*_(major II diast) (15.6 min).

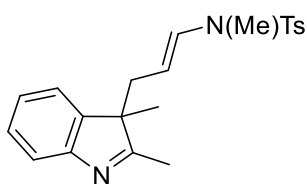
¹H-NMR (400 MHz, CDCl₃) δ (major diast.) 1.08 (s, 3H), 1.14 (d, *J* = 6.4 Hz, 3H), 1.83 (dd, *J* = 8.8, 13.6 Hz, 1H), 2.14 (dd, *J* = 6.8, 13.6 Hz, 1H), 2.43 (s, 3H), 3.50 (q, *J* = 6.8 Hz, 1H), 4.13-4.20 (m, 1H), 6.37 (d, *J* = 8.4 Hz, 1H), 6.57 (d, *J* = 2.0 Hz, 1H), 6.78 (d, *J* = 13.6 Hz, 1H), 6.90-6.93 (m, 1H), 6.97 (dd, *J* = 2.0, 8.4 Hz, 1H), 7.24-7.22 (m, 3H), 7.35-7.37 (m, 3H), 7.47 (d, *J* = 8.0 Hz, 2H). **¹³C-NMR** (100 MHz, CDCl₃) δ (major diast.) 13.8, 21.6, 22.3, 34.1, 46.8, 66.2, 108.1, 109.8, 110.5, 126.8, 127.3, 128.9, 129.5, 129.6, 129.7, 130.1, 130.8, 135.8, 136.7, 138.5, 143.7, 148.7. **LC-MS** (*m/z*): 513 [M+H]⁺, 535 [M+Na]⁺.



(*2R,3S*)-**127la**. White solid. Yield = 44% (*c*Hex-AcOEt = 90:10). *Dr* = 92:8. *Mp* = 82-84 °C. *Ee* = 94% (major), nd (minor). **HPLC**: Chiralcel-ID: eluent: *n*Hex:IPA = 90:10, flow = 0.8 mL/min, T = 40 °C, *Rt*_(*2R,3S*) (19.9 min), *Rt*_(*2S,3R*) (21.2 min), *Rt*_(minor diast.) (22.5 min). **¹H-NMR** (400

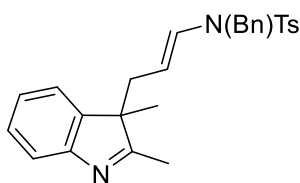
MHz, CDCl₃) δ (major diast.) 1.09 (s, 3H), 1.15 (d, *J* = 6.4 Hz, 3H), 1.51 (dd, *J* = 9.6, 13.6 Hz, 1H), 2.05 (s, 3H), 2.13 (dd, *J* = 9.6, 13.6 Hz, 1H), 2.45 (s, 3H), 3.48 (q, *J* = 7.2 Hz, 1H), 4.20-4.28 (m, 1H), 6.31 (s, 1H), 6.44 (d, *J* = 4.0 Hz, 1H), 6.70 (d, *J* = 8.0 Hz, 1H), 6.81 (d, *J* = 14.0 Hz, 1H), 6.92-6.94 (m, 2H), 7.23-7.25 (m, 3H), 7.32-7.38 (m, 3H), 7.50 (d, *J* = 8.0 Hz, 1H). **¹³C-NMR** (100 MHz, CDCl₃) δ (major diast.) 14.0, 20.8, 21.6, 22.3, 34.0, 46.4, 66.1, 109.2, 109.4, 124.5, 127.3, 127.4(2C), 128.7, 129.3(2C), 129.5(2C), 130.1(2C), 130.3, 135.8, 136.9, 138.1, 143.6, 147.3. **LC-MS** (*m/z*): 447 [M+H]⁺, 469 [M+Na]⁺.

Other substrates:

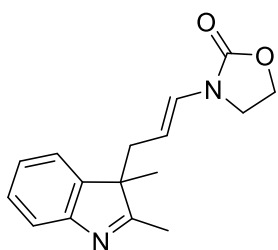


125ab. Pale orange oil. Yield = 98% (*c*Hex-AcOEt: 70:30). *Ee* = 47%. **HPLC**: Chiralcel-AD: eluent: *n*Hex:IPA = 85:15, flow = 0.6 mL/min, T = 40 °C, *Rt*_{major} (12.1 min), *Rt*_{minor} (13.0 min). **¹H-NMR** (400 MHz, CDCl₃) 1.29 (s, 3H), 2.22 (s, 3H), 2.41 (s, 3H), 2.43-2.39 (m, 1H), 2.55 (s, 3H),

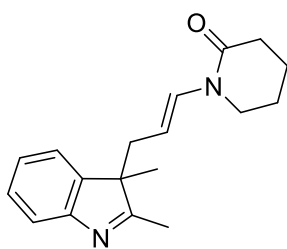
2.60 (dd, $J = 14.0$ Hz, 7.2 Hz, 1H), 4.04-3.91 (m, 1H), 6.66 (d, $J = 13.6$ Hz, 1H), 7.32-7.12 (m, 5H), 7.41 (d, $J = 8.0$ Hz, 2H), 7.46 (d, $J = 7.6$ Hz, 1H). **LC-MS** (m/z): 391 [M+Na]⁺.



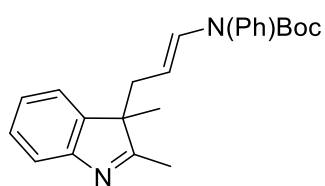
125ad. (Pale Orange solid. Yield = 63% (cHex-AcOEt: 80:20→60:40). **MP** = 50-52 °C. *Ee* = 56%. **HPLC**: Chiralcel-AD: eluent: nHex:IPA = 80:20, flow = 0.7 mL/min, T = 40 °C, $R_{t_{major}}$ (11.3 min), $R_{t_{minor}}$ (14.0 min). **¹H-NMR** (400 MHz, CDCl₃) 1.15 (s, 3H), 2.10 (s, 3H), 2.14 (d, $J = 7.6$ Hz, 1H), 2.39 (d, $J = 7.6$ Hz, 1H), 2.47 (s, 3H), 4.12-4.16 (m, 1H), 4.18 (d, $J = 15.6$ Hz, 1H), 4.32 (d, $J = 15.6$ Hz, 1H), 6.63 (d, $J = 13.6$ Hz, 1H), 6.73 (d, $J = 7.2$ Hz, 1H), 7.04 (t, $J = 7.2$ Hz, 1H), 7.09 (d, $J = 7.6$ Hz, 2H), 7.23-7.25 (m, 6H), 7.41 (d, $J = 7.2$ Hz, 1H), 7.50 (d, $J = 7.6$ Hz, 2H). **LC-MS** (m/z): 467 [M+Na]⁺.



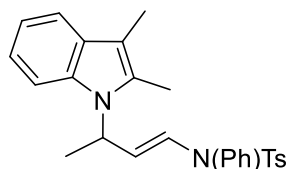
125ae. Pale yellow oil. Yield = 44% (cHex-AcOEt: 70:30→0:100). *Ee* = 54%. **HPLC**: Chiralcel-AD: eluent: nHex:IPA = 88:12, flow = 0.6 mL/min, T = 40 °C, $R_{t_{major}}$ (19.0 min), $R_{t_{minor}}$ (20.4 min). **¹H-NMR** (400 MHz, CDCl₃) δ 1.33 (s, 3H), 2.26 (s, 3H), 2.49 (dd, $J = 14.0, 8.4$ Hz, 1H), 2.66 (dd, $J = 14.0, 6.4$ Hz, 1H), 3.34 (t, $J = 8.0$ Hz, 2H), 3.96 (m, 1H), 4.30 (t, $J = 8.0$ Hz, 2H), 6.58 (d, $J = 14.0$ Hz, 1H), 7.36-7.16 (m, 3H), 7.51 (d, $J = 7.6$ Hz, 1H). **LC-MS** (m/z): 293 [M+Na]⁺, 271 [M+H]⁺.



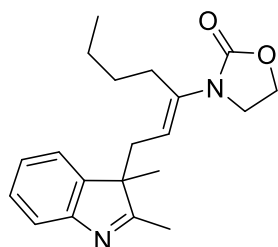
125ag. Pale yellow oil. Yield = 60% (AcOEt-MeOH: 20:1). *Ee* = 12%. **HPLC**: Chiralcel-AD: eluent: nHex:IPA = 85:15, flow = 0.7 mL/min, T = 40 °C, $R_{t_{major}}$ (9.4 min), $R_{t_{minor}}$ (10.1 min). **¹H-NMR** (400 MHz, CDCl₃) δ 1.30 (s, 3H), 1.70 (brs, 4H), 2.23 (s, 3), 2.37 (brs, 2H), 2.48 (dd, $J = 8.4, 13.6$ Hz, 1H), 2.65 (dd, $J = 5.6, 13.6$ Hz, 1H), 2.98 (brs, 2H), 4.14-4.19 (m, 1H), 7.18-7.21 (m, 1H), 7.24-7.30 (m, 3H), 7.49 (d, $J = 7.6$ Hz, 2H). **LC-MS** (m/z): 137 [M-2,3(Me)₂indole], 305 [M+Na]⁺.



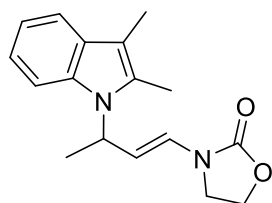
125ac. White solid. Yield = 74% (cHex-AcOEt: 90:10→80:20). *Mp* = 125-127 °C. *Ee* = 67%. **HPLC:** Chiralcel-AD: eluent: *n*Hex:IPA = 92:8, flow = 0.5 mL/min, T = 40 °C, *Rt_{minor}* (10.4 min), *Rt_{major}* (11.1 min). **¹H-NMR** (400 MHz, CDCl₃) δ 1.25 (s, 3H), 1.37 (s, 9H), 2.22 (s, 3H), 2.30 (dd, *J* = 14.0, 7.6 Hz, 1H), 2.45 (dd, *J* = 14.0, 7.6 Hz, 1H), 6.83 (d, *J* = 7.6 Hz, 2H), 3.78 (m, 1H), 7.14-7.04 (m, 2H), 6.92 (d, *J* = 14.0 Hz, 1H), 7.21 (d, *J* = 7.6 Hz, 1H), 7.31-7.22 (m, 3H), 7.48 (d, *J* = 7.6 Hz, 1H). **LC-MS** (*m/z*): 399 [M+Na]⁺.



125ai'. Pale yellow oil. Conv. = 41% (cHex-AcOEt: 90:10). *Ee* = 2%. **HPLC:** Chiralcel-IC: eluent: *n*Hex:IPA = 80:20, flow = 0.7 mL/min, T = 40 °C, *Rt* (10.7 min), *Rt* (11.4 min). **¹H-NMR** (400 MHz, CDCl₃) δ 1.58 (d, *J* = 7.2 Hz, 3H), 2.30 (s, 3H), 2.37 (s, 3H), 2.47 (s, 3H), 4.74 (dd, *J* = 4.4 Hz, 14.4 Hz, 1H), 5.06-5.10 (m, 1H), 6.93-7.24 (m, 7H), 7.30-7.36 (m, 2H), 7.46 (d, *J* = 8.0 Hz, 1H). **LC-MS** (*m/z*): 300 [M-2,3(Me)₂indole+H]⁺, 467 [M+Na]⁺, 483 [M+K]⁺.



125af. Pale yellow oil. Yield = 55% (cHex-AcOEt: 60:40→0:100). *Ee* = 3%. **HPLC:** Chiralcel-AD: eluent: *n*Hex:IPA = 90:10, flow = 0.6 mL/min, T = 40 °C, *Rt_{major}* (15.5 min), *Rt_{minor}* (16.7 min). **¹H-NMR** (400 MHz, CDCl₃) δ 0.90 (t, *J* = 7.2 Hz, 3H), 1.18-1.33 (m, 4H), 1.36 (s, 3H), 2.26 (s, 3H), 2.31-2.46 (m, 2H), 2.50 (dd, *J* = 14.8, 7.2 Hz, 1H), 2.68 (dd, *J* = 14.8, 6.8 Hz, 1H), 3.29 (td, *J* = 8.8, 7.2 Hz, 1H), 3.41 (td, *J* = 8.8, 7.2 Hz, 1H), 4.11-4.30 (m, 3H), 7.15-7.23 (m, 1H), 7.23-7.35 (m, 2H), 7.51 (d, *J* = 7.6 Hz, 1H). **LC-MS** (*m/z*): 327 [M+H]⁺, 675 [2M+Na]⁺.



125ah'. Pale yellow oil. Yield = 35% (cHex-AcOEt: 90:10 → 80:20). *Ee* = 7% (major diastereomer). **HPLC:** Chiralcel-AD: eluent: *n*Hex:IPA = 85:15, flow = 0.6 mL/min, T = 40 °C, *Rt_{minor}* (13.2 min), *Rt_{minor}* (14.1 min). **¹H-NMR** (400 MHz, CDCl₃) δ 1.71 (d, *J* = 6.8 Hz, 3H), 2.25 (s, 3H), 2.38 (s, 3H), 3.60-3.73 (m, 2H), 4.36-4.50 (m, 2H), 5.14-5.27 (m, 2H), 6.93 (d, *J* = 13.2 Hz, 1H), 7.03-7.12 (m, 2H), 7.33-7.40 (m, 1H), 7.46-7.52 (m, 1H). **LC-MS** (*m/z*): 307 [M+Na]⁺.

X-ray structure 125ka.

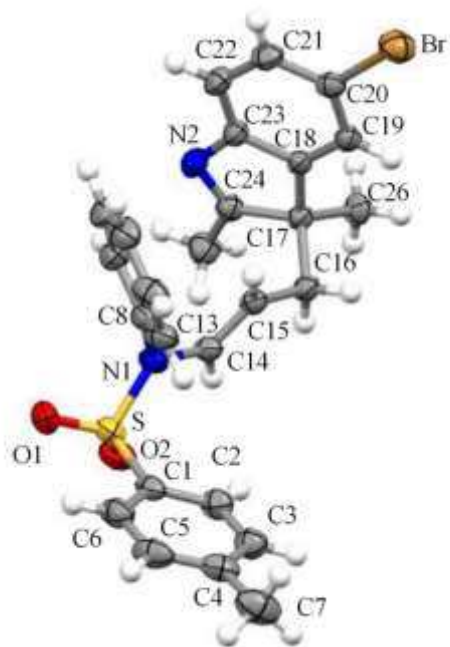


Figure S1. ORTEP drawing of (*R*)-**125ka** with partial labelling scheme. Thermal ellipsoids are drawn at 30% probability level.

Table S3. Crystal data and structure refinement for **125ka**.

Identification code	comp3ka	
Empirical formula	C ₂₆ H ₂₅ BrN ₂ O ₂ S	
Formula weight	509.45	
Temperature	296(2) K	
Wavelength	0.71073 Å	
Crystal system	Orthorhombic	
Space group	P2 ₁ 2 ₁ 2 ₁	
Unit cell dimensions	a = 7.5839(6) Å	α = 90°.
	b = 9.3135(7) Å	β = 90°.
	c = 34.311(3) Å	γ = 90°.
Volume	2423.5(3) Å ³	
Z	4	
Density (calculated)	1.396 Mg/m ³	
Absorption coefficient	1.807 mm ⁻¹	
F(000)	1048	
Crystal size	0.25 x 0.20 x 0.20 mm ³	
Theta range for data collection	2.27 to 28.00°.	
Index ranges	-9<=h<=9, -12<=k<=12, -45<=l<=45	
Reflections collected	27942	
Independent reflections	5700 [R(int) = 0.0317]	
Completeness to theta = 28.00°	99.1 %	
Absorption correction	Empirical	
Max. and min. transmission	0.698 and 0.612	
Refinement method	Full-matrix least-squares on F ²	
Data / restraints / parameters	5700 / 0 / 292	
Goodness-of-fit on F ²	0.941	
Final R indices [I>2sigma(I)]	R ₁ = 0.0351, wR ₂ = 0.0859	
R indices (all data)	R ₁ = 0.0621, wR ₂ = 0.0987	
Absolute structure parameter	0.015(8)	
Largest diff. peak and hole	0.312 and -0.258 e.Å ⁻³	

Table S4. Bond lengths [\AA] and angles [$^\circ$] for **125ka**.

Br-C(20)	1.900(3)	C(11)-H(11)	0.9300
S-O(2)	1.424(2)	C(12)-C(13)	1.382(4)
S-O(1)	1.424(2)	C(12)-H(12)	0.9300
S-N(1)	1.649(2)	C(13)-H(13)	0.9300
S-C(1)	1.754(3)	C(14)-C(15)	1.308(3)
N(1)-C(14)	1.424(3)	C(14)-H(14)	0.9300
N(1)-C(8)	1.441(3)	C(15)-C(16)	1.492(3)
N(2)-C(24)	1.281(3)	C(15)-H(15)	0.9300
N(2)-C(23)	1.425(3)	C(16)-C(17)	1.555(3)
C(1)-C(2)	1.378(4)	C(16)-H(16A)	0.9700
C(1)-C(6)	1.382(4)	C(16)-H(16B)	0.9700
C(2)-C(3)	1.372(4)	C(17)-C(18)	1.508(3)
C(2)-H(2)	0.9300	C(17)-C(24)	1.529(3)
C(3)-C(4)	1.379(4)	C(17)-C(26)	1.542(3)
C(3)-H(3)	0.9300	C(18)-C(19)	1.381(3)
C(4)-C(5)	1.377(5)	C(18)-C(23)	1.397(3)
C(4)-C(7)	1.489(5)	C(19)-C(20)	1.386(4)
C(5)-C(6)	1.394(5)	C(19)-H(19)	0.9300
C(5)-H(5)	0.9300	C(20)-C(21)	1.380(4)
C(6)-H(6)	0.9300	C(21)-C(22)	1.379(4)
C(7)-H(7A)	0.9600	C(21)-H(21)	0.9300
C(7)-H(7B)	0.9600	C(22)-C(23)	1.386(3)
C(7)-H(7C)	0.9600	C(22)-H(22)	0.9300
C(8)-C(9)	1.376(4)	C(24)-C(25)	1.493(4)
C(8)-C(13)	1.384(4)	C(25)-H(25A)	0.9600
C(9)-C(10)	1.384(5)	C(25)-H(25B)	0.9600
C(9)-H(9)	0.9300	C(25)-H(25C)	0.9600
C(10)-C(11)	1.358(6)	C(26)-H(26A)	0.9600
C(10)-H(10)	0.9300	C(26)-H(26B)	0.9600
C(11)-C(12)	1.349(5)	C(26)-H(26C)	0.9600
O(2)-S-O(1)	120.54(15)	C(12)-C(13)-H(13)	120.5
O(2)-S-N(1)	106.38(13)	C(8)-C(13)-H(13)	120.5
O(1)-S-N(1)	106.74(12)	C(15)-C(14)-N(1)	125.4(2)
O(2)-S-C(1)	108.36(13)	C(15)-C(14)-H(14)	117.3

O(1)-S-C(1)	108.04(14)	N(1)-C(14)-H(14)	117.3
N(1)-S-C(1)	105.88(12)	C(14)-C(15)-C(16)	123.1(2)
C(14)-N(1)-C(8)	119.95(19)	C(14)-C(15)-H(15)	118.4
C(14)-N(1)-S	120.02(17)	C(16)-C(15)-H(15)	118.4
C(8)-N(1)-S	118.94(16)	C(15)-C(16)-C(17)	113.59(18)
C(24)-N(2)-C(23)	106.8(2)	C(15)-C(16)-H(16A)	108.8
C(2)-C(1)-C(6)	119.4(3)	C(17)-C(16)-H(16A)	108.8
C(2)-C(1)-S	120.0(2)	C(15)-C(16)-H(16B)	108.8
C(6)-C(1)-S	120.4(2)	C(17)-C(16)-H(16B)	108.8
C(3)-C(2)-C(1)	120.3(3)	H(16A)-C(16)-H(16B)	107.7
C(3)-C(2)-H(2)	119.8	C(18)-C(17)-C(24)	99.25(18)
C(1)-C(2)-H(2)	119.8	C(18)-C(17)-C(26)	112.8(2)
C(4)-C(3)-C(2)	121.7(3)	C(24)-C(17)-C(26)	113.9(2)
C(4)-C(3)-H(3)	119.1	C(18)-C(17)-C(16)	111.7(2)
C(2)-C(3)-H(3)	119.1	C(24)-C(17)-C(16)	110.3(2)
C(3)-C(4)-C(5)	117.4(3)	C(26)-C(17)-C(16)	108.80(19)
C(3)-C(4)-C(7)	121.8(3)	C(19)-C(18)-C(23)	120.5(2)
C(5)-C(4)-C(7)	120.8(3)	C(19)-C(18)-C(17)	132.4(2)
C(4)-C(5)-C(6)	121.9(3)	C(23)-C(18)-C(17)	107.2(2)
C(4)-C(5)-H(5)	119.1	C(18)-C(19)-C(20)	117.0(2)
C(6)-C(5)-H(5)	119.1	C(18)-C(19)-H(19)	121.5
C(1)-C(6)-C(5)	119.1(3)	C(20)-C(19)-H(19)	121.5
C(1)-C(6)-H(6)	120.5	C(21)-C(20)-C(19)	123.0(2)
C(5)-C(6)-H(6)	120.5	C(21)-C(20)-Br	118.36(19)
C(4)-C(7)-H(7A)	109.5	C(19)-C(20)-Br	118.7(2)
C(4)-C(7)-H(7B)	109.5	C(22)-C(21)-C(20)	119.9(2)
H(7A)-C(7)-H(7B)	109.5	C(22)-C(21)-H(21)	120.0
C(4)-C(7)-H(7C)	109.5	C(20)-C(21)-H(21)	120.0
H(7A)-C(7)-H(7C)	109.5	C(21)-C(22)-C(23)	118.0(2)
H(7B)-C(7)-H(7C)	109.5	C(21)-C(22)-H(22)	121.0
C(9)-C(8)-C(13)	119.8(3)	C(23)-C(22)-H(22)	121.0
C(9)-C(8)-N(1)	118.5(3)	C(22)-C(23)-C(18)	121.6(3)
C(13)-C(8)-N(1)	121.7(2)	C(22)-C(23)-N(2)	126.7(2)
C(8)-C(9)-C(10)	119.6(3)	C(18)-C(23)-N(2)	111.7(2)
C(8)-C(9)-H(9)	120.2	N(2)-C(24)-C(25)	122.2(2)
C(10)-C(9)-H(9)	120.2	N(2)-C(24)-C(17)	115.0(2)
C(11)-C(10)-C(9)	120.1(3)	C(25)-C(24)-C(17)	122.8(2)
C(11)-C(10)-H(10)	119.9	C(24)-C(25)-H(25A)	109.5
C(9)-C(10)-H(10)	119.9	C(24)-C(25)-H(25B)	109.5

C(12)-C(11)-C(10)	120.6(3)	H(25A)-C(25)-H(25B)	109.5
C(12)-C(11)-H(11)	119.7	C(24)-C(25)-H(25C)	109.5
C(10)-C(11)-H(11)	119.7	H(25A)-C(25)-H(25C)	109.5
C(11)-C(12)-C(13)	120.8(3)	H(25B)-C(25)-H(25C)	109.5
C(11)-C(12)-H(12)	119.6	C(17)-C(26)-H(26A)	109.5
C(13)-C(12)-H(12)	119.6	C(17)-C(26)-H(26B)	109.5
C(12)-C(13)-C(8)	119.1(3)	H(26A)-C(26)-H(26B)	109.5
H(26A)-C(26)-H(26C)	109.5	C(17)-C(26)-H(26C)	109.5
H(26B)-C(26)-H(26C)	109.5		

3.2 Organocatalytic Enantioselective Synthesis of 1-Vinyl Tetrahydroisoquinoline

Encouraged by the satisfactory results obtained in the enantioselective dearomatization of indoles, we continued our investigation in the metal-free activation of allenamides promoted by chiral phosphoric acids.

Tetrahydroisoquinolines featuring substitution in 1 position (Figure 1) have received notable interest in medicinal and synthetic chemistry due to their pharmacological properties.^[1-3]

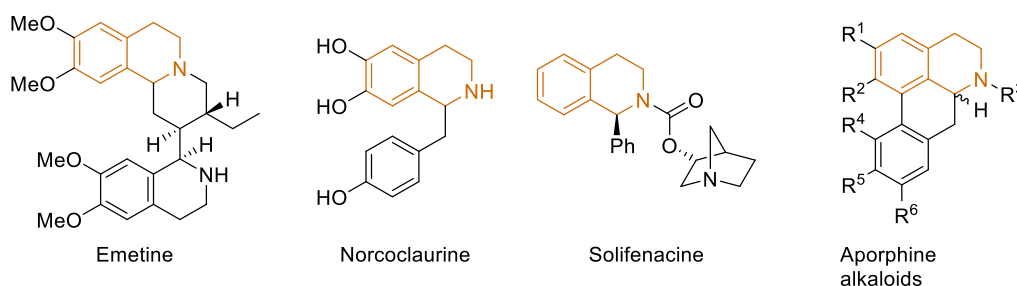
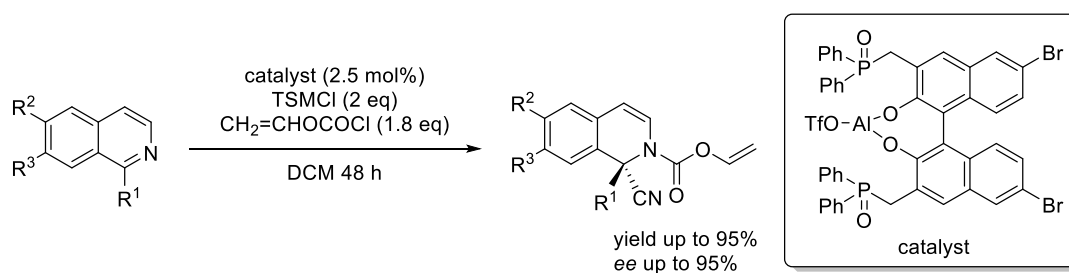


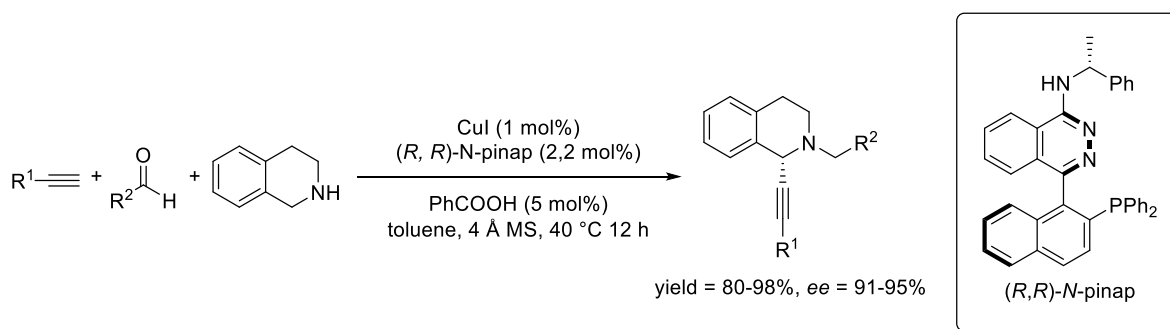
Figure 1: Alkaloids containing tetrahydroisoquinoline scaffold.

The development of new synthetic routes for their preparation must consider the asymmetric formation of a chiral carbon. For this reason, enantioselective catalysis represents a useful way for their preparation through the introduction of a substituent on the C(1)-position. The first enantioselective catalytic variant was introduced by Shibasaki in 2001 (Scheme 1).^[5]



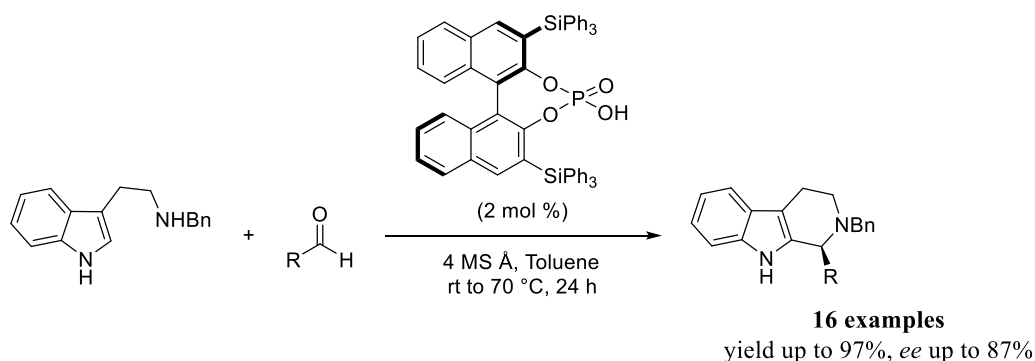
Scheme 1: Enantioselective construction of quaternary stereocenter developed by Shibasaki.

Afterward, several enantioselective methodologies^[6-8] have been reported but, no high enantiomeric excesses were recorded. Subsequently, Ma^[9] reported a new route to functionalize the tetrahydroisoquinolines using copper catalyst with high levels of enantioselectivity (Scheme 2).



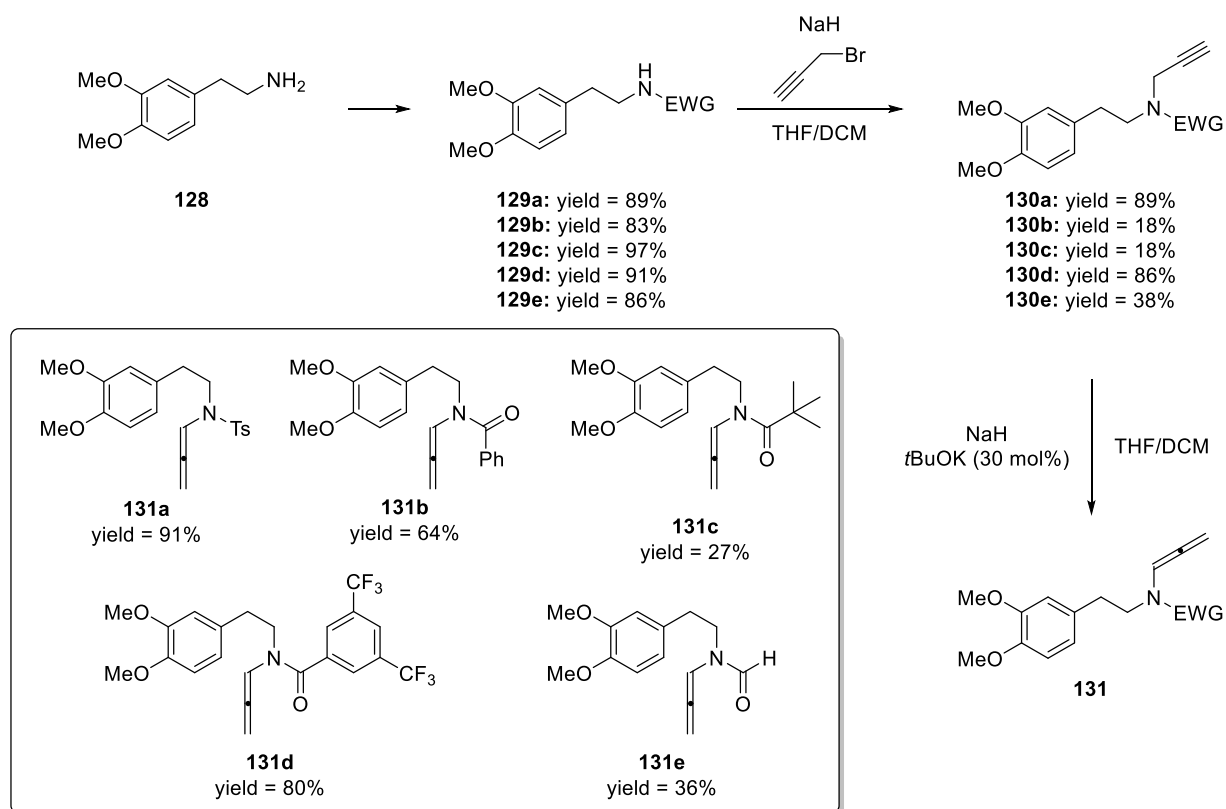
Scheme 2: Enantioselective functionalization of tetrahydroisoquinolines reported by Ma.

A direct metal-free approach for the preparation of these classes of pharmaceutical compounds is represented by the bio-mimetic Pictet-Spengler condensation^[10] of 2-phenylethylamine using Brønsted acids^[11,12] or thiourea^[13] as catalysts. However, this reaction is limited to the use of tryptamine and their derivatives as starting materials (Scheme 3). The reasons for the success of this reaction can be attributed to the presence of the indole. Indeed, the *N*(1)-free is able to form hydrogen bond interactions with the Brønsted acid or the thiourea catalysts and the indolyl core can also makes secondary interactions with aromatic substituent of the catalysts.



Scheme 3: Pictet-Spengler reaction promoted by chiral Brønsted acid

In order to remove the limitations in the use of tryptamine as starting material, we developed a new enantioselective route for the preparation of tetrahydroquinolines through a completely metal-free Friedel-Crafts-type cyclization promoted by chiral Brønsted acids.^[14] In particular, the iminium ion intermediate resulted from the electrophilic activation of allenamides by Brønsted acids could undergo a nucleophilic attack by an electron-rich aromatic ring. We started to investigate our hypothesis preparing several allenamides featuring electron-rich aromatic rings and with different electron-withdrawing groups bonded to the nitrogen (Scheme 4).

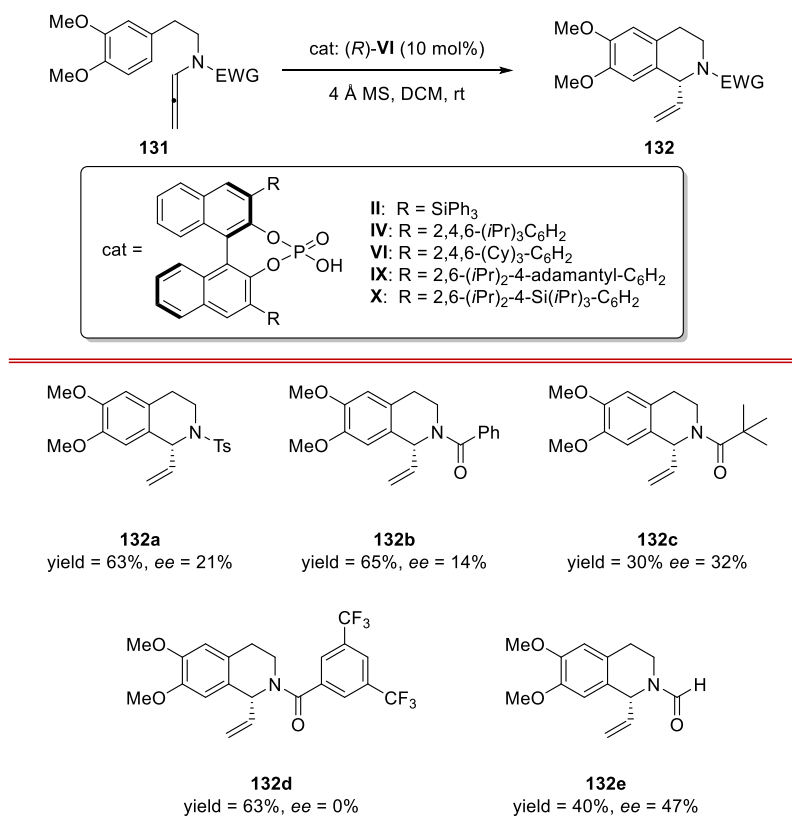


Scheme 4: Preparation of allenamides.

The synthetic procedure chosen for the preparation was not straightforward and some propargylamide **130** were isolated only in low yields despite the numerous efforts to optimize the synthetic step by changing temperature, bases and solvents. For the last step, we used a modified procedure with respect the common conditions reported in literature. Indeed, the isomerization of the propargylamide should take place using a catalytic amount of *t*BuOK, but under these conditions only traces of the allenamides desired were isolated. After considerable efforts we found a new procedure able to improve the yield which consists of the combined use of catalytic amount of *t*BuOK with 1 equivalent of NaH in a mixture of THF and DCM. Under these news reaction conditions the yields of the allenamides improved and some desired products were isolate in excellent yields.

With the starting materials in our hands, we submitted the allenamides under the Friedel-Crafts-type cyclization in the presence of (*R*)-**IV** in DCM at room temperature. As shown in Scheme 5, the allenamides featuring tosyl group and benzoyl group resulted in the products in moderate yields, but low enantiomeric excesses. The allenamides **131d** resulted in the product in good yield but as racemic mixture. Bulkier groups, such as Boc, used as protecting groups for the nitrogen increased

the *ee* of the product up to 32% but it was possible to isolate the corresponding tetrahydroisoquinoline only in 30% yield. Promising results were achieved using the formyl group as EWG for the nitrogen. Under the already described reaction condition, the corresponding product was isolated in moderate yields and 47% enantiomeric excess (Scheme 5). The presence of molecular sieves in the mixture of the reaction was essential. Indeed, the iminium ion intermediate was sensitive to water and for this reason anhydrous reaction conditions were absolutely necessary in order to avoid its undesired hydrolysis.



Scheme 5: Screening of different *N*-protecting groups.

The absolute configuration of the tetrahydroisoquinoline **132e** was established to be *R*, by comparison of optical rotation with literature data.^[15]

The higher stereoselectivity obtained using formyl group as EWG might be achieved due to the hydrogen-bond interaction formed in the transition state between the catalyst and the hydrogen atom of the formyl group as shown in Figure 2.

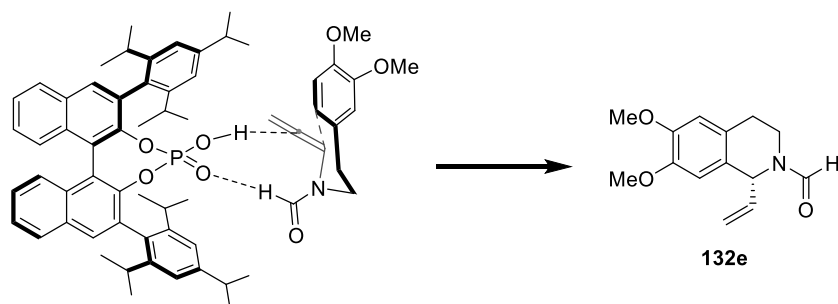


Figure 2: Proposed transition state.

Subsequently, in order to improve the yield and the enantiomeric excess, the role of the solvent was investigated. The Friedel-Crafts-type cyclization of allenamide **131e** was performed in the presence of catalyst (*R*)-**IV** using different solvents (Table 1).

Table 1: Screening of the solvents^a.

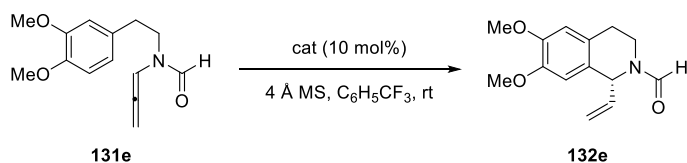
Entry	Solvent	Yield 132e (%) ^b	<i>ee</i> 132e (%) ^c
1	DCM	40	47
2	Toluene	18	72
3	C ₆ H ₅ CF ₃	48	75
4	C ₆ H ₅ F	36	70

cat IV =

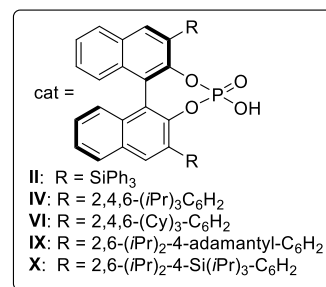
[a] All the reaction were carried out under nitrogen for 24 hours. [b] Isolated yields after flash chromatography. [c] Determined by chiral HPLC analysis performed after reduction with LiAlH₄ of the formyl group to the corresponding methyl group.

When the cyclization was performed in trifluorotoluene the desired tetrahydroisoquinoline was isolated in moderate yield and 75% *ee*. In order to further improve the yield and the stereoselectivity of the transformation, the allenamide **131e** was submitted to the Friedel-Crafts-type reaction in trifluorotoluene in the presence of different chiral BINOL-based phosphoric acids (Table 2).

Table 2: Screening of the BINOL-based phosphoric acids^a.



Entry	cat	Yield 132e (%) ^b	<i>ee</i> 132e (%) ^c
1	(<i>R</i>)- II	40	81
2	(<i>R</i>)- IV	48	75
3	(<i>R</i>)- VI	26	72
4	(<i>R</i>)- IX	27	79
5	(<i>R</i>)- X	33	78



[a] All the reaction were carried out under nitrogen for 24 hours. [b] Isolated yields after flash chromatography. [c] Determined by chiral HPLC analysis performed after reduction with $LiAlH_4$ of the formyl group to the corresponding methyl group.

No significant variations in term of the yields were observed using chiral phosphoric acids featuring different substituents in 3 and 3' position of the BINOL scaffold, but using the catalyst **II** it was possible to increase the enantiomeric excess up to 81%.

With the optimized reaction conditions in our hands, we submitted allenamides featuring different substituents on the phenyl moiety (Figure 3). Unfortunately, we were not able to obtain the corresponding products and only the amide resulted from the hydrolysis of the iminium ions intermediate were recovered.

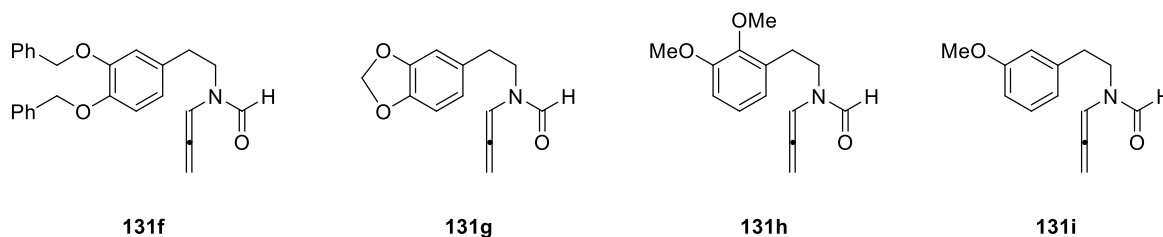


Figure 3: Substrates that failed the reaction.

In conclusion, the metal-free enantioselective Friedel-Crafts-type cyclization of allenamides promoted by chiral BINOL-based phosphoric acids was developed. With this methodology it was possible to obtain a tetrahydroisoquinoline featuring a vinyl group in 1 position which is a useful group for further functionalizations.

Bibliography

- [1] A. Gualandi, L. Mengozzi, E. Manoni, P. G. Cozzi, *Catal. Lett.* **2015**, *145*, 398–419.
- [2] A. Zhang, J. L. Neumeier, R. J. Baldessarini, *Chem. Rev.* **2007**, *107*, 274–302.
- [3] J. D. Scott, R. M. Williams, *Chem. Rev.* **2002**, *102*, 1669–1730.
- [4] M. Chrzanowska, D. Rozwadowska, *Chem. Rev.* **2004**, *104*, 3341–3370.
- [5] K. Funabashi, H. Ratni, M. Kanai, M. Shibasaki, *J. Am. Chem. Soc.* **2001**, *123*, 10784–10785.
- [6] S. Wang, C. T. Seto, *Org. Lett.* **2006**, *8*, 3979–3982.
- [7] A. M. Taylor, S. L. Schreiber, *Org. Lett.* **2006**, *8*, 143–146.
- [8] T. Hashimoto, M. Omote, K. Maruoka, *Angew. Chem. Int. Ed.* **2011**, *50*, 8952–8955.
- [9] W. Lin, T. Cao, W. Fan, Y. Han, J. Kuang, H. Luo, B. Miao, X. Tang, Q. Yu, W. Yuan, et al., *Angew. Chem. Int. Ed.* **2014**, *53*, 277–281.
- [10] E. D. E. Cox, J. M. Cook, *Chem. Rev.* **1995**, *95*, 1797–1842.
- [11] I. P. Kerschgens, E. Claveau, M. J. Wanner, S. Ingemann, J. H. van Maarseveen, H. Hiemstra, *Chem. Commun.* **2012**, *48*, 12243–12245.
- [12] N. V. Sewgobind, M. J. Wanner, S. Ingemann, R. De Gelder, J. H. Van Maarseveen, H. Hiemstra, *J. Org. Chem.* **2008**, *73*, 6405–6408.
- [13] Y. Lee, R. S. Klausen, E. N. Jacobsen, *Org. Lett.* **2011**, *13*, 5564–5567.
- [14] E. Manoni, A. Gualandi, L. Mengozzi, M. Bandini, P. G. Cozzi, *RSC Adv.* **2015**, *5*, 10546–10550.
- [15] Y. Toda, M. Terada, *Synlett* **2013**, *24*, 752–756.

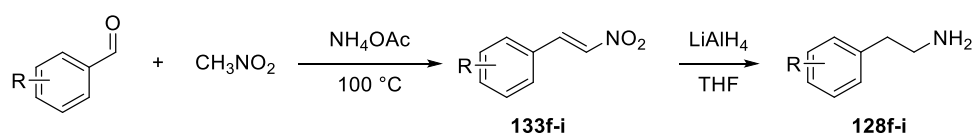
3.2.1 Experimental Section

¹H NMR spectra were recorded on Varian Gemini 200 and Varian MR400 spectrometers. Chemical shifts are reported in ppm from TMS with the solvent resonance as the internal standard (deuteriochloroform: $\delta = 7.27$ ppm). Data are reported as follows: chemical shift, multiplicity (s = singlet, d = duplet, t = triplet, q = quartet, dd = double duplet, dt = double triplet, bs = broad signal, pd = pseudo duplet, pt = pseudo triplet, m = multiplet), coupling constants (Hz). ¹³C NMR spectra were recorded on Varian Gemini 200, Varian MR400 spectrometers. Chemical shifts are reported in ppm from TMS with the solvent as the internal standard (deuteriochloroform: $\delta = 77.0$ ppm). If rotamers are present, the splitted signals are labelled as A (major rotamer) and B (minor rotamer). GC-MS spectra were taken by EI ionization at 70 eV on a Hewlett-Packard 5971 with GC injection. LC-electrospray ionization mass spectra (ESI-MS) were obtained with Agilent Technologies MSD1100 single-quadrupole mass spectrometer. They are reported as: *m/z* (rel. intense). Chromatographic purification was done with 240-400 mesh silica gel. Purification on preparative thin layer chromatography was done on Merck TLC silica gel 60 F₂₅₄. Determination of enantiomeric excess was performed on Agilent Technologies 1200 instrument equipped with a variable wave-length UV detector (reference 420 nm), using Daicel Chiralpak[®] columns (0.46 cm I.D. x 25 cm) and HPLC grade isopropanol and *n*-hexane as eluting solvents. Optical rotations were determined in a 1 mL cell with a path length of 1 dm (Na_D line). Melting points (m.p.) were determined on Bibby Stuart Scientific Melting Point Apparatus SMP3 and were not corrected.

Materials. If not otherwise stated, all reactions were carried out in sealed vials in open air without nitrogen atmosphere. Anhydrous solvents were supplied by Aldrich in Sureseal[®] bottles and were used as received avoiding further purification.

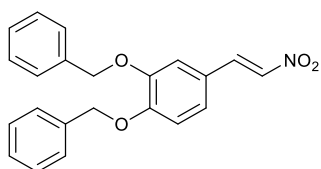
Reagents were purchased from Aldrich and used without further purification unless otherwise stated.

General procedures for the synthesis of 2-aryl-ethylamines **128f-i**.^[2]

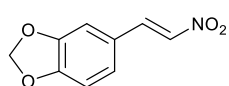


Synthesis of nitrostyrene derivatives **133f-i**.

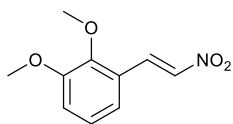
To a solution of aldehyde (15 mmol, 1 equiv.) in CH_3NO_2 (30 mL) was added NH_4OAc (3.73 mmol, 287 mg, 0.25 equiv.) in one portion. The resultant mixture was stirred at 100 °C, until complete conversion was obtained (4h, monitored by TLC), cooled at room temperature and water was added. Nitromethane was removed under reduced pressure and the residue was extracted with AcOEt (3 x 10 mL). The combined organic layers were dried over Na_2SO_4 , filtered and concentrated under reduced pressure. The crude mixture was purified by column chromatography on silica gel (cyclohexane/ethyl acetate from 10:0 to 8:2) or by re-crystallization from ethanol (80-98% yield).



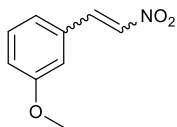
(133f): yellow solid, 4.39 g, 81% yield; m.p. 109-111 °C; ^1H NMR (400 MHz, CDCl_3): δ 5.20 (2H, s), 5.24 (2H, s), 6.97 (1H, d, $J = 8.3$ Hz), 7.08 (1H, d, $J = 2.0$ Hz), 7.12 (1H, dd, $J = 8.3$ Hz, $J = 1.9$ Hz), 7.33 (11H, m), 7.90 (1H, d, $J = 13.6$ Hz); ^{13}C NMR (101 MHz, CDCl_3): δ 70.9, 71.4, 114.1, 114.3, 123.1, 124.8, 127.1 (2C), 127.2 (2C), 128.1 (2C), 128.7 (4C), 135.6, 136.2, 136.45, 139.1, 149.1, 152.7; Spectroscopic data are according to those reported in literature.^[2]



(133g): yellow solid, 2.46 g, 85% yield; m.p. 148-150 °C; ^1H NMR (400 MHz, CDCl_3): δ 6.07 (2H, s), 6.88 (1H, d, $J = 7.7$ Hz), 7.01 (1H, d, $J = 1.6$ Hz), 7.09 (1H, dd, $J = 8.2$ Hz, $J = 1.6$ Hz), 7.48 (1H, d, $J = 13.5$ Hz), 7.94 (1H, d, $J = 13.5$ Hz); ^{13}C NMR (101 MHz, CDCl_3): δ 102.1, 107.0, 109.0, 124.2, 126.6, 135.3, 139.1, 148.7, 151.4; Spectroscopic data are according to those reported in literature.^[3]



(133h): yellow solid, 2.76 g, 88% yield; m.p. 80-83°C; Spectroscopic data are according to those reported in literature.^[3]



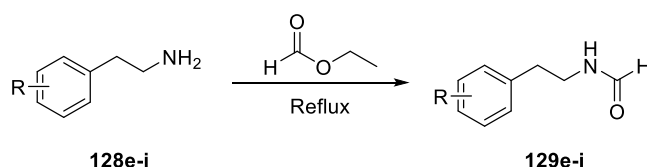
(133i): yellow sticky solid, 1.88 g, 70% yield; ¹H NMR (400 MHz, CDCl₃): δ 3.86 (3H, s), 7.04-7.07 (2H, m), 7.15 (1H, d, *J* = 7.9 Hz), 7.36-7.40 (1H, m), 7.58 (1H, d, *J* = 13.7 Hz), 7.98 (1H, d, *J* = 13.8 Hz); ¹³C NMR (101 MHz, CDCl₃): δ 55.4, 114.0, 117.9, 121.7, 130.4, 131.3, 137.3, 139.0, 160.1; Spectroscopic data are according to those reported in literature.^[3]

Reduction of nitrostyrenes derivatives **133f-i**.

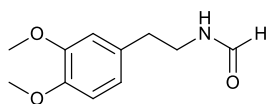
To a stirred suspension of LiAlH₄ (30 mmol, 1.14 g, 3 equiv.) in THF (30 mL) at 0 °C, a solution of nitrostyrene derivative **133f-i** (10 mmol, 1 equiv.) in THF (10 mL) was added dropwise. The mixture was allowed to reach room temperature and refluxed for 24 h. The mixture was cooled at 0 °C, diluted with Et₂O (5 mL) and water (1.14 mL) was slowly added. After 15 minutes, 15% (w/w) aqueous NaOH solution (1.14 mL) was added followed after further 15 minutes by addition of water (3.42 mL). The resultant mixture was stirred at room temperature for 30 minutes, then MgSO₄ was added and it was filtered through a Celite pad and it was washed with Et₂O (20 mL). The solvent was removed under reduced pressure to afford desired amine **128f-i** that was used as such in the next reaction steps.

General Procedure for the synthesis of allenamide derivatives 131a-i.

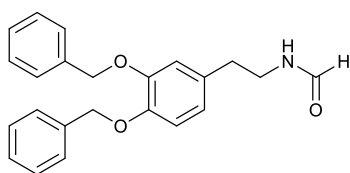
Synthesis of formamide derivatives.



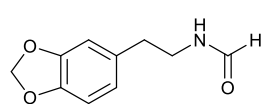
Amine **128e-i** or 3,4-dimethoxyphenethylamine (10 mmol, 1 equiv.) was dissolved in ethyl formate (20 mL) and the solution was refluxed for 24 h until complete conversion (monitored by ¹HNMR). The solvent was removed under reduced pressure and the crude residue was purified by column chromatography on silica gel (cyclohexane/ethyl acetate from 8:2 to 1:1) to afford formamides **129e-i**.



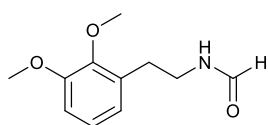
(129e): yellow oil, 1.43 g, 86% yield; Spectroscopic data are according to those reported in literature.^[4]



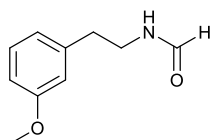
(129f): yellow oil, 1.91 g, 53% yield; ¹H NMR (400 MHz, CDCl₃, 25 °C) (two rotamers A:B, ratio 5.8:1): δ 2.70 (2H_B, t, *J* = 6.8 Hz), 2.72 (2H_A, t, *J* = 6.8 Hz), 3.39 (2H_B, q, *J* = 6.8 Hz), 3.48 (2H_A, q, *J* = 6.5 Hz), 5.16 (4H_A+2H_B, s), 5.18 (2H_B, s), 5.32 (1H_A, bs), 5.50 (1H_B, bs), 6.68-6.75 (2H_A+2H_B, m), 6.89 (1H_A+1H_B, d, *J* = 8.2 Hz), 7.30-7.46 (10H_A+10H_B, m), 7.89 (1H_B, d, *J* = 12Hz), 8.03 (1H_A, s); ¹³C NMR (101 MHz, CDCl₃): δ 34.9, 39.2, 71.3, 71.4, 115.4, 115.8, 121.6, 127.4 (2C), 127.4 (2C), 127.9, 127.9, 128.5 (4C), 132.0, 137.2, 137.3, 147.7, 148.8, 161.3;



(129g): yellow oil, 888 mg, 46% yield; ^1H NMR (400 MHz, CDCl_3) (two rotamers A:B, ratio 4.9:1): δ 2.70-2.77 ($2\text{H}_\text{A}+2\text{H}_\text{B}$, m), 3.38-3.45 (2H_B , m), 3.47-3.54 (2H_A , m), 5.92-5.94 ($2\text{H}_\text{A}+2\text{H}_\text{B}$, m), 6.60-6.76 ($3\text{H}_\text{A}+3\text{H}_\text{B}$, m), 7.90 (1H_B , t, $J = 11.7$ Hz), 8.11 (1H_A , d, $J = 7.3$ Hz); ^{13}C NMR (101 MHz, CDCl_3): δ 35.0 (1C_A), 37.1 (1C_B), 39.4 (1C_A), 43.3 (1C_B), 100.7 (1C_A), 100.8 (1C_B), 108.1 (1C_A), 108.2 (1C_B), 108.9 (1C_A), 109.0 (1C_B), 121.5 (1C_A), 121.7 (1C_B), 131.5 (1C_B), 132.4 (1C_A), 146.0 (1C_A), 146.2 (1C_B), 147.6 (1C_A), 147.7 (1C_B), 161.6 (1C_A), 164.8 (1C_B);

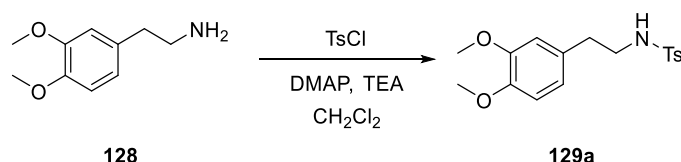


(129h): yellow oil, 1.11 g 53% yield; ^1H NMR (400 MHz, CDCl_3) (two rotamers A:B, ratio 1.1:1) : δ 2.84 (2H_B , t, $J = 6.7$ Hz), 2.87 (2H_A , t, $J = 6.7$ Hz), 3.48 (2H_A , pq, $J = 6.2$ Hz), 3.54 (2H_B , pq, $J = 6.0$ Hz), 3.85 (3H_A , s), 3.86 (3H_B , s), 3.88 ($3\text{H}_\text{A} + 3\text{H}_\text{B}$, s), 6.77-6.80 ($1\text{H}_\text{A}+1\text{H}_\text{B}$, m), 6.82-6.85 ($1\text{H}_\text{A}+1\text{H}_\text{B}$, m), 7.00-7.05 ($1\text{H}_\text{A}+1\text{H}_\text{B}$, m), 8.11 ($1\text{H}_\text{A}+1\text{H}_\text{B}$, s); ^{13}C NMR (101 MHz, CDCl_3): δ 29.57 (1C_A), 29.63 (1C_B), 39.0 (1C_A), 40.5 (1C_B), 55.6 (2C_A), 60.5 (2C_B), 110.8 (1C_B), 110.9 (1C_A), 122.16 (1C_A), 122.17 (1C_B), 124.1 (1C_B), 124.2 (1C_A), 132.5 (1C_A), 132.8 (1C_B), 146.99 (1C_B), 147.01 (1C_A), 152.57 (1C_A), 152.58 (1C_B), 161.6 (1C_A), 170.5 (1C_B);



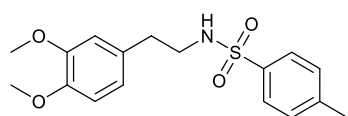
(129i): yellow oil, 1.22 g 68% yield; Spectroscopic data are according to those reported in literature.^[5]

Preparation of compound 129a.



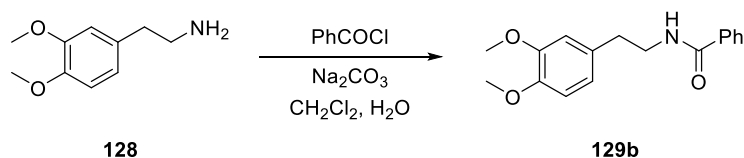
To a solution of 3,4-dimethoxyphenethylamine (3 mmol, 543 mg, 1 equiv.) in DCM (10 mL), Et_3N (4.5 mmol, 0.624 mL, 1.5 equiv.) and DMAP (0.075 mmol, 9.15 mg, 0.025 equiv.) were added. To

the resulting solution at 0 °C, tosyl chloride (3.6 mmol, 688 mg, 1.2 equiv.) was slowly added in small portions. The mixture was allowed to reach room temperature and stirred for 24 h. Subsequently, water (10 mL) was added, the organic phase was separated and the aqueous layer was extracted with DCM (3 x 5 mL). The combined organic layers were washed with HCl 1M (10 mL), NaHCO₃ sat. sln. (10 mL) and brine (10 mL). The organic layers was dried with Na₂SO₄, filtered and concentrated under reduced pressure to give pure **129a**, that was used as such, without further purification in the next steps.

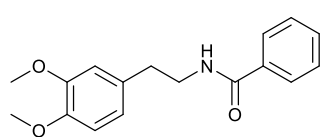


(129a): yellow solid, 894 mg, 89% yield; m.p. 133-135°C; ¹H NMR (400 MHz, CDCl₃): δ 2.43 (3H, s), 2.71 (2H, t, *J* = 6.7 Hz), 3.19 (2H, q, *J* = 6.4 Hz), 3.82 (3H, s), 3.86 (3H, s), 4.37 (1H, bs), 6.57 (1H, s), 6.63 (1H, d, *J* = 8.5 Hz), 6.77 (1H, d, *J* = 8.5 Hz), 7.29 (2H, d, *J* = 7.6 Hz), 7.68 (2H, d, *J* = 7.8 Hz); ¹³C NMR (101 MHz, CDCl₃): δ 21.5, 35.3, 44.30, 55.7, 55.9, 111.3, 111.7, 120.7, 127.0 (2C), 129.6 (2C), 130.1, 136.8, 144.3, 147.8, 149.0; EI-MS: *m/z* = 335 (60), 184 (14), 151 (100), 91 (84).

Preparation of compound 129b.

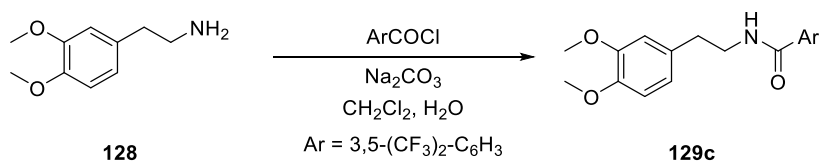


To a solution of 3,4-dimethoxyphenethylamine (3 mmol, 543 mg, 1 equiv.) and Na₂CO₃ (6 mmol, 636 mg, 2 equiv.), in H₂O/DCM (1/1, 20 mL), PhCOCl (4.5 mmol, 0.521 mL, 1.5 equiv.) was added dropwise. The mixture was stirred for 72 h, then water (10 mL) and DCM (10 mL) were added. The organic phase was separated and the aqueous layer was extracted with Et₂O (3 x 10 mL). The combined organic layers were washed with HCl 1M (15 mL), NaHCO₃ sat. sln. (15 mL) and brine (15 mL). The organic layers was dried with Na₂SO₄, filtered and concentrated under reduced pressure. The crude product was washed with *n*-hexane and then it was used such as, without further purification in the next steps.

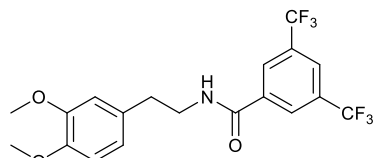


(129b): white solid, 710 mg, 83% yield; m.p. 63-65°C; ^1H NMR (400 MHz, CDCl_3): δ 2.71-2.78 (2H, m), 3.38 (2H, m), 3.84 (3H, s), 3.85 (3H, s), 6.71-6.81 (3H, m), 7.34 (5H, s); ^{13}C NMR (101 MHz, CDCl_3): δ 35.2 ($1\text{C}_\text{A}+1\text{C}_\text{B}$), 41.3 ($1\text{C}_\text{A}+1\text{C}_\text{B}$), 55.8 ($1\text{C}_\text{A}+1\text{C}_\text{B}$), 55.9 ($1\text{C}_\text{A}+1\text{C}_\text{B}$), 111.4 ($1\text{C}_\text{A}+1\text{C}_\text{B}$), 111.9 ($1\text{C}_\text{A}+1\text{C}_\text{B}$), 120.6 ($1\text{C}_\text{A}+1\text{C}_\text{B}$), 126.8 ($2\text{C}_\text{A}+2\text{C}_\text{B}$), 128.4 (1C_B), 128.5 ($2\text{C}_\text{A}+2\text{C}_\text{B}$), 130.1 (1C_A), 131.3 (1C_B), 131.4 (1C_A), 133.5 (1C_A), 134.5 (1C_B), 147.7 ($1\text{C}_\text{A}+1\text{C}_\text{B}$), 149.0 ($1\text{C}_\text{A}+1\text{C}_\text{B}$), 167.6 ($1\text{C}_\text{A}+1\text{C}_\text{B}$); EI-MS: m/z = 285 (8), 164 (100), 105 (53), 77 (48).

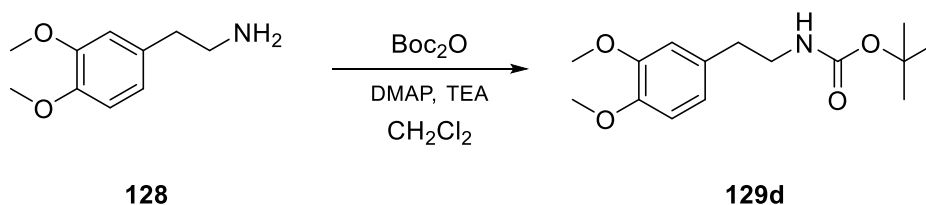
Preparation of compound 129c.



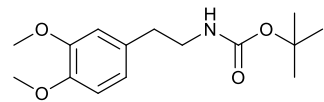
To a solution of 3,4-dimethoxyphenethylamine (3 mmol, 543 mg, 1 equiv.) and Na_2CO_3 (6 mmol, 636 mg, 2 equiv.), in $\text{H}_2\text{O}/\text{DCM}$ (1/1, 20 mL), 3,5-(CF_3) $_2$ - C_6H_3 - COCl (3.6 mmol, 0.637 mL, 1.2 equiv.) was added dropwise. The mixture was stirred for 72 h and then water (10 mL) and DCM (10 mL) were added. The organic phase was separated and the aqueous layer was extracted with Et_2O (3 x 10 mL). The combined organic layers were washed with HCl 1M (15 mL), NaHCO_3 sat. sln. (15 mL) and brine (15 mL). The organic layers was dried with Na_2SO_4 , filtered and concentrated under reduced pressure. The crude product was washed with *n*-hexane and then it was used such as, without further purification in the next steps.


(129c): white solid, 1.23 g, 97% yield; m.p. 99-101°C; ¹H NMR (400 MHz, CDCl₃): δ 2.93 (2H, t, *J* = 6.9 Hz), 3.75 (2H, q, *J* = 6.5 Hz), 3.88 (3H, s), 3.89 (3H, s), 6.18 (1H, bs), 6.77-6.80 (2H, m), 6.85 (1H, d, *J* = 7.8 Hz), 8.00 (1H, s), 8.14 (2H, s); ¹³C NMR (101 MHz, CDCl₃): δ 35.1, 41.6, 55.8, 55.9, 111.4, 111.8, 120.7, 122.7 (2C, q, *J*_{C-F} = 273.3 Hz), 124.9 (2C, t, *J*_{C-F} = 4.1 Hz), 127.1 (2C, q, *J*_{C-F} = 3.4 Hz), 130.8, 132.4, 136.7, 148.0, 149.3, 164.5; EI-MS: *m/z* = 421 (25), 241 (46), 213 (36), 164 (100).

Preparation of compound 8d.^[6]

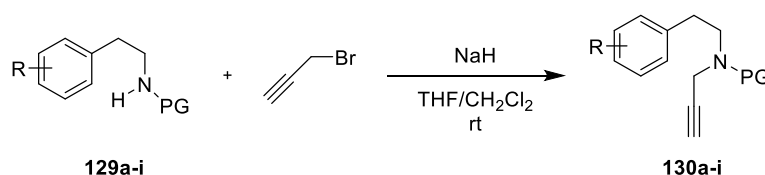


To a solution of 3,4-dimethoxyphenethylamine (3 mmol, 543 mg, 1 equiv.) in DCM (10 mL), Et₃N (4.5 mmol, 0.624 mL, 1.5 equiv.), DMAP (0.075 mmol, 9.15 mg, 0.025 equiv.) were added. To the resulting solution at 0 °C, Boc₂O (3.6 mmol, 785 mg, 1.2 equiv.) was slowly added in small portions. The mixture was allowed to reach room temperature and stirred for 24 h. Subsequently, water (10 mL) was added, the organic phase was separated and the aqueous layer was extracted with Et₂O (3 x 5 mL). The combined organic layers were washed with HCl 1M (10 mL), NaHCO₃ sat. sln. (10 mL) and brine (10 mL). The organic layers was dried with Na₂SO₄, filtered and concentrated under reduced pressure. The crude product was washed with *n*-hexane and then it was used such as, without further purification in the next steps.

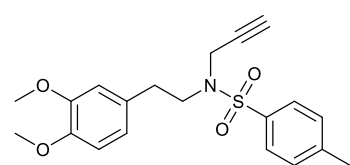

(129d): sticky yellow solid, 767 mg, 91% yield; ¹H NMR (400 MHz, CDCl₃): δ 1.45 (9H, s), 2.75 (2H, t, *J* = 7.0 Hz), 3.33-3.38 (2H, m), 3.87 (3H, s), 3.88 (3H, s), 4.54 (1H, bs), 6.72-6.75 (2H, m), 6.82 (1H, d, *J* = 8.0 Hz); ¹³C NMR (101 MHz, CDCl₃): δ 28.4 (3C), 35.7, 41.9, 55.8, 55.9, 79.2, 111.3, 111.9, 120.6,

131.5, 147.5, 148.9, 155.8; EI-MS: m/z = 281 (129, 225 (14), 209 (13), 165 (58), 151 (100), 57 (63). Spectroscopic properties are according to those reported in literature.^[6]

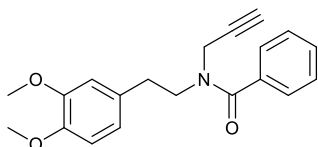
General Procedure for the propargylation of amides.



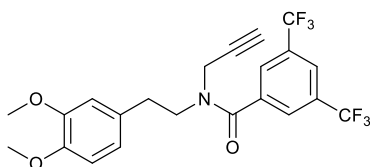
To a solution of **129a-i** (5 mmol, 1 equiv.) in anhydrous THF (15 mL) and CH₂Cl₂ (5 mL) at 0 °C, NaH (6.5 mmol, 156 mg, 1.3 equiv.) was slowly added. After 20 minutes, propargyl bromide (6 mmol, 0.539 mL, 1.2 equiv.) was added at 0 °C. The reaction mixture was allowed to reach room temperature and it was stirred for 24 h. Water (10 mL) was slowly added at 0 °C and organic volatiles were removed under reduced pressure. The residue was extracted with AcOEt (3 x 5 mL). The combined organic layers were dried over Na₂SO₄, filtered and concentrated under reduced pressure. The crude mixture was purified by column chromatography on silica gel silica gel (cyclohexane/EtOAc 7/3) to give the desired products **130a-i**.



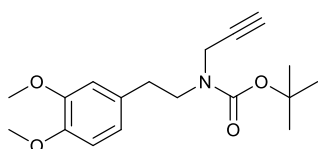
(130a): yellow solid, 1.66 g, 89% yield; m.p. 10-103 °C; ¹H NMR (400 MHz, CDCl₃): δ 2.06 (1H, t, J = 2.4 Hz), 2.42 (3H, s), 2.86 (2H, pt, J = 7.6 Hz), 3.42 (2H, pt, J = 7.6 Hz), 3.87 (3H, s), 3.88 (3H, s), 4.08 (2H, d, J = 2.5 Hz), 6.74 (1H, s), 6.75 (1H, d, J = 6.9 Hz), 6.80 (1H, d, J = 8.7 Hz), 7.28 (2H, d, J = 6.6 Hz), 7.71 (2H, d, J = 8.2 Hz); ¹³C NMR (101 MHz, CDCl₃): δ 21.5, 34.3, 36.8, 48.0, 55.86, 55.87, 73.7, 76.7, 111.3, 112.0, 120.7, 127.6 (2C), 129.4 (2C), 130.7, 135.9, 143.5, 147.7, 148.9; EI-MS: m/z = 373 (42), 222 (100), 155 (95), 151 (86), 91 (75).



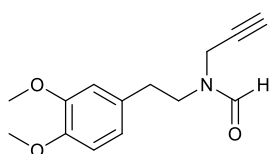
(130b): yellow oil, 291 mg, 18% yield; Although numerous attempts by changing solvent and temperature, it has never been possible to obtain a well resolved spectrum of the product; ^1H NMR (400 MHz, CDCl_3 , 25 $^\circ\text{C}$): δ 2.30 (2H, t, $J = 2.5$ Hz), 2.76 (1H, bs), 2.98 (1H, bs), 3.62 (1H, bs), 3.73 (1H, bs), 3.84 (6H, bs), 4.42 (2H, bs), 6.41 (1H, bs), 6.75 (2H, bs), 7.20 (1H, bs), 7.39 (4H, bs); ^{13}C NMR (101 MHz, CDCl_3): δ 33.0 (1C_B), 34.2 (1C_A), 40.0 ($1\text{C}_\text{A}+1\text{C}_\text{B}$), 47.3 (1C_A), 50.2 (1C_B), 55.8 (2C_A), 55.9 (2C_A), 72.4 (1C_A), 73.0 (1C_B), 78.8 ($1\text{C}_\text{A}+1\text{C}_\text{B}$), 113.3 ($1\text{C}_\text{A}+1\text{C}_\text{B}$), 111.8 (1C_B), 112.0 (1C_A), 120.7 ($2\text{C}_\text{A}+2\text{C}_\text{B}$), 126.7 ($2\text{C}_\text{A}+2\text{C}_\text{B}$), 128.4 ($1\text{C}_\text{A}+1\text{C}_\text{B}$), 129.9 (1C_B), 130.2 (1C_A), 131.3 (1C_A), 131.4 (1C_A), 135.7 ($1\text{C}_\text{A}+1\text{C}_\text{B}$), 147.7 (2C_B), 148.9 (1C_A), 171.1 ($1\text{C}_\text{A}+1\text{C}_\text{B}$); EI-MS: $m/z = 323$ (4), 164 (100), 105 (89), 77 (64).



(130c): yellow oil, 291 mg, 18% yield; Although numerous attempts by changing solvent and temperature, it has never been possible to obtain a well resolved spectrum of the product; ^1H NMR (400 MHz, CDCl_3 , 25 $^\circ\text{C}$) (two rotamers A:B, ratio 1:1): δ 2.73 ($1\text{H}_\text{A}+1\text{H}_\text{B}$, t, $J = 2.5$ Hz), 2.80 (2H_A , bs), 2.99 (2H_B , bs), 3.60 (2H_A , bs), 3.75 ($2\text{H}_\text{A}+2\text{H}_\text{B}$, bs), 3.84 ($6\text{H}_\text{A}+6\text{H}_\text{B}$, bs), 4.47 (2H_B , bs), 6.44 (1H_A , bs), 6.50 (1H_B , bs), 6.74 (2H_A , bs), 6.80 (2H_B , bs), 7.51 ($1\text{H}_\text{A}+1\text{H}_\text{B}$, bs), 7.87 (2H_A , bs), 7.96 (2H_B , bs); ^{13}C NMR (101 MHz, CDCl_3): δ 33.0 (1C_B), 33.6 (1C_A), 34.2 (1C_A), 39.9 (1C_B), 47.7 (2C_B), 50.3 (2C_A), 73.2 (1C_A), 73.8 (1C_B), 77.9 ($1\text{C}_\text{A}+1\text{C}_\text{B}$), 112.2 ($1\text{C}_\text{A}+1\text{C}_\text{B}$), 111.9 ($1\text{C}_\text{A}+1\text{C}_\text{B}$), 120.7 ($1\text{C}_\text{A}+1\text{C}_\text{B}$), 122.9 ($2\text{C}_\text{A}+2\text{C}_\text{B}$, q, $J_{\text{C-F}} = 271.5$ Hz), 123.3 (1C_A), 123.7 (1C_B), 124.1 ($1\text{C}_\text{A}+1\text{C}_\text{B}$), 127.0 ($1\text{C}_\text{A}+1\text{C}_\text{B}$, bs), 129.3 (1C_B), 130.8 (1C_A), 131.2 ($2\text{C}_\text{A}+2\text{C}_\text{B}$), 137.7 ($1\text{C}_\text{A}+1\text{C}_\text{B}$), 147.9 (1C_A), 148.0 (1C_B), 149.1 ($1\text{C}_\text{A}+1\text{C}_\text{B}$), 168.0 (1C_B), 168.5 (1C_A); EI-MS: $m/z = 459$ (9), 241 (88), 213 (67), 164 (100).

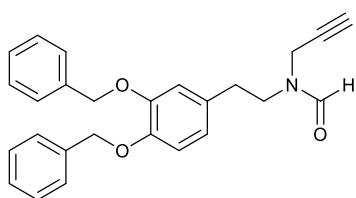


(130d): sticky white solid, 1.37 g, 86% yield; ^1H NMR (400 MHz, CDCl_3): δ 1.46 (9H, s), 2.22 (1H, s), 2.83 (2H, bs), 3.52 (2H, pt, $J = 7.4$ Hz), 3.86 (3H, s), 3.88 (3H, s), 4.03 (2H, bs), 6.74-6.82 (3H, m); ^{13}C NMR (101 MHz, CDCl_3): δ 28.3, 29.7, 30.9, 48.5, 55.8, 55.9, 71.5, 79.9, 80.1, 111.3, 111.0, 120.7, 131.7, 147.5, 148.9, 154.8; EI-MS: $m/z = 319$ (31), 246 (25), 151 (100), 57 (87).



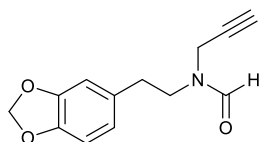
(130e): yellow oil, 469 mg, 38% yield; ^1H NMR (400 MHz, CDCl_3) (two rotamers A:B, ratio 2:1): δ 2.28 (1 H_B , t, J = 2.3 Hz), 2.34 (1 H_A , t, J = 2.5 Hz), 2.85 (2 H_A , pt, J = 6.8 Hz), 2.86 (2 H_B , pt, J = 6.4 Hz), 3.60 (2 H_A , pt, J = 6.8 Hz), 3.63 (2 H_B , pt, J = 6.8 Hz), 3.86 (3 H_A , s), 3.87 (3 H_A +3 H_B , s), 3.88

(3 H_B , s), 4.18 (2 H_A +2 H_B , d, J = 2.4 Hz), 6.67-6.83 (3 H_A +3 H_B , m), 7.80 (1 H_A , bs), 8.10 (1 H_B , bs); ^{13}C NMR (101 MHz, CDCl_3): δ 31.4 (1 C_A), 32.8 (1 C_B), 34.4 (1 C_A), 37.5 (1 C_B), 43.9 (1 C_B), 48.7 (1 C_A), 55.8 (2 C_A +2 C_B), 72.5 (1 C_A), 73.6 (1 C_B), 77.7 (1 C_B), 78.0 (1 C_A), 111.3 (1 C_B), 111.4 (1 C_A), 111.8 (1 C_B), 111.9 (1 C_A), 120.6 (1 C_B), 120.8 (1 C_A), 130.1 (1 C_A), 130.9 (1 C_B), 147.6 (1 C_B), 147.8 (1 C_A), 148.9 (1 C_B), 149.0 (1 C_A), 162.1 (1 C_A), 162.1 (1 C_B); ESI-MS: m/z = 248.2 [$\text{M}+\text{H}$] $^+$, 270.0 [$\text{M}+\text{Na}$] $^+$, 495.2 [$2\text{M}+\text{H}$] $^+$; ESI-MS: m/z = 248.0 [$\text{M}+\text{H}$] $^+$, 270.0 [$\text{M}+\text{Na}$] $^+$, 495.2 [$2\text{M}+\text{H}$] $^+$.



(130f): brown oil, 1.26 g, 63% yield; ^1H NMR (400 MHz, CDCl_3) (two rotamers A:B, ratio 1.7:1): δ 2.23 (1 H_A , t, J = 2.2 Hz), 2.29 (1 H_B , t, J = 2.0 Hz), 2.78 (2 H_A , t, J = 6.8 Hz), 2.80 (2 H_B , t, J = 7.02 Hz), 3.49 (2 H_B , t, J = 6.9 Hz), 3.52 (2 H_A , t, J = 6.8 Hz), 3.68 (2 H_B , d,

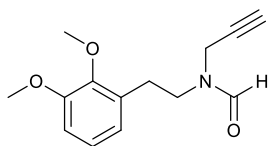
J = 1.6 Hz), 4.13 (2 H_A , d, J = 2.2 Hz), 5.14 (2 H_A +2 H_B , s), 5.16 (2 H_A , s), 5.18 (2 H_B , s), 6.67 (1 H_A , d, J = 8.3 Hz), 6.73 (1 H_A , s), 6.74 (1 H_B , s), 6.80 (1 H_B , s), 6.88 (1 H_A +1 H_B , d, J = 8.0 Hz), 7.30-7.45 (10 H_A +10 H_B , m), 7.71 (1 H_A , s), 8.00 (1 H_B , s); ^{13}C NMR (101 MHz, CDCl_3) (two rotamers A:B, ratio 6:1): δ 31.4 (1 C_A), 32.9 (1 C_B), 34.3 (1 C_A), 37.6 (1 C_B), 44.1 (1 C_B), 48.5 (1 C_A), 71.4 (1 C_B), 71.4 (1 C_A), 71.5 (1 C_A), 73.5 (1 C_B), 77.8 (1 C_B), 78.0 (1 C_A), 115.4 (1 C_A), 115.5 (1 C_B), 115.8 (1 C_B), 116.0 (1 C_A), 121.6 (1 C_B), 121.8 (1 C_A), 127.3 (4 C_A), 127.4 (4 C_B), 127.76 (2 C_B), 127.80 (1 C_A), 127.82 (1 C_A), 128.44 (2 C_B), 128.46 (2 C_A), 128.48 (2 C_B), 128.5 (2 C_A), 131.0 (1 C_A), 132.0 (1 C_B), 137.2 (1 C_A +1 C_B), 137.2 (1 C_A +1 C_B), 147.6 (1 C_B), 147.9 (1 C_A), 148.9 (1 C_B), 149.0 (1 C_A), 162.1 (1 C_A), 162.1 (1 C_B); ESI-MS: m/z = 400.2 [$\text{M}+\text{H}$] $^+$, 422.2 [$\text{M}+\text{Na}$] $^+$, 799.4 [$2\text{M}+\text{H}$] $^+$.



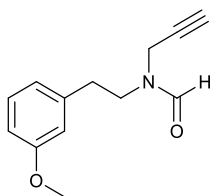
(130g): yellow oil, 658 mg, 57% yield; ^1H NMR (400 MHz, CDCl_3) (two rotamers A:B, ratio 1.9:1): δ 2.28 (1 H_A , t, J = 2.6 Hz), 2.34 (1 H_B , t, J = 2.5 Hz), 2.83 (2 H_A +2 H_B , t, J = 6.7 Hz), 3.58 (2 H_A , t, J = 7.5 Hz), 3.62 (2 H_B , pt, J = 7.4 Hz), 3.90 (2 H_B , d, J = 2.1 Hz), 4.19 (2 H_A , d, J = 2.2 Hz), 5.94 (2 H_B , s), 5.95 (2 H_A , s), 6.60-

6.76 (3 H_A +3 H_B , m), 7.82 (1 H_A , s), 8.11 (1 H_B , s); ^{13}C NMR (101 MHz, CDCl_3): δ 31.2 (1 C_A), 32.9 (1 C_B), 34.4 (1 C_A), 37.4 (1 C_B), 44.1 (1 C_B), 48.5 (1 C_A), 72.6 (1 C_A), 73.7 (1 C_B), 77.9 (1 C_B), 78.0 (1 C_A), 100.8 (1 C_B), 100.9 (1 C_A), 108.2 (1 C_B), 108.3 (1 C_A), 108.9 (1 C_A), 109.0 (1 C_B), 121.5 (1 C_B),

121.7 (1C_A), 131.3 (1C_A), 132.2 (1C_B), 146.0 (1C_B), 146.3 (1C_A), 147.6 (1C_B), 147.8 (1C_A), 162.0 (1C_A), 162.1 (1C_B); ESI-MS: $m/z = 232.2$ [M+H]⁺, 254.0 [M+Na]⁺, 463.2 [2M+H]⁺.

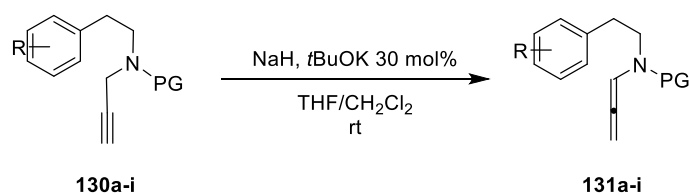


(130h): yellow oil, 630 mg, 51% yield; ¹H NMR (400 MHz, CDCl₃) (two rotamers A:B, ratio 2.2:1): δ 2.26 (1H_A, t, $J = 2.6$ Hz), 2.31 (1H_B, t, $J = 2.5$ Hz), 2.91 (2H_A, t, $J = 6.9$ Hz), 2.92 (2H_B, t, $J = 7.0$ Hz), 3.61 (2H_A, t, $J = 7.0$ Hz), 3.67 (2H_B, t, $J = 7.3$ Hz), 3.85 (6H_B, s), 3.87 (6H_A, s), 3.92 (2H_B, d, $J = 2.5$ Hz), 4.22 (2H_A, d, $J = 2.5$ Hz), 6.72 (1H_A, dd, $J_1 = 7.7$ Hz, $J_2 = 1.4$ Hz), 6.81-6.84 (1H_A + 2H_B, m), 6.99 (1H_A + 1H_B, pt, $J = 8.0$ Hz), 7.82 (1H_A, s), 8.10 (1H_B, s); ¹³C NMR (101 MHz, CDCl₃): δ 27.6 (1C_B), 29.4 (1C_A), 31.1 (1C_A), 37.3 (1C_B), 43.0 (1C_B), 47.3 (1C_A), 55.50 (1C_B), 55.51 (1C_A), 60.4 (1C_A), 60.6 (1C_B), 72.4 (1C_A), 73.5 (1C_B), 78.0 (1C_B), 78.1 (1C_A), 110.9 (1C_B), 111.3 (1C_A), 122.11 (1C_A), 122.13 (1C_B), 123.9 (1C_B), 124.0 (1C_A), 131.2 (1C_A), 132.1 (1C_B), 147.15 (1C_A), 147.23 (1C_B), 152.55 (1C_B), 152.62 (1C_A), 162.0 (1C_A), 162.1 (1C_B); ESI-MS: $m/z = 248.2$ [M+H]⁺, 270.0 [M+Na]⁺, 494.2 [2M+H]⁺.

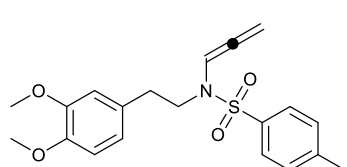


(130i): yellow oil, 521 mg, 48% yield; ¹H NMR (400 MHz, CDCl₃) (two rotamers A:B, ratio 1.8:1): δ 2.28 (1H_A, t, $J = 2.5$ Hz), 2.34 (1H_B, t, $J = 2.5$ Hz), 2.87-2.91 (2H_A+2H_B, m), 3.63 (2H_A, t, $J = 7.1$ Hz), 3.68 (2H_B, t, $J = 7.5$ Hz), 3.80 (3H_A, s), 3.81 (3H_B, s), 3.88 (2H_B, d, $J = 2.6$ Hz), 4.20 (2H_A, d, $J = 2.6$ Hz), 6.72-6.85 (3H_A+3H_B, m), 7.21-7.26 (1H_A+1H_B), 7.84 (1H_A, s), 8.11 (1H_B, s); ¹³C NMR (101 MHz, CDCl₃): δ 31.3 (1C_A), 33.3 (1C_B), 34.7 (1C_A), 37.4 (1C_B), 43.8 (1C_B), 48.3 (1C_A), 55.01 (1C_B), 55.02 (1C_A), 72.6 (1C_A), 73.8 (1C_B), 77.9 (1C_B), 78.1 (1C_A), 111.88 (1C_B), 111.91 (1C_A), 114.3 (1C_B), 114.6 (1C_A), 120.96 (1C_A), 120.98 (1C_B), 129.5 (1C_B), 129.7 (1C_A), 139.3 (1C_A), 140.1 (1C_B), 159.7 (1C_B), 159.8 (1C_A), 162.0 (1C_B), 162.3 (1C_A); ESI-MS: $m/z = 218.2$ [M+H]⁺, 240.2 [M+Na]⁺, 435.2 [2M+H]⁺.

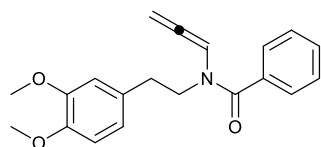
General Procedure for the isomerization to allenamide compounds **131a-i**.



To a solution of propargylic amide **130a-i** (1.5 mmol, 1 equiv.) in THF (8 mL) at 0°C, *t*BuOK (0.3 mmol, 33.6 mg, 0.2 equiv.) and NaH (1.5 mmol, 36 mg, 1 equiv.) were added. The reaction was stirred for 24 h at room temperature, and then it was quenched with water (5 mL) at 0 °C. THF was removed under reduced pressure and the aqueous layer was extracted with ethyl acetate (3 x 5 mL). The combined organic layers were dried over Na₂SO₄, filtered and concentrated under reduced pressure. The crude mixture was purified by column chromatography on silica gel silica gel (cyclohexane/EtOAc 7/3) to give the desired products **131a-i**.

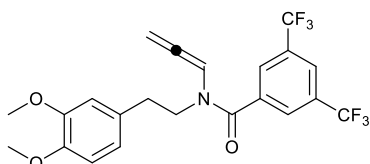


(131a): yellow oil, 509 mg, 91% yield; ¹H NMR (400 MHz, CDCl₃): δ 2.42 (3H, s), 2.82 (2H, pt, *J* = 8.0 Hz), 3.32 (2H, pt, *J* = 8.0 Hz), 3.85 (3H, s), 3.87 (3H, s), 5.39 (2H, d, *J* = 6.4 Hz), 6.70 (2H, bs), 6.77-6.79 (1H, m), 6.88 (1H, t, *J* = 6.2 Hz), 7.30 (2H, d, *J* = 7.8 Hz), 7.68 (2H, d, *J* = 7.80 Hz); ¹³C NMR (101 MHz, CDCl₃): δ 21.4, 34.0, 48.1, 55.6, 55.7, 87.6, 100.0, 111.1, 112.0, 120.6, 126.9 (2C), 129.6 (2C), 130.8, 135.3, 143.6, 147.5, 148.7, 201.4; ESI-MS: *m/z* = 374.0 [M+H]⁺, 396.0 [M+Na]⁺, 769.0 [2M+H]⁺.



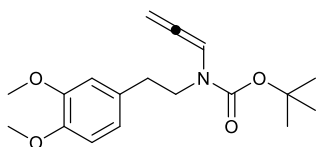
(131b): brown oil, 49 mg, 64% yield; although numerous attempts by changing solvent and temperature, it has never been possible to obtain a well resolved spectrum of the product. ¹H NMR (400 MHz, CDCl₃, 25 °C) (two rotamers A:B, ratio 2:1): δ 2.78 (2H_B, bs), 2.94 (2H_A, bs), 3.64 (2H_B, bs), 3.77 (2H_A, bs), 3.89 (6H_A+6H_B, bs), 5.40 (2H_A, bs), 5.53 (2H_B, bs), 6.68 (3H_b, bs), 6.83 (3H_A, bs), 7.18 (1H_A+1H_B, m), 7.46 (5H_A+5H_B, bs); ¹³C NMR (50 MHz, CDCl₃): δ 35.4 (1C_A+1C_B), 41.3 (1C_A+1C_B), 55.9 (1C_A+1C_B), 56.0 (1C_A+1C_B), 111.4 (1C_B), 111.5 (1C_B), 111.6 (1C_A), 112.1 (1C_A), 120.8 (1C_A),

120.9 (1C_A), 121.0 (2C_B), 126.9 (2C_A+2C_B), 128.5 (1C_A+1C_B), 128.7 (2C_A+2C_B), 131.5 (1C_A+1C_B), 134.7 (1C_A+1C_B), 147.9 (1C_A), 149.0 (1C_B), 149.1 (1C_B), 149.2 (1C_A), 151.1 (1C_B), (1C_A+1C_B), 167.5 (1C_A+1C_B), 198.1 (1C_A+1C_B); ESI-MS: $m/z = 324.2$ [M+H]⁺.



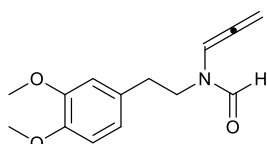
(131c): yellow oil, 185 mg, 27% yield; although numerous attempts by changing solvent and temperature, it has never been possible to obtain a well resolved spectrum of the product. ¹H NMR (400 MHz, CDCl₃, 25 °C) (two rotamers A:B, ratio 3:1):

δ 2.77 (2H_B, bs), 2.93 (2H_B, t, $J = 7.2$ Hz), 2.80 (2H_A, bs), 3.59 (2H_B, bs), 3.75 (2H_A, bs), 3.84 (6H_A+6H_B, bs), 5.40 (2H_A, d, $J = 5.9$ Hz), 5.57 (2H_B, bs), 6.36-6.45 (1H_A+1H_B, bs), 6.71-6.80 (2H_A+2H_B, bs), 7.40 (2H_A, bs), 7.62 (2H_B, bs), 7.86 (2H_A, bs), 7.94 (2H_B, bs); ¹³C NMR (101 MHz, CDCl₃): δ 33.1, 46.4, 55.9 (2C), 87.5, 101.4, 112.3, 113.2, 121.0 (2C), 122.3 (2C, q, $J_{C-F} = 272.4$ Hz), 123.9 (1C, m), 128.3 (2C, bs), 131.9 (2C), 137.4, 149.1, 151.1, 168.3, 198.1; ESI-MS: $m/z = 460.2$ [M+H]⁺, 492.0 [M+Na]⁺.



(131d): yellow oil, 325 mg, 80% yield; Although numerous attempts by changing solvent and temperature, it has never been possible to obtain a well resolved spectrum of the product; ¹H NMR (200 MHz, CDCl₃, 25

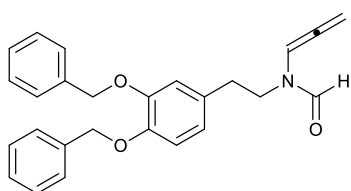
°C) (two rotamers A:B, ratio 1:1): δ 1.38 (9H_A, bs), 1.47 (9H_B, bs), 2.73 (2H_A+2H_B, bs), 3.52 (2H_A+2H_B, bs), 3.83 (3H_A+3H_B, bs), 3.84 (3H_A+3H_B, bs), 5.37 (2H_A+2H_B, bs), 6.65-6.78 (3H_A+3H_B, m), 6.98 (1H_A, m), 7.16 (1H_A, m); ESI-MS: $m/z = 319.1$ [M+H]⁺, 342.0 [M+Na]⁺, 639.2 [2M+H]⁺.



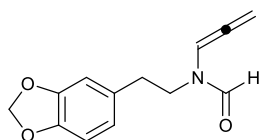
(131e): brown oil, 133 mg, 36% yield; ¹H NMR (400 MHz, CDCl₃) (two rotamers A:B, ratio 1.2:1): δ 2.77-2.83 (2H_A + 2H_B, m), 3.56 (2H_A, t, $J = 6.6$ Hz), 3.63-3.67 (2H_B, m), 3.86 (6H_B, s), 3.87 (3H_A, s), 3.88 (3H_A, s), 5.48

(2H_B, d, $J = 6.3$ Hz), 5.51 (2H_A, d, $J = 6.6$ Hz), 6.58 (1H_A, t, $J = 6.3$ Hz), 6.64-6.82 (3H_A + 3H_B, m), 7.30 (1H_B, t, $J = 6.4$ Hz), 7.76 (1H_B, s), 8.20 (1H_A, s); ¹³C NMR (101 MHz, CDCl₃): δ 32.8 (1C_B), 34.0 (1C_A), 43.5 (1C_B), 48.2 (1C_A), 55.8 (2C_B), 55.9 (2C_A), 87.3 (1C_A), 87.9 (1C_B), 97.4 (1C_A), 100.4 (1C_B), 111.2 (1C_B), 111.4 (1C_A), 112.0 (1C_B), 112.0 (1C_A), 120.7 (1C_B), 120.9 (1C_A), 130.4

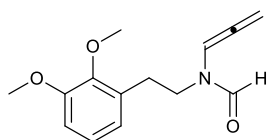
(1C_A), 131.0 (1C_B), 147.6 (1C_A), 147.9 (1C_B), 148.8 (1C_B), 149.0 (1C_A), 160.3 (1C_B), 160.5 (1C_A), 200.4 (1C_A), 202.2 (1C_B); ESI-MS: $m/z = 248.0 [M+H]^+$, 270.0 $[M+Na]^+$, 495.2 $[2M+H]^+$.



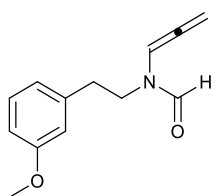
(131f): yellow oil, 479 mg, 80% yield; ¹H NMR (400 MHz, CDCl₃) (two rotamers A:B, ratio 1.7:1): δ 2.71-2.75 (2H_A+2H_B, m), 3.46-3.52 (2H_A, m), 3.59 (2H_B, t, $J = 7.7$ Hz), 5.14 (4H_A, s), 5.15 (2H_B, s), 5.17 (2H_B, s), 5.38 (2H_B, d, $J = 6.2$ Hz), 5.45 (2H_A, d, $J = 6.4$ Hz), 6.45 (1H_A, t, $J = 6.3$ Hz), 6.64 (1H_A, d, $J = 8.3$ Hz), 6.69 (1H_B, s), 6.72 (1H_B, d, $J = 8.3$ Hz), 6.79 (1H_A, s), 6.87 (1H_A+1H_B, d, $J = 8.0$ Hz), 7.25 (1H_A, t, $J = 6.6$ Hz), 7.30-7.47 (10H_A+10H_B, m), 7.67 (1H_A, s), 8.10 (1H_B, s); ¹³C NMR (101 MHz, CDCl₃): δ 32.7 (1C_B), 33.4 (1C_A), 43.4 (1C_B), 48.1 (1C_A), 71.2 (1C_A), 71.35 (1C_B), 71.40 (1C_B), 71.5 (1C_A), 87.2 (1C_A), 87.9 (1C_B), 95.4 (1C_A), 100.4 (1C_B), 115.27 (1C_B), 115.31 (1C_A), 115.9 (1C_A), 116.1 (1C_B), 121.7 (1C_B), 121.9 (1C_A), 127.27 (2C_B), 127.31 (2C_B+2C_A), 127.3 (2C_A), 127.7 (1C_A+1C_B), 127.7 (1C_A), 127.9 (1C_B), 128.44 (2C_B), 128.46 (2C_A+2C_B), 128.49 (2C_A), 131.2 (1C_B), 131.9 (1C_A), 137.3 (1C_A+1C_B), 137.4 (1C_A+1C_B), 147.6 (1C_B), 148.0 (1C_A), 148.8 (1C_A), 149.0 (1C_B), 160.3 (1C_A), 160.5 (1C_B), 200.3 (1C_A), 202.2 (1C_B); ESI-MS: $m/z = 400.0 [M+H]^+$, 422.0 $[M+Na]^+$, 799.0 $[2M+H]^+$.



(131g): yellow oil, 208 mg, 60% yield; ¹H NMR (400 MHz, CDCl₃) (two rotamers A:B, ratio 1.1:1): δ 2.74-2.80 (2H_A+2H_B, m), 3.54 (2H_A, t, $J = 6.8$ Hz), 3.62 (2H_B, pt, $J = 7.8$ Hz), 5.48 (2H_B, d, $J = 6.2$ Hz), 5.50 (2H_A, d, $J = 6.2$ Hz), 5.93 (2H_B, s), 5.95 (2H_A, s), 6.56-6.76 (3H_A+4H_B, m), 7.30 (1H_A, t, $J = 6.3$ Hz), 7.79 (1H_A, s), 8.10 (1H_B, s); ¹³C NMR (101 MHz, CDCl₃): δ 32.9 (1C_B), 34.1 (1C_A), 43.5 (1C_B), 48.2 (1C_A), 87.3 (1C_A), 88.0 (1C_B), 95.4 (1C_A), 100.4 (1C_B), 100.8 (1C_B), 100.9 (1C_A), 108.2 (1C_B), 108.4 (1C_A), 109.0 (1C_A), 109.2 (1C_B), 121.7 (1C_B), 121.9 (1C_A), 131.5 (1C_A), 132.1 (1C_B), 146.1 (1C_A), 146.4 (1C_B), 147.5 (1C_B), 147.8 (1C_A), 160.3 (1C_B), 160.5 (1C_A), 200.24 (1C_B), 202.18 (1C_A); ESI-MS: $m/z = 270.0 [M+Na]^+$.



(131h): yellow oil, 256 mg, 69% yield; ^1H NMR (400 MHz, CDCl_3) (two rotamers A:B, ratio 1.3:1): δ 2.86-2.90 ($2\text{H}_\text{A}+2\text{H}_\text{B}$, m), 3.59 (2H_A , t, $J = 7.2$ Hz), 3.67 (2H_B , t, $J = 7.7$ Hz), 3.84-3.87 ($6\text{H}_\text{A}+6\text{H}_\text{B}$, m), 5.43 (2H_B , d, $J = 6.2$ Hz), 5.50 (2H_A , d, $J = 6.5$ Hz), 6.56 (1H_B , t, $J = 6.6$ Hz), 6.68 (1H_A , d, $J = 7.5$ Hz), 6.82 ($1\text{H}_\text{A}+2\text{H}_\text{B}$, pt, $J = 7.9$ Hz), 6.98 ($1\text{H}_\text{A}+1\text{H}_\text{B}$, pt, $J = 7.5$ Hz), 7.26-7.29 (1H_A , m), 7.83 (1H_A , s), 8.20 (1H_B , s); ^{13}C NMR (101 MHz, CDCl_3): δ 27.8 (1C_B), 29.6 (1C_A), 42.5 (1C_B), 46.9 (1C_A), 55.6 ($1\text{C}_\text{A} + 1\text{C}_\text{B}$), 60.6 (1C_A), 60.7 (1C_B), 87.2 (1C_A), 87.9 (1C_B), 95.5 (1C_A), 100.4 (1C_B), 110.9 (1C_B), 111.3 (1C_A), 122.4 (1C_B), 122.4 (1C_A), 123.8 (1C_B), 124.1 (1C_A), 131.5 (1C_A), 132.3 (1C_B), 147.2 (1C_A), 147.5 (1C_B), 152.7 (1C_B), 152.8 (1C_A), 160.4 (1C_B), 160.6 (1C_A), 200.1 (1C_B), 200.2 (1C_A); ESI-MS: $m/z = 248.0$ [$\text{M}+\text{H}$] $^+$, 270.0 [$\text{M}+\text{Na}$] $^+$, 495.2 [$2\text{M}+\text{H}$] $^+$.

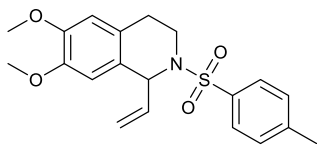


(131i): brown oil, 208 mg, 64% yield; ^1H NMR (400 MHz, CDCl_3) (two rotamers A:B, ratio 1.1:1): δ 2.80-2.86 ($2\text{H}_\text{A}+2\text{H}_\text{B}$, m), 3.58 (2H_A , t, $J = 7.2$ Hz), 3.67 (2H_B , pt, $J = 7.8$ Hz), 3.80 (3H_A , s), 3.81 (3H_B , s), 5.48 (2H_B , d, $J = 6.5$ Hz), 5.51 (2H_A , d, $J = 6.6$ Hz), 6.58 (1H_B , t, $J = 6.1$ Hz), 6.68-6.83 ($3\text{H}_\text{A}+3\text{H}_\text{B}$, m), 7.20-7.25 ($1\text{H}_\text{A}+1\text{H}_\text{B}$, m), 7.30 (1H_A , t, $J = 6.5$ Hz), 7.80 (1H_A , s), 8.20 (1H_B , s); ^{13}C NMR (101 MHz, CDCl_3): δ 33.3 (1C_B), 34.5 (1C_A), 43.2 (1C_B), 47.9 (1C_A), 55.1 (1C_B), 55.1 (1C_A), 87.3 (1C_A), 87.9 (1C_B), 95.4 (1C_A), 100.4 (1C_B), 111.8 (1C_B), 111.9 (1C_A), 114.5 (1C_A), 114.7 (1C_B), 121.10 (1C_B), 121.13 (1C_A), 129.4 (1C_B), 129.7 (1C_A), 139.5 (1C_B), 140.0 (1C_A), 159.6 (1C_B), 159.8 (1C_A), 160.3 (1C_B), 160.5 (1C_A), 200.3 (1C_B), 202.2 (1C_A); ESI-MS: $m/z = 218.0$ [$\text{M}+\text{H}$] $^+$, 240 [$\text{M}+\text{Na}$] $^+$.

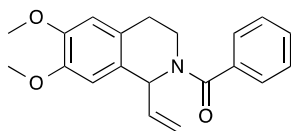
General Procedure for the organocatalytic enantioselective cyclization of compounds 131a-i.

To a solution of allenamide (0.1 mmol, 1 equiv.) in trifluorotoluene (1 mL), Brønsted acid (0.01 mmol, 0.1 equiv.) and MS 4Å (0.05 g) were added and the reaction was stirred for 24h. The solvent

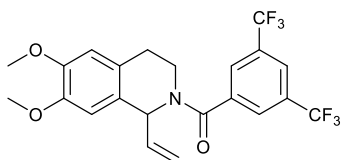
was removed under reduced pressure and the crude was purified by flash chromatography on silica gel (cyclohexane/ethyl acetate 3/7) to obtain the desired products.



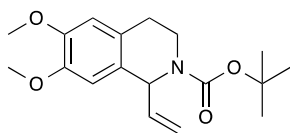
(132a): sticky white solid, 23.5 mg, 63% yield, 21% *ee*; the *ee* was determined by HPLC analysis, Daicel Chiralpak[®] IA column: hexane/*i*-PrOH from 70:30, flow rate 1.0 mL/min, 40°C, $\lambda = 280$ nm: $\tau_{major} = 8.18$ min., $\tau_{minor} = 6.98$ min; ¹H NMR (400 MHz, CDCl₃): δ 2.38 (3H, s), 2.48-2.54 (1H, m), 2.65-2.74 (1H, m), 3.27-3.34 (1H, m), 3.82 (3H, s), 3.84 (3H, s), 3.85-3.89 (1H, m), 5.05 (1H, d, $J = 17.14$ Hz), 5.18 (1H, d, $J = 10.20$ Hz), 5.46 (1H, d, $J = 5.98$ Hz), 5.91 (1H, ddd, $J = 5.72$ Hz, $J = 10.12$ Hz, $J = 16.98$ Hz), 6.47 (1H, s), 6.53 (1H, s), 7.20 (2H, d, $J = 8.08$ Hz), 7.67 (2H, d, $J = 8.33$ Hz); ¹³C NMR (101 MHz, CDCl₃): δ 21.5, 27.2, 39.1, 55.8, 55.9, 57.7, 110.4, 111.3, 117.7, 125.4, 125.6, 127.1 (2C), 129.4 (2C), 137.3, 137.9, 143.9, 147.4, 148.0; EI-MS: $m/z = 373$ (12), 346 (84), 308 (75), 217 (82), 198 (87), 91 (100); ESI-MS: $m/z = 374.0$ [M+H]⁺, 396.0 [M+Na]⁺, 769.0 [2M+Na]⁺; HMRS calcd for C₁₈H₁₉N: 373.13478; found 373.13486.



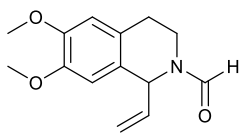
(132b): sticky white solid, 21.0 mg, 65% yield, 14% *ee*; the *ee* was determined by HPLC analysis, Daicel Chiralpak[®] IA column: hexane/*i*-PrOH from 60:40, flow rate 0.50 mL/min, 40°C, $\lambda = 280$ nm: $\tau_{major} = 11.62$ min., $\tau_{minor} = 16.86$ min; Although numerous attempts by changing solvent and temperature, it has never been possible to obtain a well resolved spectrum of the product; ¹H NMR (400 MHz, CDCl₃, 25 °C) (two rotamers A:B, ratio 2:1): δ 2.61 (1H_A, bs), 2.89 (1H_A, bs), 3.22 (1H_B, bs), 3.40 (1H_B, bs), 3.75 (2H_A+2H_B, bs), 3.85 (6H_A+6H_B, bs), 4.72-5.11 (2H_A+2H_B, m), 5.26 (1H_A+1H_B, bs), 6.07 (1H_A+1H_B, bs), 6.17 (1H_A, bs), 6.36 (1H_B, bs), 6.61 (2H_A, bs), 6.67 (2H_B, bs), 7.38 (5H_A+5H_B, bs); ¹³C NMR (101 MHz, CDCl₃): δ 28.9 (1C_B), 29.7 (1C_A), 41.2 (1C_A+1C_B), 54.2 (1C_A+1C_B), 55.8 (1C_A+1C_B), 56.0 (1C_A+1C_B), 111.4 (1C_A+1C_B), 117.4 (1C_A+1C_B), 120.6 (1C_A+1C_B), 126.0 (1C_A+1C_B), 126.7 (2C_A+2C_B), 128.5 (2C_A+2C_B), 129.2 (2C_A+2C_B), 131.4 (1C_A+1C_B), 136.3 (1C_A), 137.1 (1C_B), 147.6 (1C_A+1C_B), 148.1 (1C_A+1C_B), 170.4 (1C_A+1C_B); ESI-MS: $m/z = 323$ (25), 308 (20), 280 (6), 264 (11), 218 (34), 105 (100), 77 (85); ESI-MS: $m/z = 324.2$ [M+H]⁺, 346.0 [M+Na]⁺, 669.2 [2M+Na]⁺;



(132c): sticky yellow solid, 28.9 mg, 63% yield, 0% *ee*; the *ee* was determined by HPLC analysis, Daicel Chiralpak® IA column hexane/*i*-PrOH from 90:10, flow rate 0.5 mL/min, 40°C, $\lambda = 285$ nm: $\tau_{major} = 14.66$ min., $\tau_{minor} = 16.76$ min; Although numerous attempts by changing solvent and temperature, it has never been possible to obtain a well resolved spectrum of the product; ^1H NMR (400 MHz, CDCl_3 , 25 °C) (two rotamers A:B, ratio 2:1): δ 2.60 (1H_A+1H_B, bs), 2.89 (1H_A+1H_B, bs), 3.00 (2H_A, bs), 3.28 (1H_B, bs), 3.53 (1H_A, bs), 3.85 (6H_A+6H_B, bs), 4.72-5.16 (2H_A+2H_B, m), 5.34 (1H_A+1H_B, d, $J = 9.4$ Hz), 6.09 (1H_A, bs), 6.37 (1H_B, bs), 6.67 (2H_A+2H_B, bs), 7.45 (1H_A+1H_B, bs), 7.89 (2H_A+2H_B, bs); The presence of rotamers avoids the detection of some signals, that result too broad to be identified from the noise; ^{13}C NMR (101 MHz, CDCl_3): δ 34.2 (1C_A), 35.1 (1C_B), 41.6 (1C_A), 41.7 (1C_B), 55.9 (2C_A), 56.0 (1C_B), 77.2 (1C_A+1C_B), 110.9 (1C_A+1C_B), 111.4 (1C_A+1C_B), 117.2 (1C_A), 118.3 (1C_B), 119.8 (2C_B, q, $J_{\text{C-F}} = 274.2$ Hz), 122.8 (2C_A, q, $J_{\text{C-F}} = 272.4$ Hz), 123.6 (2C_A+2C_B), 124.9 (1C_B), 125.1 (1C_A), 125.4 (1C_B), 125.6 (1C_A), 127.2 (1C_A+1C_B, bs), 136.5 (1C_A), 136.8 (1C_B), 138.1 (1C_A+1C_B), 147.9 (1C_A+1C_B), 148.4 (1C_A+1C_B); EI-MS: $m/z = 459$ (22), 430 (76), 241 (100), 213 (84); ESI-MS: $m/z = 460.0$ [M+H]⁺, 482.0 [M+Na]⁺, 941.0 [2M+Na]⁺;



(132d): yellowish oil, 10.0 mg, 30% yield, 32% *ee*; the *ee* was determined by HPLC analysis, Daicel Chiralpak® ia column: hexane/*i*-PrOH from 90:10, flow rate 0.70 mL/min, 40°C, $\lambda = 280$ nm: $\tau_{major} = 11.80$ min., $\tau_{minor} = 18.4$ min; ^1H NMR (400 MHz, CDCl_3 , 25 °C): δ 1.47 (9H, s), 2.60 (1H, dt, $J = 3.4$ Hz, $J = 15.5$ Hz), 2.71-2.77 (1H, m), 2.80-2.88 (1H, m), 3.13 (1H, bs), 3.83 (3H, s), 3.84 (3H, s), 3.85 (1H, d, $J = 4.0$ Hz), 5.05 (1H, d, $J = 17.0$ Hz), 5.14 (1H, dt, $J = 1.4$ Hz, $J = 10.2$ Hz), 5.89-5.97 (1H, m), 6.58 (s, 1H), 6.59 (s, 1H); Due to the presence of rotamers, it was not possible to obtain suitable spectra performing a ^{13}C NMR experiment; the signals have been determined from gHSQC and gHMBC experiments; ^{13}C NMR (101 MHz, CDCl_3): δ 28.9 (1C_A+1C_B), 29.6 (3C_A), 32.5 (3C_B), 42.3 (1C_A+1C_B), 56.0 (1C_A+1C_B), 56.5 (1C_A+1C_B), 57.3 (1C_A+1C_B), 80.4 (1C_A), 85.6 (1C_B), 111.4 (1C_A), 111.3 (1C_A), 111.6 (1C_B), 112.4 (1C_B), 116.8 (1C_A+1C_B), 127.3 (1C_A), 128.7 (1C_B), 129.2 (1C_A+1C_B), 148.3 (1C_A+1C_B), 148.8 (1C_A+1C_B), 149.5 (1C_A+1C_B), 181.6 (1C_A+1C_B); ESI-MS: $m/z = 342.2$ [M+Na]⁺, 661.2 [2M+Na]⁺;



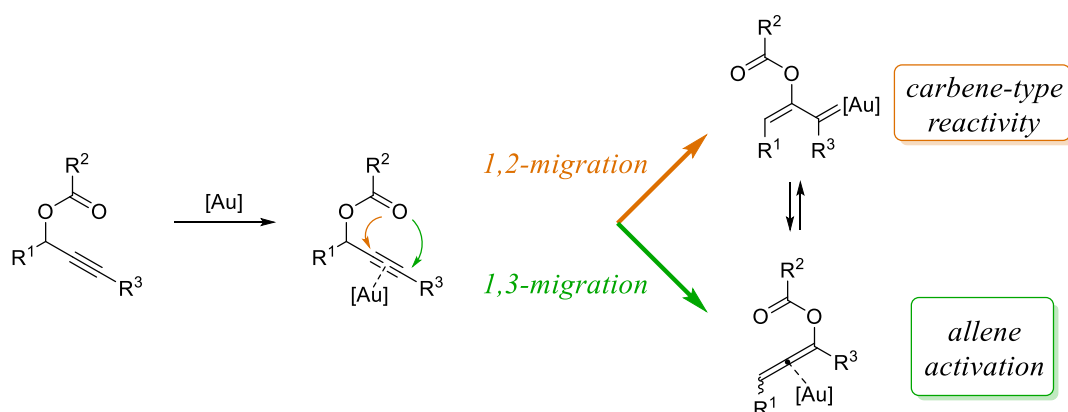
(132e): sticky white solid, 9.9 mg, 40% yield, 81% *ee*; to perform the HPLC analysis of product **132e**, it was necessary to reduce the amide moiety to methyl group LiAlH₄ (1.5 equiv.) was added to **132e**. After 2h, a few drops of water were added, followed by MgSO₄. The mixture was filtered and directly subjected to HPLC analysis; Daicel Chiralpak[®] OD-H column: hexane/*i*-PrOH from 90:10, flow rate 0.70 mL/min, 40°C, λ = 285 nm: τ_{major} = 7.87 min., τ_{minor} = 14.93 min; ¹H NMR (400 MHz, CDCl₃) (two rotamers A:B, ratio 1:1): δ 2.62-2.72 (2H_B, m), 2.78-2.91 (2H_A, m), 3.13 (1H_B, ddd, *J* = 4.7 Hz, *J* = 11.0 Hz, *J* = 15.6 Hz), 3.45 (1H_A, ddd, *J* = 4.2 Hz, *J* = 13.0 Hz, *J* = 13.0 Hz), 3.65 (1H_A, dd, *J* = 5.8 Hz, *J* = 13.2 Hz), 3.80 (3H_A, s), 3.81 (3H_A + 3H_B, bs), 3.82 (3H_B, s), 4.29 (1H_B, m), 5.02 (1H_B, d, *J* = 5.7 Hz), 5.09 (1H_A, d, *J* = 17 Hz), 5.11 (1H_B, d, *J* = 17.0 Hz), 5.19 (1H_A, d, *J* = 10.1 Hz), 5.20 (1H_B, d, *J* = 10.1 Hz), 5.78 (1H_A, d, *J* = 5.6 Hz), 5.86-5.99 (1H_A + 1H_B, m), 6.55 (1H_A, s), 6.56 (1H_A + 1H_B, bs), 6.59 (1H_B, s), 8.15 (1H_A, s), 8.25 (1H_B, s); ¹³C NMR (101 MHz, CDCl₃): δ 27.6 (1C_B), 29.2 (1C_A), 35.1 (1C_B), 40.2 (1C_A), 52.7 (1C_A), 55.8 (1C_A), 55.8 (1C_A), 55.9 (1C_A), 56.0 (1C_B), 58.7 (1C_B), 110.1 (1C_B), 110.6 (1C_A), 111.3 (1C_A), 111.5 (1C_B), 117.0 (1C_B), 117.3 (1C_A), 125.2 (1C_A + 1C_B), 125.4 (1C_A), 126.5 (1C_B), 136.4 (1C_A), 138.0 (1C_B), 147.6 (1C_B), 147.7 (1C_A), 148.0 (1C_A), 148.3 (1C_B), 161.1 (1C_A), 161.6 (1C_B); ESI-MS: *m/z* = 248.2 [M+H]⁺, 270.0 [M+Na]⁺, 495.2 [2M+H]⁺; HMRS calcd for C₁₈H₁₉N: 247.12084; found 247.12075.

References

1. F. Romanov-Michailidis, L. Guénée and A. Alexakis, *Angew. Chem. Int. Ed.*, 2013, **52**, 9266-9270; F. Romanov-Michailidis, L. Guénée and A. Alexakis, *Org. Lett.*, 2013, **15**, 5890-5893; V. Rauniyar, A. D. Lackner, G. L. Hamilton and F. D. Toste, *Science*, 2011, **334**, 1681-1684; Y.-M. Wang, J. Wu, C. Hoong, V. Rauniyar and F. D. Toste, *J. Am. Chem. Soc.*, 2012, **134**, 12928-12931; V. Rauniyar, Z. J. Wang, H. E. Burks and F. D. Toste, *J. Am. Chem. Soc.*, 2011, **133**, 8486-8489; T. Akiyama, H. Morita and K. Fuchibe, *J. Am. Chem. Soc.*, 2006, **128**, 13070-13071.
2. J. Párraga, N. Cabedo, S. Andujar, L. Piqueras, L. Moreno, A. Galán, E. Angelina, R. D. Enriz, M. D. Ivorra, M. J. Sanz and D. Cortes, *Eur. J. Med. Chem.*, 2013, **68**, 150-166.
3. S. H. Yang, C.-H. Song, H. T. M. Van, E. Park, D. B. Khadka, E.-Y. Gong, K. Lee and W.-J. Cho, *J. Med. Chem.*, 2013, **56**, 3414-3418.
4. C. Zhang, Z. Xu, T. Shen, G. Wu, L. Zhang and N. Jiao *Org. Lett.* 2012, **14**, 2362–2365.
5. T. M. Böhme, C. E. Augelli-Szafran, H. Hallak, T. Pugsley, K. Serpa and R. D. Schwarz, *J. Med. Chem.*, 2002, **45**, 3094-3102.
6. D. S. Ermolat'ev, J. B. Bariwal, H. P. L. Steenackers, S. C. J. De Keersmaecker and E. V. Van der Eycken, *Angew. Chem. Int. Ed.*, 2010, **49**, 9465-9468.

4. INTRODUCTION: ALLENOATES

Another type of heteroatom-substituted allenes is represented by allenoates where the amide group of the allenamides is replaced with an ester group. One easy way to obtain allenoates consists of the gold-catalysed [3,3]-sigmatropic rearrangement of propargylic carboxylates. Indeed, it is already known that in gold catalysis these propargylic esters can undergo 1,2-acyloxy migration leading to a gold vinyl carbenoid species or 1,3-acyloxy migration resulting in a gold allenic intermediate (Scheme 1).



Scheme 1: Au-catalysed 1,2- or 1,3-acyloxy migration of propargylic carboxylates.

The intermediates obtained through the 1,2- or 1,3-migration are in equilibrium.^[1] Recently, it was reported a computation study to rationalize the rearrangement selectivity.^[2] In particular, two resonance structure models were associated to the selectivity of the cyclization (Figure 1).

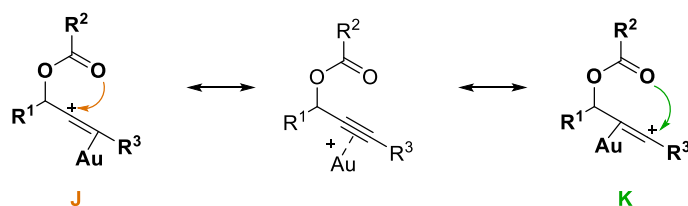


Figure 1: Resonance structure models.

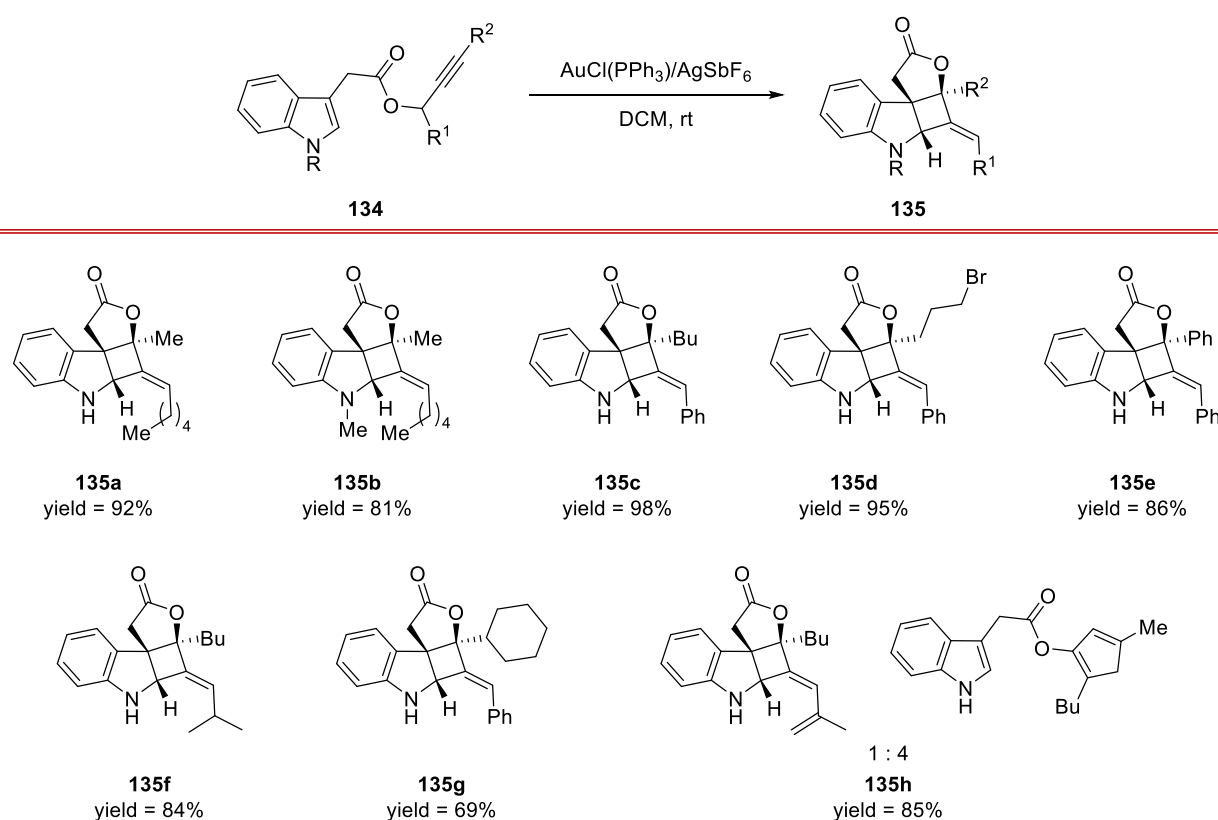
Substrates are more likely to be stabilized to the resonance structure **K** and the C3 atom is more likely to accept the electron from the ester group except for the substrates featuring hydrogen or EWG for R³, which undergo the gold-catalysed 1,2-acyloxy migration.

The gold vinyl carbenoid species are principally employed in cyclopropanation reaction of alkenes and dienes, as well as insertion into C–H bonds.^[3–5] On the contrary, the allenic intermediate can follow two different routes:

- ✓ the allenates intermediate can undergo a gold-catalysed electrophilic activation and subsequent nucleophilic trapping;
- ✓ the allene moiety can act as nucleophilic reagent.

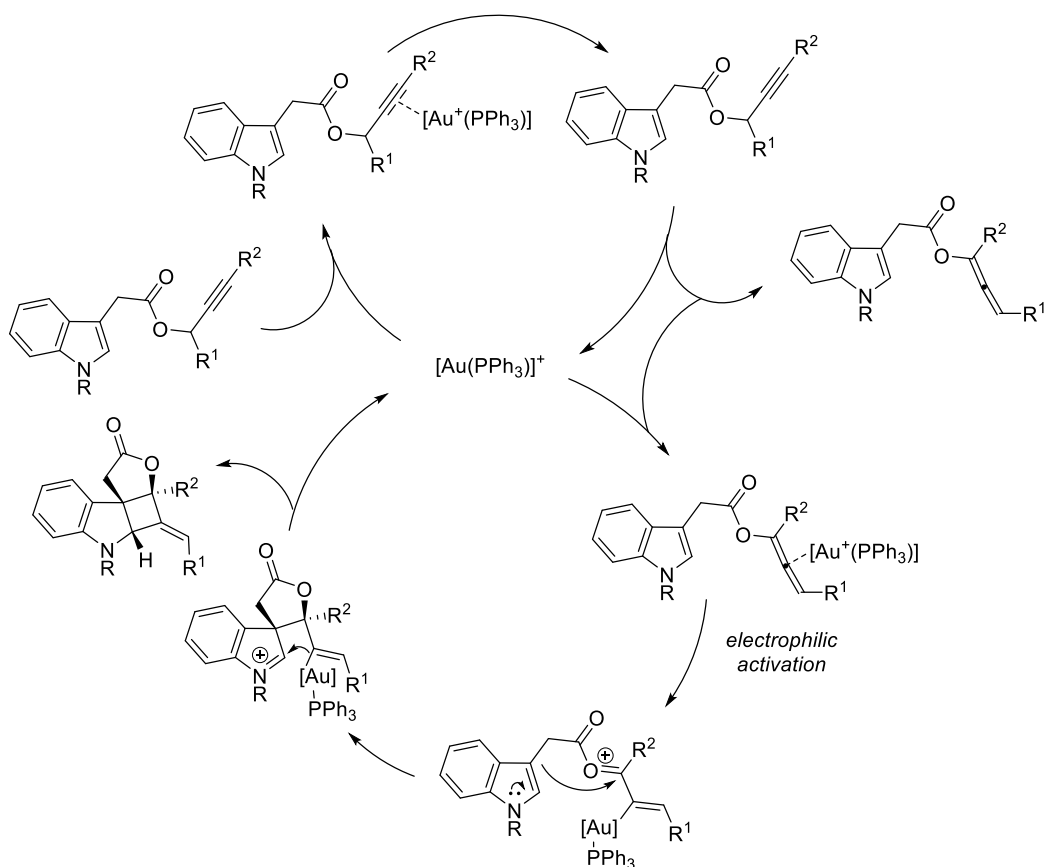
4.1 Electrophilic Activation

The first type of reactivity was used by Zhang in 2005^[6] to develop an new efficient procedure to prepare highly functionalized 2,3-indoline-fused cyclobutanes. In particular, in the presence of gold(I) catalyst, the propargylic indole-3-acetates resulted after 2 hours in the corresponding products in good yields (Scheme 2).



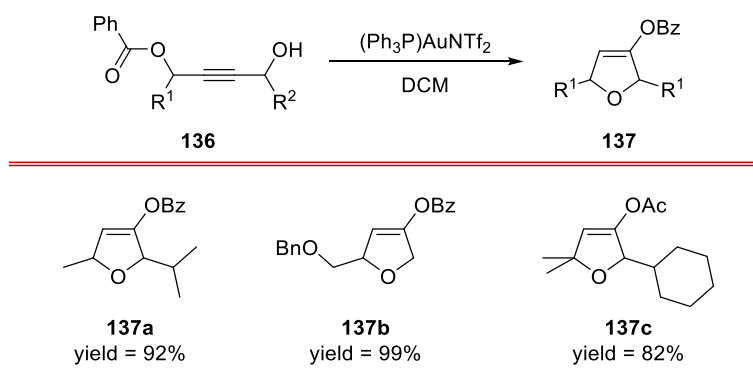
Scheme 2: Scope of the Au-catalysed synthesis of 2,3-indoline-fused cyclobutanes.

In the proposed reaction mechanism reported in Scheme 3, the [3,3]-sigmatropic rearrangement promoted by the catalyst, led to an allenolate intermediate that can be efficiently activated by the gold(I) specie toward the subsequent nucleophilic attack by the C(3)-indole.



Scheme 3: Proposed reaction mechanism.

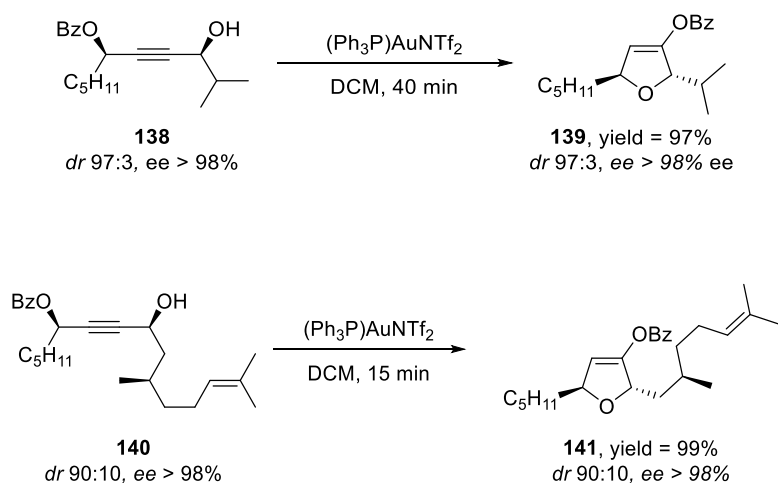
The electrophilic activation followed by nucleophilic trapping can be also used to prepare polysubstituted 2,5-dihydrofurans as reported by Gagosz.^[7] The methodology proved to be flexible and several substituted butynediol monobenzoates resulted in the corresponding products in the presence of 2 mol% of $(\text{Ph}_3\text{P})\text{AuNTf}_2$ (Scheme 4).



Scheme 4: Application in the synthesis of 2,5-dihydrofurans.

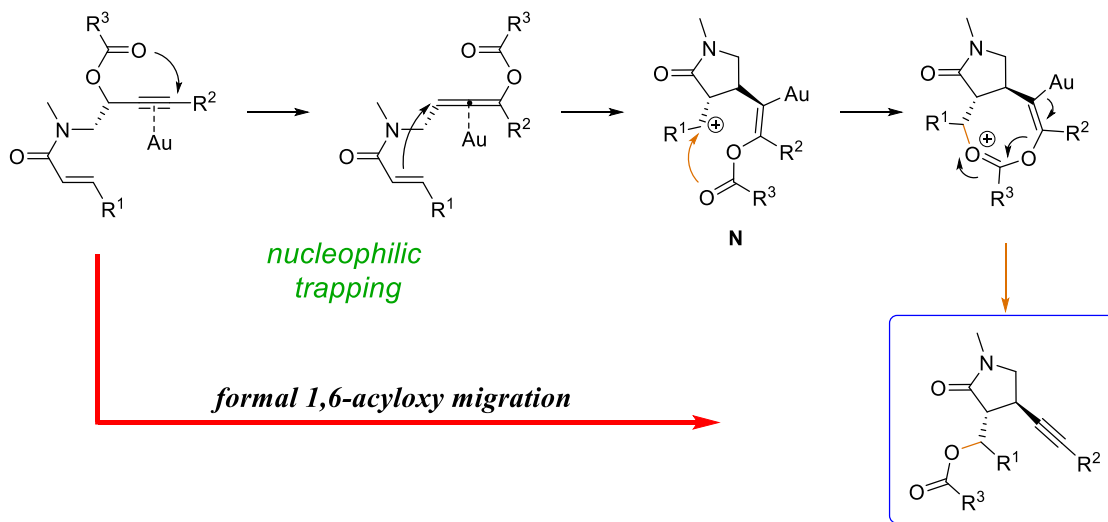
Also enantioenriched butynediol monobenzoates were submitted under the same experimental conditions and in most of these cases the desired products were isolated without loss of optical purity. Also propargylic ester featuring three stereogenic centers was used as starting material by

providing the corresponding *trans*-2,5-disubstituted dihydrofuran in 99% yield and complete transfer of the stereochemical information (Scheme 5).



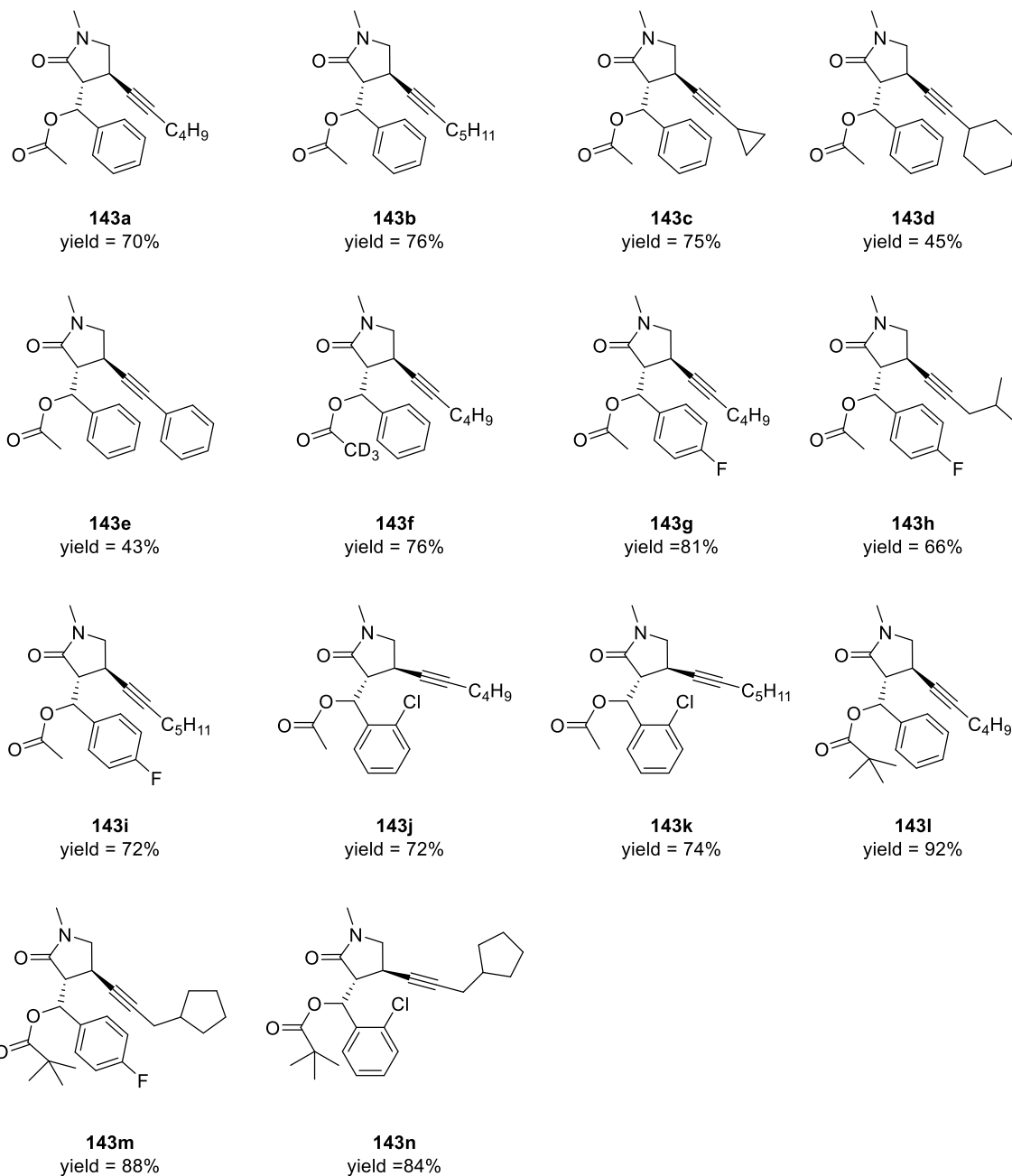
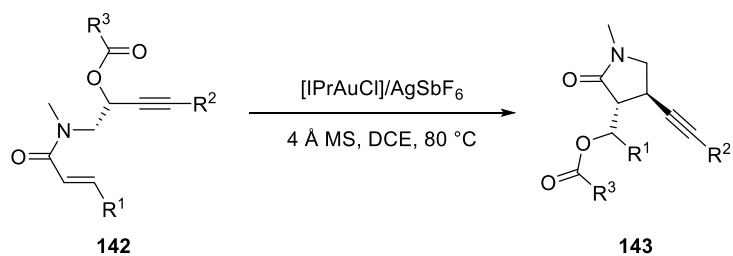
Scheme 5: Complete transfer of optical purity using enantioenriched substrates.

Recently, Hashmi and co-workers employed the electrophilic activation of the *in situ* formed allenates in order to prepare 3,4-disubstituted pyrrolidin-2-ones through tandem 1,3- and 1,5-acyloxy migration.^[8] In particular, the substituted propargylic ester undergoes the [3,3]-sigmatropic rearrangement resulting in the allenate intermediate which is attacked by the olefin forming the intermediate N. The final 1,5-acyloxy migration leads to the desired product (Scheme 6).



Scheme 6: Tandem 1,3-1,5-acyloxy migration.

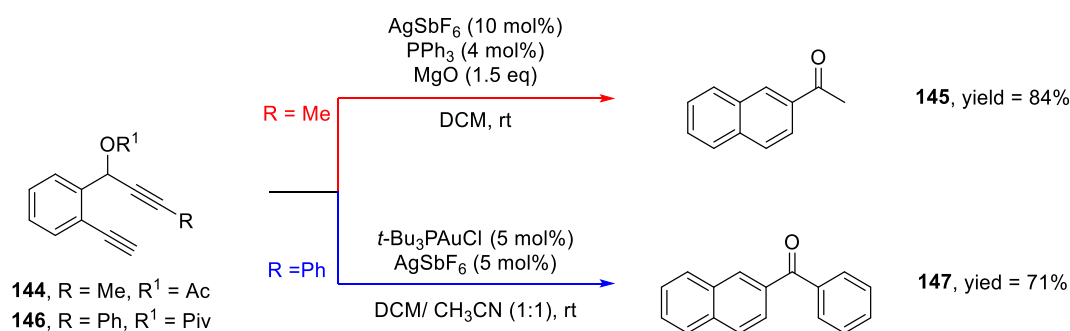
The large flexibility exhibited by the methodology makes this new route a useful and easy way to prepare diastereomerically pure butyrolactams, which are important building blocks for the total synthesis of various natural products and for the development of new compounds with pharmaceutical activities^[9] (Scheme 7).



Scheme 7: Scope of the formal 1,6-acyloxy migration promoted by Au(I)-catalyst.

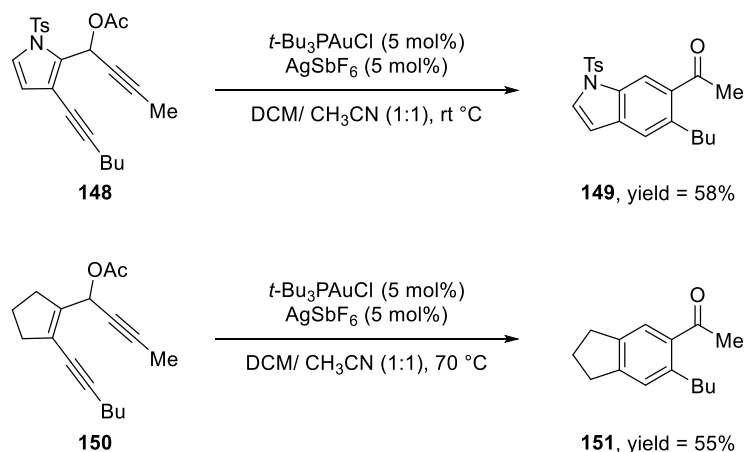
4.2 Nucleophilic Activation

The presence of the oxygen directly bonded to the allene moiety in the allenates, allows at the allenates undergoing nucleophilic activation. Toste and co-workers in 2006^[10] used this type of reactivity of the allenates to develop a very efficient synthesis of aromatic ketones promoted by transition metal, in particular silver- and gold-catalysts (Scheme 8).



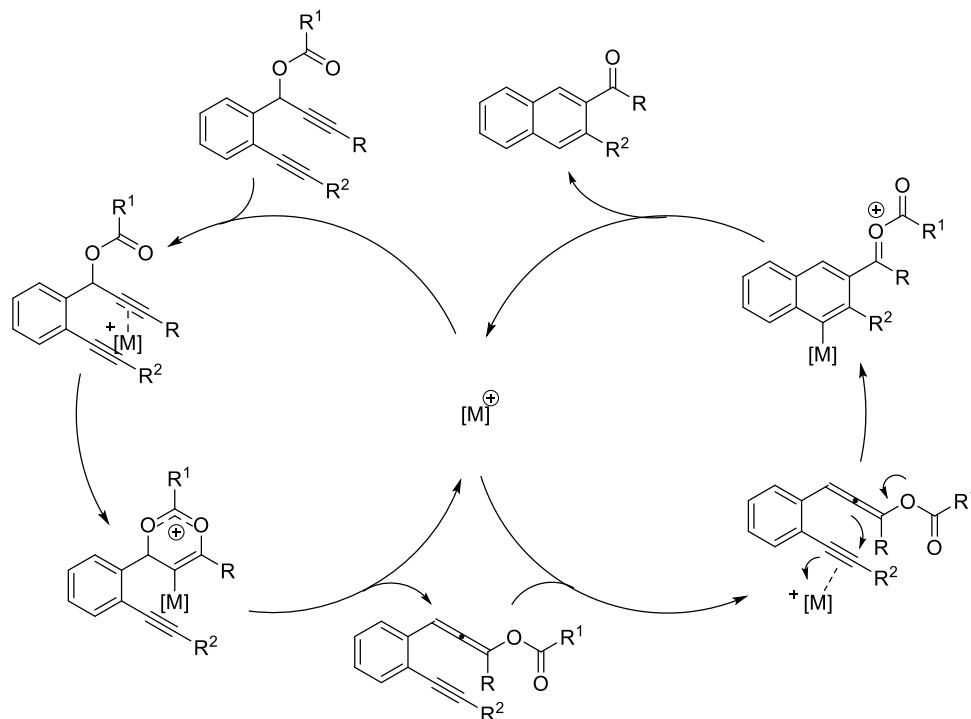
Scheme 8: Synthesis of aromatic ketones promoted by transition metal-catalysts.

The AgSbF₆ in the presence of PPh₃ was able to promote the reaction in good yield when acetyl group was employed as ester and the terminal substituent of the propargylic acetate was a methyl group, but no traces of the corresponding product were observed when pivalic ester **146** were used instead of **144**. To obtain the desired naphthylphenyl ketone **147** was developed a new catalyst-system using gold(I) catalyst in a mixture of dichloromethane and acetonitrile as solvent. An ample scope with ten differently substituted ketones isolated with good to excellent yields proved the flexibility of the catalytic process promoted by silver catalyst. The gold(I)-catalytic system demonstrated to be complementary to the silver-protocol because in all of the cases where the silver-conditions failed, the gold(I)-catalytic system produced the desired products (Scheme 9).



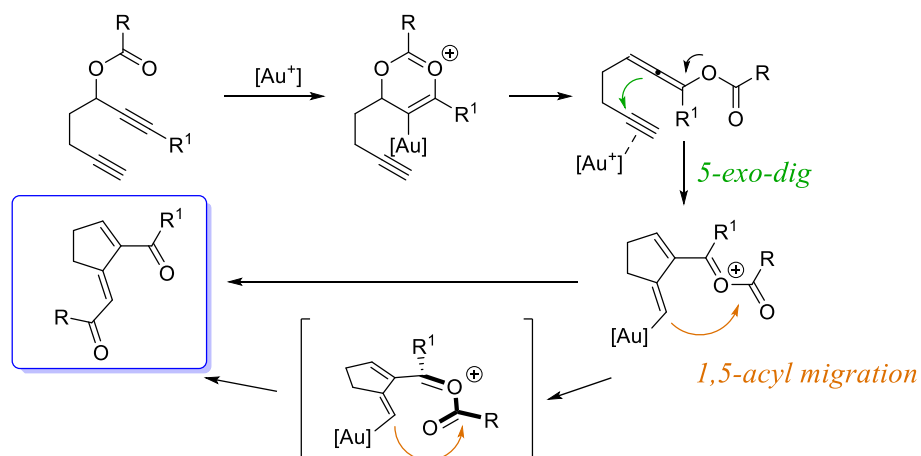
Scheme 9: Complementarity of the Au(I)-catalytic system with the Ag(I) ones.

Mechanistically, as it is shown in Scheme 10, the formation of the allenates promoted by the metal-catalyst is followed by activation of the remaining alkyne which undergoes the nucleophilic trapping from the allene moiety.



Scheme 10: Proposed reaction mechanism.

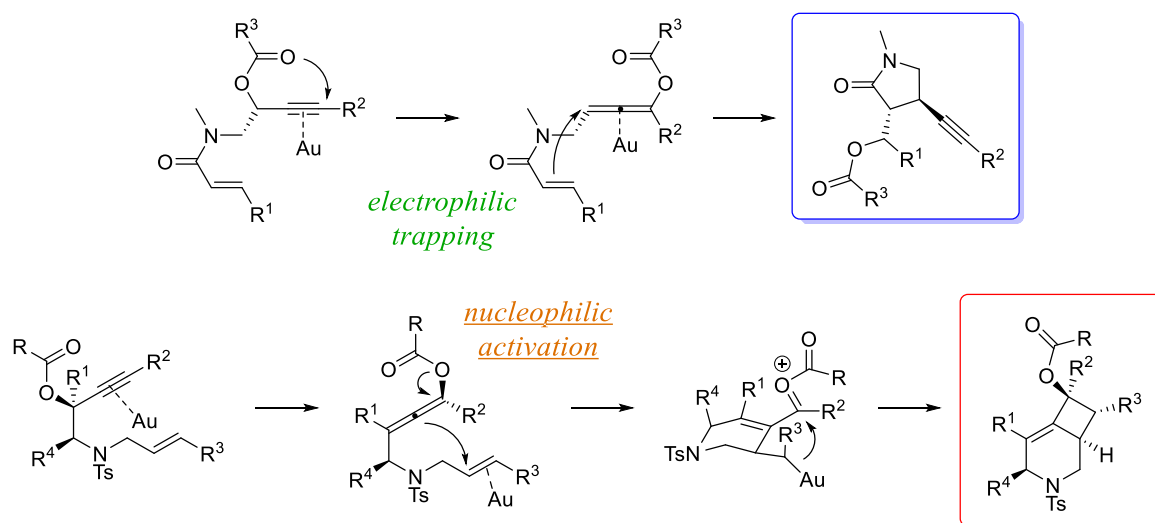
An efficient method to prepare δ -diketones through nucleophilic trapping by allenate intermediates was reported by Fensterbank and co-workers.^[11] In particular, the nucleophilic attack by the allene moiety on the alkyne, resulted in an intermediate which undergoes 1,5-acyl migration and leads to the desired product (Scheme 11).



Scheme 11: Synthesis of δ -diketones through 1,5-acyloxy migration.

Not only gold(I) catalyst could promote this reaction, but also complexes of Au^{III}, Pt^{II} and Pt^{IV} gave the desired product in good to excellent yield. All the products isolated exhibited only the *E* configuration for the exocyclic double bond. The DFT computational studies demonstrated that the *E* configuration was the favourite and the formation of the *Z* stereoisomer was kinetically very difficult to achieve. A scope with more than twenty diketones was obtained and the methodology resulted to be very tolerant toward several functional groups; only one limitation related to the triple bond was found: when substituted propargyl ester was employed, the second triple bond must remain monosubstituted.

Above it was reported that the allenolate intermediates underwent nucleophilic trapping by inactivated alkene in order to prepare disubstituted pyrrolidinone.^[8] Subsequently, Chan and co-workers demonstrated that the allene moiety can also react as nucleophile in a reaction with alkenes. In particular, they developed a gold-catalysed tandem 1,3-migratory/[2,2] cycloaddition of propargylic esters in order to prepare azabicyclo[4.2.0]oct-5-enes.^[12]



Scheme 12: Au-catalysed tandem 1,3-migratory/[2,2] cycloaddition of propargylic esters.

Several 1,7-enyne benzoates, prepared from the opportune *L*- α -aminoacids, were submitted under optimized reaction conditions resulting in a variety of highly substituted bicycles in good to excellent yields. The reaction demonstrated efficient transfer of chirality from the enantiopure substrates leading to the products. Moreover, when mixtures of diastereoisomers were employed as starting materials the reactions exhibited highly stereoconvergence since the corresponding products were isolated as single diastereoisomers.

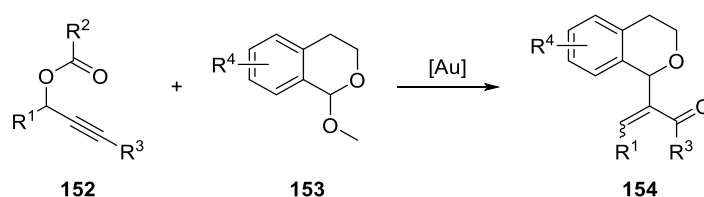
Bibliography

- [1] N. Marion, S. P. Nolan, *Angew. Chem. Int. Ed.* **2007**, *46*, 2750–2752.
- [2] J. Jiang, Y. Liu, C. Hou, Y. Li, Z. Luan, C. Zhao, Z. Ke, *Org. Biomol. Chem.* **2016**, *14*, 3558–3563.
- [3] C. Fehr, J. Galindo, *Angew. Chem. Int. Ed.* **2006**, *45*, 2901–2904.
- [4] A. Fürstner, P. Hannen, *Chem. Eur. J.* **2006**, *12*, 3006–3019.
- [5] N. D. Shapiro, Y. Shi, F. D. Toste, *J. Am. Chem. Soc.* **2009**, *131*, 11654–11655.
- [6] L. Zhang, **2005**, 16804–16805.
- [7] A. Buzas, F. Istrate, F. Gagosz, *Org. Lett.* **2006**, *8*, 1957–1959.
- [8] A. S. K. Hashmi, W. Yang, Y. Yu, M. M. Hansmann, M. Rudolph, F. Rominger, *Angew. Chem. Int. Ed.* **2013**, *52*, 1329–1332.
- [9] W. Xu, A. Kong, X. Lu, *J. Org. Chem.* **2006**, *71*, 3854–3858.
- [10] J. Zhao, C. O. Hughes, F. D. Toste, *J. Am. Chem. Soc.* **2006**, *128*, 7436–7437.
- [11] D. Leboeuf, A. Simonneau, C. Aubert, M. Malacria, V. Gandon, L. Fensterbank, *Angew. Chem. Int. Ed.* **2011**, *50*, 6868–6871.
- [12] W. Rao, D. Susanti, P. W. H. Chan, *J. Am. Chem. Soc.* **2011**, *133*, 15248–15251.

5. GOLD(I)-CATALYSED [3,3]-SIGMATROPIC REARRANGEMENT OF PROPARGYLIC CARBOXYLATES

5.1 Catalytic α -Allylation of Enones with Alcohols

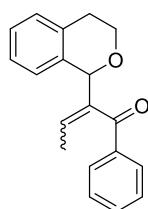
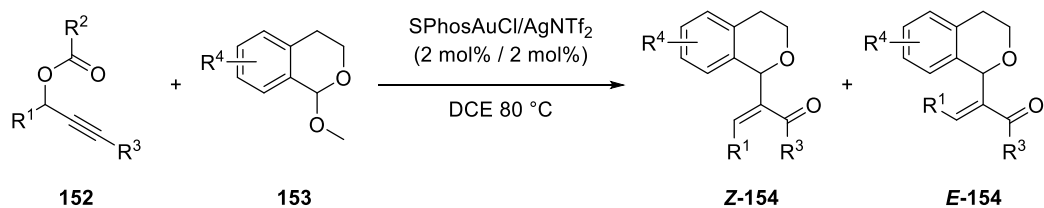
The few examples reported above for the electrophilic trapping of the allenates were limited to studies of intramolecular process. Hashmi and co-workers in 2013 developed the first intermolecular reaction involving nucleophilic gold allenic intermediates.^[1] In particular, they developed an efficient catalytic protocol able to prepare various isochromane derivatives which are powerful building blocks for the synthesis of natural products (Scheme 1).



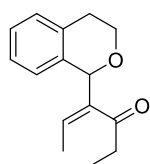
Scheme 1: Synthesis of isochromanes promoted by Au-catalysts.

Several gold(I) catalysts were tested in different solvents demonstrating that the SPhosAuCl/AgNTf₂ in DCE was the best catalytic system for the process leading to the corresponding product in 68% yield and with complete stereocontrol toward the formation of the *Z* isomer. Moreover, it was also observed that the replacement of the acetate group with the pivalate group increased the yield of the product up to 85%. Subsequently, the scope of the reaction was investigated submitting under optimized reaction conditions differently substituted isochromane acetal derivatives in combination with several propargylic pivalates (Scheme 2).

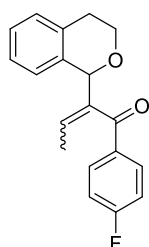
The large scope reported below shows the versatility of the protocol and its tolerance toward different functional groups. Propargylic pivalates featuring aliphatic as well as aromatic groups resulted in the corresponding products in good to excellent yields. In most of the cases the *Z* isomers were isolated as single products or as major stereoisomer in a mixture with the *E* products.



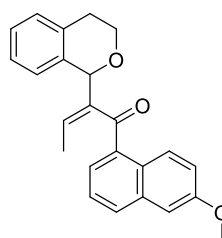
yield = 93%
Z/E = 11:1



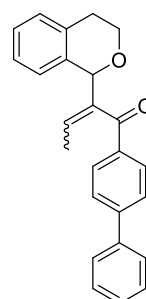
yield = 64%



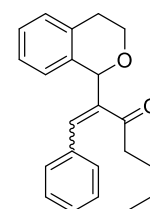
yield = 80%
Z/E = 22:1



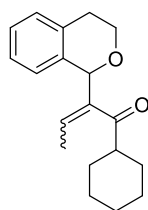
yield = 50%



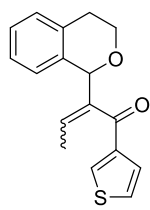
yield = 88%
Z/E = 12:1



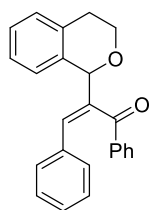
yield = 78%
Z/E = 2:1



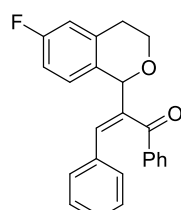
yield = 40%
Z/E = 3:2



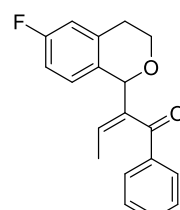
yield = 72%
Z/E = 3:2



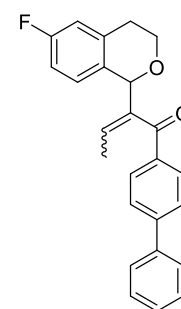
yield = 92%



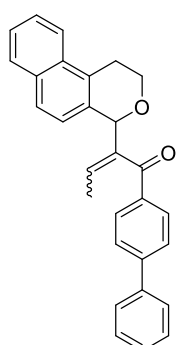
yield = 87%



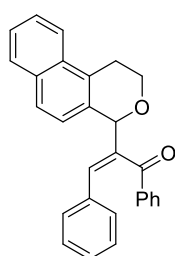
yield = 71%



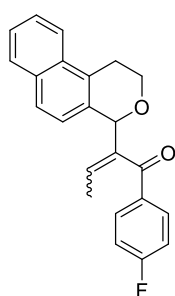
yield = 84%
Z/E = 15:1



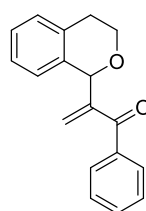
yield = 88%
Z/E = 13:1



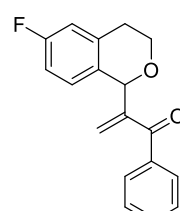
yield = 99%



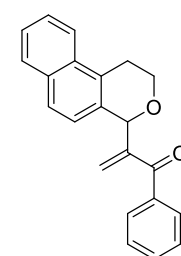
yield = 92%
Z/E = 39:1



yield = 80%



yield = 60%

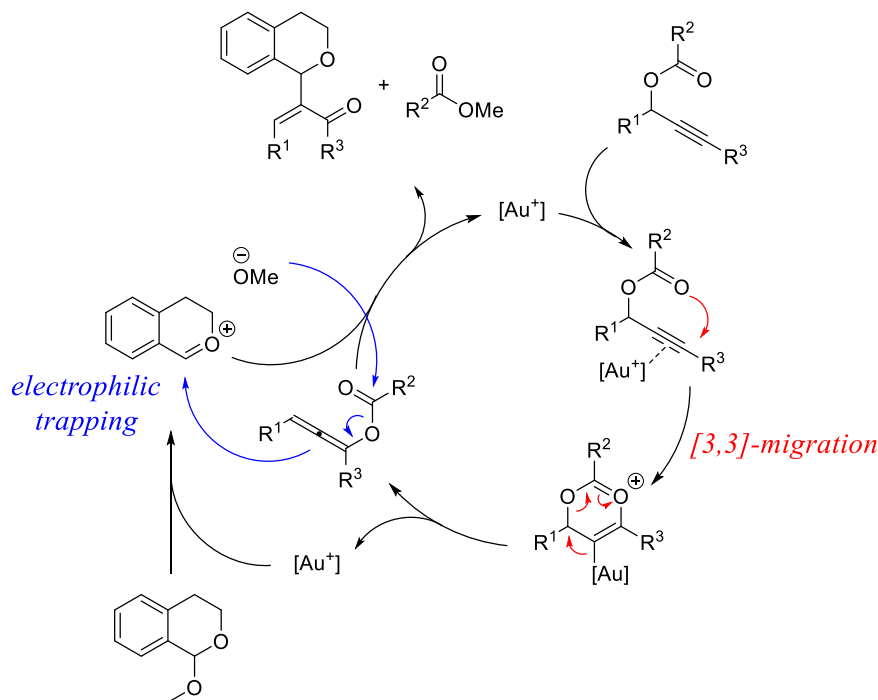


yield = 98%

Scheme 2: Scope of the reaction.

Mechanistically, the oxocarbenium ion, resulted from the gold activation of the isochromane acetate, underwent the nucleophilic attack by the allenolate intermediate, the latter generated by gold-catalyzed 1,3-pivalate migration (Scheme 3). In order to support this pathway, the allenolate

intermediate was isolated and submitted with the isochromane acetate under optimized reaction conditions. The corresponding product was isolated in 85% yield.



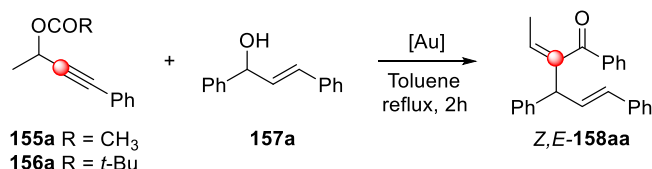
Scheme 3: Proposed reaction mechanism.

Inspired by this type of reactivity and considering our interest in the manipulation of allenol derivatives^[2–5], we envisioned the possibility to use this nucleophilic reactivity of the allenolates in order to develop the direct α -allylation of enones using activated alcohols as alkylating agents.^[6] We started our investigation considering the condensation between the easily accessible propargylic acetate **155a** and the activated alcohol **157a** in the presence of different gold-catalysts (Table 1).

Interestingly, the carbene-gold catalyst^[7] promoted moderately the reaction providing the desired product in 40% yield (entry 1, Table 1). The phosphine-based complexes furnished not homogenous results; in particular only the JohnPhosAuCl/AgNTf₂ provided the allylated product in satisfactory yield and good *cis*-diastereoselectivity (entry 3, Table 1).^[8] The optimization continued evaluating the effect of the counterion: weakly coordinating anions performed better the catalytic reaction than that the more nucleophilic ones.^[9,10] The obtained results elected the commercially available silver-free [JohnPhosAu(CH₃CN)SbF₆]^[11,12] as the best catalyst for the titled transformation furnishing the corresponding α -allylated product in 74% yield and excellent diastereoselectivity (entry 10, Table 1). It was also demonstrated that the AgSbF₆ was not able to promote the catalytic reaction (entry 6, Table 1). Moreover, the well-known attitude of pivalates as better 1,3-migrating group respect to the acetate group, suggested us to replace the acetyl group with bulkier pivalate. Gratifyingly, under

the latter conditions, the desired product was isolated in higher yield (86%) without loss of diastereoselectivity (entry 11, Table 1).

Table 1: Optimization table.^[a]



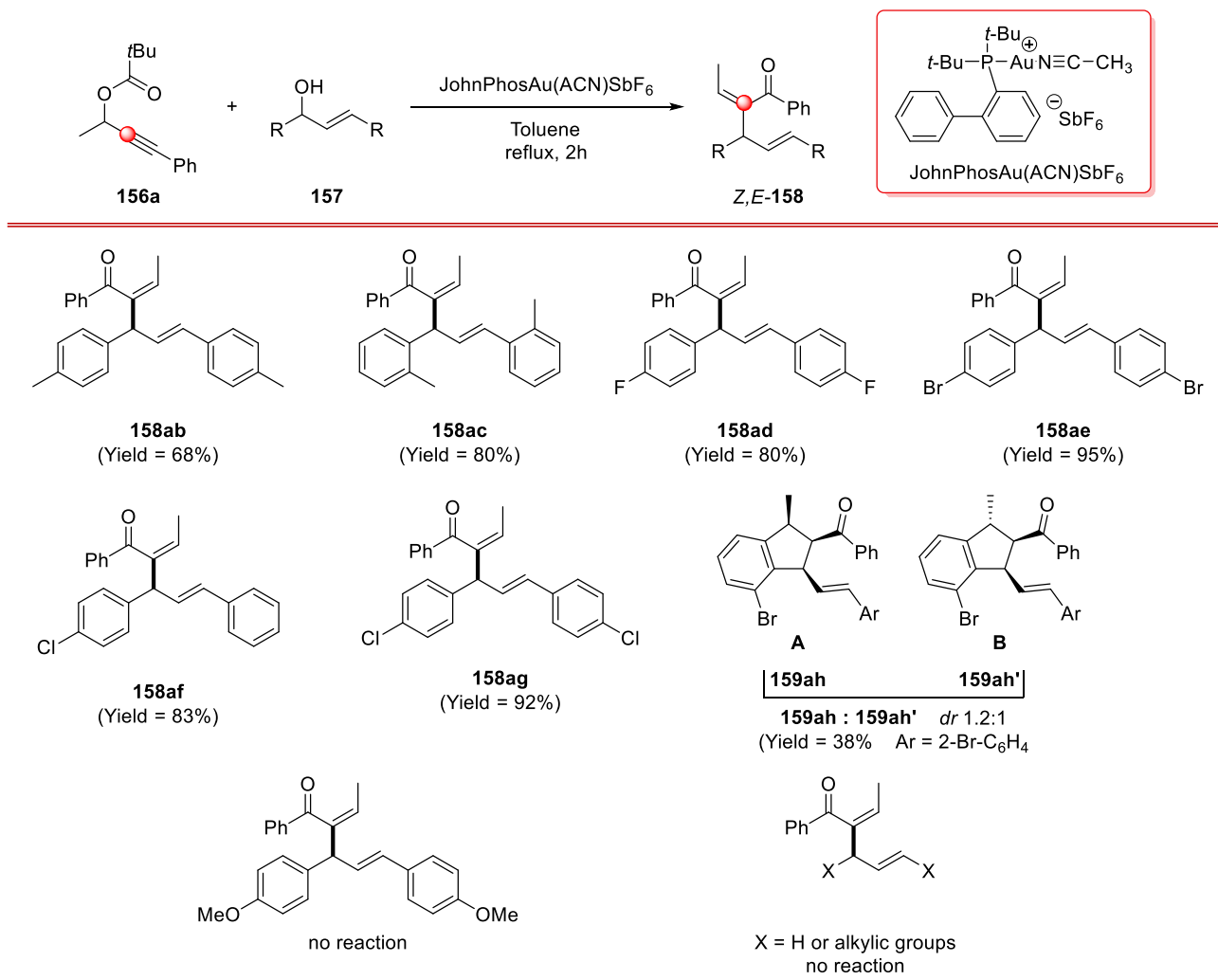
Entry	[Au] (2 mol%)	155a/156a	Yield 158aa (%) ^[b]	Z : E ^[c]
1 ^[d]	[Au(IPr)NTf ₂]	155a	40	95:5
2 ^[e]	PPh ₃ AuNTf ₂	155a	23	95:5
3	JohnPhosAuCl/AgNTf ₂	155a	65	97:3
4 ^[d]	JackiePhosAuNTf ₂	155a	12	--:--
5 ^[d,e]	Me-Dalpos-AuNTf ₂	155a	38	95:5
6	AgNTf ₂	155a	n. r.	--:--
7 ^[e]	JohnPhosAuOTs	155a	48	95:5
8 ^[e]	JohnPhosAuTFA	155a	45	95:5
9 ^[e]	JohnPhosAuBARf	155a	61	95:5
10	JohnPhosAu(ACN)SbF ₆	155a	74	97:3
11	JohnPhosAu(ACN)SbF ₆	156a	86	97:3
12 ^[f]	JohnPhosAu(ACN)SbF ₆	156a	76	98:2

[a] All the reaction were carried out under nitrogen. Ratio **155a/156a:157a:[Au]** = 1:1.5:0.02 unless otherwise specified. All the reagents used and the products obtained should be considered as racemic mixtures. [b] Isolated yield after flash chromatography. [c] Yield determined *via* GC-MS on the reaction crude. [d] Large amount of unreacted acetate **155a** was recovered. Reaction time 48 h. [e] the catalyst was prepared *in situ* by treating equimolar amounts of LAuCl and AgX. [f] A **156a:157a:[Au]** = 1:1:0.02 ratio was utilized. n.r. = no reaction.

Subsequently, in order to further increase the yield and the diastereoselectivity, the reaction was performed in different solvents. In particular, dichloromethane, benzene and trifluorotoluene proved to be efficient in the reaction, but no significant improvement in term of yield or diastereoselectivity was recorder.

With the optimized reaction conditions in our hand, we tested the scope and limitations of the protocol submitted differently substituted activate alcohols with propargylic pivalate **156a** in the presence of JohnPhosAu(ACN)SbF₆ in Toluene at reflux (Scheme 4). All the corresponding products were isolated in good to excellent yields demonstrating that the synthetic procedure was tolerant toward different functional groups. Indeed, activated alcohols featuring electron-withdrawing groups as well as moderate electron-donating groups resulted in the corresponding allylated products in satisfactory yields. Only the strong electron-withdrawing group, such as OMe, was not tolerated and no traces of the product were found after the reaction. In that case a

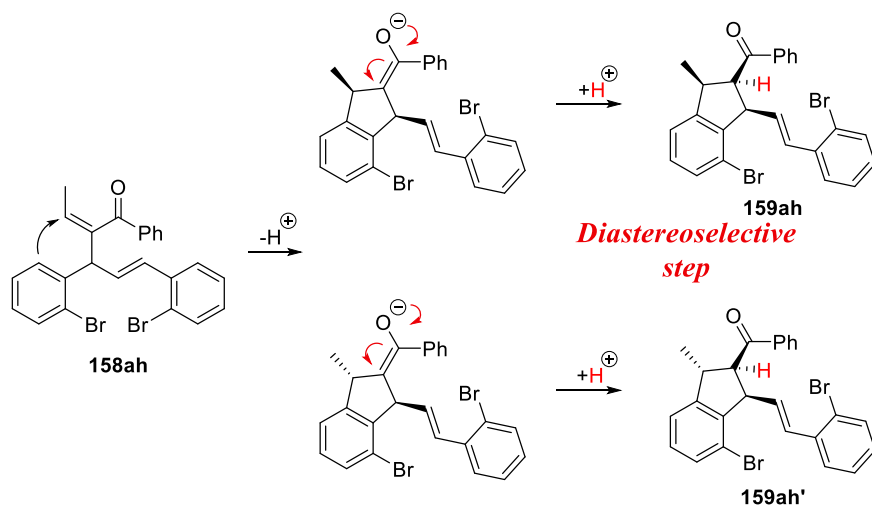
disproportion of the alcohol to the corresponding chalcone and 1,3-diphenylpropene was observed.^[13] Furthermore, the replacement of one or both the aromatic substituents of the alcohols with hydrogen atom or alkylic substituents caused the failure of the reactions.



Scheme 4: Scope of the reaction with different activated alcohols.

When asymmetric alcohol **157f** was employed in the reaction, a 1:1 mixture of regioisomers was isolated; this evidence supports a S_N1-type mechanism reaction.

Furthermore, in several cases the formation of traces of trisubstituted dihydroindenyl compounds was observed. It is noteworthy that the bicycle **159ah** was isolated as major product in 1.2:1 mixture of diastereoisomers A:B. The formation of these compounds can be rationalized in term of a cascade Friedel-Crafts-type alkylation by the aromatic ring to the β -position of the enone intermediate (Scheme 5).



Scheme 5: Cascade Friedel-Crafts-type alkylation.

Only two diastereoisomers were obtained and it was demonstrated by NMR studies that the diastereoselective protonation occurred always at the opposite face respect the styrene group. (Figure 1)

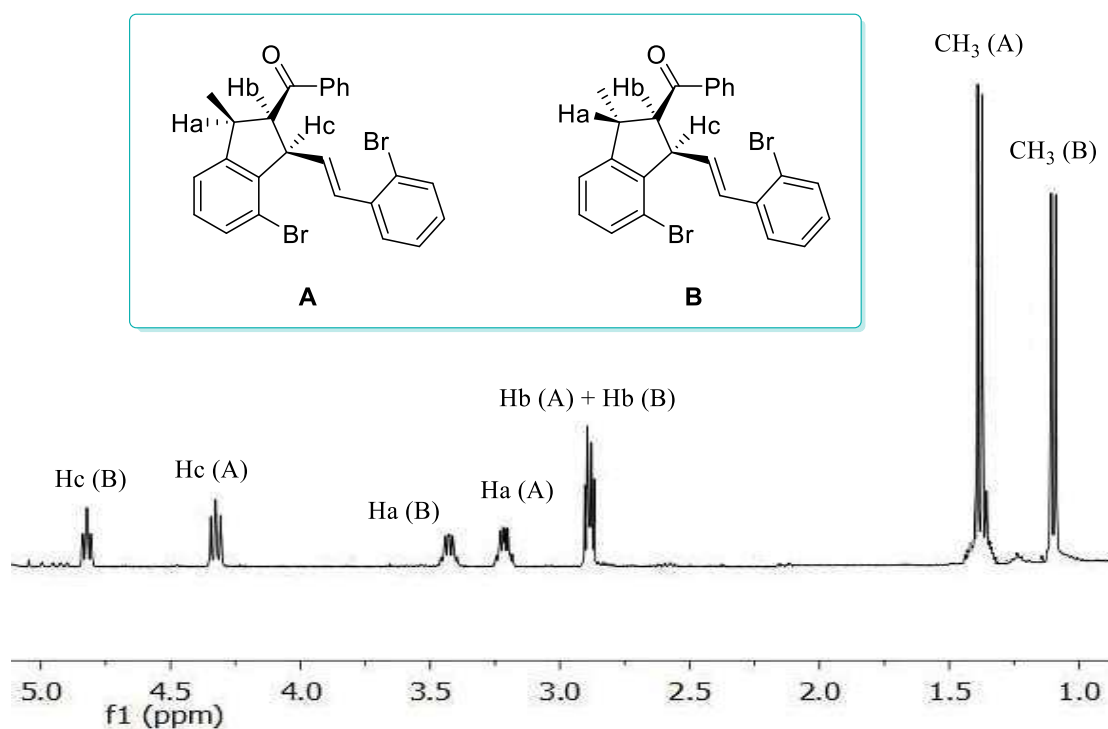


Figure 1: Peak assignment of the products in ¹H NMR spectrum.

After that, the NOE experiments have been carried out by irradiation of the Hb proton of both diastereoisomers.

As it can see in Figure 2, only the Ha of the diastereoisomer A (major diastereoisomer) is visible in the spectrum as well as the Hc of both isomers. With these results it is easy to determinate that the carbonyl group and the styrene group are always in *cis* position while the methyl group is in *cis* in the major diastereoisomer (A) and *anti* in the minor one (B).

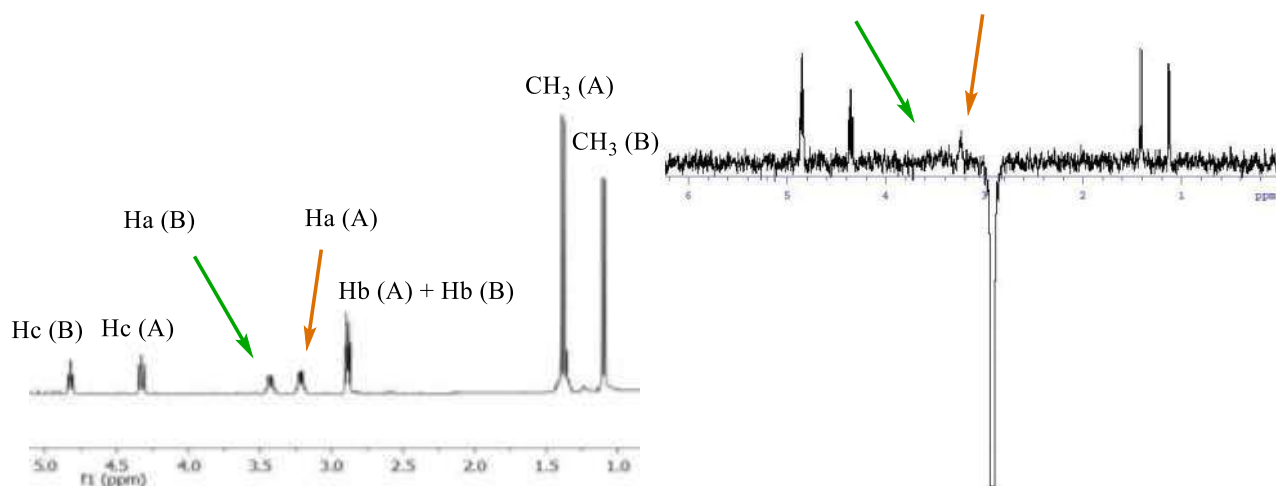
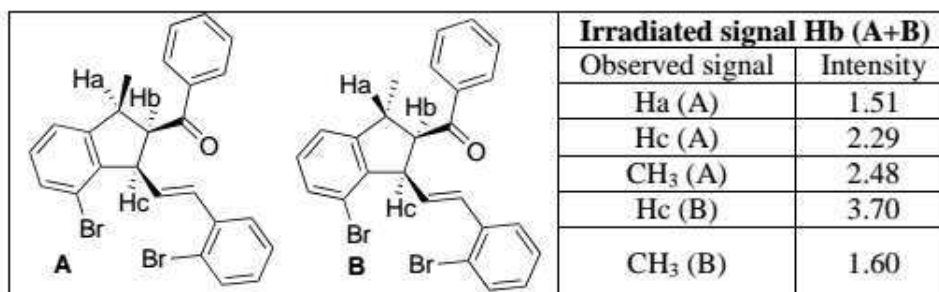
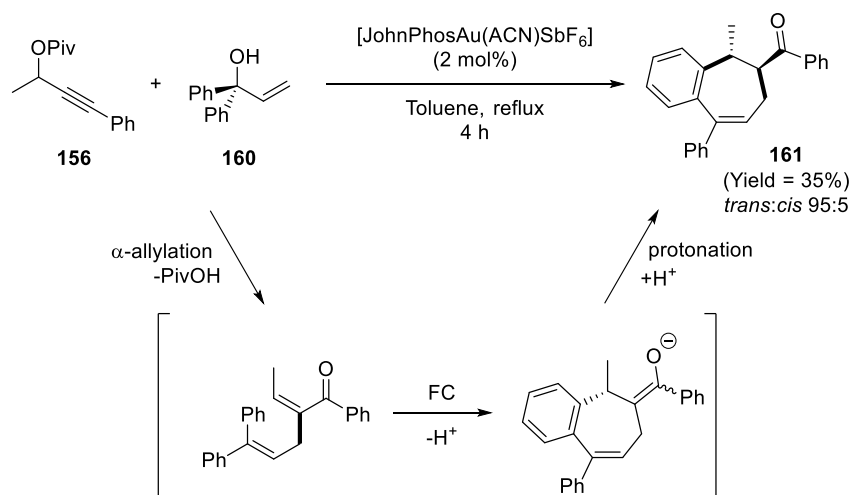


Figure 2: **159ah** and **159ah'** NOE experiments.

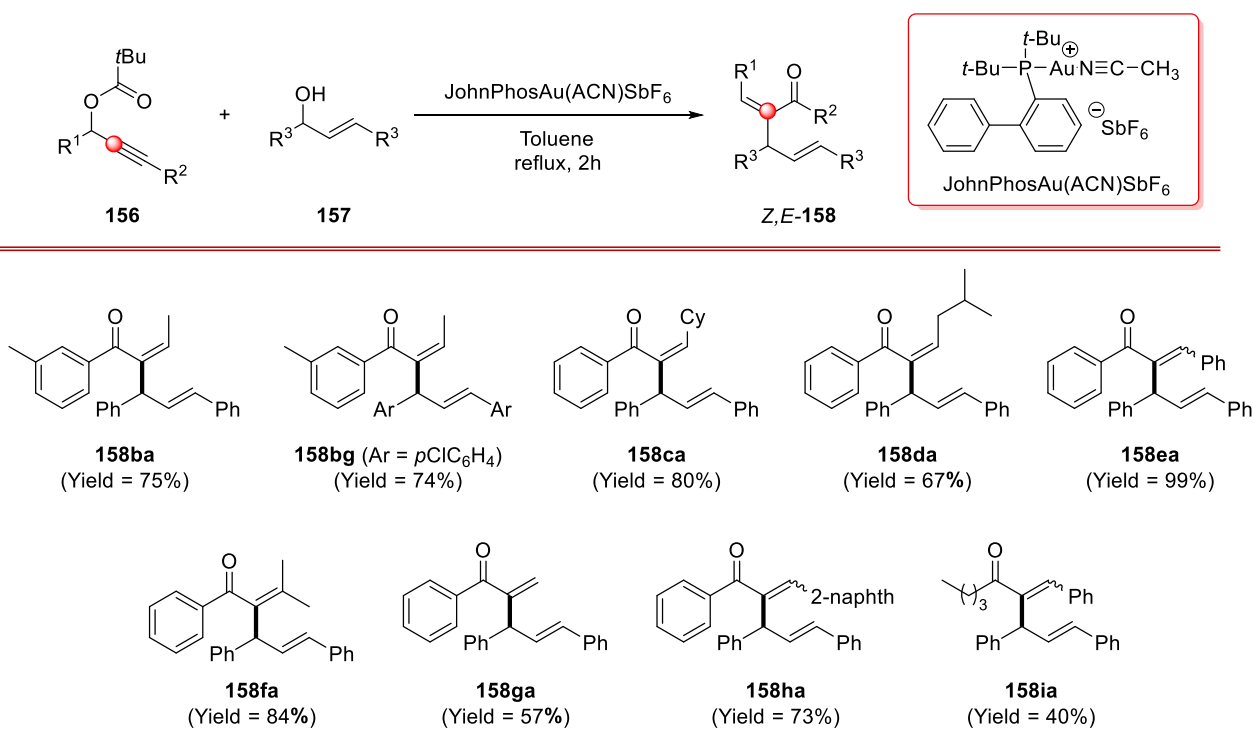
The same Michael-type-Friedel-Crafts alkylation was observed when tertiary allylic alcohol **160** was employed in the transformation with propargylic pivalates **156a** in the presence of JohnPhosAu(ACN)SbF₆ (Scheme 6).



Scheme 6: Michael-type-Friedel-Crafts alkylation observed with tertiary allylic alcohol **160**.

The bicycle **161** was isolated in moderate yield and high *trans*-diastereoselectivity; the configuration of the dihydrobenzo[7]annulene was unambiguously determined through NMR experiments.

Additionally, in order to further prove the flexibility of the synthetic protocol, differently substituted propargylic pivalates were prepared and submitted under optimized reaction conditions (Scheme 7).



Scheme 7: Scope of the reaction with different propargylic pivalates.

Propargylic pivalates featuring aliphatic as well as aromatic groups as R¹ substituent resulted in the desired products in good to excellent yields (up to 99%). Not only secondary, but also primary and tertiary esters were employed in the reaction and the corresponding products were isolated in good yields. Only modest yield was achieved when propargylic pivalate featuring aliphatic group as R² substituent was used as starting material.

The structure of enone **158ag** was determined by single crystal X-ray diffraction. In particular, the data collected demonstrated that the enone unit adopts the *Z* configuration. The geometry of the molecule in the crystal is influenced by high steric hindrance. Indeed, the enone moiety exhibits a significant deviation from planarity forming a torsion angle of 52.3 (3)° between the C=C double bond and the carbonyl group. This particular arrangement allows weak intermolecular π - π stackings among the phenyl groups linked to the carbonyl (Figure 3).

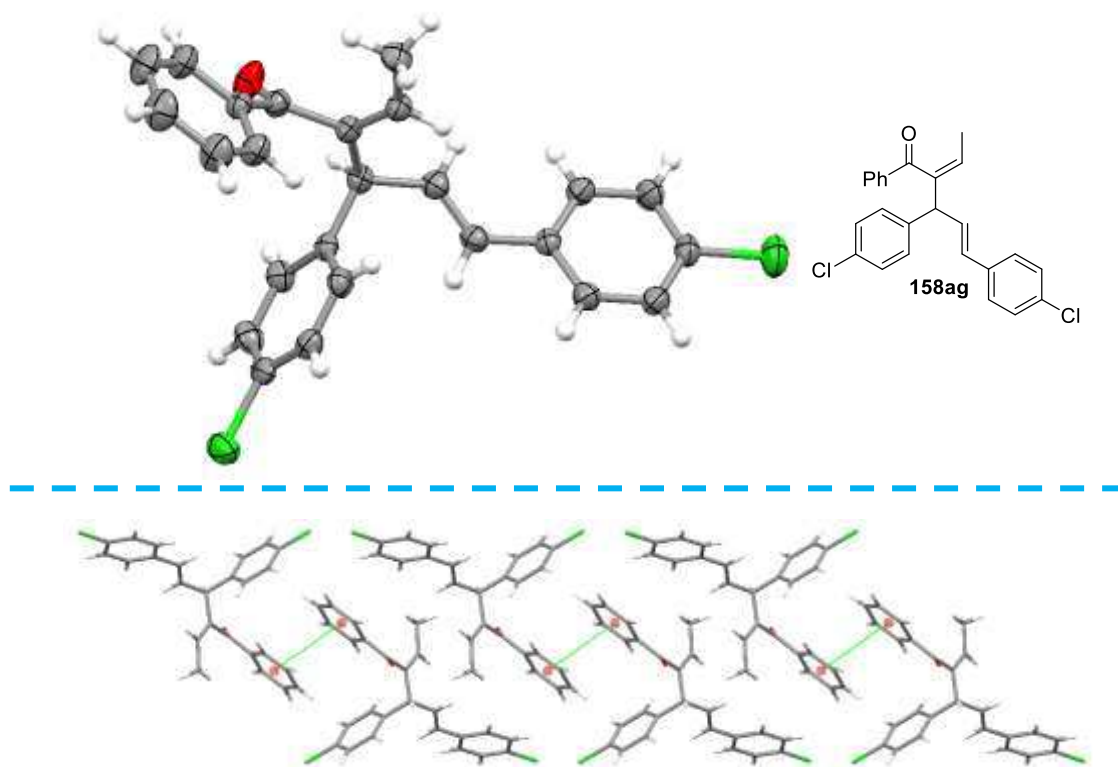
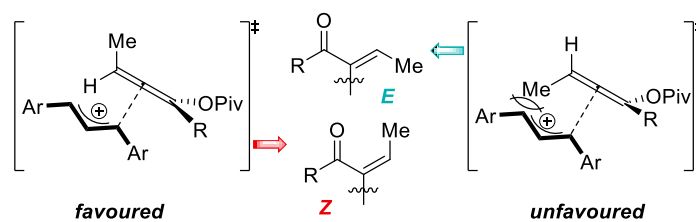


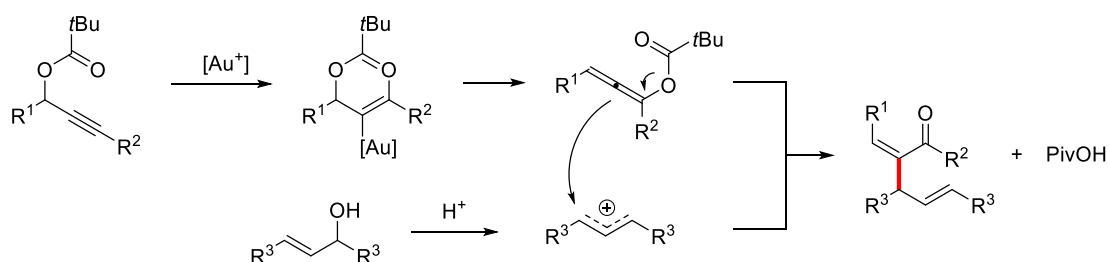
Figure 3: X-ray structure of **158ag**.

The unexpected *Z* configuration of the enones was rationalized as shown in Scheme 8: in the unfavoured approaching trajectory is present an interaction between the allyl moiety and the methyl group in γ position on the allenyl framework which is not present in the transition state that will result in a *Z* configuration.



Scheme 8: Favoured and unfavoured approaches in the transition state.

Finally, the role of the *in situ* formed pivalic acid was investigated. Some reactions were performed in the presence of different organic and inorganic bases and no traces of product were observed. No traces of product were observed even when a stoichiometric amount of pivalic acid was utilized in the absence of the gold catalyst. These results demonstrated that the concomitant presence of the gold catalyst and the Brønsted acid is necessary for the success of the reaction. Moreover, it was rationalized that the role of the gold-catalyst is the formation of the nucleophilic species through [3,3]-sigmatropic rearrangement of the propargylic ester, while the pivalic acid activates the alcohol toward the nucleophilic trapping (Scheme 9).



Scheme 9: Proposed reaction mechanism.

In conclusion, an unprecedented gold(I)/H⁺ co-catalysed α -allylation of enones using activated alcohols as electrophilic partner was developed. The catalytic protocol demonstrated to be tolerant toward different functional groups furnishing all the desired products in good to excellent yields and very high *Z*-stereocontrol. In some cases it was also possible to obtain fused bicycles in moderate yields and good diastereoselectivity.

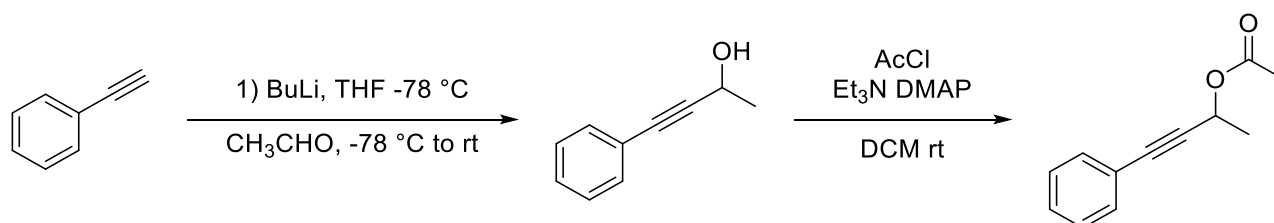
Bibliography

- [1] Y. Yu, W. Yang, F. Rominger, A. S. K. Hashmi, *Angew. Chem. Int. Ed.* **2013**, 7586–7589.
- [2] M. M. Mastandrea, N. Mellonie, P. Giacinto, A. Collado, S. P. Nolan, G. P. Miscione, A. Bottoni, M. Bandini, *Angew. Chem. Int. Ed.* **2015**, 54, 14885–14889.
- [3] R. Ocello, A. De Nisi, M. Jia, Q.-Q. Yang, M. Monari, P. Giacinto, A. Bottoni, G. P. Miscione, M. Bandini, *Chem. Eur. J.* **2015**, 21, 18445–18453.
- [4] M. Jia, M. Monari, Q.-Q. Yang, M. Bandini, *Chem. Commun.* **2015**, 51, 2320–2323.
- [5] E. Manoni, M. Bandini, *Eur. J. Org. Chem.* **2016**, 3135–3142.
- [6] E. Manoni, M. Daka, M. M. Mastandrea, A. De Nisi, M. Monari, M. Bandini, *Adv. Synth. Catal.* **2016**, 358, 1404–1409.
- [7] S. Gaillard, C. S. J. Cazin, S. P. Nolan, *Acc. Chem. Res.* **2012**, 45, 778–787.
- [8] N. Mézailles, L. Ricard, F. Gagosz, *Org. Lett.* **2005**, 7, 4133–4136.
- [9] M. Jia, M. Bandini, *ACS Catal.* **2015**, 5, 1638–1652.
- [10] B. Ranieri, I. Escofet, A. M. Echavarren, *Org. Biomol. Chem.* **2015**, 13, 7103–7118.
- [11] C. Nieto-Oberhuber, S. López, A. M. Echavarren, *J. Am. Chem. Soc.* **2005**, 127, 6178–6179.
- [12] E. Herrero-Gómez, C. Nieto-Oberhuber, S. López, J. Benet-Buchholz, A. M. Echavarren, *Angew. Chem. Int. Ed.* **2006**, 45, 5455–5459.
- [13] J. Wang, W. Huang, Z. Zhang, X. Xiang, R. Liu, X. Zhou, *J. Org. Chem.* **2009**, 74, 3299–3304.

5.1.1 Experimental Section

¹H-NMR spectra were recorded on Varian 200 (200 MHz) or Varian 400 (400 MHz) spectrometers. Chemical shifts are reported in ppm from TMS with the solvent resonance as the internal standard (deuteriochloroform: 7.27 ppm). Data are reported as follows: chemical shift, multiplicity (s = singlet, d = doublet, t = triplet, q = quartet, sext = sextet, sept = septet, p = pseudo, b = broad, m = multiplet), coupling constants (Hz). ¹³C-NMR spectra were recorded on a Varian 200 (50 MHz), Varian 400 (100 MHz) spectrometers with complete proton decoupling. Chemical shifts are reported in ppm from TMS with the solvent as the internal standard (deuteriochloroform: 77.0 ppm). GC-MS spectra were taken by EI ionization at 70 eV on a Hewlett-Packard 5971 with GC injection. They are reported as: *m/z*. LC-electrospray ionization mass spectra were obtained with Agilent Technologies MSD1100 single-quadrupole mass spectrometer. Chromatographic purification was done with 240-400 mesh silica gel. Anhydrous solvents were supplied by Fluka or Sigma Aldrich in Sureseal® bottles and used without any further purification. Commercially available chemicals were purchased from Sigma Aldrich, Stream and TCI and used without any further purification.

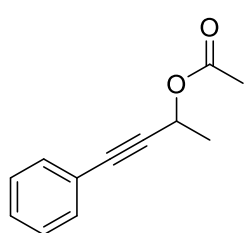
Synthesis of 4-phenylbut-3-yn-2-yl acetate (1)



To a solution of alkyne phenylacetylene (5 mmol) in THF (15 mL) under nitrogen atmosphere, n-BuLi was added dropwise at -78 °C. The mixture was stirred at -78 °C for 2h and then acetaldehyde (1 eq, 5 mmol) was added at the same temperature and then the mixture was allow to reach at room temperature and stirred for 4h. Subsequently, brine (15 mL) was added and the aqueous layer was extracted with AcOEt (3 x 10 mL). The combined layers were washed with brine (15 mL) and then dried with Na₂SO₄, filtered and concentrated under reduced pressure. The crude product was used such as, without further purification in the next step.

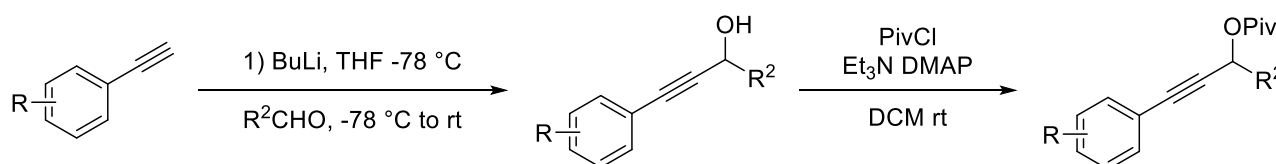
To a solution of 4-phenylbut-3yn-2ol, Et₃N (10eq, 50mmol, 7mL), and DMAP (5%, 0,25mmol, 31 mg) in DCM (10 mL) was added acetylchloride (1,2 eq, 6 mmol, 429 μL) and the mixture was stirred at rt overnight. Then the mixture was quenched with water (10 mL) and the aqueous layer

was extracted with DCM (3 x 10 mL). The combined organic layers were washed with brine (15 mL) and dried with Na₂SO₄, filtered and concentrated under reduced pressure. The crude product was purified by column chromatography on silica gel (cyclohexane:AcOEt 98:2) to give 4-phenylbut-3-yn-2-yl acetate (**155a**).



155a Yellow oil; Y = 78%; Spectroscopic data are according to those reported in literature; ^[1] GC-MS (m/z): 188 (M).

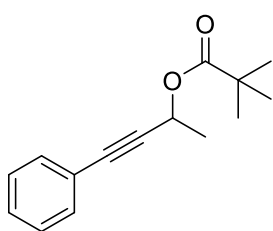
General procedure for the synthesis of pivaloyl derivatives (**156a-h**):



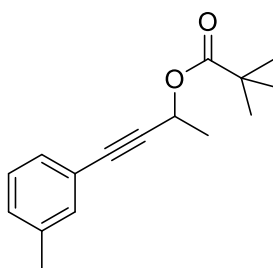
To a solution of alkyne (5 mmol) in THF (15 mL) under nitrogen atmosphere, n-BuLi was added dropwise at -78 °C. The mixture was stirred at -78 °C for 2h and then the opportune aldehyde (1 eq, 5 mmol) was added and then the mixture was allowed to reach at room temperature and stirred for 4h. Subsequently, brine (15 mL) was added and the aqueous layer was extracted with AcOEt (3 x 10 mL). The combined layers were washed with brine (15 mL) and then dried with Na₂SO₄, filtered and concentrated under reduced pressure. The crude product was used such as, without further purification in the next step.

To a solution of propargyl alcohol, Et₃N (10eq, 50mmol, 7mL), and DMAP (5%, 0,25mmol, 31 mg) in DCM (10 mL) was added trimethylacetylchloride (1,2 eq, 6 mmol, 742 μL) and the mixture was stirred at rt overnight. Then the mixture was quenched with water (10 mL) and the aqueous layer

was extracted with DCM (3 x 10 mL). The combined organic layers were washed with brine (15 mL) and dried with Na₂SO₄, filtered and concentrated under reduced pressure. The crude product was purified by column chromatography on silica gel (cyclohexane:AcOEt 98:2) to give the desired product.

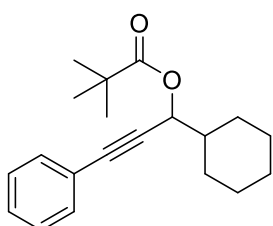


156a Yellow oil; Y = 76% (un-optimized yield); Spectroscopic data are according to those reported in literature.^[2] GC-MS (m/z): 230 (M).



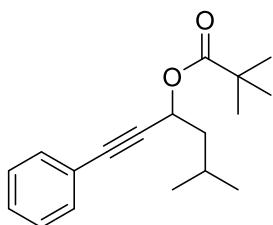
244 (M).

156b Yellow oil; Y = 73% (un-optimized yield); ¹H-NMR (400 MHz, CDCl₃), δ 1.16 (s, 9H), 1.48 (d, 3H, J = 6.7 Hz), 2.25 (s, 3H), 5.59 (q, 1H, J = 6.6 Hz), 7.05 (d, 1H, J = 7.5 Hz), 7.11 (t, 1H, J = 7.5 Hz), 7.20-7.15 (m, 2H); ¹³C-NMR (100 MHz, CDCl₃), δ 21.1, 21.3, 27.0 (3C), 38.6, 60.6, 84.4, 87.3, 122.2, 128.1, 128.8, 129.3, 132.4, 137.8, 177.3; GC-MS (m/z):



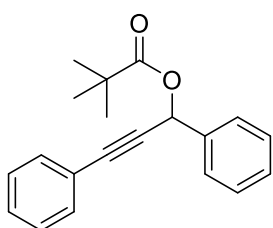
156c Yellow oil; Y = 77% (un-optimized yield); ¹H-NMR (400 MHz, CDCl₃), δ 1.10-1.32 (m, 13H), 1.66-1.91 (m, 6H), 5.39 (d, 1H, J = 6.1 Hz), 7.24-7.29 (m, 3H), 7.40-7.43 (m, 2H); ¹³C-NMR (100 MHz, CDCl₃), δ 25.8(2C), 26.3, 27.1 (3C), 28.4, 28.5, 38.9, 42.1, 68.4, 85.4, 86.0, 122.6,

128.2 (2C), 128.3, 131.8 (2C), 177.4. GC-MS (m/z): 298 (M)

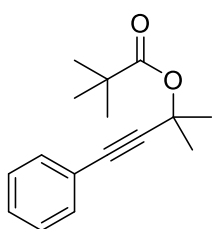


156d White solid; Y = 68% (un-optimized yield); mp = 38 °C; ¹H-NMR (400 MHz, CDCl₃), δ 0.98 (d, 3H, J = 4.5 Hz), 1.00 (d, 3H, J = 4.4 Hz), 1.25 (s, 9H), 1.93- 1.70 (m, 3H), 5.64 (t, 1H, J = 7.0 Hz), 7.31-7.29 (m, 3H), 7.45-7.43 (m, 2H); ¹³CNMR (100 MHz, CDCl₃), δ 22.4, 22.5, 24.9, 27.0 (3C), 38.7, 43.6, 63.0, 84.8, 87.0, 122.5, 128.2 (2C), 128.4, 131.8 (2C),

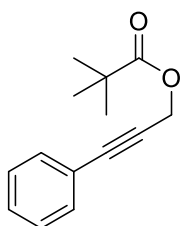
177.4; GC-MS (m/z): 272 (M).



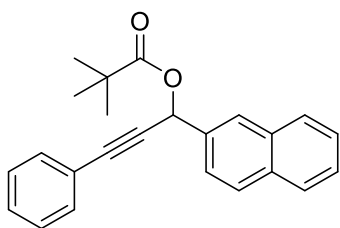
156e White solid; Y = 78% (un-optimized yield); mp = 44 °C; spectroscopic data are in accordance to those reported in literature. ^[2] GC-MS (m/z): 292 (M).



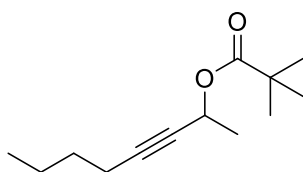
156f Yellow oil; Y = 48% (un-optimized yield); ¹H-NMR (400 MHz, CDCl₃), δ 1.19 (s, 9H), 1.72 (s, 6H), 7.28-7.24 (m, 3H), 7.42-7.39 (m, 2H); ¹³C-NMR (100 MHz, CDCl₃), δ 27.0 (3C), 28.9 (2C), 39.1, 72.0, 83.6, 90.4, 122.8, 128.1 (2C), 128.1, 131.8 (2C), 176.6. GC-MS (m/z): 244 (M)



156g Yellow oil; Y = 65% (un-optimized yield); Spectroscopic data are according to those reported in literature. ^[2] GC-MS (m/z): 216 (M).

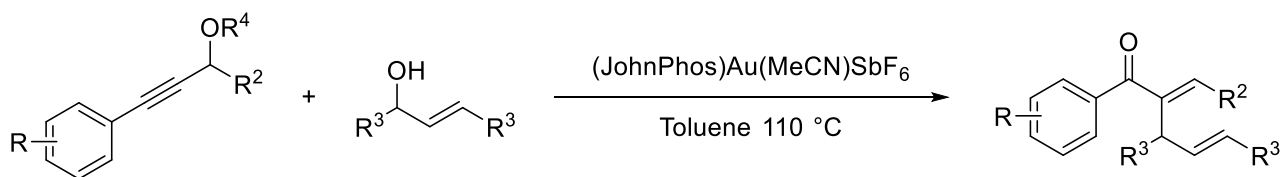


156h White solid; Y = 71% (un-optimized yield); mp = 79 °C. ¹H-NMR (400 MHz, CDCl₃), δ 1.26 (s, 9H), 6.85 (s, 1H), 7.35-7.32 (m, 3H), 7.54-7.49 (m, 4H), 7.68 (dd, 1H, J = 8.6 Hz, J = 1.5 Hz), 7.87-7.86 (m, 1H), 7.90 (d, 2H, J = 8.8 Hz), 8.06 (s, 1H); ¹³C-NMR (100 MHz, CDCl₃), δ 27.0 (3C), 38.8, 66.0, 85.0, 87.0, 122.3, 124.9, 126.3, 126.5, 127.8, 127.7, 128.2, 128.3, 128.5, 128.7, 131.9 (2C), 133.0, 133.3, 134.8, 177.2; GC-MS (m/z): 342 (M).

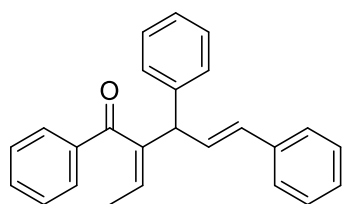


156i Yellow oil; Y = 60% (un-optimized yield); Spectroscopic data are in accordance to those reported in literature.^[2]

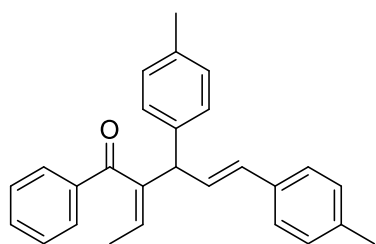
Gold-catalysed α -allylation of enons (158aa-fh)



A dried two-necked round bottom flask was charged with anhydrous toluene (1 mL), the desired carboxylate (**155a**, **156a-h**) (0.1 mmol), the allylic alcohol (0.15 mmol) and the [JohnPhosAu(ACN)]SbF₆ (2 mol%). The mixture was poured in a pre-heated oil bath (110 °C) and the reaction left stirring at the same temperature for the indicated time. After cooling to room temperature, the reaction crude was directly charged into a column for purification by flash chromatography (cHex:AcOEt 98:2).

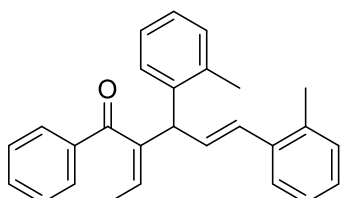


(*Z,E*)-**158aa** Yellow oil, Y = 77%. ¹H-NMR (400 MHz, CDCl₃), δ 1.58 (dd, 3H, J = 7.1 Hz, J = 1.3 Hz), 4.66 (dd, 1H, J = 7.9 Hz, J = 1.0 Hz), 5.86 (dq, 1H, J = 7.1 Hz, J = 1.4 Hz), 6.39 (d, 1H, J = 15.9 Hz), 6.54 (dd, 1H, J = 15.8 Hz, J = 7.9 Hz), 7.23-7.18 (m, 2H), 7.35-7.27 (m, 8H), 7.44-7.37 (m, 2H), 7.55-7.51 (m, 1H), 7.83-7.81 (m, 2H); ¹³C-NMR (100 MHz, CDCl₃), δ 16.0, 53.0, 126.4 (2C), 126.9, 127.5, 128.5, 128.60 (2C), 128.64 (2C), 128.7 (2C), 128.8 (2C), 129.3 (2C), 130.7, 132.0, 133.1, 137.3, 137.7, 141.0, 143.3, 199.6; GC-MS (m/z): 338 (M); anal. calcd for (C₂₅H₂₂O: 338.17): C, 88.72; H, 6.55; found: C, 88.56, H, 6.64.

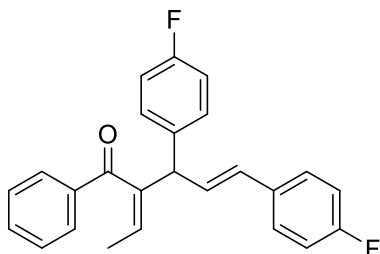


(*Z,E*)-**158ab** Yellow oil, Y = 68%. ¹H-NMR (400 MHz, CDCl₃), δ 1.55 (dd, 3H, J = 7.2 Hz, J = 1.1 Hz), 2.29 (s, 3H), 2.30 (s, 3H), 4.59 (d, 1H, J = 7.8 Hz), 5.82 (dq, 1H, J = 7.0 Hz, J = 1.2 Hz), 6.32 (d, 1H, J = 15.9 Hz), 6.43 (dd, 1H, J = 15.8 Hz, J = 7.8 Hz), 7.08 (t, 3H, J = 7.6 Hz), 7.24-7.15 (m, 5H), 7.40 (t, 2H, J = 7.6 Hz), 7.50 (t, 1H, J = 7.4 Hz), 7.82 (d, 2H, J = 7.3 Hz); ¹³C-NMR (100 MHz, CDCl₃), δ 15.8, 21.0, 52.4, 126.2 (2C), 128.1, 128.51 (2C), 128.54 (2C), 129.07, 129.09 (2C), 129.15 (2C), 129.17 (2C), 129.7, 131.4,

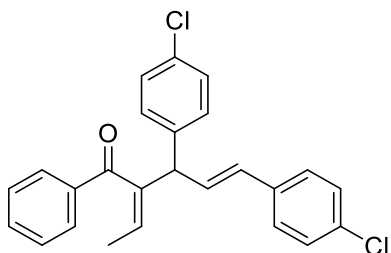
132.9, 134.4, 136.2, 137.0, 137.5, 137.9, 143.4, 199.6; GC-MS (m/z): 366 (M); anal. calcd for (C₂₇H₂₆O: 366.20): C, 88.48; H, 7.15; found: C, 88.39, H, 7.11.



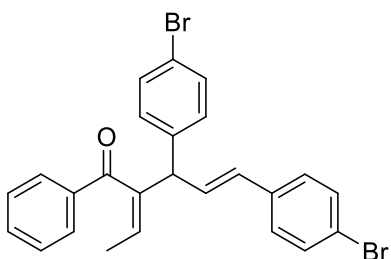
(*Z,E*)-**158ac** Yellow oil, Y = 80%. ¹H-NMR (400 MHz, CDCl₃), δ 1.59 (dd, 3H, J = 7.2 Hz, J = 1.4 Hz), 2.20 (s, 3H), 2.34 (s, 3H), 4.97 (d, 1H, J = 7.8 Hz), 5.79 (dq, 1H, J = 7.1 Hz, J = 1.4 Hz), 6.34 (dd, 1H, J = 15.7 Hz), 7.25-7.08 (m, 6H), 7.47-7.36 (m, 4H), 7.55-7.51 (m, 1H), 7.86 (dd, 2H, J = 8.4 Hz, J = 1.3 Hz); ¹³C-NMR (100 MHz, CDCl₃), δ 16.0, 19.5, 19.7, 48.8, 125.7, 125.9 (2C), 126.6, 127.2, 128.4, 128.5 (2C), 128.7, 129.1 (2C), 128.8, 130.1, 130.6, 131.6, 132.9, 135.3, 136.4, 136.5, 137.8, 139.0, 142.6, 199.5; LC-ESI-MS: 367 [M+H⁺], 389 [M+Na⁺]; anal. calcd for (C₂₇H₂₆O: 366.20): C, 88.48; H, 7.15; found: C, 88.55, H, 7.26.



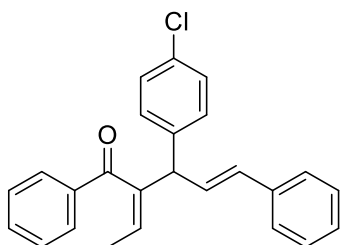
(*Z,E*)-**158ad** Yellow oil, Y = 80%. ¹H-NMR (400 MHz, CDCl₃), δ 1.58 (d, 3H, J = 7.1 Hz), 4.63 (d, 1H, J = 7.5 Hz), 5.86 (q, 1H, J = 7.1 Hz), 6.31 (d, 1H, J = 15.9 Hz), 6.41 (dd, 1H, J = 7.6 Hz, J = 15.8 Hz), 6.98 (dt, 4H, J = 8.6 Hz, J = 3.6 Hz), 7.30-7.23 (m, 4H), 7.43 (t, 2H, J = 7.6 Hz), 7.56-7.52 (m, 1H), 7.81 (d, 2H, J = 7.9 Hz); ¹³C-NMR (100 MHz, CDCl₃), δ 15.8, 52.0, 115.3 (d, 2C, J = 21.0 Hz), 115.4 (d, 2C, J = 21.0 Hz), 127.8 (d, 2C, J = 7.0 Hz), 128.5, 128.6 (2C), 129.1 (2C), 130.1 (d, 2C, J = 8.0 Hz), 130.1, 130.8, 133.1, 133.1 (d, 1C, J = 3.0 Hz), 136.4 (d, 1C, J = 4.0 Hz), 137.36, 142.9, 161.6 (d, 1C, J = 244.0 Hz), 162.2 (d, 1C, J = 244.0 Hz), 199.3; ESI-MS: 375 [M+H⁺], 395 [M+Na⁺]; anal. calcd for (C₂₅H₂₀F₂O: 374.15): C, 80.20; H, 5.38; found: C, 80.06, H, 5.15.



(Z,E)-4ag White solid, Y = 92%. ¹H-NMR (400 MHz, CDCl₃), δ 1.58 (dd, 3H, J = 7.1 Hz, J = 1.0 Hz), 4.63 (d, 1H, J = 7.7 Hz), 5.86 (dq, 1H, J = 7.1 Hz, J = 1.2 Hz), 6.30 (d, 1H, J = 15.7 Hz), 6.46 (dd, 1H, J = 7.8 Hz, J = 15.8 Hz), 7.21-7.30 (m, 9H), 7.43 (t, 2H, J = 7.7 Hz), 7.49-7.60 (m, 2H), 7.81 (d, 2H, J = 7.1 Hz); ¹³C-NMR (100 MHz, CDCl₃), δ 15.9, 52.2, 127.5 (2C), 128.63 (2C), 128.65 (2C), 128.68 (2C), 128.9, 129.1 (2C), 130.0 (2C), 130.7, 130.9, 132.6, 133.1, 133.2, 135.4, 137.3, 139.1, 142.4, 199.1; ESI-MS: 407 [M+H⁺], 429 [M+Na⁺]; anal. calcd for (C₂₅H₂₀Cl₂O: 406.09): C, 73.72; H, 4.95; found: C, 73.60, H, 4.81.

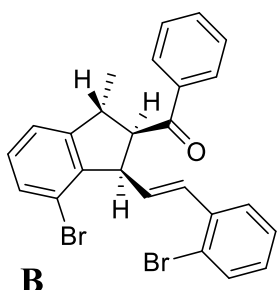
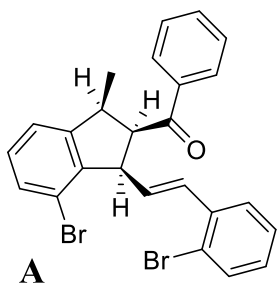


(Z,E)-4ae White solid, Y = 95%. ¹H-NMR (400 MHz, CDCl₃), δ 1.58 (d, 3H, J = 7.2 Hz), 4.61 (d, 1H, J = 7.7 Hz), 5.86 (q, 1H, J = 7.1 Hz), 6.28 (d, 1H, J = 15.8 Hz), 6.47 (dd, 1H, J = 7.8 Hz, J = 15.8 Hz), 7.17 (dd, 3H, J = 8.2 Hz, J = 5.1 Hz), 7.28-7.23 (m, 1H), 7.45-7.40 (m, 5H), 7.56-7.50 (m, 2H), 7.81 (d, 2H, J = 7.5 Hz); ¹³C-NMR (100 MHz, CDCl₃), δ 15.9, 52.2, 120.8, 121.3, 127.8 (2C), 128.7 (2C), 129.1, 129.1 (2C), 130.4 (2C), 130.8, 131.0, 132.6 (2C), 131.7 (2C), 133.2, 135.8, 137.3, 139.6, 142.3, 199.0; ESI-MS: 497 [M+H⁺], 519 [M+Na⁺]; anal. calcd for (C₂₅H₂₀Br₂O: 493.99): C, 60.51; H, 4.06; found: C, 60.35, H, 3.85.

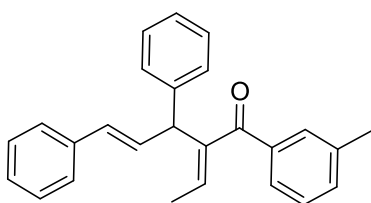


4af Yellow oil, Y = 83%. ¹H-NMR (400 MHz, CDCl₃), (two regioisomers A:B, ratio 1.25:1), δ 1.54-1.57 (m, 3HA + 3HB), 4.62 (d, 1HA + 1HB, J = 7.9 Hz), 5.78-5.89 (m, 1HA + 1HB), 6.29-6.35 (m, 1HA + 1HB), 6.52-6.43 (m, 1HA + 1HB), 7.32-7.20 (m, 9HA + 9HB), 7.35-7.43 (m, 2HA + 2HB), 7.48-7.54 (m, 1HA + 1HB), 7.78-7.80 (m, 2HA + 2HB); ¹³C-NMR (100 MHz, CDCl₃), (two regioisomers A:B, ratio 1.25:1), δ 15.8 (1CA), 15.9 (1CB), 52.2 (1CB), 52.8 (1CA), 126.3 (2CB), 126.8 (1CA), 127.5 (2CA), 128.43 (1CA), 128.49 (2CB), 128.54 (2CA), 128.56 (4CA), 128.63 (4CB), 128.66 (2CA), 129.11 (2CA), 129.12 (4CB), 129.99 (2CB), 130.01 (2CB), 130.6 (2CA), 131.2 (1CA), 132.2 (1CB), 133.0 (1CA), 133.1

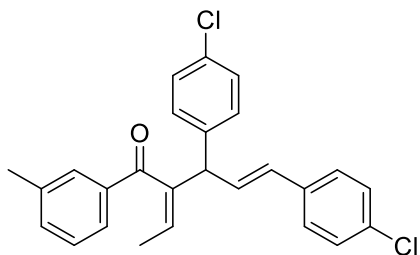
(1CB), 135.6 (1CA), 136.9 (1CB), 137.4 (1CB), 137.5 (1CB), 139.4 (1CA), 140.6 (1CA), 142.6 (1CB), 142.9 (1CA), 199.2 (1CB), 199.4 (1CA); GC-MS (m/z): 372 (M)



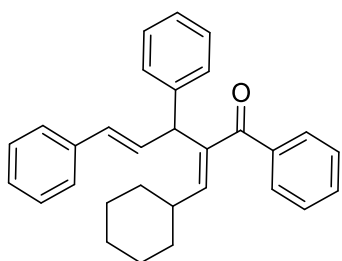
159ah Yellow solid, Y = 38%. ¹H-NMR (400 MHz, CDCl₃), (as a mixture of diastereoisomers A:B, ratio 1.2:1), diagnostic signals δ 1.12 (d, 3HA, J = 7.0 Hz), 1.40 (d, 3HB, J = 7.1 Hz), 2.89-2.92 (m, 1HA + 1HB), 3.23 (dt, 1HA, J = 11.0 J = 7.0 Hz), 3.45 (dt, 1HB, J = 11.0 J = 7.0 Hz), 4.35 (t, 1HB, J = 7.5 Hz), 4.84 (ddd, 1HA, J = 6.9 Hz J = 5.6 Hz J = 1.2 Hz), 6.33 (dd, 1HA, J = 15.9 Hz J = 7.2 Hz), 6.53 (dd, 1HB, J = 15.7 Hz J = 8.5 Hz), 6.68 (d, 1HA, J = 16.0 Hz), 6.73 (d, 1HB, J = 15.7 Hz); ¹³C-NMR (100 MHz, CDCl₃), (two diastereoisomers A:B, ratio 1.2:1), diagnostic signals δ 20.4 (1CA), 20.7 (1CB), 36.1 (1CB), 39.2 (1CA), 47.4 (1CB), 49.0 (1CA), 59.0 (1CB), 59.4 (1CA), 140.6 (1CB), 141.3 (1CA), 157.8 (1CA), 158.0 (1CB), 205.4 (1CA), 205.8 (1CB); ESI-MS: 497 [M+H⁺], 519 [M+Na].



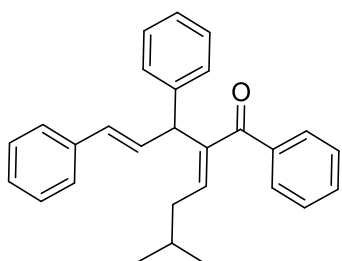
(Z,E)-158ba Yellow oil, Y = 75%. ¹H-NMR (400 MHz, CDCl₃), δ 1.55 (dd, 3H, J = 7.1 Hz, J = 1.3 Hz), 2.35 (s, 3H), 4.63 (d, 1H, J = 7.8 Hz), 5.82 (q, 1H, J = 7.1 Hz), 6.36 (d, 1H, J = 15.8 Hz), 6.52 (dd, 1H, J = 7.9 Hz, J = 15.8 Hz), 7.20-7.16 (m, 2H), 7.32-7.24 (m, 10H), 7.57-7.60 (m, 2H); ¹³C-NMR (100 MHz, CDCl₃), δ 15.8, 21.3, 52.8, 126.3 (2C), 126.6, 126.7, 127.3, 128.1, 128.4, 128.4 (2C), 128.5 (2C), 128.7 (2C), 129.5, 130.6, 131.8, 133.8, 137.2, 137.5, 138.3, 140.9, 143.4, 199.7; GC-MS (m/z): 352 (M); anal. calcd for (C₂₆H₃₄O): 352.18; C, 88.60; H, 6.86; found: C, 88.45, H, 6.71.



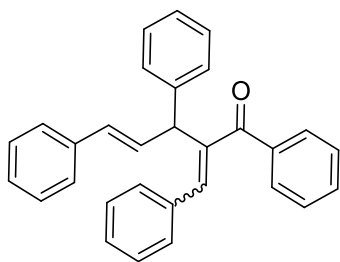
(Z,E)-158bg Yellow oil, Y = 74%. ¹H-NMR (400 MHz, CDCl₃), δ 1.58 (d, 3H, J = 7.1 Hz), 2.38 (s, 3H), 4.62 (d, 1H, J = 7.7 Hz), 5.84 (q, 1H, J = 7.1 Hz), 6.30 (d, 1H, J = 15.4 Hz), 6.46 (dd, 1H, J = 15.8 Hz, J = 7.7 Hz), 7.21-7.36 (m, 10H), 7.59 (d, 2H, J = 11.0 Hz); ¹³C-NMR (100 MHz, CDCl₃), δ 15.8, 21.3, 52.2, 126.5, 127.5 (2C), 127.9, 128.2, 128.5, 128.6 (2C), 128.7 (2C), 128.7, 128.8, 129.4, 130.0, (2C), 130.8, 130.9, 134.0, 135.4, 138.5, 139.2, 142.6, 199.3; ESI-MS: 421 [M+H⁺], 443 [M+Na⁺]; anal. calcd for (C₃₆H₂₂Cl₂O: 420.10): C, 74.11; H, 5.26; found: C, 73.91, H, 5.03.



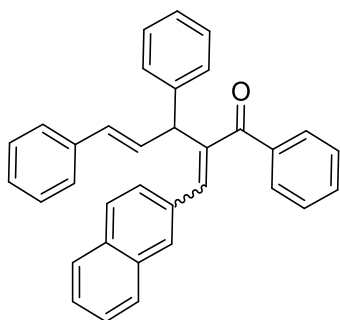
(Z,E)-158ca Yellow oil, Y = 80%. ¹H-NMR (400 MHz, CDCl₃), δ 1.08- 0.96 (m, 4H), 1.28-1.21 (m, 2H), 1.63-1.50 (m, 4H), 1.97-1.88 (m, 1H), 4.55 (d, 1H, J = 7.8 Hz), 5.55 (d, 1H, J = 10.4 Hz), 6.33 (d, 1H, J = 15.8 Hz), 6.48 (dd, 1H, J = 7.8 Hz, J = 15.8 Hz), 7.21-7.15 (m, 2H), 7.32- 7.24 (m, 8H), 7.39 (t, 2H, J = 7.6 Hz), 7.50 (t, 1H, J = 7.4 Hz), 7.79 (d, 2H, J = 7.7 Hz); ¹³C-NMR (100 MHz, CDCl₃), δ 25.3, 25.4, 25.7, 32.7, 32.8, 38.6, 52.6, 126.3 (2C), 126.7, 127.3, 128.3 (2C), 128.4 (4C), 128.7 (2C), 129.1 (2C), 130.7, 131.7, 132.9, 137.2, 137.6, 139.1, 140.2, 140.8, 199.5; GC-MS (m/z): 406 (M); anal. calcd for (C₃₀H₃₀O: 406.23): C, 88.63; H, 7.44; found: C, 88.51, H, 7.28.



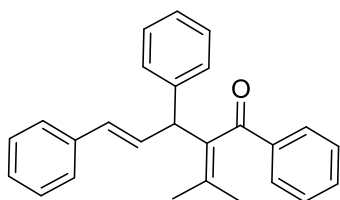
(Z,E)-158da Yellow oil, Y = 67%. ¹H-NMR (400 MHz, CDCl₃), δ 0.78 (d, 3H, J = 6.6 Hz), 0.79 (d, 3H, J = 6.6 Hz), 1.59 (ept, 1H, J = 6.7 Hz), 1.80 (t, 1H, J = 7.4 Hz), 4.62 (d, 1H, J = 7.8 Hz), 5.75 (dt, 1H, J = 7.6 Hz, J = 1.2 Hz), 6.37 (d, 1H, J = 15.8 Hz), 6.51 (dd, 1H, J = 7.8 Hz, J = 15.8 Hz), 7.21-7.15 (m, 2H), 7.32-7.24 (m, 8H), 7.40-7.36 (m, 2H), 7.50 (t, 1H, J = 7.4 Hz), 7.80-7.78 (m, 2H); ¹³C-NMR (100 MHz, CDCl₃), δ 22.3, 22.3, 28.7, 38.7, 52.9, 126.3 (2C), 126.7, 128.4 (4C), 128.5 (2C), 128.7 (2C), 129.2 (2C), 130.6, 131.8, 132.9, 132.95, 137.2, 137.5, 140.9, 142.8, 199.5; GC-MS: 380 (M); anal. calcd for (C₂₈H₂₈O: 380.21): C, 88.38; H, 7.42; found: C, 88.19, H, 7.39.



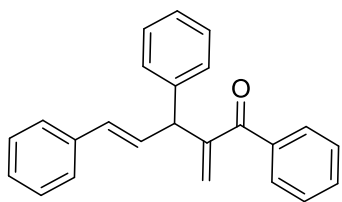
158ea Yellow oil, Y = 99%. ¹H-NMR (400 MHz, CDCl₃), δ 4.81 (d, 1H, J = 7.8 Hz), 6.44 (d, 1H, J = 15.8 Hz), 6.63 (dd, 1H, J = 7.8 Hz, J = 15.8 Hz), 6.81 (s, 1H), 7.05-7.11 (m, 3H), 7.14 (d, 2H, J = 6.6 Hz), 7.24-7.20 (m, 4H), 7.41-7.28 (m, 9H), 7.75 (d, 2H, J = 7.3 Hz); ¹³C-NMR (100 MHz, CDCl₃), δ 53.8, 126.4 (2C), 126.9, 127.4, 127.7, 128.06 (2C), 128.14 (2C), 128.5 (2C), 128.6 (2C), 128.7 (2C), 128.8 (2C), 129.4 (2C), 130.1, 132.0, 132.4, 132.9, 135.6, 136.2, 137.1, 140.3, 143.3, 199.8; GCMS (m/z): 400 (M); anal. calcd for (C₂₈H₂₈O: 400.18): C, 89.97; H, 6.04; found: C, 89.81, H, 5.91.



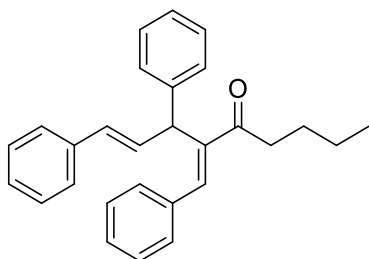
158fa Yellow oil, Y = 73%. ¹H-NMR (400 MHz, CDCl₃), δ 4.86 (d, 1H, J = 7.8 Hz), 6.47 (d, 1H, J = 15.8 Hz), 6.67 (dd, 1H, J = 7.8 Hz, J = 15.8 Hz), 6.96 (s, 1H), 7.13 (t, 3H, J = 7.7 Hz), 7.36-7.19 (m, 10H), 7.42-7.40 (m, 2H), 7.51 (d, 2H, J = 8.5 Hz), 7.64-7.59 (m, 3H), 7.77-7.75 (m, 2H); ¹³C-NMR (100 MHz, CDCl₃), δ 54.0, 126.1, 126.2, 126.2, 126.4 (2C), 127.0, 127.4, 127.5, 127.7, 128.0, 128.2 (2C), 128.5 (2C), 128.6, 128.6 (2C), 128.9 (2C), 129.3 (2C), 130.1, 131.9, 132.5, 132.5, 132.9, 132.9, 133.1, 136.3, 137.1, 140.4, 143.6, 200.0; ESI-MS: 451 [M+H⁺], 473 [M+Na]; anal. calcd for (C₃₄H₂₆O: 450.20): C, 90.63; H, 5.82; found: C, 90.51, H, 5.61.



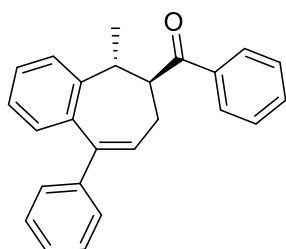
158ga Yellow oil, Y = 84%. ¹H-NMR (400 MHz, CDCl₃), δ 1.60 (s, 3H), 1.90 (s, 3H), 4.81 (t, 1H, J = 3.6 Hz), 4.49 (s, 1H), 6.50 (d, 1H, J = 1.0 Hz), 7.20-7.26 (m, 6H), 7.33-7.36 (m, 5H), 7.43-7.48 (m, 2H), 7.79-7.82 (m, 2H); ¹³C-NMR (100 MHz, CDCl₃), δ 20.5, 23.3, 50.4, 126.3, 126.3 (2C), 127.1, 128.20 (2C), 128.3 (2C), 128.3 (2C), 128.4 (2C), 129.3 (2C), 130.5, 131.3, 132.7, 134.0, 135.6, 137.3, 138.1, 141.9, 200.6; ESIMS: 352 (M); anal. calcd for (C₂₆H₂₄O: 352.18): C, 88.60; H, 6.86; found: C, 88.45, H, 6.71.



158ha Yellow oil, Y = 57%. ¹H-NMR (400 MHz, CDCl₃), δ 5.08 (d, 1H, J = 7.4 Hz), 5.81 (s, 1H), 5.87 (s, 1H), 6.40 (d, 1H, J = 15.9 Hz), 6.54 (dd, 1H, J = 7.4 Hz, J = 15.9 Hz), 7.22-7.18 (2H, m), 7.36-7.24 (8H, m), 7.41 (t, 2H, J = 7.5 Hz), 7.51 (t, 1H, J = 7.4 Hz), 7.74 (d, 2H, J = 7.3 Hz); ¹³C-NMR (100 MHz, CDCl₃), δ 49.6, 126.3 (2C), 126.4, 126.7, 127.4, 128.2 (2C), 128.5 (2C), 128.6 (2C), 128.7 (2C), 129.6 (2C), 130.5, 132.0, 132.3, 137.1, 137.5, 140.9, 150.2, 197.0; ESI-MS: 324 (M); anal. calcd for (C₂₄H₂₀O: 324.15): C, 88.85; H, 6.21; found: C, 88.51, H, 6.02.



158ia Yellow oil, Y = 40%. ¹H-NMR (400 MHz, CDCl₃), δ 0.59 (t, 3H, J = 7.3 Hz), 0.92 (dd, 2H, J = 15.0 Hz, J = 7.4 Hz), 1.83-1.91 (m, 2H), 2.04- 2.12 (m, 2H), 4.73 (d, 1H, J = 7.5 Hz), 6.35 (d, 1H, J = 15.9 Hz), 6.56 (dd, 1H, J = 15.9 Hz, J = 7.5 Hz), 6.67 (s, 1H), 7-16-7.38 (m, 15H); ¹³C-NMR (100 MHz, CDCl₃), δ 13.6, 21.7, 25.6, 43.5, 52.9, 126.3 (2C), 127.0, 127.4, 128.0, 128.4 (2C), 128.5 (2C), 128.5 (2C), 128.6 (2C), 128.8 (2C), 130.2, 130.7, 132.3, 136.3, 137.0, 140.2, 147.1, 200.0; HPLC-MS: 381 [M+H⁺], 403 [M+Na]; anal. calcd for (C₂₈H₂₈O: 380.21): C, 88.38; H, 7.42; Found: C, 88.49, H, 7.61.



(+/-)-**trans-161** Yellow solid, Y = 35%; ¹H-NMR (400 MHz, CDCl₃), δ 1.44 (d, 3H, J = 7.0 Hz), 2.36 (dt, 1H, J = 8.7 Hz, J = 4.5 Hz), 2.49 (dt, 1H, J = 14.7 Hz, J = 8.1 Hz), 2.78 (ddd, 1H, J = 14.7 Hz, J = 6.9 Hz, J = 4.8 Hz), 3.04 (m, 1H), 6.15 (t, 1H, J = 7.4 Hz), 7.17-7.21 (m, 4H), 7.22-7.23 (m, 2H), 7.25-7.26 (m, 1H), 7.30-7.31 (m, 1H), 7.35-7.39 (m, 3H), 7.46 (d, 1H, J = 7.7 Hz), 7.60 (dt, 1H, J = 7.7 Hz, J = 1.0 Hz), 7.72 (d, 1H, J = 7.6 Hz); ¹³C-NMR (100 MHz, CDCl₃), δ 20.1, 30.2, 39.0, 56.5, 123.5, 124.9, 126.5, 127.0, 127.1, 127.2 (2C), 127.4, 128.1 (2C), 128.3 (2C), 129.8 (2C), 134.9, 135.9, 139.8, 142.3, 143.4, 158.1, 207.1; ESI-MS: 339 [M+H⁺], 355 [M+NH₄⁺], 361 [M+Na], 377 [M+K]; anal. calcd for (C₂₅H₂₂O: 338.17): C, 88.72; H, 6.55; found: C, 88.52, H, 6.31.

Crystallographic Data Collection and Structure Determination for (Z,E)-158ag.

The X-ray intensity data were measured on a Bruker SMART Apex II CCD area detector diffractometer. Cell dimensions and the orientation matrix were initially determined from a least-squares refinement on reflections measured in three sets of 20 exposures, collected in three different ω regions, and eventually refined against all data. A full sphere of reciprocal space was scanned by 0.3° ω steps. The software SMART^[3] was used for collecting frames of data, indexing reflections, and determination of lattice parameters. The collected frames were then processed for integration by the SAINT program^[4] and an empirical absorption correction was applied using SADABS.^[4] The structures were solved by direct methods (SIR 2004)^[5] and subsequent Fourier syntheses and refined by full-matrix least-squares on F^2 (SHELXTL)^[6], using anisotropic thermal parameters for all non-hydrogen atoms. All hydrogen atoms were added in calculated positions, included in the final stage of refinement with isotropic thermal parameters, $U(\text{H}) = 1.2 U_{\text{eq}}(\text{C})$ [$U(\text{H}) = 1.5 U_{\text{eq}}(\text{C-Me})$], and allowed to ride on their carrier carbons. Crystal data and details of the data collection for (Z,E)-158ag are reported in Table S1.

X-ray crystal structure of (Z,E)-158ag.

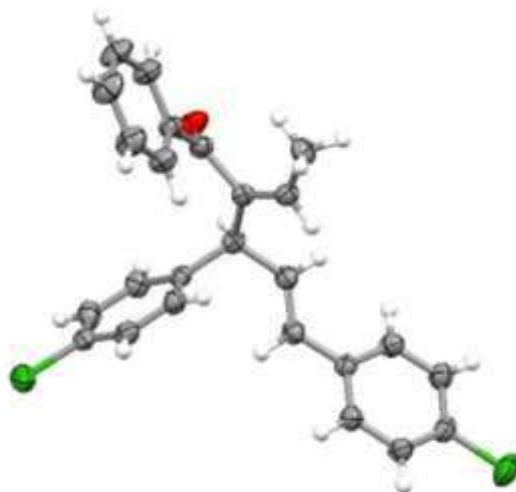


Figure S1. a) Molecular structure of (Z,E)-158ag.

Table S1. Crystal data and structure refinement for **(Z,E)-158ag**.

	(Z,E)-158ag
Empirical formula	C ₂₅ H ₂₀ Cl ₂ O
Formula weight	407.31
Temperature/K	296 (2)
Crystal system	monoclinic
Space group	<i>P</i> 2 ₁ / <i>n</i>
<i>a</i> , Å	6.1008(8)
<i>b</i> , Å	13.366(2)
<i>c</i> , Å	26.012(3)
α , °	90
β , °	90.785(2)
γ , °	90
Cell volume, Å ³	2121(5)
Z	4
ρ_c , mg m ⁻³	1.276
μ (Mo-K α), mm ⁻¹	0.318
F(000)	848
Crystal size mm	0.25 × 0.10 × 0.07
θ limits, °	1.566 to 24.978
Refl. collected, unique (R_{int})	13542 / 3697 [R_{int}] = 0.0447]
Goodness-of-fit-on F ²	1.019
$R_1(F)^a$, $wR_2(F^2)$ [$I > 2\sigma(I)$] ^b	$R_1 = 0.0502$, $wR_2 = 0.1186$
Largest diff. peak and hole, e. Å ⁻³	0.462 and -0.384

^a $R_1 = \Sigma||F_o| - |F_c|| / \Sigma|F_o|$, ^b $wR_2 = [\Sigma w(F_o^2 - F_c^2)^2 / \Sigma w(F_o^2)^2]^{1/2}$ where $w = 1/[\sigma^2(F_o^2) + (aP)^2 + bP]$ where $P = (F_o^2 + F_c^2)/3$.

Reference:

- [1] S. Wang, L. Zhang, *J. Am. Chem. Soc.* 2006, 128, 8414-8415.
- [2] Y. Yu, W. Yang, F. Rominger, A. S. Hashmi, *Angew. Chem. Int. Ed.* 2013, 52, 7586-7589.
- [3] SMART & SAINT Software Reference Manuals, version 5.051 (Windows NT Version), Bruker Analytical X-ray Instruments Inc.: Madison, WI, 1998.
- [4] G. M. Sheldrick, SADABS, program for empirical absorption correction, University of Göttingen, Germany, 1996.
- [5] M. C. Burla, R. Caliandro, M. Camalli, B. Carrozzini, Cascarano, G. L. De Caro, C. Giacovazzo, G. Polidori, R. Spagna, *J. Appl. Crystallogr.* 2005, 38, 381-388.
- [6] G. M. Sheldrick, SHELXTLplus (Windows NT Version) Structure Determination Package, Version 5.1. Bruker Analytical X-ray Instruments Inc.: Madison, WI, USA, 1998.

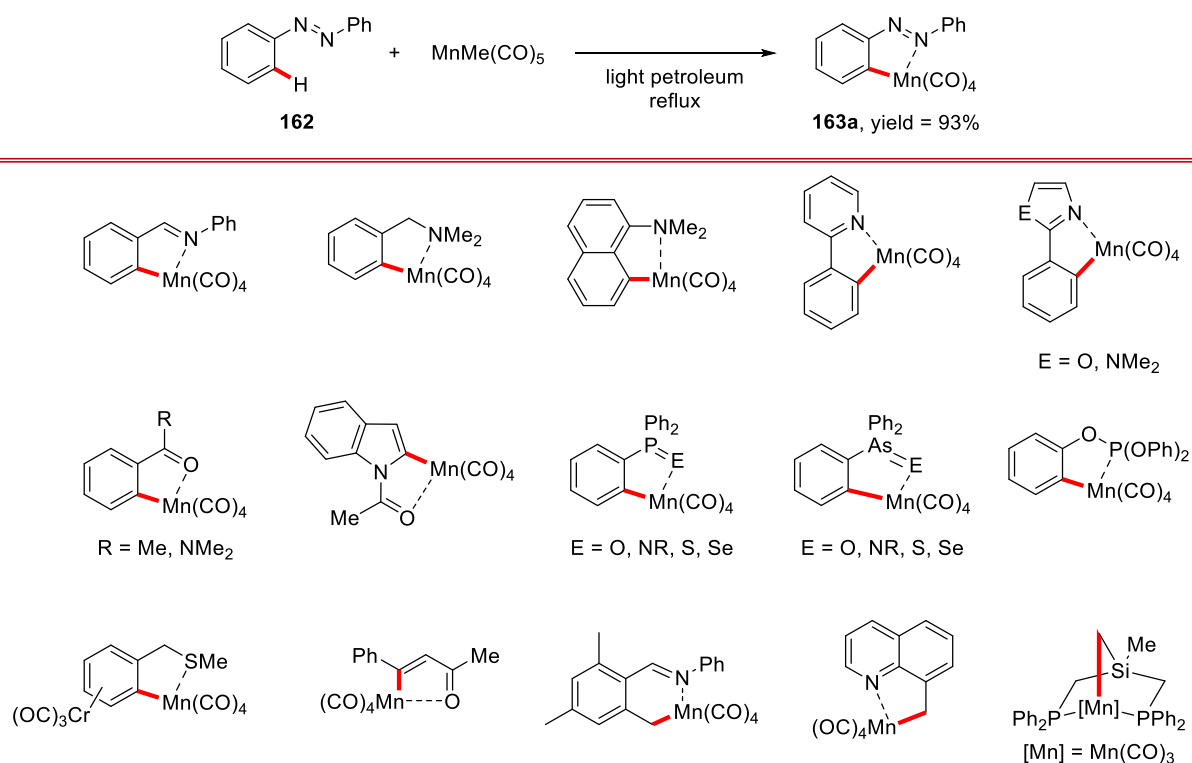
6. INTRODUCTION: C–H ACTIVATION

In the past 10 years, C–H activation has emerged as a powerful alternative method to traditional cross-coupling reactions, for the formation of new C–C or C–X bonds. The most attractive advantage in this type of approach relies in the possibility to avoid the pre-activation of the substrates, improving the atom- and step-economy, and the reduction of toxic wastes. In the past, this type of reactions was promoted principally by 4d and 5d transition metals. Only recently, the interest in the development of C–H activation catalysed by first-row transition-metals, increased due to their high abundance in the Earth's crust and their low costs. In particular, cobalt, nickel and iron have received considerable interest while the interest in manganese has been increased only in the last 3-5 years.

Manganese is the twelfth most abundant element in the Earth and the third transition metal only after iron and titanium.

6.1 Stoichiometric Reaction

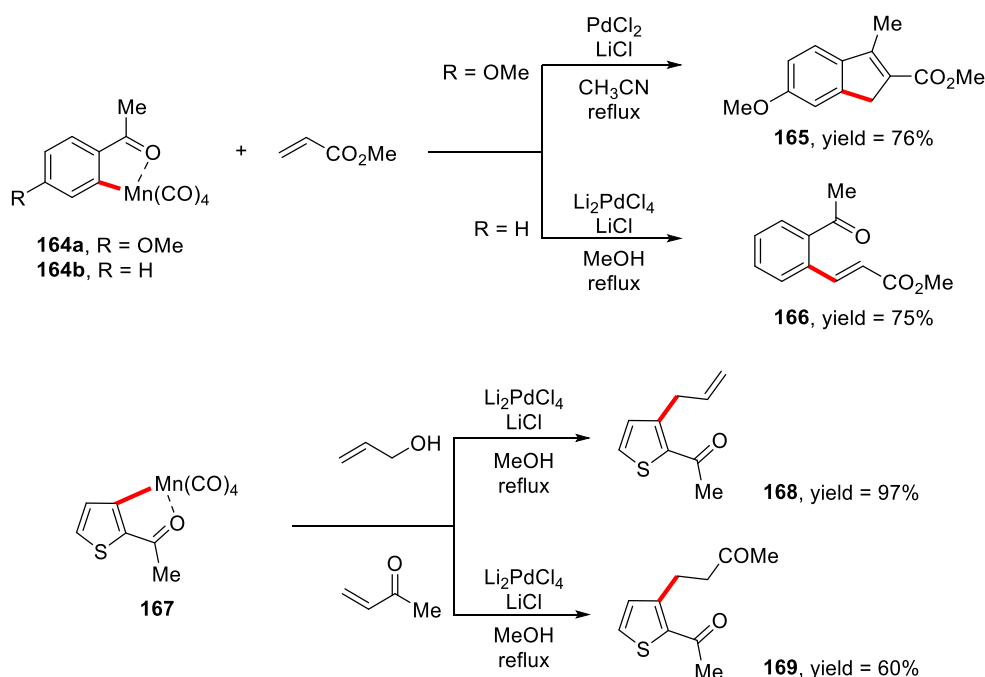
The first C–H activation promoted by manganese complex was developed by Stone and Bruce in 1970^[1] using stoichiometric amount of $\text{MnMe}(\text{CO})_5$.



Scheme 1: First C–H activation promoted by manganese complex.

Under the optimized reaction conditions it was possible to isolate different five-membered manganacycles in excellent yields (Scheme 1).

Subsequently, Nicholson and Main studied in depth the reactivity of these compounds. In particular in 1987^[2] they treated the manganacycle **164** with activated alkene in the presence of palladium catalysts. Different products were isolated from the same substrates when different palladium catalysts were employed in the reaction. Moreover, when manganacycle derived from 2-acetylthiophene was submitted under the same conditions in the presence of methyl vinyl ketone or allyl alcohol, the alkylated thiophene or allylic thiophene were achieved in good yields (Scheme 2).

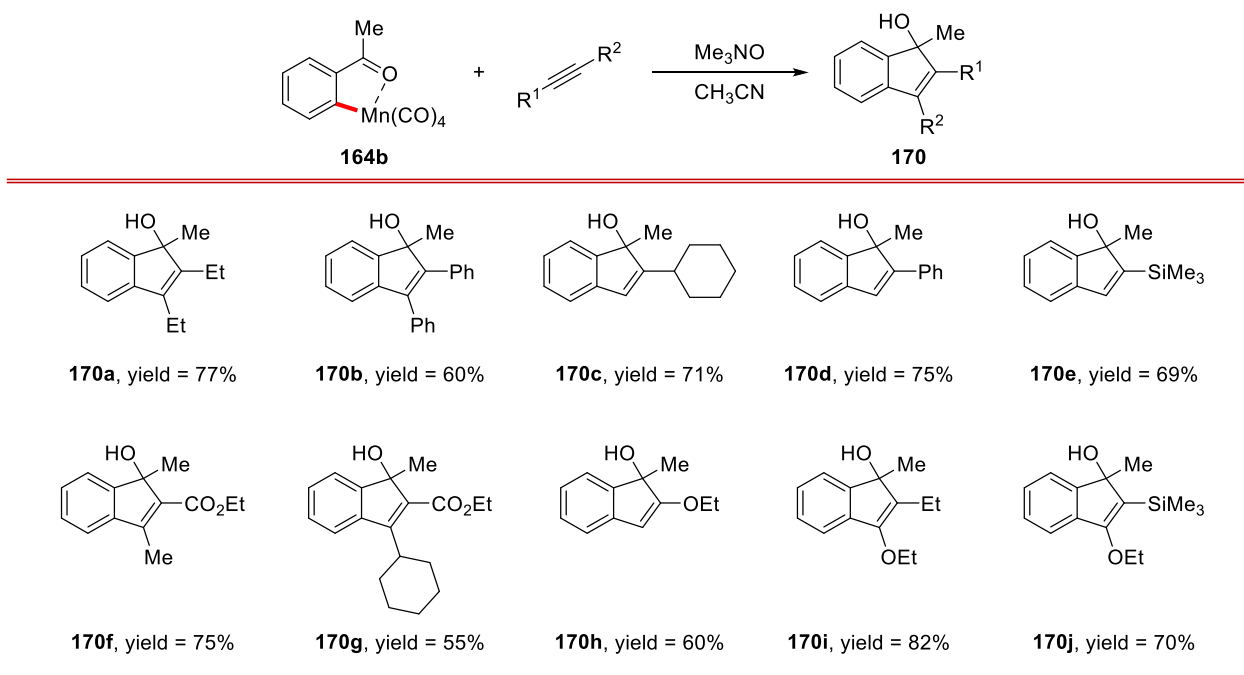


Scheme 2: Reactivity of the manganacycles.

Not only aromatic but also olefinic manganacycles can react with methyl acrylate resulting in the corresponding products in good yields as reported by the same authors in 1995.^[3] Several applications in the use of manganacycles with activated olefins were reported; for example, Woodgate and co-workers^[4,5] developed a procedure using a manganacycle derived from podocarpic acid, while Nicholson^[6] employed a cyclomanganated triphenylphosphine chalcogenide obtaining in both cases the corresponding products in satisfactory yields.

Moreover, the coupling of manganacycles with alkynes was investigated in order to extend the applications of these compounds. In particular, Liebeskind and co-workers reported in 1989 the annulation reaction of ketone-based mangacycles with differently substituted alkynes.^[7] The desired products were achieved when anhydrous trimethylamine *N*-oxide (TMANO)^[8] was added in the

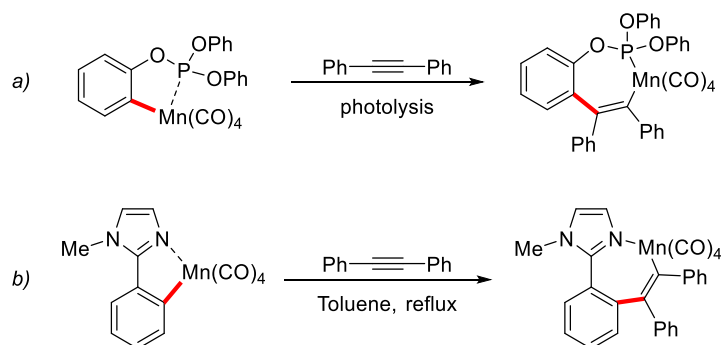
reaction. Several substituted alkynes were submitted in the reaction with manganacycle **164b** in acetonitrile and in the presence of TMANO resulting in the corresponding products in good yields (Scheme 3). The procedure demonstrated to be tolerant toward different functional groups and the reactions proceeded smoothly with terminal, internal, electron-rich as well as electron-deficient alkynes.



Scheme 3: Coupling with alkynes.

On the basis of the observed regiochemistry of the products, the authors rationalized that the insertion of the alkyne into the Mn–C bond of the manganacycle has been controlled by steric effects; indeed, the large alkyne substituent occupied the 2-position of the indenol, predominantly. It was assumed that the desired products were achieved through the formation of seven-member metallacycle intermediate generated by insertion of alkyne into the Mn–C bond and subsequently the nucleophilic attack of the Mn–C bond to the carbonyl group led to the corresponding indenol.

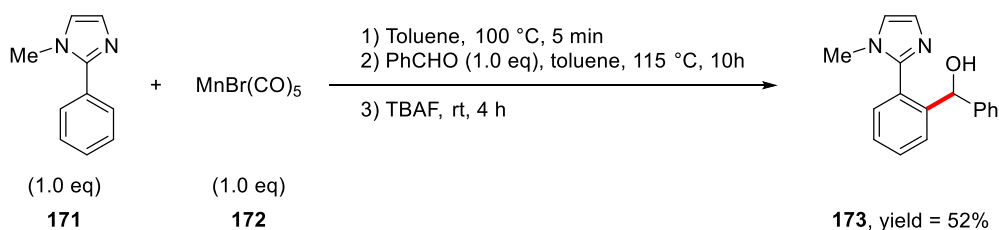
The formation of the seven-member manganacycle was demonstrated by Nicholson and Main^[9,10] one year later when they examined again the photochemical reaction of *ortho*-manganated triphenylphosphite with diphenylacetylene reported the first time by Onaka and co-workers.^[11] In that situation, they were able to isolate the seven-member manganacycle which was unambiguously characterized by X-ray diffraction analysis (Scheme 4a). Subsequently, Suárez and co-workers reported the synthesis of the first N-containing seven-membered manganacycle achieved by reaction of phenylimidazole-based manganacycle with diphenylacetylene (Scheme 4b)



Scheme 4: Isolation of the seven-membered manganacycle (a) and preparation of the first *N*-containing seven-membered manganacycle (b).

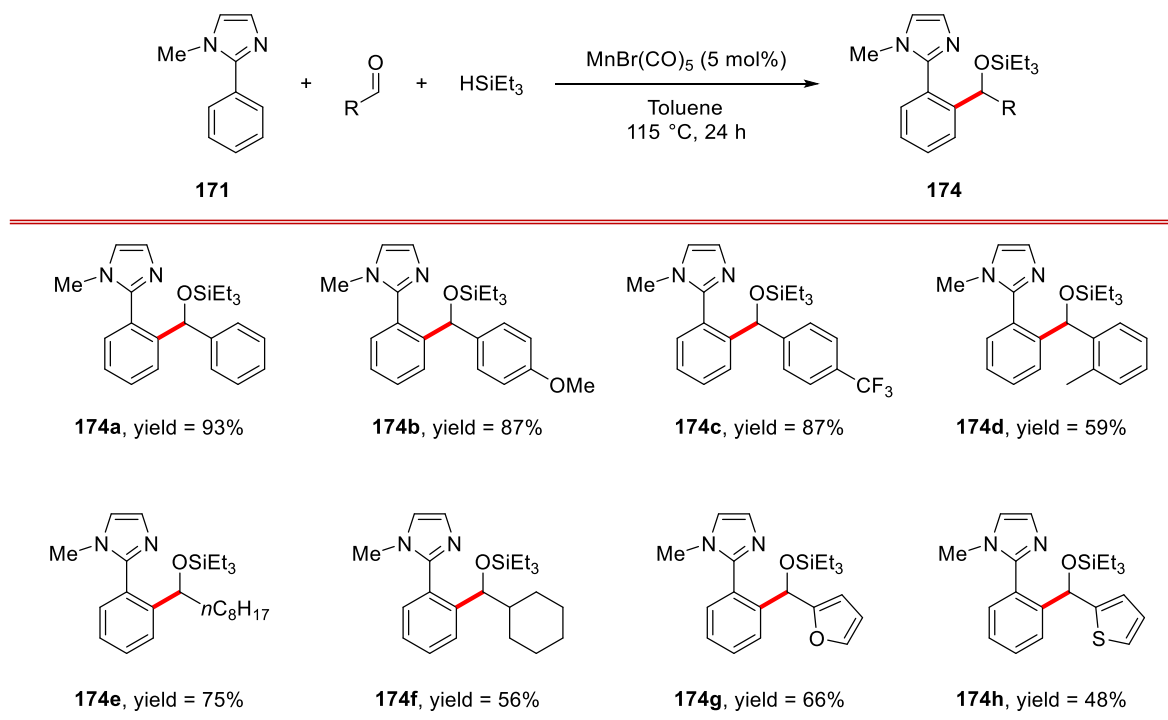
6.2 Catalytic Reaction

Pioneering results in manganese-catalysed C–H activation were reported by Kuninobu and Takai in 2007^[12] when they started to investigate the stoichiometric C–H bond activation of 1-methyl-2-phenyl-1*H*-imidazole and consequent insertion of aldehydes promoted by MnBr(CO)₅. In particular, using benzaldehyde the authors were able to isolate the corresponding product in 52% yield (Scheme 5).



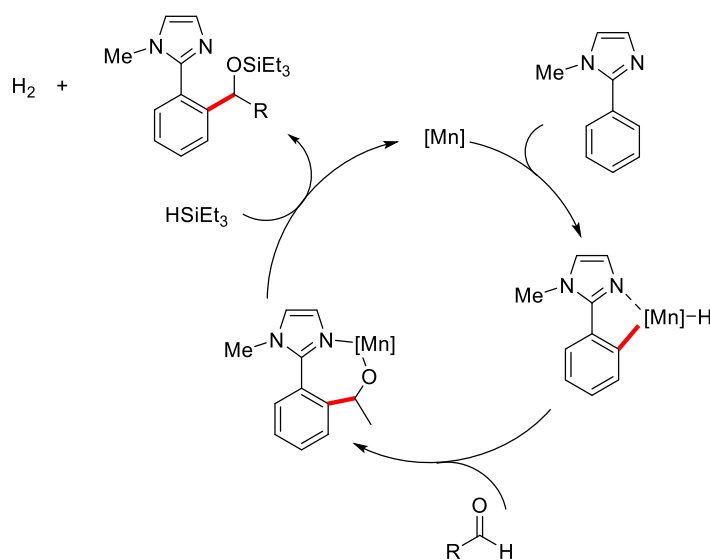
Scheme 5: Stoichiometric C–H bond activation.

Unfortunately, when the manganese complex was used in catalytic amount, only traces of the product have been produced. However, they detected a possible method to recycle the catalyst in order to use only catalytic amount of manganese complex. In particular, they demonstrated that adding 2.0 equivalent of triethylsilane in the reaction mixture from the beginning it was possible to obtain the corresponding product in 93% yield. Subsequently, they proved the scope of the methodology by submitting several aldehydes under optimized catalytic conditions. The protocol revealed to be tolerant toward differently substituted aromatic as well as aliphatic aldehydes resulting in the corresponding products in satisfactory yields (Scheme 6).



Scheme 6: Scope of the Mn-catalysed C–H activation.

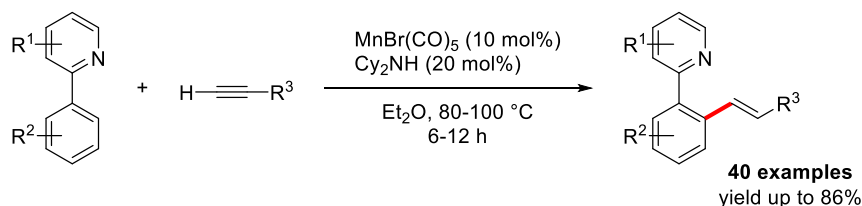
The authors investigated the mechanism through several experiments finding that the hydrosilane promoted the reductive elimination of manganese by silylation of the alkoxy moiety; the proposed mechanism is illustrated in Scheme 7.



Scheme 7: Proposed reaction mechanism.

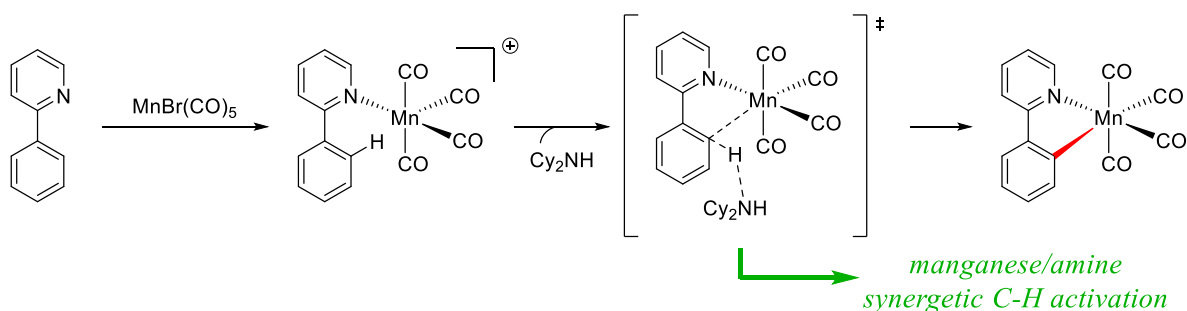
Subsequently in 2013, Chen and Wang reported a manganese-catalysed aromatic C–H alkenylation.^[13] In particular, arylpyridines reacted with terminal alkynes in the presence of $\text{MnBr}(\text{CO})_5$ and dicyclohexylamine (Cy_2NH) resulting in the corresponding *E*-alkenylated products.

The protocol demonstrated high chemo-, regio- and stereoselectivity and the ample scope shows its flexibility (Scheme 8).



Scheme 8: Mn-catalysed aromatic C–H alkenylation

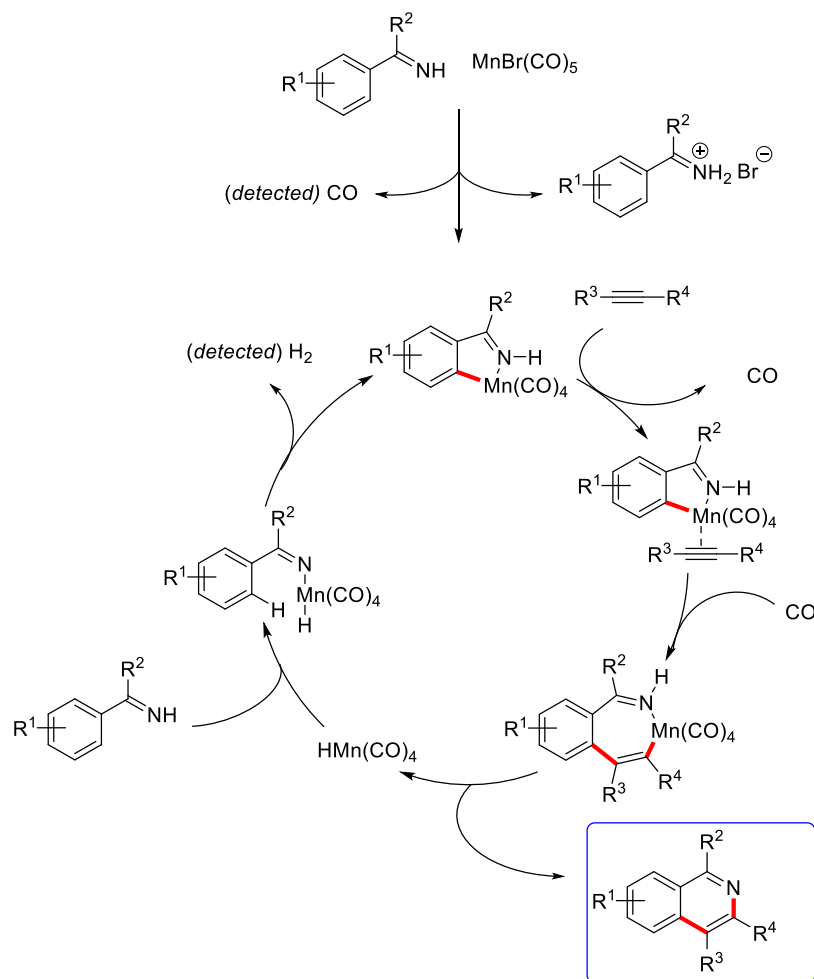
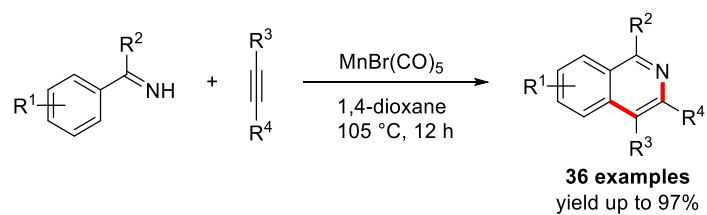
It is noteworthy that in stoichiometric reaction of MnBr(CO)_5 and 2-phenylpyridine only traces of the product were observed in the absence of Cy_2NH , while the rate reaction increased when the base was used as an additive. This result has been rationalized considering the cooperation of the manganese catalyst with the base in the C–H activation step (Scheme 9). In particular, using Cy_2NH the C–H bond cleavage resulted to be easier to achieve. This preliminary hypothesis has been subsequently confirmed by deuterium-labeling experiments and DFT calculations.



Scheme 9: Base-assisted C–H activation.

Subsequently, Wang and co-worker increased the applications in manganese-catalysed C–H activation reporting two different procedures for the dehydrogenative [4+2] annulation of N–H imines with alkynes^[14] and the C–H conjugate addition to α,β -unsaturated carbonyl compounds^[15] respectively.

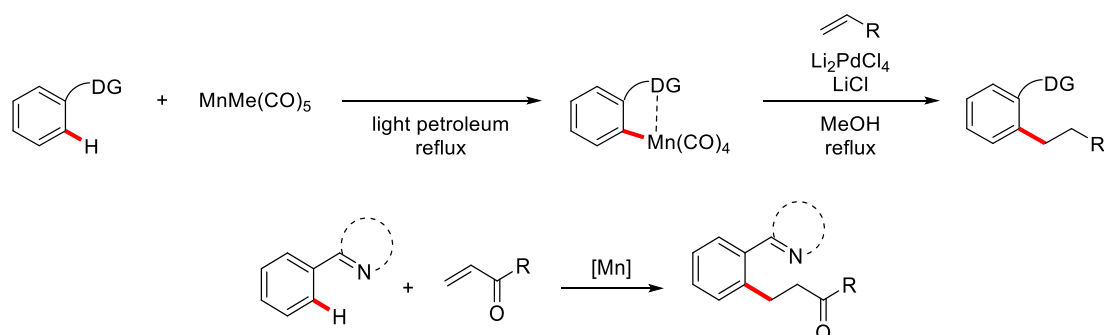
The dehydrogenative [4+2] annulation of imines with alkynes is a useful protocol to prepare differently substituted isoquinolines. The methodology demonstrated to be tolerant toward different functional groups due to the mild reaction conditions which do not require any oxidants, external ligands or additives.



Scheme 10: Dehydrogenative [4+2] annulation of imines with alkynes and proposed reaction mechanism.

As it is shown in the catalytic cycle in Scheme 10, the production of H₂ and CO as by-products was detected by analytical methods, confirming consequently the proposed reaction mechanism.

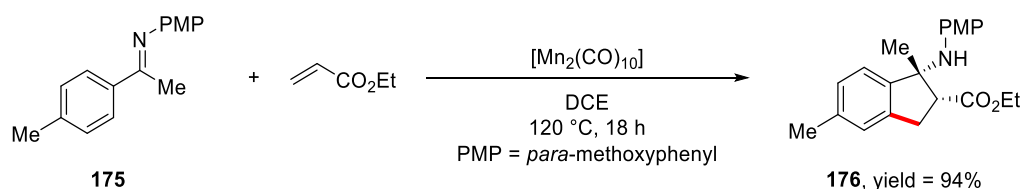
Continuing with their interest in manganese-catalysed C–H activation, the same authors reported an alternative one-step catalysed-reaction^[15] for the stoichiometric methodology reported by Nicholson and Main and above illustrated (Scheme 11).^[2]



Scheme 11: One-step catalysed-reaction for the stoichiometric methodology reported by Nicholson and Main.

Several 2-arylpyridines featuring electron-donating as well as electron-withdrawing groups were submitted under optimized reaction conditions, furnishing the corresponding products in good yields. The reaction showed high levels of regio-control when arylpyridines featuring two adjacent C–H bonds were available for the activation favouring the addition of less sterically congested one. Subsequently, it was further tested the scope of the reaction employing primary, secondary and also tertiary alkylacrylates. The methodology revealed to be tolerant toward different functional groups furnishing the corresponding products in good yields. Only styrene cannot be used as reagent highlighting the importance of the carbonyl group. On the base of the experimental results obtained it was proposed a hypothetical reaction mechanism which was then confirmed by DFT calculations. Moreover, it was also demonstrated that the use of dicyclohexylamine increased the C–H bond cleavage through its cooperation with manganese catalyst.

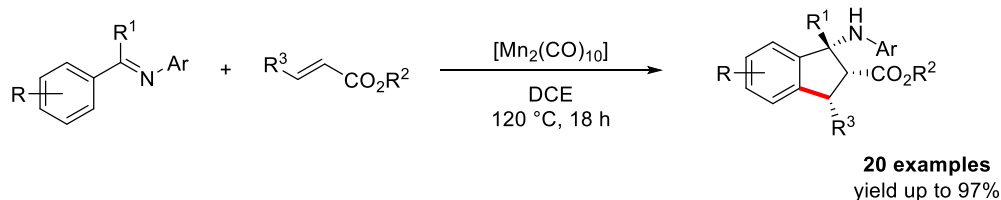
In 2015 Ackermann and co-workers developed a new powerful route to synthesize β -amino acid derivatives from manganese-catalysed C–H activation of easily available imines.^[16] The authors started their investigation choosing the transformation of ketimine **175** with ethyl acrylate as model reaction. The desired product was isolated in 94% yield when the reaction was promoted by $[\text{Mn}_2(\text{CO})_{10}]$ in DCE at 120 °C (Scheme 12).



Scheme 12: Synthesize β -amino acid derivatives from Mn-catalysed C–H activation.

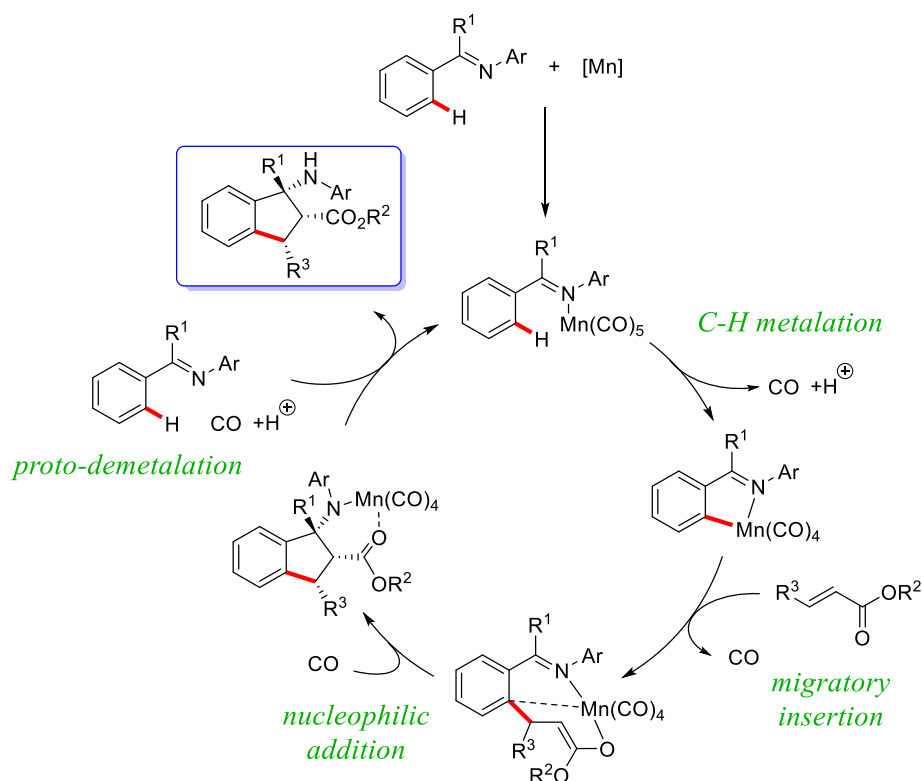
The unusual *cis*-configuration exhibited by the obtained product was determined in unambiguous way by bidimensional NMR studies.

Subsequently, the scope of the reaction was investigated, by submitting differently substituted ketimines and alkenes under optimized reaction conditions. All the corresponding products were achieved in good to excellent yields (Scheme 13).



Scheme 13: Scope of the Mn-catalysed C–H activation of imines.

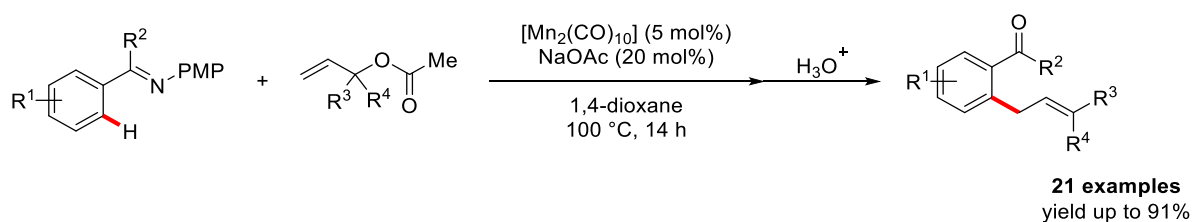
The methodology demonstrated to be tolerant toward different functional groups such as cyclopropyl, ester and halogen substituents and moreover the reaction was not limited to terminal alkenes but also internal alkenes resulted in the corresponding products in good yields. Finally, several experiments were carried out in order to shed light on the reaction mechanism which is illustrated in Scheme 14.



Scheme 14: Reaction mechanism.

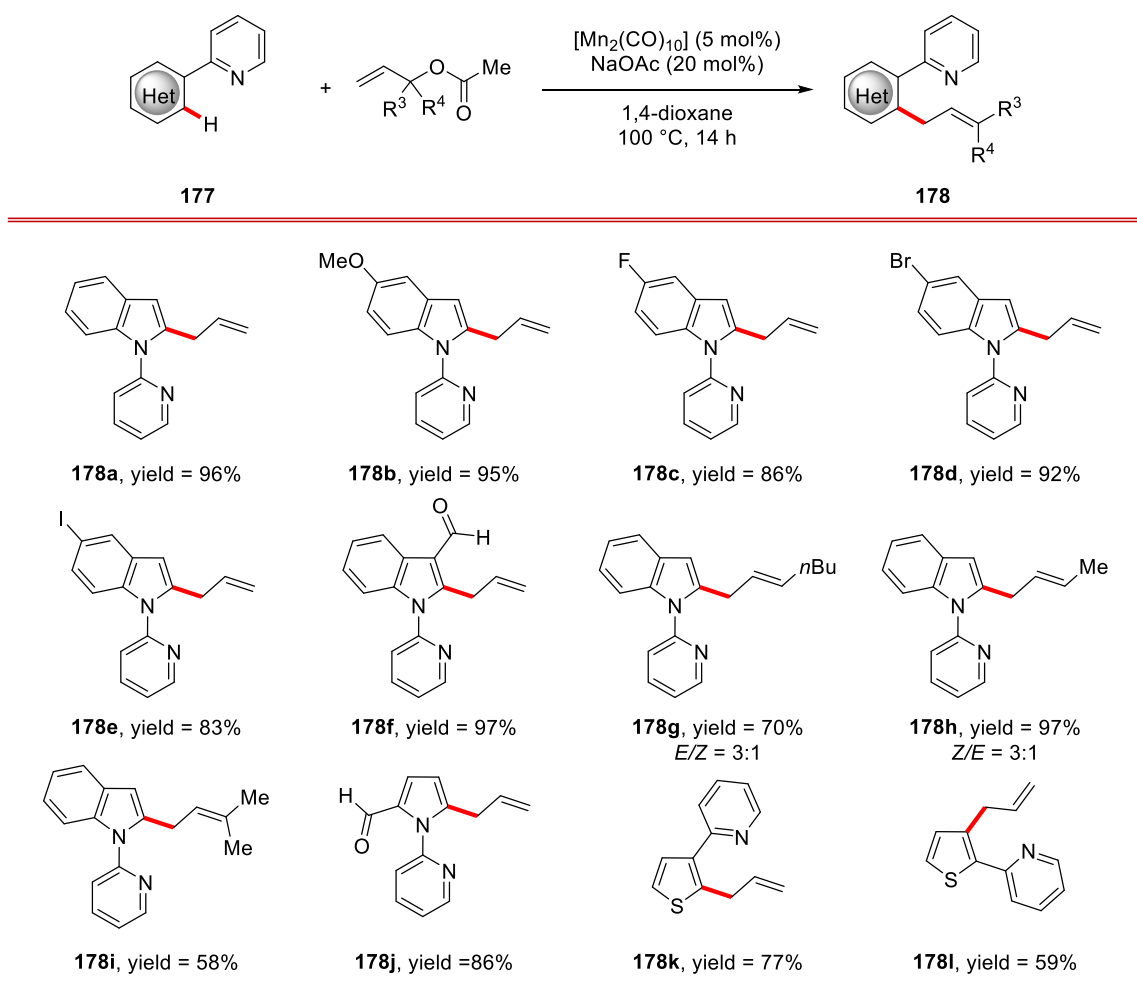
Subsequently, it was also reported the first manganese(I)-catalysed intermolecular C–H allylation of ketimines.^[17] In particular, it was demonstrated that using $[\text{Mn}_2(\text{CO})_{10}]$ and NaOAc as catalytic

system it was possible using allyl-carbonate derivatives for the C–H allylation of ketimines (Scheme 15).



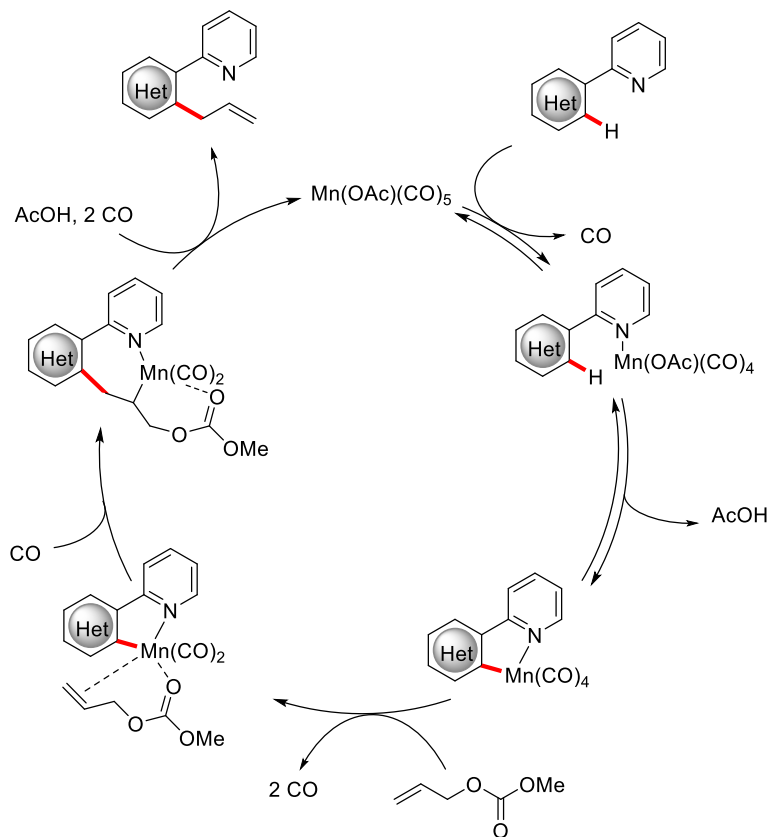
Scheme 15: Mn-catalysed intermolecular C–H of ketimines.

The methodology resulted to be tolerant toward several functional groups and all the corresponding products were isolated in good to excellent yields. Subsequently, it was discovered that the methodology was not limited to the use of arenes. Indeed, indole as well as pyrrole and thiophene heterocycles can be employed in the transformation resulting in the desired products in good yields (Scheme 16).



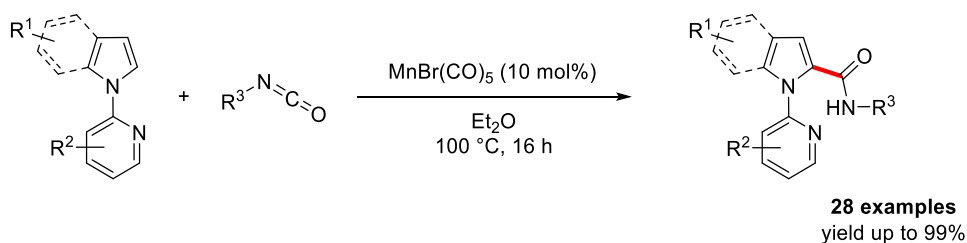
Scheme 16: Scope of the Mn-catalysed C–H allylation.

The authors investigated the reaction mechanism through several mechanistic experiments in order to determine the catalytic cycle which allows the formation of desired allylated products (Scheme 17).



Scheme 17: Reaction mechanism.

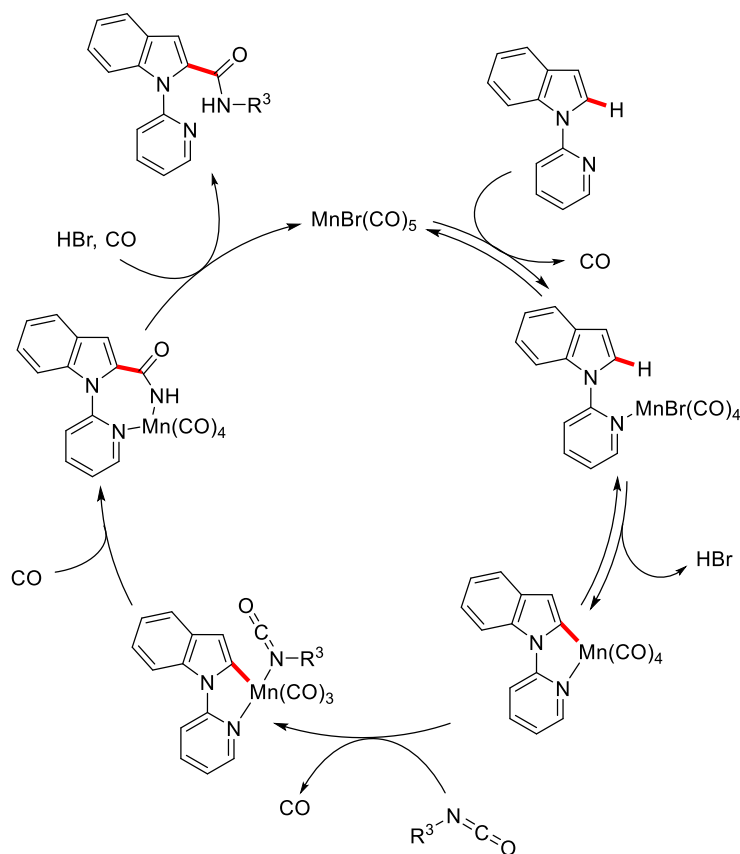
In the same line, Ackermann and co-workers reported a highly efficient manganese-catalyzed C–H aminocarbonylation of heteroarenes.^[18] The authors were able to develop a method where challenging sterically bulky alkyl isocyanates could be used and moreover the success of the reaction was not dependent to the presence of additional ligands or additives.



Scheme 18: Mn-catalyzed aminocarbonylation of heteroarenes.

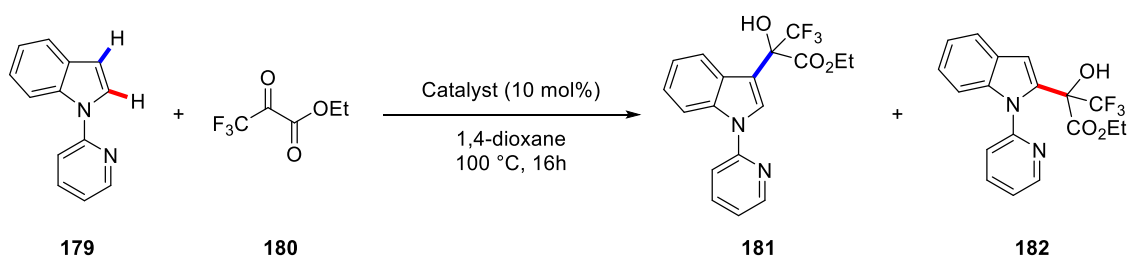
The ample scope reveals the large flexibility of the protocol and the tolerance toward several functional groups. Furthermore, intermolecular competition experiments demonstrated that

electron-deficient isocyanates and electron-rich indoles were more reactive in the transformation. These evidences can be rationalized considering the nucleophilic attack of the metallated indole on the coordinated isocyanate the rate-determining step. Finally, through several experimental mechanistic studies the authors proposed a mechanism reaction which is shown in Scheme 19.



Scheme 19: Proposed reaction mechanism.

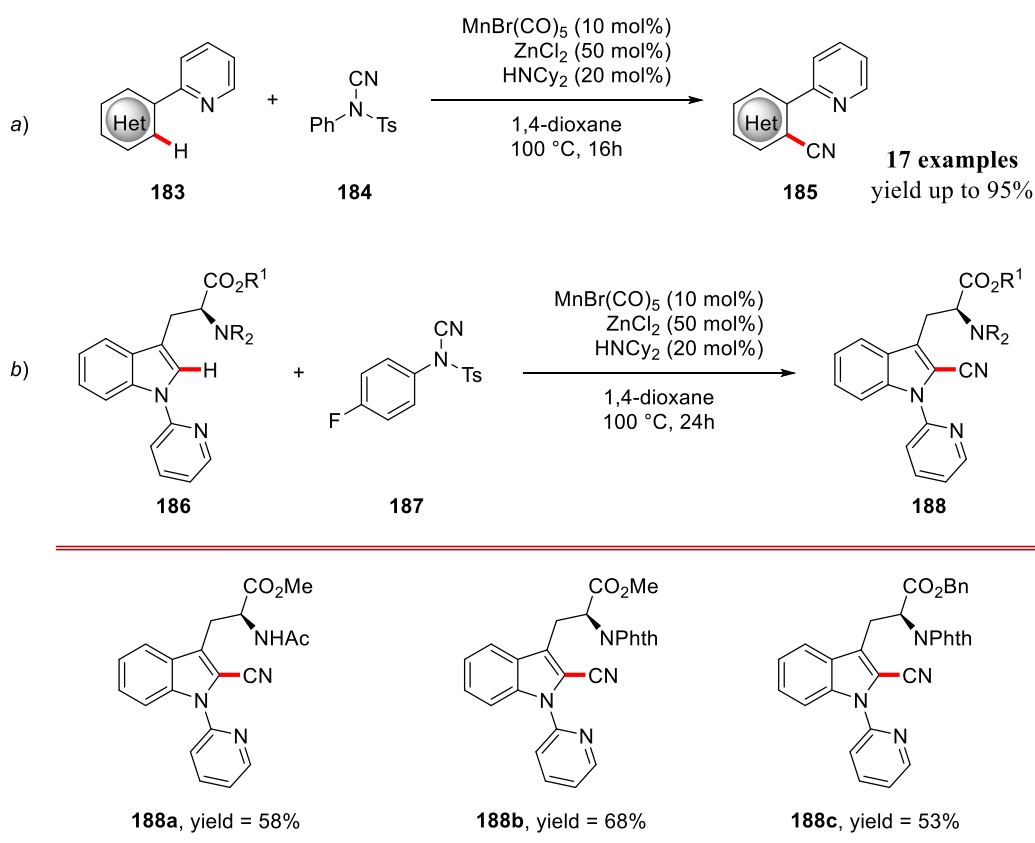
The large benefit in manganese-catalysed C–H activation has been demonstrated by Ackermann in 2016 when with his co-workers developed a highly efficient hydroarylation of ketones with heteroarenes.^[19] They started their investigation considering the reaction of indole **179** with ketone **180** in the presence of different transition-metal-catalysts (Scheme 20).



Scheme 20: Hydroarylation of ketones.

When the reaction was carried out in the presence of catalysts derived from palladium, ruthenium, rhodium, iridium, rhenium, cobalt, nickel and iron, only the C3-functionalized indole **181** was isolate in quantitative yields. Only manganese-catalysts were able to lead to the selective formation of the C2-derivate **182** in excellent yield. In particular, $\text{Mn}_2(\text{CO})_{10}$ promoted the reaction furnishing the desired product in 90% yield, while $\text{MnBr}(\text{CO})_5$ provided the C2-adduct in 88% yield only when NaOAc was used as additive. Subsequently the authors demonstrated that not only ketones but also aldehydes and imines could be used in the reaction resulting in the corresponding products in excellent yields. Moreover, the protocol demonstrated to be not limited to the indole scaffold and, also pyrroles and thiophene derivatives were employed in the reaction resulting in the desired products in satisfactory yields.

Continuing with the interest toward manganese-catalysed C–H activation, very recently Ackermann and co-workers reported the first C–H cyanation of heteroarenes promoted by manganese(I)-catalysts.^[20] They started the investigation studying the reaction between indole **183** and Beller's NCTS (*N*-cyano-*N*-phenyl-*p*-toluenesulfonamide) **184** in the presence of $\text{MnBr}(\text{CO})_5$. Unfortunately, under these reaction conditions, only unsatisfactory yields of the desired products were achieved. In contrast, when ZnCl_2 and HNCy_2 were added in the mixture as additive and base respectively, the desired product was isolated in good yield. They also demonstrated that catalytic amount of Zn(II) were enough to guarantee the success of the reaction (Scheme 21a).



Scheme 21: First C–H cyanation of heteroarenes promoted by Mn(I)-catalysts (a) and its application with tryptophan derivatives (b).

The ample scope showed the large tolerance of the methodology toward different functional groups and moreover, the authors were able to obtain the first manganese-catalysed C–H cyanation of tryptophan derivatives in good yields and without racemization of the stereogenic centers (Scheme 21b).

This new heterobimetallic catalytic system for the C–H cyanation was deeply studied through DFT calculations. In particular, it was demonstrated that the coordinative interaction of the Zn(II) additive allowed a stabilizing effect on the cyclomanganated transition state of 30 kcal mol⁻¹ (Figure 1).

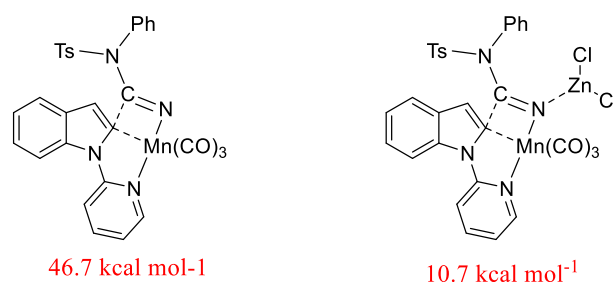


Figure 1: Stabilizing effect of the Zn(II) additive on the cyclomanganated transition state.

Bibliography

- [1] M. I. Bruce, M. Z. Iqbal, F. G. A. Stone, *J. Chem. Soc. A* **1970**, 3204–3209.
- [2] L. H. P. Gommans, L. Main, B. K. Nicholson, *J. Chem. Soc., Chem. Commun.* **1987**, 761–762.
- [3] W. Tully, L. Main, B. I. S. Nicholson, *J. Organomet. Chem.* **1995**, 503, 75–92.
- [4] R. C. Cambie, M. R. Metzler, P. S. Rutledge, P. D. Woodgate, *J. Organomet. Chem.* **1990**, 381, C26–C30.
- [5] R. C. Cambie, M. R. Metzler, P. S. Rutledge, P. D. Woodgate, *J. Organomet. Chem.* **1990**, 398, C22–C24.
- [6] G. J. Depree, L. Main, B. K. Nicholson, *J. Organomet. Chem.* **1998**, 551, 281–291.
- [7] L. S. Liebeskind, J. R. Gasdaska, J. S. McCallum, S. J. Tremont, *J. Org. Chem.* **1989**, 54, 669–677.
- [8] J. A. Soderquist, C. L. Anderson, *Tetrahedron Lett.* **1986**, 27, 3961–3962.
- [9] W. J. Grigsby, L. Main, B. K. Nicholson, *Bull. Chem. Soc. Jpn.* **1990**, 63, 649–651.
- [10] W. J. Grigsby, L. Main, B. K. Nicholson, *Organometallics* **1993**, 12, 397–407.
- [11] S. Onaka, N. Furuichi, Y. Tatematsu, *Bull. Chem. Soc. Jpn.* **1987**, 60, 2280–2282.
- [12] Y. Kuninobu, Y. Nishina, T. Takeuchi, K. Takai, *Angew. Chem. Int. Ed.* **2007**, 46, 6518–6520.
- [13] B. Zhou, H. Chen, C. Wang, *J. Am. Chem. Soc.* **2013**, 135, 1264–1267.
- [14] R. He, Z.-T. Huang, Q.-Y. Zheng, C. Wang, *Angew. Chem. Int. Ed.* **2014**, 53, 4950–4953.
- [15] B. Zhou, P. Ma, H. Chen, C. Wang, *Chem. Commun.* **2014**, 50, 14558–14561.
- [16] W. Liu, D. Zell, M. John, L. Ackermann, *Angew. Chem. Int. Ed.* **2015**, 54, 4092–4096.
- [17] W. Liu, S. C. Richter, Y. Zhang, L. Ackermann, *Angew. Chem. Int. Ed.* **2016**, 55, 7747–7750.

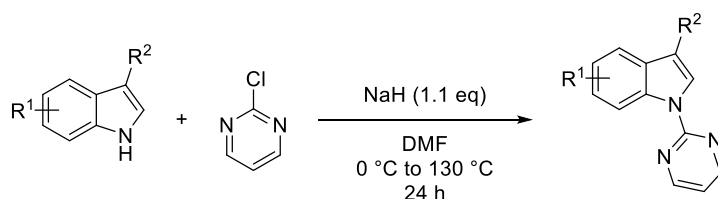
- [18] W. Liu, J. Bang, Y. Zhang, L. Ackermann, *Angew. Chem. Int. Ed.* **2015**, *54*, 14137–14140.
- [19] Y.-F. Liang, L. Massignan, W. Liu, L. Ackermann, *Chem. Eur. J.* **2016**, *22*, 14856–14859.
- [20] W. Liu, S. C. Richter, R. Mei, M. Feldt, L. Ackermann, *Chem. Eur. J.* **2016**, *22*, 17958–17961.

7. MANGANESE-CATALYSED C–H ACTIVATION

7.1 Mn-Catalysed C–H Alkynylation

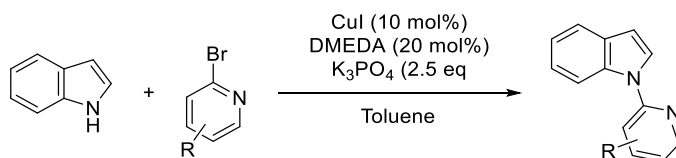
During the third year of my PhD I spent five months in Göttingen (Germany) where I joined in the Ackermann's group. In particular, in collaboration with Z. Ruan and N. Sauermann, the goal was the development of a very efficient strategy for a manganese-catalysed C–H alkynylation of indoles. Below, all the results obtained in this project to give a complete overview about the powerful methodology will be described, highlighting the collaborative nature of the investigation.

We started to prepare differently substituted indole derivatives featuring the pyridine or pyrimidine as directing group. To prepare the 1-(pyrimidin-2-yl)-1*H*-indoles and 1-(pyrimidin-2-yl)-1*H*-pyrrole, the synthetic procedure already reported in literature was followed.^[1] In particular, the indoles reacted smoothly with 2-chloropyrimidine in the presence of NaH in DMF at 130 °C after 24 h (Scheme 1).



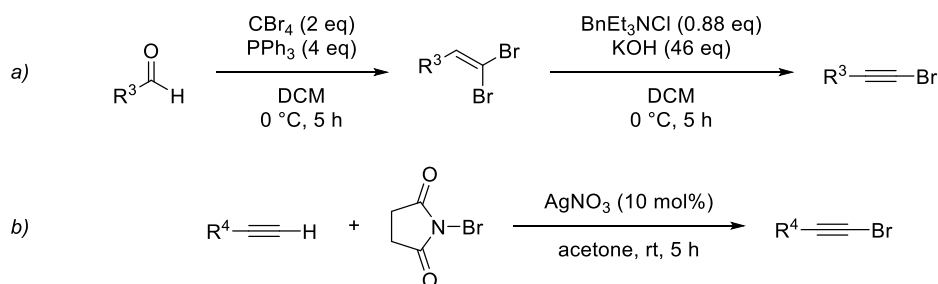
Scheme 1: Synthetic procedure for 1-(pyrimidin-2-yl)-1*H*-indoles.

The synthetic procedure for the preparation of the 1-(pyridine-2-yl)-1*H*-indole consists of a coupling reaction between indole and 2-bromopyridine promoted by CuI in the presence of *N,N'*-dimethyl-ethylenediamine and K₃PO₄ (Scheme 2).^[1]



Scheme 2: Synthetic procedure for 1-(pyridine-2-yl)-1*H*-indoles.

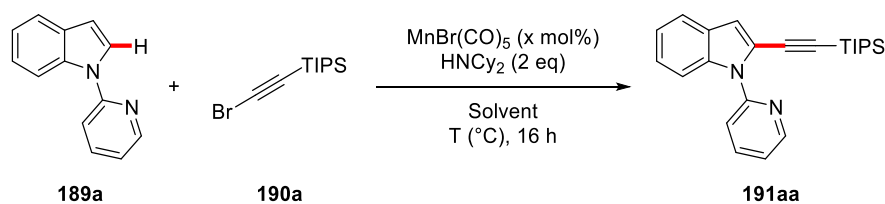
Subsequently the bromoacetylenes were prepared using the already known procedure reported by Bolm (Scheme 3).^[2]



Scheme 3: Synthetic procedure for the bromoacetylenes from corresponding aldehydes (a) or from alkynes (b).

We started the investigation studying the condensation between indole **189a** with silyl bromoalkyne **190a** in the presence of $\text{MnBr}(\text{CO})_5$ as catalyst and HNCy_2 as base. We evaluated the loading the Mn(I) catalyst and the solvent of the reaction. It was demonstrated that using 1,4-dioxane as solvent, the product **191aa** has been isolated in excellent yield when 10 mol% of catalyst has been used and 78% yield when the catalyst has been used in 5 mol% (Table 1).

Table 1: Optimization table for the catalyst loading.^[a]

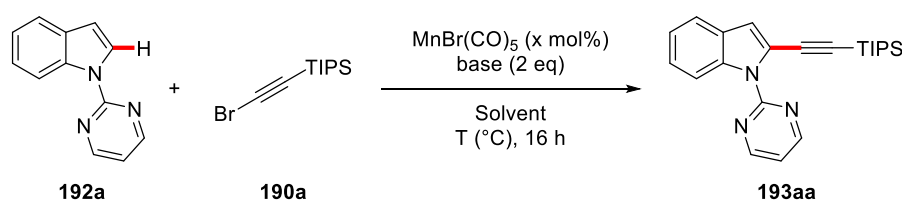


Entry	$\text{MnBr}(\text{CO})_5$ (x mol%)	T (°C)	Solvent	Yield 191aa (%) ^[b]
1	10.0	120	1,4-dioxane	93
2	5.0	100	1,4-dioxane	78
3	5.0	80	DCE	85

[a] Reaction condition: **189a** (0.5 mmol), **190a** (0.75 mmol), $\text{MnBr}(\text{CO})_5$ (x mol%), HNCy_2 (1.0 mmol), T (°C), 16 h. [b] Yield of isolated product. TIPS = triisopropylsilyl.

Subsequently, pyrimidine instead of pyridine was used as directing group and different bases were tested in the transformation. The HNCy_2 led to the formation of the desired products in highest yield. Finally, different solvents and temperatures were investigated and the product was isolated in excellent yield using DCE as solvent at 80 °C (entry 9, Table 2).

Table 2: Screening of bases, solvents, and temperatures.^[a]

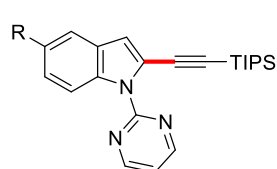
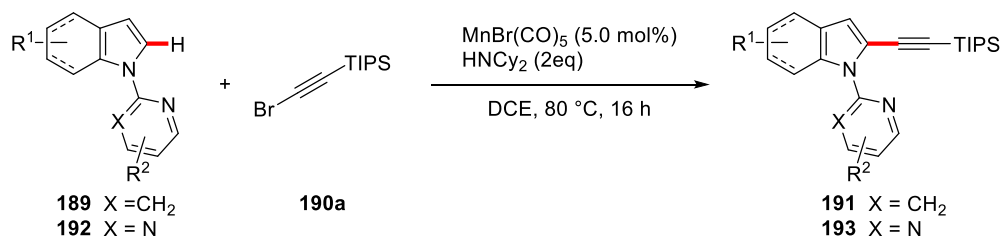


Entry	MnBr(CO) ₅ (x mol%)	Base	Solvent	T (°C)	Yield 193aaa (%) ^[b]
1	10.0	HNCy ₂	1,4-dioxane	120	94
2	5.0	HNCy ₂	1,4-dioxane	120	71
3	5.0	NaOAc	1,4-dioxane	120	41 ^[c]
4	5.0	Na ₂ CO ₃	1,4-dioxane	120	33 ^[c]
5	5.0	HNCy ₂	TFE	120	15 ^[c]
6	5.0	HNCy ₂	DCE	120	96
7	2.5	HNCy ₂	DCE	120	71
8	5.0	HNCy ₂	DCE	100	92
9	5.0	HNCy₂	DCE	80	95 (99)^[d]
10	5.0	HNCy ₂	DCE	60	71 ^[e]
11	5.0	HNCy ₂	DCE	40	23 ^[e]
12	-	HNCy ₂	DCE	80	0
13	5.0	-	DCE	80	<5

[a] Reaction conditions: **192a** (0.5 mmol), **190a** (0.75 mmol), MnBr(CO)₅ (x mol%), HNCy₂ (1.0 mmol), T (°C), 16 h. [b] Yield of isolated product. [c] Determined by GC conversion using *n*-dodecane as the internal standard. [d] **190a** (0.6 mmol). [e] Personal contribution. DCE = 1,2-dichloroethane, TFE = 2,2,2-trifluoroethanol, TIPS = triisopropylsilyl.

With the optimal catalytic conditions in our hands, we proved the scope of the reaction by submitting differently substituted indoles in the reaction with **190a** in the presence of MnBr(CO)₅ (Scheme 4).

The ample scope showed in Scheme 4 highlights the versatility of the methodology. Indoles featuring electron-withdrawing groups as well as electron-donating groups resulted in the corresponding products with comparable levels of yields. Sensitive groups such as bromo, ester and cyano were fully tolerated in the transformations. Moreover, the methodology resulted to be not limited to the use of indoles; indeed, pyrrole derivatives demonstrated to be suitable substrates for the manganese-catalysed C–H alkylation as well.

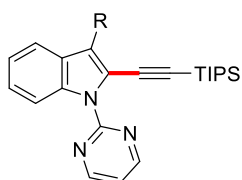


193ba, R = OMe, yield = 78%

193ca, R = F, yield = 88%

193da, R = Br, yield = 91%

193ea, R = NO₂, yield = 63%

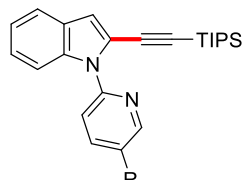


193fa, R = Me, yield = 82%^[a]

193ga, R = CN, yield = 70%

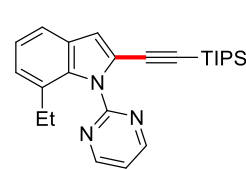
193ha, R = Ac, yield = 34%^[a]

193ia, R = CH₂CO₂Me, yield = 87%^[a]

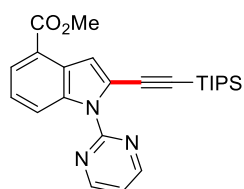


191ba, R = Me, yield = 98%

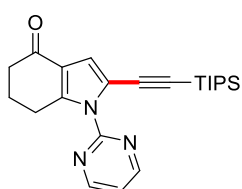
191ca, R = Br, yield = 73%



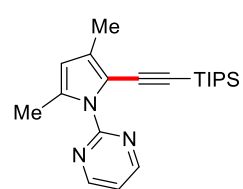
193ja, yield = 79%^[a]



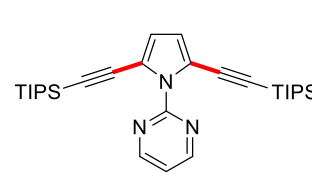
193ka, yield = 85%^[a]



193la, yield = 96%



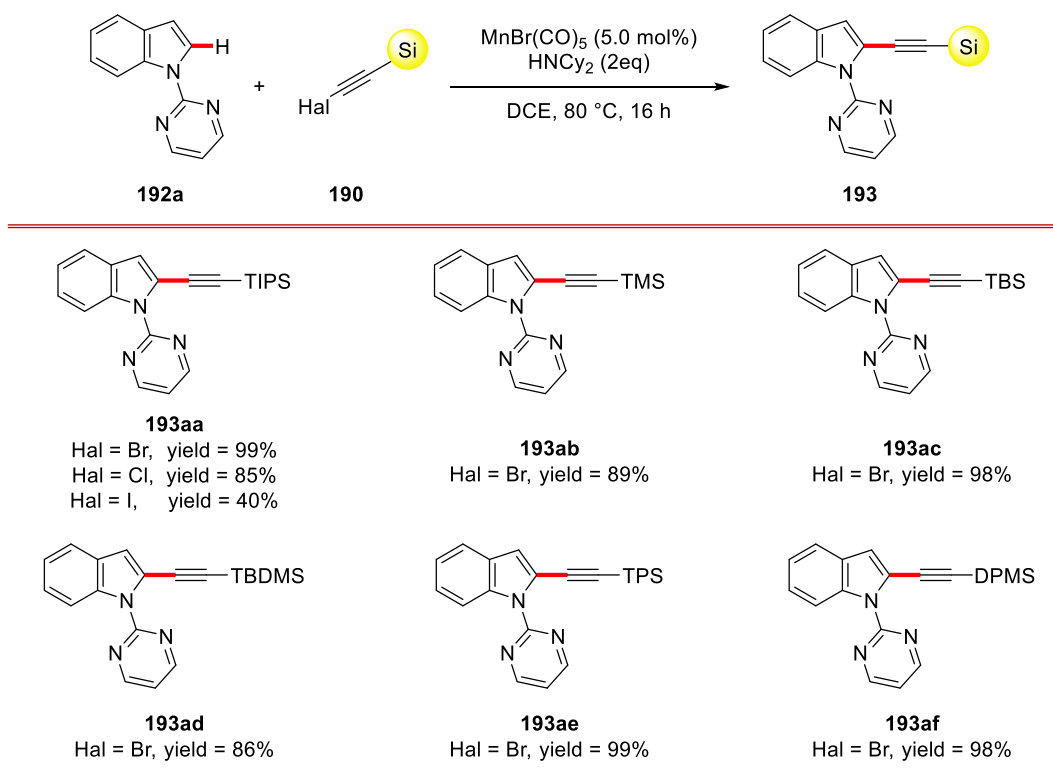
193ma, yield = 92%



193na, yield = 89%^[a]

Scheme 4: Scope of the reaction with different indoles. [a] Personal contribution.

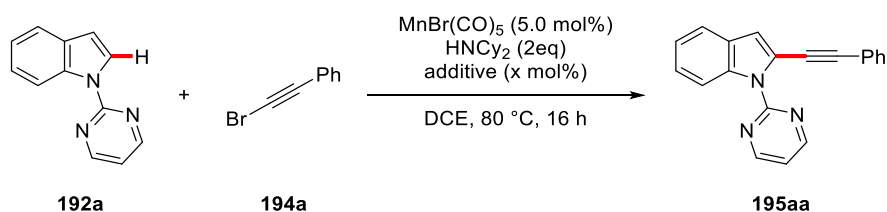
Subsequently, the scope of the reaction was further investigated by submitting different silyl haloacetylenes under optimized catalytic conditions with indole **192a**. Bromoacetylene as well as chloroacetylene reacted smoothly with the 1-(pyrimidin-2-yl)-1*H*-indole allowing the formation of the products in excellent yields. On the contrary, the iodoacetylene resulted in the desired product only in moderate yield. Satisfyingly, all the bromoacetylenes featuring different silyl groups reacted smoothly with the indole and all the corresponding products were isolated in quantitative yields (Scheme 5).



Scheme 5: Manganese-catalysed C–H alkylation with different silyl haloalkynes. TMS = trimethylsilyl, TBS = tri-*n*-butylsilyl, TBDMS = *tert*-butyldimethylsilyl, DPMS = diphenylmethylsilyl.

So far, all methodologies for the metal-catalysed C–H alkylation were limited to the use of activated alkynes featuring silyl groups. To overcome this limitation, we developed a new protocol which allows the use of aryl, alkenyl and alkyl bromoacetylenes. We started the investigation by analysing the results obtained carrying out the manganese-catalysed C–H alkylation of indole **192a** with phenylacetylene bromide in the presence of different additive (Table 3). Only the BPh_3 gave promising results in the formation of the product **195aa**. In particular, with a 5 mol% of loading the desired product was isolated in 61% yield. In order to check that the concomitant presence of the additive and the manganese catalyst was necessary for the success of the reaction, two reaction were carried out with the only presence of manganese catalyst (entry 1, Table 3) and with the only presence of BPh_3 (entry 3, Table 3) and both of them failed in the formation of the product.

Table 3: Screening of the additives.^[a]

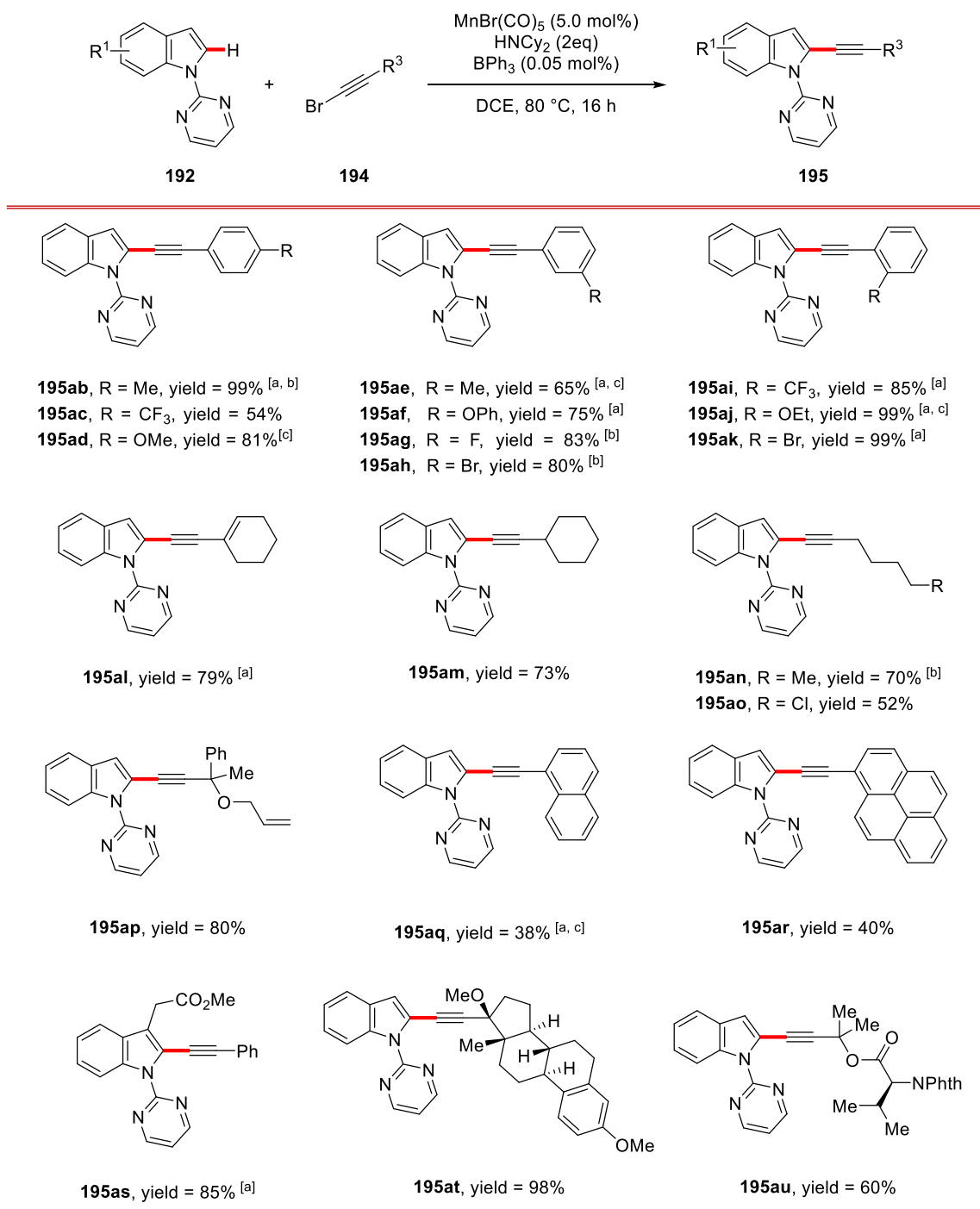


Entry	Additive	x mol% additive	Yield 195aa (%) ^[b]
1	-	-	0 ^[c]
2	BPh ₃	5.0	61 ^[c] (99) ^[c, e]
3	BPh ₃	5.0	0 ^[c, d]
4	CuBr ₂	5.0	0 ^[c]
5	AlCl ₃	5.0	32
6	BBr ₃	5.0	56
7	ZnCl ₂	5.0	Trace
8	ZnBr ₂	5.0	Trace
9	ZnI ₂	5.0	0
10	FeCl	2.5	0
11	MgCl ₂	5.0	0
12	BPh ₃	0.05	92 ^[c] (95) ^[c, e]
13	BPh ₃	0.05	86 ^[c, f]

[a] reaction conditions: **192a** (0.5 mmol), **194a** (0.6 mmol), MnBr(CO)₅ (5 mol%), HNCy₂ (1.0 mmol), DCE (1 mL), 80 °C, 16 h. [b] Yield of isolated product. [c] Personal contribution. [d] Without [Mn]. [e] 1 h. [f] [Mn] (2.5 mol%)

Surprisingly, when the loading of the additive was decreased up to 0.05 mol%, the yield of the product increased up to 92% (entry 12, Table 3) and moreover, after 1 h we were able to isolate the desired product in 95% yield. Since the great catalytic efficacy of the protocol we evaluated the possibility to lower the manganese-catalyst loading and with 2.5 mol% of MnBr(CO)₅ and 0.05 mol% of BPh₃, the product was obtained in 86% yield (entry 13, Table 3).

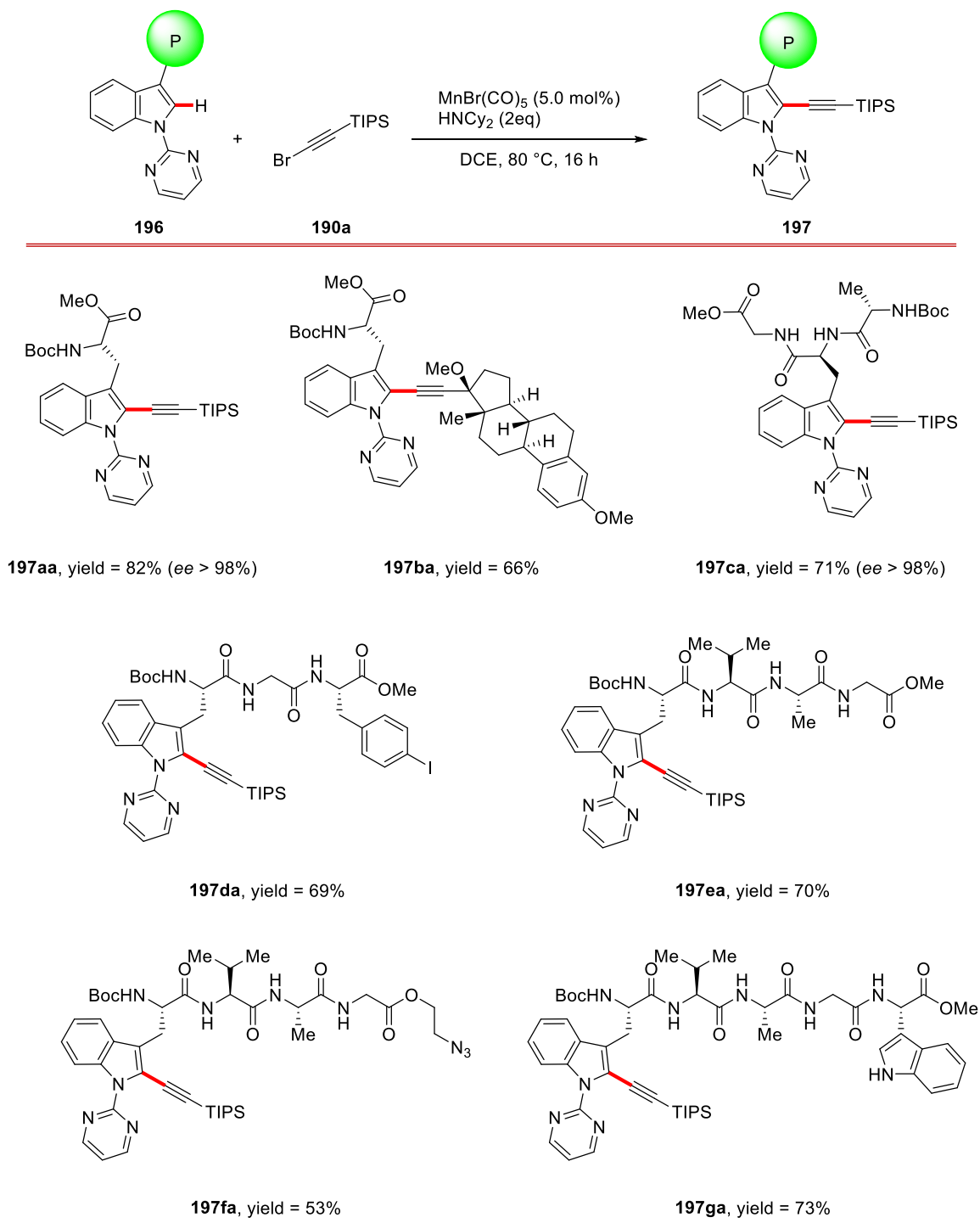
With the optimized reaction conditions in our hands, we proved the flexibility of the new methodology by testing bromoalkynes featuring different aryl, alkyl and alkenyl substituents (Scheme 6). The methodology demonstrated to be tolerant toward different functional groups. The corresponding products were isolated in good to excellent yields. Moreover, the protocol was extended to more complex substrates. Indeed, the bromoalkynes featuring complex steroid motif resulted in the corresponding product **195at** in quantitative yield and aminoacid derivative from the (S)-valine was converted in the product **195au** without loss of enantiomeric excess.



Scheme 6: Manganese-catalysed C–H alkylation with bromo alkynes featuring aryl, alkenyl and alkyl substituents. [a] Personal contribution. [b] 1 h. [c] [Mn] (2.5 mol%).

Since the great result obtained with the aminoacid derivative in this transformation, we wanted to test if the methodology could be used with more complex peptides as well, in order to develop an efficient route for their diversification. We started to prepare different peptides through peptidic coupling reaction of several enantiopure aminoacids including the tryptophan, where the nitrogen of the indole moiety was protected with a pyrimidyl group. Satisfactory results were achieved when

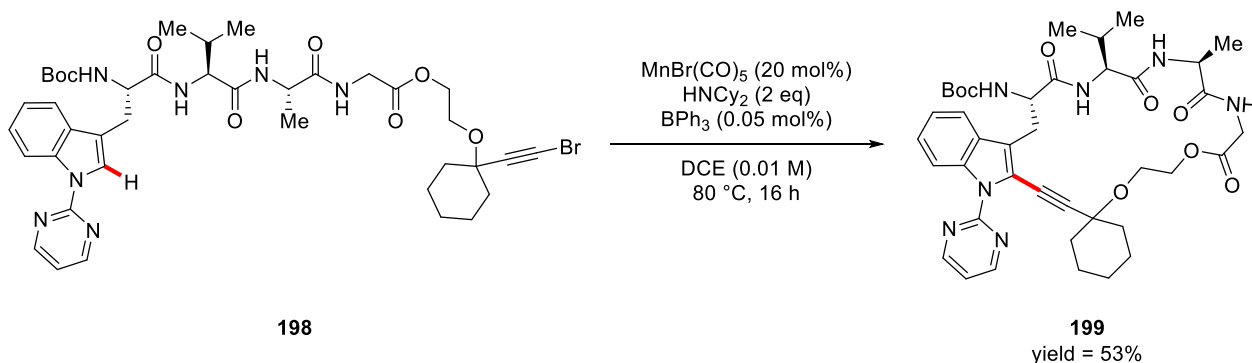
these peptides were submitted under optimized reaction conditions with the silyl bromoacetylene **190a** (Scheme 7).



Scheme 7: Mn-catalysed C–H alkylation with peptide derivatives.

All the corresponding peptides were isolated in good to excellent yields. The presence of powerful functional groups such as the iodo- and the azido- groups could be exploited for further modification of the alkynylated peptides. It was possible to synthesize cyclic peptides through Sonogashira-coupling and click chemistry respectively, after silyl deprotection of the opportune alkynes.

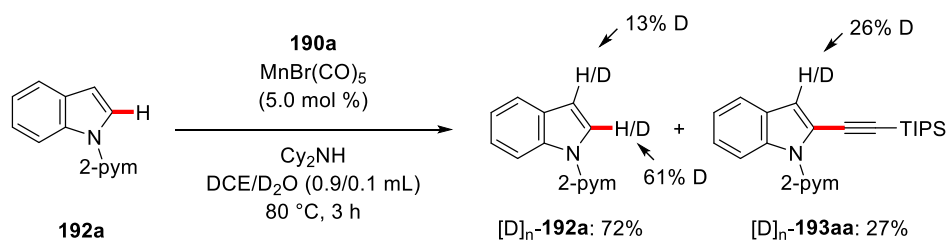
Furthermore, we investigated the possibility to use the manganese-catalysed C–H alkylation to directly prepare cyclic peptide through intramolecular reaction. In particular, we prepared the acyclic peptide **198** featuring a bromoalkynyl moiety which was submitted under optimized catalytic conditions (Scheme 8). Gratefully, the corresponding 21-membered-macrocycle was isolated in 53% yield.



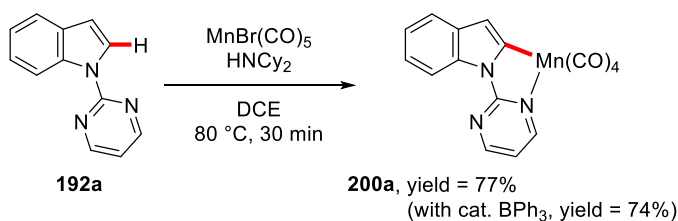
Scheme 8: Synthesis of cyclic peptide through intramolecular Mn-catalysed C–H alkylation of indole.

In order to shed light on the mode of action of the manganese-catalysed C–H alkylation, mechanistic experiments were performed (Scheme 9). In particular, through experiments with a mixture of DCE and D_2O in ratio 9:1 as solvent, it was revealed an major H/D scrambling at C2-position with respect the C3-position which is even observed also in the absence of the metal-catalyst due to its nucleophilic nature (Scheme 9a). Moreover, we were also able to demonstrate that the organometallic complex is a key intermediate in the catalytic cycle. To do this, we prepared the intermediate **200a** (Scheme 9b) and subsequently it has been used as substrate in a stoichiometric reaction with TIPS-bromoalkyne **190a** and with bromophenylacetylene **194a** (Scheme 9c). Moreover, intermediate **200a** was used as catalyst (5.0 mol%) in a catalytic reaction with indole **192a** and TIPS-bromoalkyne **190a** (Scheme 9d). In both of the cases it was possible to isolate the desired product in good yields.

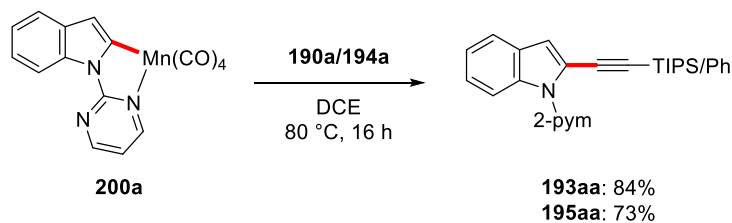
(a) facile H/D exchange



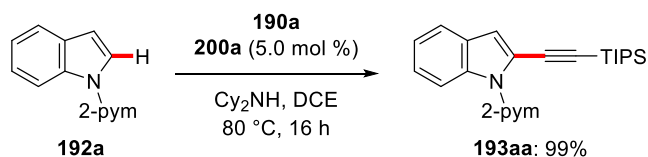
(b) Synthesis of complex **200a**



(c) stoichiometric alkylation with complex **200a**



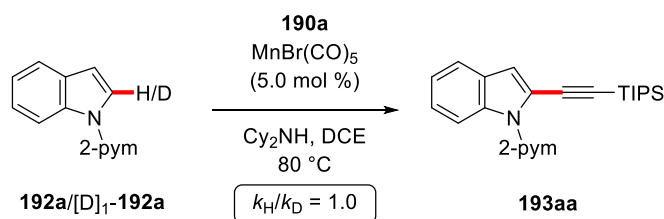
(d) complex **200a** as catalyst



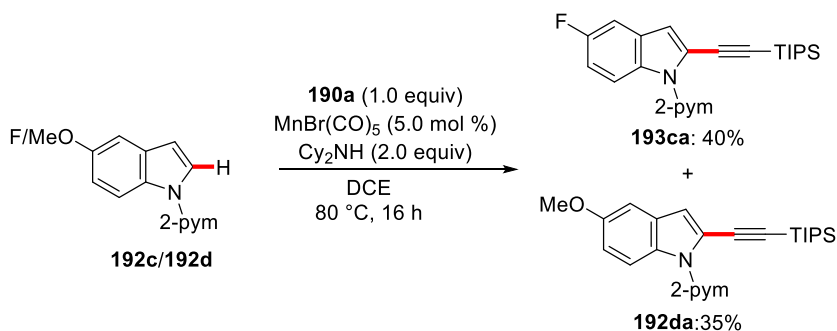
Scheme 9: Mechanistic experiments.

Studies with isotopically labeled substrate **192a** revealed a minor kinetic isotope effect (KIE) which is indicative of a fast C–H manganeseation process (Scheme 10a) and intermolecular competition experiments between indole featuring electron-donating group and electron-withdrawing group demonstrated a slight preference toward the latter one (Scheme 10b).

(a) KIE experiments

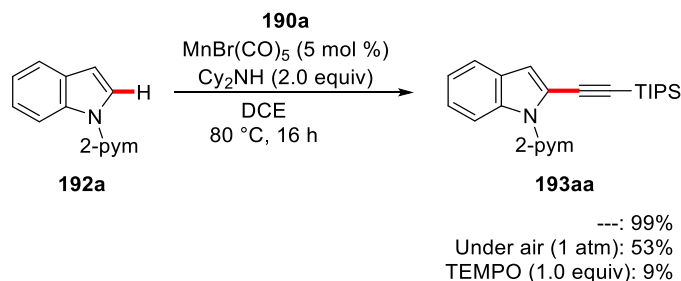


(b) Intermolecular competition experiment



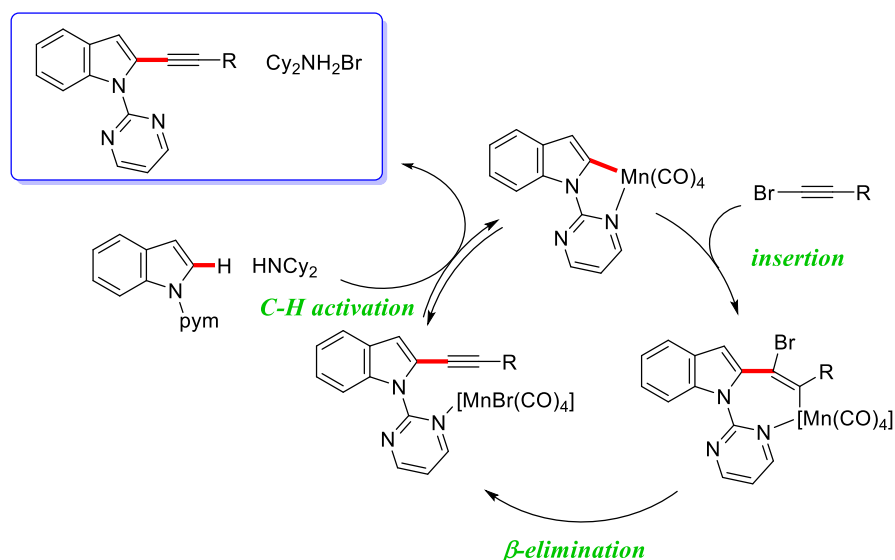
Scheme 10: KIE experiments and intermolecular competition experiments.

In stark contrast with the previously reported manganese-catalysed C–H activation^[3–7], the catalytic efficacy dropped down when the reaction was performed under air or in the presence of the radical scavenger TEMPO (Scheme 11).



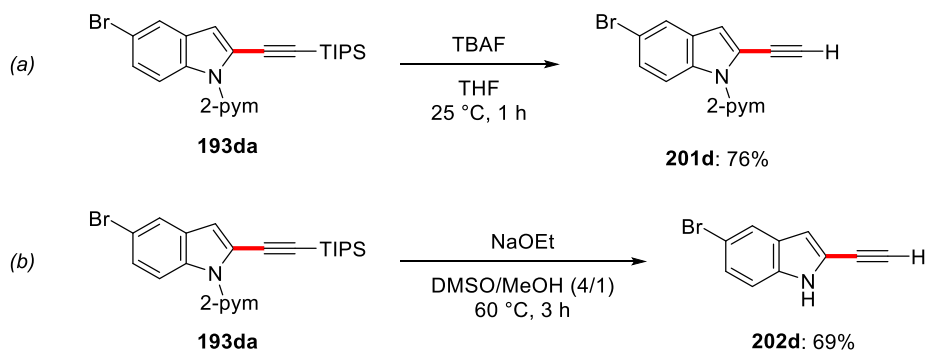
Scheme 11: Experiments performed under air or in the presence of TEMPO.

On the bases of the experimental collected data, a plausible catalytic cycle is shown in Scheme 12 starting with a fast and facile C–H metallation and formation of metallated intermediate **200a**. Subsequently, the seven-membered manganacycle was formed by migratory insertion of the bromoalkyne derivatives in the compound **200a**. Finally, β -Br elimination delivered the desired alkynylated indole (Scheme 12). We proposed that in the presence of haloalkynes featuring aryl, alkenyl and alkyl substituents, the rate of the β -Br elimination step, is increased by the BPh_3 additive. However, an oxidative addition followed by reductive elimination mechanism cannot be ruled out.



Scheme 12: Proposed reaction mechanism.

Last, but not least, it was also demonstrated the easiness in the removal of the protecting groups. In particular, the chemoselective removal of the silyl-group (Scheme 13a) or the concomitant removal of both silyl-group and directing group (Scheme 13b) were achieved in good yields.



Scheme 13: Removal of silyl group or concomitant removal of silyl group and directing group.

In conclusion the first manganese-catalysed C–H activation of indole derivatives to develop a new C–H alkylation protocol was reported. The methodology resulted to be tolerant toward differently substituted indoles and silyl haloalkynes. Moreover the transformation revealed to be not limited to the use of haloalkynes featuring silyl groups but can be extended to the less employed aryl, alkenyl and alkyl moiety adding to the mixture sub-catalytic amount of BPh_3 . The protocol demonstrated to be also suitable for functionalization of more complex substrates such as alkyne featuring steroids or acyclic peptides. The corresponding alkynylated peptides were isolated without loss of chiral purity. Finally, it was also illustrated the possibility to perform an intramolecular manganese-catalysed C–H alkylation to synthesize macrocycle.

Bibliography

- [1] L. Ackermann, A. V. Lygin, *Org. Lett.* **2011**, *13*, 3332–3335.
- [2] X. Y. Chen, L. Wang, M. Frings, C. Bolm, *Org. Lett.* **2014**, *16*, 3796–3799.
- [3] W. Liu, D. Zell, M. John, L. Ackermann, *Angew. Chem. Int. Ed.* **2015**, *54*, 4092–4096.
- [4] W. Liu, J. Bang, Y. Zhang, L. Ackermann, *Angew. Chem. Int. Ed.* **2015**, *54*, 14137–14140.
- [5] Y.-F. Liang, L. Massignan, W. Liu, L. Ackermann, *Chem. Eur. J.* **2016**, *22*, 14856–14859.
- [6] W. Liu, S. C. Richter, R. Mei, M. Feldt, L. Ackermann, *Chem. Eur. J.* **2016**, *22*, 17958–17961.
- [7] W. Liu, S. C. Richter, Y. Zhang, L. Ackermann, *Angew. Chem. Int. Ed.* **2016**, *55*, 7747–7750.

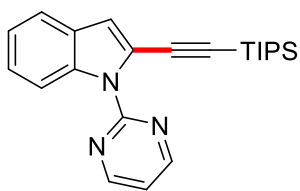
7.1.1 Experimental Section

Catalytic reactions were performed under N₂ atmosphere using pre-dried glassware and standard Schlenk techniques. 1,4-Dioxane and toluene were dried with sodium and freshly distilled under N₂, DCE and TFE were dried with CaH₂ and freshly distilled under N₂. The substrates **189a-c** **192a-1n**,^[1,2] [D]₁-**192a**,^[2] **190**,^[3, 4] **194**,^[3, 5] **196**^[2, 6] and **198**^[2, 6] were synthesized according to previously described methods. Other chemicals were obtained from commercial sources and were used without further purification. Yields refer to isolated compounds, estimated to be >95% pure as determined by ¹H-NMR and GC. TLC: Macherey-Nagel, TLC plates Alugram®Sil G/UV254. Detection under UV light at 254 nm. Chromatography: Separations were carried out on Merck Silica 60 (0.040–0.063 mm, 70–230 mesh ASTM). All IR spectra were recorded on a BRUKER ALPHA-P spectrometer. MS: EI-MS: Finnigan MAT 95, 70eV; ESI-MS: Finnigan LCQ. High resolution mass spectrometry (HRMS): APEX IV 7T FTICR, Bruker Daltonic. M. p. Stuart® Melting Point Apparatus SMP3 melting point apparatus, values are uncorrected. ¹H, ¹³C, ¹⁹F NMR-spectra were recorded at 300 (¹H), 400 (¹H), 500 (¹H), 600 (¹H), 75, 100, 125 {¹³C, APT (Attached Proton Test)} and 283 MHz (¹⁹F), respectively, on Varian Unity-300 (600) and AMX 300 instruments in CDCl₃ solutions. If not otherwise specified, chemical shifts (δ) are given in ppm.

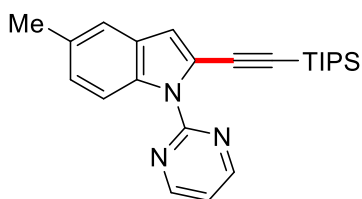
General Procedure for the manganese-catalysed C-H alkynylation

General Procedure A: To a solution of substrates **192** (0.5 mmol), MnBr(CO)₅ (6.9 mg, 5.0 mol %) and Cy₂NH (181 mg, 1.0 mmol) in DCE (1.0 mL), silyl bromoalkynes **190** (0.6 mmol) was added. The mixture was stirred at 80 °C for 16 h. After completion of the reaction, CH₂Cl₂ (3.0 mL) was added at ambient temperature and the volatiles were removed in *vacuo*. Purification by chromatography on silica gel afforded the desired product **193**.

General Procedure B: To a solution of substrates **192** (0.5 mmol), MnBr(CO)₅ (6.9 mg, 5.0 mol %), Cy₂NH (181 mg, 1.0 mmol) and BPh₃ (25 μL, 0.05 mol %, 0.01 M stock solution in DCE) in DCE (1 mL), aryl or alkyl bromoalkynes **194** (0.6 mmol) was added. The mixture was stirred at 80 °C for 16 h. After completion of the reaction, CH₂Cl₂ (3 mL) was added at ambient temperature and the volatiles were removed in *vacuo*. Purification by chromatography on silica gel afforded the desired product **195**.

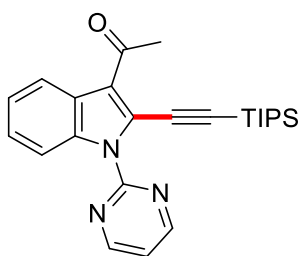


(193aa): The general procedure **A** was followed using substrate **192a** (98 mg, 0.5 mmol) and **190a** (157 mg, 0.6 mmol). Isolation by column chromatography (*n*-hexane/EtOAc: 9/1) yielded **193aa** (186 mg, 99%) as a colorless liquid. ¹H NMR (400 MHz, CDCl₃) δ = 8.75 (d, *J* = 4.8 Hz, 2H), 8.30 (dd, *J* = 8.5, 0.9 Hz, 1H), 7.58 (dd, *J* = 8.0, 1.0 Hz, 1H), 7.34 (ddd, *J* = 8.5, 7.1, 1.3 Hz, 1H), 7.23 (ddd, *J* = 8.0, 7.1, 1.0 Hz, 1H), 7.12 (t, *J* = 4.8 Hz, 1H), 7.10 (s, 1H), 1.15–1.14 (m, 21H). ¹³C NMR (100 MHz, CDCl₃) δ = 157.9 (CH), 157.2 (C_q), 136.1 (C_q), 128.4 (C_q), 124.7 (CH), 122.3 (CH), 120.8 (C_q), 120.6 (CH), 117.5 (CH), 115.6 (CH), 114.0 (CH), 98.7 (C_q), 97.7 (C_q), 18.6 (CH₃), 11.3 (CH). IR (neat): 2957, 2151, 1561, 1421, 1248, 839, 746 cm⁻¹. MS (EI) *m/z* (relative intensity) 375 (30) [M⁺], 332 (100). HR-MS (ESI) *m/z* calcd for C₂₃H₃₀N₃Si [M+H⁺] 375.2131, found 375.2125. The analytical data are in accordance with those previously published in the literature.^[1]

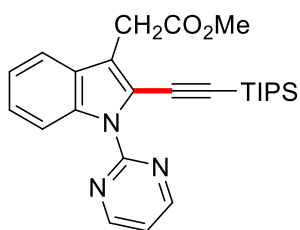


(193fa): The general procedure **A** was followed using substrate **1f** (105 mg, 0.5 mmol) and **190a** (157 mg, 0.6 mmol). Isolation by column chromatography (*n*-pentane/EtOAc: 9/1) yielded **193fa** (160 mg, 82%) as a yellow liquid. ¹H NMR (500 MHz, CDCl₃) δ = 8.74 (d, *J* = 4.8 Hz, 2H), 8.32 (d, *J* = 8.4 Hz, 1H), 7.53 (d, *J* = 7.8 Hz, 1H), 7.31 (ddd, *J* = 8.4, 7.1, 1.0 Hz, 1H), 7.21 (ddd, *J* = 8.0, 7.1, 1.0 Hz, 1H), 7.11 (t, *J* = 4.8 Hz, 1H), 2.45 (s, 3H), 1.13 (m, 21H). ¹³C NMR (125 MHz, CDCl₃) δ = 157.9 (CH), 157.4 (C_q), 135.8 (C_q), 129.4 (C_q), 125.1 (C_q), 125.0 (CH), 121.9 (CH), 119.0 (CH), 118.7 (C_q), 117.0 (CH), 114.2 (CH), 100.7 (C_q), 98.3 (C_q), 18.7 (CH₃), 11.4 (CH), 9.9 (CH₃). IR (neat): 2940, 2862, 2142, 1561, 1426, 728 cm⁻¹. MS (EI) *m/z* (relative intensity) 389 (56) [M⁺], 346 (100), 330 (49). HR-MS (ESI) *m/z* calcd for C₂₄H₃₂N₃Si [M+H⁺] 390.2365, found 390.2360.

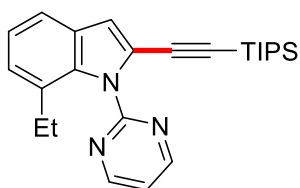
The analytical data are in accordance with those previously published in the literature.^[1]



(193ha): The general procedure **A** was followed using substrate **192h** (119 mg, 0.5 mmol) and **190a** (157 mg, 0.6 mmol). Isolation by column chromatography (*n*-Pentane/EtOAc : 9/1) yielded **193ha** (70 mg, 34%) as yellow oil. ¹H NMR (300MHz, CDCl₃) δ = 8.88 (d, *J* = 4.8 Hz, 2H), 8.47 (dt, *J* = 6.3, 2.5 Hz, 1H), 7.83–7.78 (m, 1H), 7.37–7.29 (m, 3H), 2.86 (s, 3H), 1.06 (s, 18H), 1.04 (s, 3H). ¹³C NMR (126 MHz, CDCl₃) δ = 194.8 (C_q), 158.5 (CH), 156.7 (C_q), 136.0 (C_q), 126.2 (C_q), 125.7 (CH), 124.7 (C_q), 124.1 (CH), 124.0 (C_q), 123.2 (CH), 119.2 (CH), 112.0 (CH), 107.3 (C_q), 97.6 (C_q), 30.8 (CH₃), 18.6 (CH₃), 11.3 (CH). IR (neat): 2942, 2864, 2149, 1651, 1563, 1419, 1384, 1193, 721 cm⁻¹; MS (EI) *m/z* (relative intensity) 417 (29) [M⁺], 402 (9), 375 (100), 332 (77), 290 (76). HR-MS (EI) *m/z* calcd for C₂₅H₃₁N₃OSi [M⁺] 417.2236, found 417.2231.



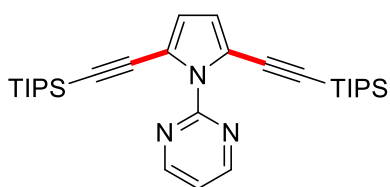
(193ia): The general procedure **A** was followed using substrate **192i** (134 mg, 0.5 mmol) and **190a** (157 mg, 0.6 mmol). Isolation by column chromatography (*n*-pentane/EtOAc: 9/1) yielded **193ia** (195 mg, 87%) as a yellow solid. M.p. = 68–70 °C. ¹H NMR (500 MHz, CDCl₃) δ = 8.75 (d, *J* = 4.8 Hz, 2H), 8.34 (d, *J* = 8.5 Hz, 1H), 7.58 (d, *J* = 7.7 Hz, 1H), 7.33 (ddd, *J* = 8.4, 7.2, 1.1 Hz, 1H), 7.25–7.22 (m, 1H), 7.14 (t, *J* = 4.8 Hz, 1H), 3.96 (s, 2H), 3.65 (s, 3H), 1.13–1.12 (m, 21H). ¹³C NMR (125 MHz, CDCl₃) δ = 171.1 (C_q), 158.0 (CH), 157.3 (C_q), 135.7 (C_q), 128.4 (C_q), 125.2 (CH), 122.4 (CH), 121.0 (C_q), 120.2 (C_q), 119.3 (CH), 117.4 (CH), 114.4 (CH), 101.7 (C_q), 97.4 (C_q), 52.0 (CH₃), 31.3 (CH₂), 18.6 (CH₃), 11.3 (CH). IR (neat): 2942, 2863, 2142, 1737, 1566, 1426, 655 cm⁻¹. MS (ESI) *m/z* (relative intensity) 470 [M+Na⁺] (100), 448 [M+H⁺] (60). HR-MS (ESI) *m/z* calcd for C₂₆H₃₄N₃O₂Si [M+H⁺] 448.2420, found 448.2415.



(193ja): The general procedure **A** was followed using substrate **192j** (112 mg, 0.5 mmol) and **190a** (157 mg, 0.6 mmol). Isolation by column chromatography (*n*-pentane/EtOAc: 9/1) yielded **193ja** (160 mg, 79%) as a yellow solid. M.p. = 74–76 °C. ¹H NMR (500 MHz, CDCl₃) δ = 8.85 (d, *J* = 4.7 Hz, 2H), 7.44 (d, *J* = 7.6 Hz, 1H), 7.34 (t, *J* = 4.8 Hz, 1H), 7.13–7.06 (m, 2H), 6.97 (s, 1H),

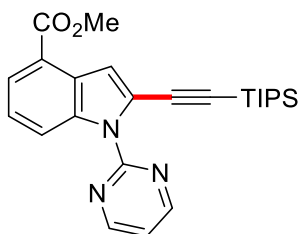
2.29 (q, $J = 7.4$ Hz, 2H), 0.99–0.98 (m, 21H), 0.93 (t, $J = 7.4$ Hz, 3H). ^{13}C NMR (125 MHz, CDCl_3) $\delta = 158.9$ (C_q), 158.3 (CH), 135.4 (C_q), 128.7 (C_q), 128.1 (C_q), 124.6 (CH), 122.8 (C_q), 121.9 (CH), 119.7 (CH), 119.0 (CH), 112.4 (CH), 97.8 (C_q), 97.4 (C_q), 25.4 (CH_2), 18.5 (CH_3), 13.9 (CH_3), 11.2 (CH). IR (neat): 2940, 2864, 2146, 1560, 1420, 734, 669 cm^{-1} . MS (EI) m/z (relative intensity) 403 (51) [M^+], 360 (100), 332 (18), 318 (29). HR-MS (ESI) m/z calcd for $\text{C}_{25}\text{H}_{34}\text{N}_3\text{Si}$ [$\text{M}+\text{H}^+$] 404.2522, found 404.2517.

The analytical data are in accordance with those previously published in the literature.^[1]



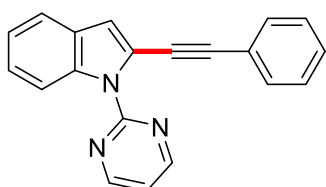
(193na): The general procedure **A** was followed using substrate **1n** (73 mg, 0.5 mmol) and **190a** (261 mg, 1.0 mmol). Isolation by column chromatography (*n*-pentane/EtOAc: 9/1) yielded **193na** (225 mg, 89%) as a yellow solid. M.p. = 72–74 °C. ^1H NMR (400 MHz, CDCl_3) $\delta = 8.76$ (d, $J = 4.8$ Hz, 2H), 7.26 (t, $J = 4.8$ Hz, 1H), 6.51 (s, 2H), 0.99 (m, 42H). ^{13}C NMR (100 MHz, CDCl_3) $\delta = 158.3$ (CH), 156.5 (C_q), 119.4 (CH), 117.6 (CH), 117.3 (C_q), 97.7 (C_q), 95.2 (C_q), 18.5 (CH_3), 11.2 (CH). IR (neat): 2941, 2863, 2146, 1563, 1422, 1014, 767, 653 cm^{-1} . MS (ESI) m/z (relative intensity) 528 [$\text{M}+\text{Na}^+$] (100), 506 [$\text{M}+\text{H}^+$] (92). HR-MS (ESI) m/z calcd for $\text{C}_{30}\text{H}_{48}\text{N}_3\text{Si}_2$ [$\text{M}+\text{H}^+$] 506.3387, found 506.3381.

The analytical data are in accordance with those previously published in the literature.^[1]

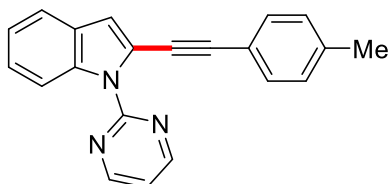


(193ka): The general procedure **A** was followed using substrate **192k** (127 mg, 0.5 mmol) and **190a** (157 mg, 0.6 mmol). Isolation by column chromatography (*n*-pentane/EtOAc: 9/1) yielded **193ka** (185 mg, 85%) as a white solid. M.p. = 140–142 °C. ^1H NMR (500 MHz, CDCl_3) $\delta = 8.79$ (d, $J = 4.8$ Hz, 2H), 8.45 (d, $J = 8.4$ Hz, 1H), 7.96 (dd, $J = 7.5, 1.0$ Hz, 1H), 7.70 (s, 1H), 7.34 (dd, $J = 8.1, 8.1$ Hz, 1H), 7.21 (t, $J = 4.8$ Hz, 1H), 3.99 (s, 3H), 1.11 (m, 21H). ^{13}C NMR (125 MHz, CDCl_3) $\delta = 167.4$ (C_q), 158.2 (CH), 157.1 (C_q), 136.7 (C_q), 128.3 (C_q), 125.5 (CH), 123.9 (CH), 122.9 (C_q), 121.5 (C_q), 118.6 (CH), 118.0 (CH), 116.1 (CH), 99.3 (C_q), 98.3 (C_q), 51.9 (CH_3), 18.6 (CH_3), 11.3 (CH). IR (neat): 2943, 2865, 2143, 1705, 1567, 1414, 732

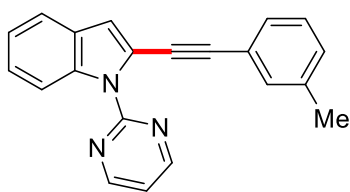
cm⁻¹. MS (ESI) *m/z* (relative intensity) 456 [M+K⁺] (100), 434 [M+H⁺] (73). HR-MS (ESI) *m/z* calcd for C₂₅H₃₂N₃O₂Si [M+H⁺] 434.2264, found 434.2258.



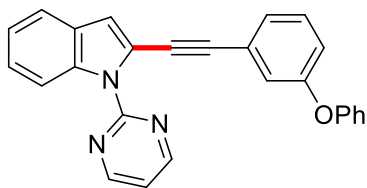
(195aa): The general procedure **B** was followed using substrate **192a** (98 mg, 0.5 mmol) and **194a** (108 mg, 0.6 mmol) for 1 h. Isolation by column chromatography (*n*-pentane/EtOAc: 5/1) yielded **195aa** (141 mg, 95%) as a colorless oil. ¹H NMR (500 MHz, CDCl₃) δ = 8.85 (d, *J* = 4.9 Hz, 2H), 8.31 (d, *J* = 8.4 Hz, 1H), 7.60 (d, *J* = 7.6 Hz, 1H), 7.52–7.48 (m, 2H), 7.35–7.31 (m, 4H), 7.25–7.21 (m, 1H), 7.21 (t, *J* = 4.9 Hz, 1H), 7.08 (s, 1H). ¹³C NMR (125 MHz, CDCl₃) δ = 158.1 (CH), 157.4 (C_q), 136.4 (C_q), 131.3 (CH), 128.8 (C_q), 128.4 (CH), 128.3 (CH), 124.8 (CH), 123.3 (C_q), 122.4 (CH), 120.9 (C_q), 120.8 (CH), 117.7 (CH), 114.6 (CH), 114.1 (CH), 95.0 (C_q), 82.5 (C_q). IR (neat): 3048, 2963, 2851, 1560, 1418, 1081, 741, 686, 521 cm⁻¹. MS (ESI) *m/z* (relative intensity) 296 (5) [M⁺], 214 (11), 196 (100), 173 (20), 149 (15). HR-MS (ESI) *m/z* calcd for C₂₀H₁₄N₃ [M+H⁺] 296.1182, found 296.1188.



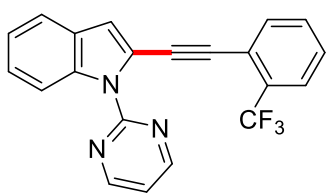
(195ab): The general procedure **B** was followed using substrate **192a** (98 mg, 0.5 mmol) and **194b** (117 mg, 0.6 mmol) for 1 h. Isolation by column chromatography (*n*-pentane/EtOAc: 9/1) yielded **195ab** (153 mg, 99%) as a colorless solid. M.p. = 100–102 °C. ¹H NMR (500 MHz, CDCl₃) δ = 8.84 (d, *J* = 4.8 Hz, 2H), 8.30 (d, *J* = 8.4 Hz, 1H), 7.59 (d, *J* = 7.8 Hz, 1H), 7.39 (d, *J* = 8.0 Hz, 2H), 7.32 (ddd, *J* = 8.3, 6.9, 1.0 Hz, 1H), 7.24–7.21 (m, 1H), 7.19 (t, *J* = 4.8 Hz, 1H), 7.14 (d, *J* = 7.9 Hz, 2H), 7.06 (s, 1H), 2.35 (s, 3H). ¹³C NMR (125 MHz, CDCl₃) δ = 158.1 (CH), 157.4 (C_q), 138.5 (C_q), 136.3 (C_q), 131.2 (CH), 129.1 (CH), 128.8 (C_q), 124.6 (CH), 122.4 (CH), 121.0 (C_q), 120.7 (CH), 120.2 (C_q), 117.7 (CH), 114.3 (CH), 114.0 (CH), 95.1 (C_q), 81.8 (C_q), 21.5 (CH₃). IR (neat): 3046, 2920, 2851, 1557, 1422, 800, 739, 526 cm⁻¹. MS (EI) *m/z* (relative intensity) 309 (100) [M⁺], 294 (15). HR-MS (ESI) *m/z* calcd for C₂₁H₁₆N₃ [M+H⁺] 310.1344, found 310.1339.



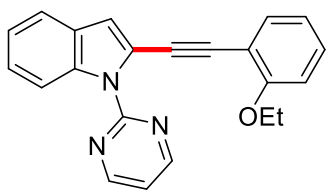
(195ae): The general procedure **B** was followed using substrate **192a** (98 mg, 0.5 mmol), **194e** (117 mg, 0.6 mmol) and $\text{MnBr}(\text{CO})_5$ (3.4 mg, 2.5 mol %). Isolation by column chromatography (*n*-pentane/EtOAc: 8/2) yielded **195ae** (100 mg, 65%) as a colorless solid. M.p. = 111–113 °C. ^1H NMR (300 MHz, CDCl_3) δ = 8.84 (d, J = 4.8 Hz, 2H), 8.31 (dd, J = 8.4, 0.9 Hz, 1H), 7.60 (d, J = 7.7 Hz, 1H), 7.36–7.28 (m, 3H), 7.25–7.18 (m, 3H), 7.13 (d, J = 7.7 Hz, 1H), 7.07 (s, 1H), 2.34 (s, 3H). ^{13}C NMR (125 MHz, CDCl_3) δ = 158.0 (CH), 157.3 (C_q), 137.9 (C_q), 136.3 (C_q), 131.8 (CH), 129.2 (CH), 128.7 (C_q), 128.3 (CH), 128.1 (CH), 124.6 (CH), 123.0 (C_q), 122.3 (CH), 120.9 (C_q), 120.7 (CH), 117.6 (CH), 114.5 (CH), 114.0 (CH), 95.1 (C_q), 82.1 (C_q), 21.3 (CH_3). IR (neat): 3038, 2916, 2204, 1558, 1451, 1416, 810, 791, 746 cm^{-1} . MS (EI) m/z (relative intensity) 309 (85), 308 (100), 294 (14). HR-MS (EI) m/z calcd for $\text{C}_{21}\text{H}_{15}\text{N}_3$ [M^+] 309.1266, found 309.1264.



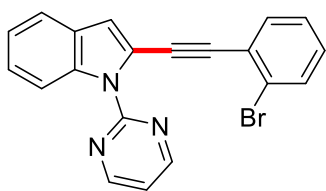
(195af): The general procedure **B** was followed using substrate **192a** (98 mg, 0.5 mmol) and **194f** (164 mg, 0.6 mmol). Isolation by column chromatography (*n*-pentane/EtOAc: 8/2) yielded **195af** (146 mg, 75%) as a colorless oil. ^1H NMR (400 MHz, CDCl_3) δ = 8.75 (d, J = 5.7 Hz, 2H), 8.31 (d, J = 8.4 Hz, 1H), 7.59 (d, J = 7.9 Hz, 1H), 7.38–7.27 (m, 4H), 7.23–7.21 (m, 2H), 7.16–7.13 (m, 2H), 7.09–7.03 (m, 4H), 6.99 (ddd, J = 8.2, 2.5, 1.1 Hz, 1H). ^{13}C NMR (100 MHz, CDCl_3) δ = 158.1 (CH), 157.3 (C_q), 157.2 (C_q), 156.6 (C_q), 136.4 (C_q), 129.9 (CH), 129.7 (CH), 128.7 (C_q), 126.0 (CH), 124.9 (CH), 124.7 (C_q), 123.7 (CH), 122.5 (CH), 120.9 (CH), 120.8 (CH), 120.5 (C_q), 119.4 (CH), 119.0 (CH), 117.7 (CH), 114.8 (CH), 114.2 (CH), 94.4 (C_q), 83.1 (C_q). IR (neat): 3039, 2205, 1734, 1562, 1421, 1238, 1212, 748 cm^{-1} . MS (ESI) m/z (relative intensity) 410 [$\text{M}+\text{Na}^+$] (78), 388 [$\text{M}+\text{H}^+$] (100). HR-MS (ESI) m/z calcd for $\text{C}_{26}\text{H}_{18}\text{N}_3\text{O}$ [$\text{M}+\text{H}^+$] 388.1450, found 388.1444.



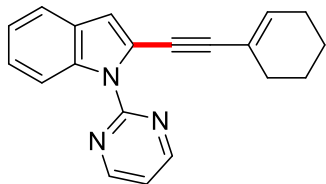
(195ai): The general procedure **B** was followed using substrate **192a** (98 mg, 0.5 mmol) and **194i** (149 mg, 0.6 mmol). Isolation by column chromatography (*n*-pentane/EtOAc: 9/1) yielded **195ai** (155 mg, 85%) as a colorless oil. ^1H NMR (300 MHz, CDCl_3) δ = 8.83 (d, J = 4.8 Hz, 2H), 8.36 (dd, J = 8.4, 0.6 Hz, 1H), 7.68–7.60 (m, 3H), 7.50 (dd, J = 7.4, 7.4 Hz, 1H), 7.40–7.33 (m, 2H), 7.26–7.17 (m, 3H). ^{13}C NMR (75 MHz, CDCl_3) δ = 158.2 (CH), 157.2 (C_q), 136.5 (C_q), 133.8 (CH), 131.3 (CH), 130.7 (q, $^2J_{\text{CF}}$ = 30.5 Hz, C_q), 128.7 (C_q), 127.8 (CH), 125.8 (q, $^3J_{\text{CF}}$ = 5.1 Hz, CH), 125.1 (CH), 123.5 (q, $^1J_{\text{CF}}$ = 273.4 Hz, C_q), 122.5 (CH), 121.6 (q, $^3J_{\text{CF}}$ = 2.1 Hz, C_q), 120.9 (CH), 120.2 (C_q), 117.6 (CH), 116.1 (CH), 114.3 (CH), 91.0 (C_q), 88.1 (C_q). ^{19}F NMR (282 MHz, CDCl_3) δ = -62.16. IR (neat): 3050, 2205, 1562, 1422, 1314, 1125, 744 cm^{-1} . MS (EI) m/z (relative intensity) 363 (100) [M^+], 294 (28). HR-MS (ESI) m/z calcd for $\text{C}_{21}\text{H}_{14}\text{F}_3\text{N}_3$ [$\text{M}+\text{H}^+$] 364.1062, found 364.1056.



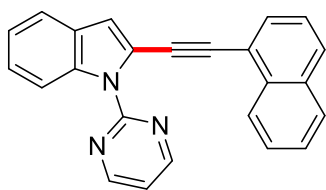
(195aj): The general procedure **B** was followed using substrate **192a** (98 mg, 0.5 mmol), **194j** (135 mg, 0.6 mmol) and $\text{MnBr}(\text{CO})_5$ (3.4 mg, 2.5 mol %). Isolation by column chromatography (*n*-pentane/EtOAc: 8/2) yielded **195aj** (168 mg, 99%) as a colorless oil. ^1H NMR (400 MHz, CDCl_3) δ = 8.84 (d, J = 4.8 Hz, 2H), 8.29 (dd, J = 8.4, 0.9 Hz, 1H), 7.59 (d, J = 7.8 Hz, 1H), 7.45 (dd, J = 7.6, 1.7 Hz, 1H), 7.31 (ddd, J = 8.4, 7.1, 1.3 Hz, 1H), 7.27–7.20 (m, 2H), 7.18 (dd, J = 4.8, 4.8 Hz, 1H), 7.10 (s, 1H), 6.90 (ddd, J = 7.5, 7.5, 1.1 Hz, 1H), 6.86 (d, J = 8.3 Hz, 1H), 4.11 (q, J = 7.0 Hz, 2H), 1.42 (t, J = 7.0 Hz, 3H). ^{13}C NMR (100 MHz, CDCl_3) δ = 159.4 (C_q), 158.1 (CH), 157.4 (C_q), 136.3 (C_q), 133.3 (CH), 129.7 (CH), 128.9 (C_q), 124.6 (CH), 122.3 (CH), 121.3 (C_q), 120.7 (CH), 120.4 (CH), 117.5 (CH), 114.5 (CH), 114.0 (CH), 113.1 (C_q), 112.3 (CH), 91.9 (C_q), 86.2 (C_q), 64.3 (CH_2), 14.8 (CH_3). IR (neat): 2979, 2928, 1733, 1421, 804, 746 cm^{-1} . MS (ESI) m/z (relative intensity) 362 [$\text{M}+\text{Na}^+$] (100), 340 [$\text{M}+\text{H}^+$] (38). HR-MS (ESI) m/z calcd for $\text{C}_{22}\text{H}_{18}\text{N}_3\text{O}$ [$\text{M}+\text{H}^+$] 340.1450, found 340.1444.



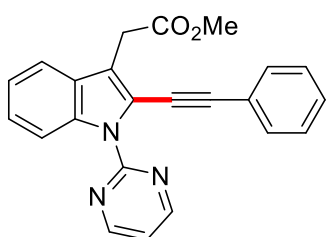
(195ak): The general procedure **B** was followed using substrate **192a** (98 mg, 0.5 mmol) and **194k** (156 mg, 0.6 mmol). Isolation by column chromatography (*n*-pentane/EtOAc:8/2) yielded **195ak** (185 mg, 99%) as a colorless oil. ^1H NMR (400 MHz, CDCl_3) δ = 8.84 (d, J = 4.8 Hz, 2H), 8.34 (dd, J = 8.5, 0.9 Hz, 1H), 7.61 (dd, J = 7.9, 1.0 Hz, 1H), 7.57 (dd, J = 8.1, 1.2 Hz, 1H), 7.54 (dd, J = 7.7, 1.7 Hz, 1H), 7.35 (ddd, J = 8.4, 7.1, 1.3 Hz, 1H), 7.30–7.21 (m, 2H), 7.18 (t, J = 4.8 Hz, 1H), 7.17–7.12 (m, 2H). ^{13}C NMR (125 MHz, CDCl_3) δ = 158.1 (CH), 157.2 (C_q), 136.4 (C_q), 133.2 (CH), 132.4 (CH), 129.2 (CH), 128.7 (C_q), 126.9 (CH), 125.5 (C_q), 124.9 (CH), 124.8 (C_q), 122.4 (CH), 120.8 (CH), 120.4 (C_q), 117.6 (CH), 115.5 (CH), 114.2 (CH), 93.5 (C_q), 86.9 (C_q). IR (neat): 3049, 2925, 2202, 1990, 1911, 1562, 1422, 1024, 745, 459 cm^{-1} . MS (EI) m/z (relative intensity) 375 (79) [M^+] (^{81}Br), 374, (100) [$\text{M}-\text{H}^+$] (^{81}Br), 373 (79) [M^+] (^{79}Br), 372 (88) [$\text{M}-\text{H}^+$] (^{79}Br), 293 (50), 214 (22), 147 (28). HR-MS (EI) m/z calcd for $\text{C}_{20}\text{H}_{12}\text{BrN}_3$ [M^+] 373.0215 (^{79}Br), found 373.0199 (^{79}Br).



(195al): The general procedure **B** was followed using substrate **192a** (98 mg, 0.5 mmol) and **194l** (111 mg, 0.6 mmol). Isolation by column chromatography (*n*-pentane/EtOAc: 9/1) yielded **195al** (118 mg, 79%) as a colorless oil. ^1H NMR (300 MHz, CDCl_3) δ = 8.81 (d, J = 4.8 Hz, 2H), 8.24 (dd, J = 8.4, 0.9 Hz, 1H), 7.55 (ddd, J = 7.8, 1.0, 1.0 Hz, 1H), 7.28 (ddd, J = 8.4, 7.2, 1.2 Hz, 1H), 7.21–7.16 (m, 2H), 6.94 (s, 1H), 6.18 (tt, J = 4.0, 1.8 Hz, 1H), 2.22–2.18 (m, 2H), 2.15–2.11 (m, 2H), 1.68–1.57 (m, 4H). ^{13}C NMR (125 MHz, CDCl_3) δ = 158.0 (CH), 157.3 (C_q), 136.2 (C_q), 135.3 (CH), 128.7 (C_q), 124.3 (CH), 122.2 (CH), 121.3 (C_q), 120.7 (C_q), 120.5 (CH), 117.5 (CH), 113.9 (CH), 113.7 (CH), 96.8 (C_q), 79.8 (C_q), 28.8 (CH_2), 25.9 (CH_2), 22.3 (CH_2), 21.6 (CH_2). IR (neat): 2962, 2927, 1561, 1449, 1259, 1014, 796, 742 cm^{-1} . MS (ESI) m/z (relative intensity) 338 [$\text{M}+\text{K}^+$] (41), 322 [$\text{M}+\text{Na}^+$] (100), 300 [$\text{M}+\text{H}^+$] (95). HR-MS (ESI) m/z calcd for $\text{C}_{20}\text{H}_{18}\text{N}_3$ [$\text{M}+\text{H}^+$] 300.1501, found 300.1495.



(195aq): The general procedure **B** was followed using substrate **192a** (98 mg, 0.5 mmol), **194q** (139 mg, 0.6 mmol) and $\text{MnBr}(\text{CO})_5$ (3.4 mg, 2.5 mol %). Isolation by column chromatography (*n*-Pentane/EtOAc : 9/1) yielded **195aq** (66 mg, 38%) as brown oil. ^1H NMR (400MHz, CDCl_3) δ = 8.87 (d, J = 4.8 Hz, 2H), 8.55 (d, J = 8.1 Hz, 1H), 8.40 (d, J = 8.4 Hz, 1H), 7.84 (dd, J = 14.6, 7.9 Hz, 2H), 7.75 (d, J = 7.1 Hz, 1H), 7.63 (d, J = 7.8 Hz, 1H), 7.57–7.50 (m, 2H), 7.47–7.43 (m, 1H), 7.36 (ddd, J = 8.3, 6.9, 1.0 Hz, 1H), 7.27–7.20 (m, 3 H). ^{13}C NMR (101 MHz, CDCl_3) δ = 158.2 (CH), 157.5 (C_q), 136.5 (C_q), 133.4 (C_q), 133.2 (C_q), 130.2 (CH), 128.9 (C_q), 128.7 (CH), 128.2 (CH), 126.6 (CH), 126.5 (CH), 126.4 (CH), 125.3 (CH), 124.9 (CH), 122.5 (CH), 121.1 (C_q), 121.0 (C_q), 120.8 (CH), 117.6 (CH), 115.1 (CH), 114.4 (CH), 93.5 (C_q), 87.4 (C_q). IR (neat): 3044, 2924, 2851, 1733, 1561, 1419, 798, 771, 744 cm^{-1} . HR-MS (ESI) m/z calcd for $\text{C}_{24}\text{H}_{15}\text{N}_3$ [$\text{M}+\text{H}^+$] 346.1344, found 346.1332.



(195as): The general procedure **B** was followed using substrate **192a** (133 mg, 0.5 mmol) and **194s** (109 mg, 0.6 mmol). Isolation by column chromatography (*n*-pentane/EtOAc:8/2) yielded **195as** (157 mg, 85%) as a brown solid. M.p. = 135–137 °C. ^1H NMR (300 MHz, CDCl_3) δ = 8.83 (d, J = 4.8 Hz, 1H), 8.82 (d, J = 4.8 Hz, 1H), 8.37 (d, J = 8.4 Hz, 1H), 7.61 (d, J = 7.8 Hz, 1H), 7.55–7.50 (m, 2H), 7.38–7.30 (m, 4H), 7.29–7.22 (m, 1H), 7.18 (dd, J = 4.8, 4.8 Hz, 1H), 4.02 (s, 2H), 3.69 (s, 3H). ^{13}C NMR (125 MHz, CDCl_3) δ = 171.0 (C_q), 157.9 (CH), 157.2 (C_q), 136.0 (C_q), 131.2 (CH), 128.5 (C_q), 128.3 (CH), 128.2 (CH), 125.1 (CH), 123.2 (C_q), 122.4 (CH), 119.9 (C_q), 119.8 (C_q), 119.1 (CH), 117.5 (CH), 114.4 (CH), 98.6 (C_q), 81.2 (C_q), 52.1 (CH_3), 31.4 (CH_2). IR (neat): 3048, 2953, 2848, 2197, 1730, 1561, 745, 691 cm^{-1} . MS (EI) m/z (relative intensity) 367 (47), 352, (5), 308 (100). HR-MS (EI) m/z calcd for $\text{C}_{23}\text{H}_{17}\text{N}_3\text{O}_2$ [M^+] 367.1321, found 367.1305.

References

- [1] N. Sauermann, M. J. Gonzalez, L. Ackermann, *Org. Lett.* **2015**, *17*, 5316–5319.
- [2] L. Ackermann, A. V. Lygin, *Org. Lett.* **2011**, *13*, 3332–3335.
- [3] J. P. Brand, J. Waser, *Angew. Chem. Int. Ed.* **2010**, *49*, 7304–7307
- [4] Z. Ruan, S. Lackner, L. Ackermann, *ACS Catal.* **2016**, *6*, 4690–4693.
- [5] Y.-S. Feng, Z.-Q. Xu, L. Mao, F.-F. Zhang, H.-J. Xu, *Org. Lett.* **2013**, *15*, 1472–1475
- [6] (a) W. Liu, S. C. Richter, R. Mei, M. Feldt, L. Ackermann, *Chem. Eur. J.* **2016**, *22*, DOI: 10.1002/chem.201604621; (b) Y. Zhu, M. Bauer, L. Ackermann, *Chem. Eur. J.* **2015**, *21*, 9980–9983.
- [7] (a) F. Xie, Z. Qi, S. Yu, X. Li, *J. Am. Chem. Soc.* **2014**, *136*, 4780–4787; (b) Z.-Z. Zhang, B. Liu, C.-Y. Wang, B.-F. Shi, *Org. Lett.* **2015**, *17*, 4094–4097.

8. CONCLUSIONS

In conclusion, in this work it was reported different employments of allene-derivatives in organic chemistry. In particular, it was reported the first metal-free enantioselective dearomatization of indoles using allenamides.

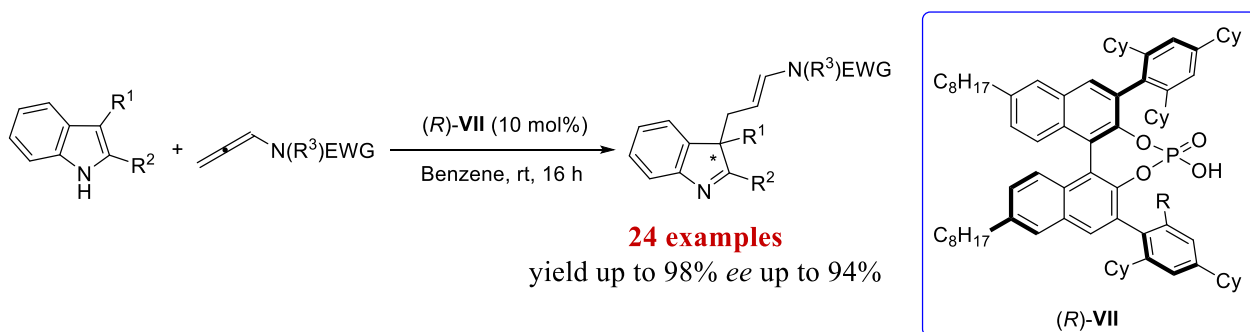


Figure 1: First metal-free enantioselective dearomatization of indoles.

The methodology resulted to be tolerant toward several functional groups. The indolenines were isolated in good to excellent yields and very high enantiomeric excesses. Moreover, it was also developed a one-pot three-component reaction for the dearomatization/hydrogenation cascade reaction that involving indoles, allenamides and a Hantzsch ester. The corresponding indolines were obtained in moderate yields and excellent diastereoisomeric ratios as well as enantiomeric excesses.

Inspired by these satisfactory results obtained in electrophilic activation of allenamides promoted by BINOL-based phosphoric acids, we developed an enantioselective Friedel-Crafts reaction of allenamides in order to prepare 1-vinyl tetrahydroisoquinolines.

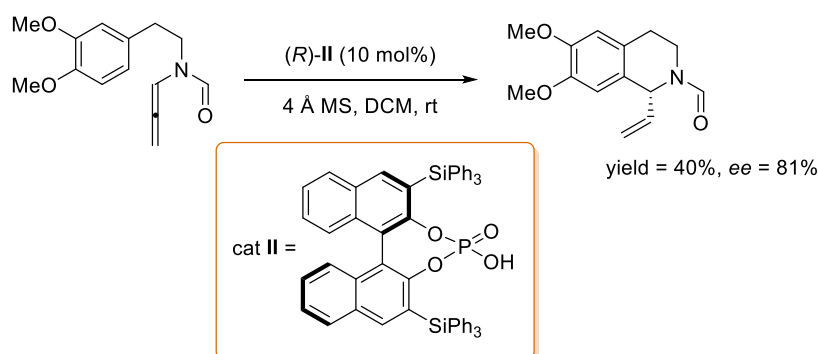


Figure 2: Enantioselective synthesis of 1-vinyl tetrahydroisoquinolines from electrophilic activation of allenamides promoted by chiral BINOL-based phosphoric acids.

The tetrahydroisoquinolines obtained with this methodology present a vinyl group in 1 position which is a powerful building block for further functionalizations.

Not only allenamides but also allenates were considered in this work. Indeed, it was also reported an efficient α -allylation of enones promoted by gold(I)/H⁺ co-catalyst. In particular the allenate intermediates generated by [3,3]-sigmatropic rearrangements of propargylic pivalates underwent electrophilic trapping by activated allylic alcohols.

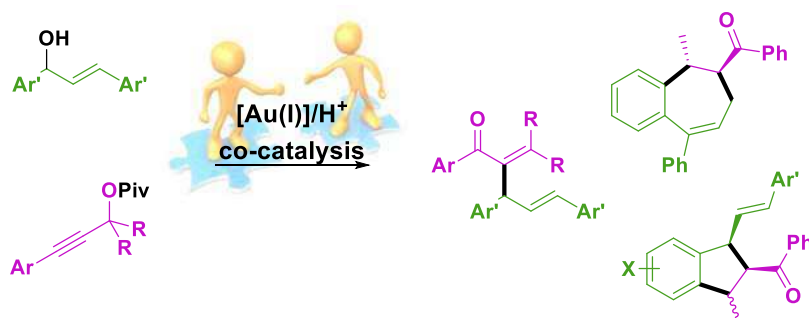


Figure 3: Gold(I)/H⁺ co-catalysed α -allylation of enones with activated alcohols.

The transformation demonstrated large flexibility in the employment of different functional groups, and the corresponding α -allylated enones were obtained in good to excellent yields. In some of the cases it was possible to isolate bicycles compound delivered by an allylic alkylation/Michael-type Friedel-Crafts alkylation.

Finally, the Mn-catalysed C–H alkylation of indoles was reported. The methodology resulted to be tolerant toward several functional groups. Several silyl haloalkynes as well as aryl, alkenyl and alkyl bromoacetylenes resulted in the corresponding products in good to excellent yields. Moreover, the protocol is suitable for the functionalization of more complex substrates such as peptides without loss of chiral purity. It is also reported the possibility to perform an intramolecular Mn-catalysed C–H alkylation to synthesize macrocycles.

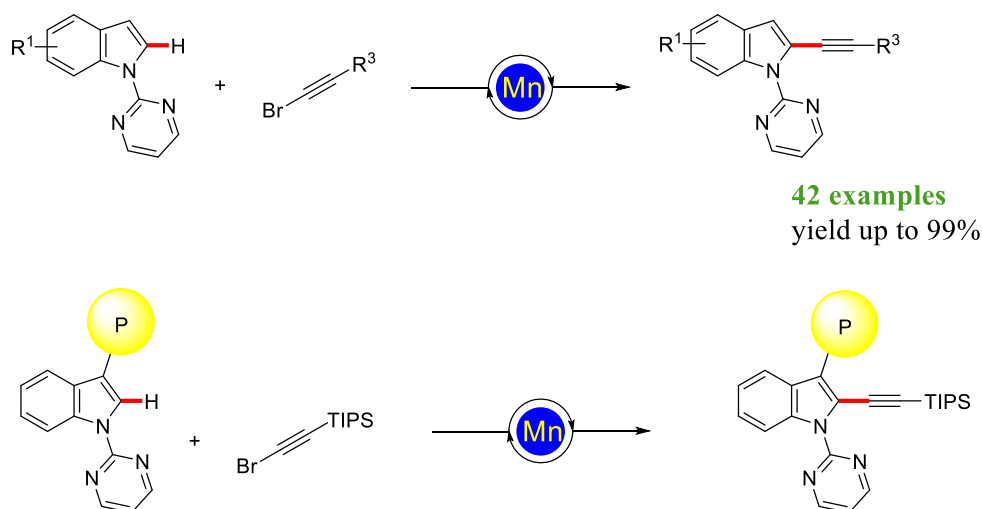


Figure 4: Mn-catalysed C–H alkylation of indoles.